Complexity

Energy and Complexity

Lead Guest Editor: Zofia Lukszo
Guest Editors: Ettore Bompard, Paul Hines, and Liz Varga

Energy and Complexity

Complexity

Energy and Complexity

Lead Guest Editor: Zofia Lukszo
Guest Editors: Ettore Bompard, Paul Hines, and Liz Varga

Editorial Board

Contents

Hindawi
Complexity
Volume 2018, Article ID 6937505, 2 pages
https://doi.org/10.1155/2018/6937505

Editorial
Energy and Complexity

Zofia Lukszo,[1,2] **Ettore Bompard**,[2] **Paul Hines**,[3] **and Liz Varga**[4]

[1]*Delft University of Technology, Delft, Netherlands*
[2]*Politecnico di Torino, Turin, Italy*
[3]*University of Vermont, Burlington, VT, USA*
[4]*Cranfield University, Swindon, UK*

Correspondence should be addressed to Zofia Lukszo; z.lukszo@tudelft.nl

Received 8 April 2018; Accepted 8 April 2018; Published 13 June 2018

Sustainable energy systems are complex sociotechnical systems with a social network of many players that "together" develop, operate, and maintain the technical infrastructure. No single player controls the system, but their actions are coordinated through a range of institutions—informal and formal rules—and regulations. As the control is distributed among actors, the overall system behaviour (at different time scales) emerges from operating practices and characteristics, from (dis)investment decisions, and from other aspects of the players' strategies.

A successful realization of sustainable energy systems depends on their societal acceptability, market dynamics, regulations, and the support of different stakeholder groups. To facilitate the introduction of flexibility sources like storage, demand-side response, flexible clean generation, and interconnections between different power systems, different sociotechnical designs have to be considered.

Sustainable energy systems require a complex, irreducible approach for design and operation and for robust what-if analyses. Essential aspects of the overall system behaviour or structure might be misunderstood or even overlooked if traditional methods continue to be applied; that is, methods which examine the connections between the heterogeneous parts and the whole system of systems are needed. Multidisciplinary research including engineering science, economics, political science, and behavioural science is needed to meet ambitions.

This special issue addresses recent advances regarding complexity in energy systems. From 10 submissions, 7 papers are published in this special issue. Each paper was reviewed by at least two reviewers and revised according to review comments. The accepted papers show that insights into the possible consequences of design choices and operational modes can be provided by engineering science, advanced modelling, and optimization techniques, but at the same time new market structures, organizational interactions, and institutional designs should be taken into consideration.

In the paper "Structural Evaluation for Distribution Networks with Distributed Generation Based on Complex Network," F. Xue et al. addressed challenges of the operation of distribution grid with a high participation of distributed generators (DG) and energy storage systems. They stressed that in the field of complex networks the performance and vulnerabilities of networked infrastructures are tightly related to the original topology and structural factors as positions of generation and load buses and capacities. However, when integrating distributed generating systems with distribution networks two perspectives should be taken into account: local perspective from individual viewpoint of DGs and global perspective from overall viewpoint of the original network. Case studies were used to illustrate the proposed Power-Supply-Ability metrics to identify potential structural vulnerabilities of distribution networks in general and the impact of DGs on security in particular. Also site selection for DGs can benefit from these metrics by providing evaluation of different location possibilities.

In the paper "A Stability Analysis of Thermostatically Controlled Loads for Power System Frequency Control," E. Webborn and R. S. Mackay investigated thermostatically controlled loads (TCLs) functioning as a flexible demand

resource with the potential to play a significant role in supporting electricity grid operation. The mathematical modelling and simulation study showed the short-term benefits of using identical TCLs for frequency response and discussed long-term issues indicating that a population of refrigerators might perform a valuable service to the grid without requiring centralised or stochastic control.

In the paper "Enabling the Analysis of Emergent Behavior in Future Electrical Distribution Systems Using Agent-Based Modeling and Simulation," S. Kolen et al. investigated emergent system behaviour of future electrical distribution grids and in particular cyber-physical interactions and communication through electrical lines as well as control systems. They developed an agent-based modelling and simulation tool DistAIX to be used for large-scale system analysis addressing the need for scalable capability to observe emergent behaviour that is vital for the development of decentralized control strategies.

In the paper "Sociotechnical Network Analysis for Power Grid Resilience in South Korea," D. A. Eisenberg et al. showed that to improve power grid resilience technological solutions to reduce the probability of losses are not sufficient. Policies and protocols for social processes should be taken into consideration, too. Case study of the Korean power grid illustrated that both technological and social analyses are needed to provide important information regarding power grid resilience, and both are necessary to avoid unintended consequences for future blackouts.

In the paper "Assessing the Plurality of Actors and Policy Interactions: Agent-Based Modelling of Renewable Energy Market Integration," M. Deissenroth et al. discussed to what extent and how growing participation of renewable energy sources (RES) should be integrated into energy markets with new regulations. They proposed an agent-based model to study the impact of changing energy policy instruments on the economic performance of RES operators and marketers. They concluded that changes in the political framework cannot be mapped directly to RES operators without considering intermediary market actors, the characteristics and strategies of these being an important factor for successful RES marketing and further deployment.

In the paper "Conceptualization of Vehicle-to-Grid Contract Types and Their Formalization in Agent-Based Models," E. H. Park Lee et al. looked at a specific application of fuel cell electric vehicles (FCEVs) which can be used as flexible power plants in future energy systems. Technical and economic feasibility of such an innovative concept should be accompanied by an institutional analysis. They investigate by agent-based simulation how different types of contracts, that is, price-based, volume-based, and control-based contracts, can be used not only for the benefits of car owners but also for balancing local energy supply in microgrids.

The paper "Creating Agent-Based Energy Transition Management Models That Can Uncover Profitable Pathways to Climate Change Mitigation" by A. Hoekstra et al. closes this special issue. The authors of the last paper presented a literature review comparing equilibrium models, system dynamics, and discrete event simulation with agent-based models to address general energy transition and climate change problems. Exploring these problems using agent-based modeling is often the most promising strategy as interactions between the global, national, local, and individual level can be taken into account.

The papers in this special issue represent exciting and insightful observations into energy problems from the complexity perspective. We hope that this special issue will attract attention to the many important opportunities for further research into complexity and energy and will function as a valuable resource to further develop the knowledge needed for energy transition.

Zofia Lukszo
Ettore Bompard
Paul Hines
Liz Varga

Hindawi
Complexity
Volume 2018, Article ID 3569129, 11 pages
https://doi.org/10.1155/2018/3569129

Research Article

Conceptualization of Vehicle-to-Grid Contract Types and Their Formalization in Agent-Based Models

Esther H. Park Lee, Zofia Lukszo, and Paulien Herder

Faculty of Technology, Policy and Management, Delft University of Technology, Jaffalaan 5, 2628 BX Delft, Netherlands

Correspondence should be addressed to Esther H. Park Lee; h.parklee@tudelft.nl

Received 30 June 2017; Revised 8 January 2018; Accepted 30 January 2018; Published 7 March 2018

Academic Editor: Pietro De Lellis

Fuel cell electric vehicles (FCEVs) have the potential to be used as flexible power plants in future energy systems. To integrate FCEVs through vehicle-to-grid (V2G), agreements are needed between the FCEV owners and the actor that coordinates V2G on behalf of them, usually considered the aggregator. In this paper, we argue that, depending on the purpose of providing V2G and the goal of the system or the aggregator, different types of contracts are needed, not currently considered in the literature. We propose price-based, volume-based, and control-based contracts. Using agent-based modeling and simulation we show how price-based contracts can be applied for selling V2G in the wholesale electricity market and how volume-based contracts can be used for balancing the local energy supply and demand in a microgrid. The models can provide a base to explore strategies in the market and to improve performance in a system highly dependent on V2G.

1. Introduction

Flexibility can be defined as the ability of a system to deal with the variability and uncertainty in the balance of generation and consumption of electricity [1]. One of the potential flexibility resources that can be exploited by residential consumers for electric power systems is the energy stored in electric vehicles (EVs), which could be used whenever they are parked, to provide storage, demand-side response, or vehicle-to-grid (V2G) [2–4]. This has been an area of interest for over a decade [5] due to the increasing electrification of transport systems [6]. In many cases, the supply of flexibility with EVs is an opportunity but also a need, due to the effect that EV charging has on the distribution networks. In the case of fuel cell electric vehicles (FCEVs), hydrogen is used as an energy carrier and therefore it can be stored centrally but also in the vehicles. Thus, the energy demand for mobility does not affect the grid directly, while the energy available in the vehicles can be used for supplying flexible vehicle-to-grid power [7].

Research on Battery Electric Vehicles (BEVs) is usually focused on ancillary services (spinning reserves and regulation) due to the ability of BEVs to provide regulation up and down [8–12]. As Kempton and Tomić [2] indicate, BEVs are better for providing regulation and FCEVs are more suitable for spinning reserves and peak power. Wholesale markets have also been considered [13–15] as it is expected that a growing EV capacity will eventually saturate the balancing markets [16–18]. The supply of power in microgrids for load leveling has also been considered [19, 20]. Regarding FCEVs, most of the literature is focused on local energy supply, for example, vehicle-to-building power [21, 22] and more recently microgrids [23–25] and smart cities [26]. The role of FCEVs in the wholesale market in systems with high wind penetration is also being explored [27]. The more recent research presents FCEVs within the Car as Power Plant (CaPP) concept, which combines renewable energy generation, conversion to hydrogen, and storage [4, 7].

The technical and economic potential of V2G has been widely explored [2, 21, 22], but due to political and regulatory barriers [28, 29] implementation is still limited to controlled environments and pilot projects [30]. In the case of FCEVs, the slow adoption of FCEVs and limited hydrogen infrastructure are additional barriers, as well as the public acceptance of hydrogen [31]. When implemented, the operation V2G will depend on the participation of drivers, who must be willing to activate the flexibility from their vehicles when needed. The

aggregator role is considered to be important for the implementation of V2G, given that an actor in the electricity system is needed to participate in markets on behalf of the drivers (prosumers) [9, 32]. In local energy systems/microgrids, the controller or microgrid operator takes the role of aggregator. The use of vehicles for flexible power supply by an aggregator implies the need of an agreement between vehicle owners and the aggregator, which can be made in the form of a contract [32, 33]. Contracts can provide the aggregator with information about the availability and activation criteria of the vehicles, to make decisions about when to operate which resources. The literature on V2G contracts, however, is quite limited as only one form of contract is usually considered for different markets.

The goal of this paper is to (1) contribute to the V2G contract literature by adding new types of contracts to provide different ways to manage EVs (FCEVs in particular) for different markets and types of V2G power and (2) demonstrate in two models how price-based contracts can be used to sell power in the wholesale market and how volume-based contracts can be used to coordinate V2G in a microgrid. For the first goal we provide the current insights into the V2G contract literature and propose new V2G contract types within a classification that is used in the demand response (DR) literature: price-based, volume-based, and control-based contracts. We briefly introduce the contract parameters in each one and explain when they may be suitable. For the second goal, we present two agent-based models in which the different energy systems are represented as complex sociotechnical systems.

The rest of the paper is structured as follows: In Section 2 we present a review of the relevant literature that deals with contracts for V2G. In Section 3 we describe three contract types: price-based, volume-based, and control-based. In Section 4 we describe the two models used and the results of the simulations. We end in Section 5 with conclusions about our research.

2. Literature Review

2.1. Vehicle-to-Grid and Its Value Chain. The Universal Smart Energy Framework (USEF) defines the relationships in flexibility trading using prosumer-side resources [34]. Since all electric vehicles (EVs) can be considered prosumer-side flexibility resources, the framework can also be used to describe the V2G value chain (Figure 1). Drivers provide V2G to the electricity system via an aggregator that may interact with balance responsible parties (BRP), the Transmission System Operator (TSO), and/or the Distribution System Operator (DSO) for the supply of V2G in different markets. The framework also indicates the several stages in flexibility trading, in which the interactions among actors occur [35]: Contract, Plan, Validate, Operate, and Settle. The Contract phase can include the agreements between prosumer and aggregator on the capacity available and the conditions for activation. The Plan and Validate stages are similar to the processes in current markets, where market actors make plans for energy supply and demand, which are validated if feasible. The Operate stage refers to the dispatch of resources,

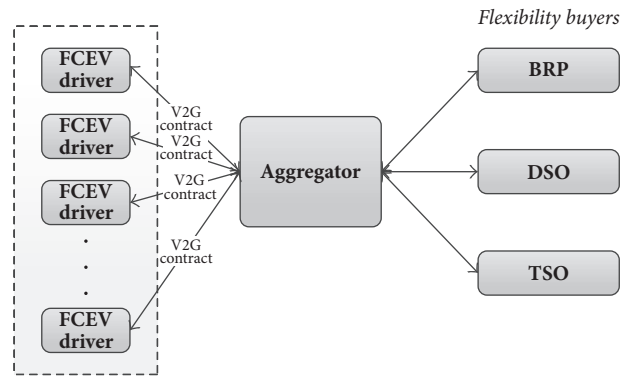

Figure 1: Relationships of actors in the V2G value chain, based on [35].

which would refer to the use of vehicles to provide electricity. While generally the V2G literature is focused on the Plan and Operate stages and the participation in electricity markets [8, 36, 37], there is limited knowledge on the Contract phase and how it affects the daily operations.

2.2. Role of Contracts in the Coordination of Vehicle-to-Grid. We define operational coordination of V2G as the set of decisions that are made to operate individual vehicles in order to achieve a certain goal in the technical system. Although the aggregator offers aggregated energy or capacity in the markets, it also has to make decisions about the operation of individual vehicles, taking into account the different needs and preferences of the drivers and the technical characteristics of the vehicles. These aspects which define the *availability* and *activation criteria* of each car delineate how it can be operated by the aggregator and have to be explicitly defined in a contract.

Guille and Gross [32] present a V2G implementation framework that consists of using contracts to get the commitment from vehicles before the aggregator can make a contract with the system operator. A package deal is formed, consisting of preferential rates for purchasing the battery but also discounts for charging and parking. The obligations indicated in the contract consist of plugging in at times that are predefined in the contract. Failing to comply with the contract terms leads to penalties. The authors in [33] describe two options for the relationship between the aggregator and EV driver: a contractual and a noncontractual form. The former would involve obligations for the service and a yearly cash payment and the second a free participation and "pay-as-you-go" type of remuneration. A choice experiment about V2G-enabled EVs is carried out, using a simple contract concept. Required plug-in hours (ranging from 5 to 20 hours) and a guaranteed minimum range (ranging from 25 to 175 miles) are two of the contract terms. One of the conclusions is that the upfront payments for V2G to drivers might not be enough to participate in V2G.

One econometric study quantifies the influence of contract parameters on the economic potential of V2G in the German secondary reserve markets [37]. The contract parameters used are those presented in [33]. Driver characteristics

from mobility data are used to assume contract parameters (based on the theoretical participation potential) and to make subsets of drivers with similar characteristics. Using the subsets, the value of different vehicle characteristics for the aggregator are determined. Although the authors use market data of a whole year, they extract two weeks with the highest and lowest reserve market demands to calculate the optimal car pool size, as well as the annual profits. Broneske and Wozabal [37] conclude that the value of certain contract parameters for the aggregator depends on the characteristics of the market; that is, markets where more energy is supplied will value drivers that are able to provide enough energy (lower guaranteed minimum range) while also providing enough availability, while markets where less energy is supplied, the availability (plug-in hours) will be more valued.

2.3. Different Vehicle-to-Grid Contract Types. For all types of markets and services, the supply of V2G has different characteristics and needs. As Broneske and Wozabal [37] concluded, in markets with different "energy throughput" characteristics, different contract parameters are suitable and thus valuable for the aggregator. Kempton and Tomić [2] also suggest that when providing ancillary services the availability (capacity) is more valuable than the actual energy supplied, since even when there is a loss for selling electricity, the capacity payments sufficiently make up for the costs incurred [2]. Since the characteristics for participation in V2G differ in each market and system, different types of contracts should be made to account for the different needs.

In the demand response (DR) literature, demand response programs can be categorized into "explicit" (volume-based) and "implicit" (price-based) mechanisms [38]. The first one refers to explicitly defining the level of flexibility to be activated and is appropriate for system reliability purposes. The latter refers to the reaction of consumers to prices and thus the provision of flexibility without a previous agreement on the volume [39]. He et al. [40] emphasize the importance of *activating* consumers for demand response to be successful. To achieve that, the authors present different types of contracts that can cater to consumers with distinct technical capabilities and preferences: *price-based*, *volume-based*, and *control-based* contracts, all of which have different technical characteristics and high level implications for prosumers.

The concepts from demand response can be extended to V2G, although there are fundamental differences between DR and V2G. In the case of DR, the service is a deviation of the normal consumption pattern, usually provided through household load or EV charging. V2G on the other hand implies allowing the use of a vehicle as a dispatchable generation unit. These are two different ways to provide flexibility in electricity systems [1] and have in common the fact that small prosumers can participate. The concepts from [40] and the DR literature can be used as a guideline to define different ways in which the V2G service can be activated, although specific characteristics related to mobility have to be applied to activate drivers for V2G supply. In the case of FCEVs, which are usually not connected to the grid, it can be a challenge since additional efforts are needed by the prosumer to plug in the vehicle and provide energy.

Currently only one type of contract is considered in the literature, which is defined by the plug-in time (timing and length) and the guaranteed driving range after V2G. In [13], different strategies for V2G participation with BEVs in the wholesale market are explored. One of them allows the driver to define a selling price for V2G, leading to the lowest battery cycles and highest savings (net profits) when compared to other strategies where the driver does not control the minimum price. Although the aggregator's role is implied, there are no details about the contractual relationships and there seems to be no profit sharing with the aggregator. This example demonstrates that in some cases allowing drivers to set a minimum price for activating V2G would help them control the level of expected revenues and thus make participation more attractive.

2.4. Conclusions. In conclusion, the need for contracts in V2G supply is evident from the literature and is in line with the processes of flexibility trading defined in [35]. The use of V2G contracts is mentioned in the literature either to imply agreements on the level of participation of the vehicles [8], or as a means to ensure or increase participation [32, 33]. Broneske and Wozabal [37] demonstrated that contract parameters influence profitability in the market and that different market characteristics value contract parameters differently. The only V2G contract type explicitly mentioned in the literature (based on plug-in time and energy available) [32, 33, 37] may not be enough to engage drivers in different markets. This is supported by the distinction made in DR programs and contract types [38, 40] and the possibility that setting a selling V2G price can be more profitable for drivers in some cases [13]. There is still limited focus in the literature on V2G contract design or on how contracts made with drivers with different needs and behaviors affect the operational coordination in the system in which the vehicles are integrated. When viewing future energy systems with V2G as complex sociotechnical systems, we cannot ignore the interactions between actors in the whole V2G value chain and the role of V2G contracts on the operation of the system. For aggregators to sell V2G power in different markets, the contract parameters used to coordinate drivers must be aligned with the characteristics of both individual drivers and the markets. Therefore, there is a clear need to define new V2G contract types and their corresponding parameters and to explore their possible effects on the operation of future energy systems.

3. A Classification of Vehicle-to-Grid Contract Types

In this section we present three V2G contract types and introduce the distinct sets of parameters. To conceptualize these contracts we use the generic classification of contracts from the DR literature [38, 40], which can be applied to V2G: *price-based*, *volume-based*, and *control-based* V2G contracts. We use the characteristics of V2G as explored in [13, 23, 32, 33]

Table 1: Price-based contract parameters.

Contract parameter	Description
Min. V2G price	Minimum price for activation, defined by driver
Guaranteed fuel level	Minimum level of hydrogen in the tank guaranteed after operation
V2G remuneration	Remuneration for energy supply, for example, min. V2G price

Table 2: Volume-based contract parameters.

Contract parameter	Description
Time interval	Time interval (start + duration) for availability
Max. volume	Maximum volume usable for V2G
V2G remuneration	Energy and capacity remuneration
Guaranteed fuel level	Minimum level of fuel guaranteed after operation
Min. fuel required at plug-in	*Calculated level of fuel required in the vehicle before plug-in*

Table 3: Control-based contract parameters.

Contract parameter	Description
Time interval	Plug-in time (voluntary or precommitted)
V2G remuneration	Energy and capacity remuneration
Guaranteed fuel level	Minimum level of energy guaranteed after operation, requested by driver

and define the contract parameters corresponding to each type.

The contract types presented here can be used to for plug-in EVs as well as FCEVs. Although the coordination of smart charging with plug-in EVs can also be arranged through contracts with an aggregator, V2G refers strictly to the power flows from vehicle-to-grid, and therefore we exclude the arrangements of power flows from grid-to-vehicle (G2V). For the implementation of combined smart charging and vehicle-to-grid (charging and discharging) with battery EVs, we suggest adding or adjusting the contract parameters to provide the appropriate limits to use the battery. In the rest of this paper we will conceptualize and explain the contract parameters assuming they are used to manage FCEVs, which technically allow exclusively power flows from vehicle-to-grid.

3.1. Price-Based Contracts. Price-based vehicle-to-grid contracts involve a price signal for the activation of V2G. As shown in Table 1, the driver defines a minimum price he wants to receive for V2G. Therefore, the aggregator will use the vehicle only when he can provide this remuneration (e.g., market price is higher) and as long as there is enough energy in the vehicle. The availability or time at which the FCEV is plugged in is voluntary and therefore not committed. Depending on the market, the aggregator may define a remuneration structure such that the driver gets the minimum price and a percentage of the additional profit (difference between the market price and the minimum V2G price). This percentage could depend on the available energy at plug-in or the plug-in duration so that availability is rewarded.

This type of contract could be used for drivers to participate in the wholesale market, where average prices may not be high enough but peak prices can make V2G profitable [13].

3.2. Volume-Based Contracts. Volume-based contracts involve commitment of a predefined volume of energy within a certain time interval, as shown in Table 2. Thus, drivers can limit the amount of energy they are willing to provide (maximum volume). Since the fuel capacity in the FCEV tank is limited, this means that FCEVs need to have a certain amount of volume at plug-in. By defining the guaranteed fuel level, the required fuel amount can be also calculated for drivers to comply with the commitment.

Volume-based contracts can be attractive for drivers who have a very predictable driving schedule and can be plugged in regularly, for example, at the workplace parking facilities or at home. This type of contract can be used when the commitment of availability and energy is important such as in local energy systems depending on variable RES and FCEVs [23, 24, 26] or when providing reserve capacity. Since there is a commitment on the time and volume, the remuneration structure could be designed such that the commitment is rewarded.

3.3. Control-Based Contracts. With control-based contracts the driver cedes control to the aggregator as soon as the car is plugged in. The availability is defined by the time interval, which could be precommitted or informed at plug-in by indicating the expected departure time. As shown in Table 3, the activation criterion is defined by the guaranteed fuel level to be left after V2G. Although it is similar to the volume-based contract, there is no commitment on the maximum volume available. Implicitly, it is defined once the car is plugged in, by the initial level of fuel and the guaranteed fuel level. However, the total available volume can change every time.

This may be the contract form with lowest complexity and in the absence of a time interval commitment it gives freedom to the driver to plug in anytime. However, when plugged in,

the driver cannot limit how much energy may be used by the aggregator. High levels of availability or fuel levels may be incentivized by designing V2G remuneration structures that consist of a V2G tariff plus a capacity remuneration that is linked to the time duration and the fuel level at plug-in.

This type of contract is in practice implied in the assumptions made in the microgrid in [23], where all FCEVs are assumed to be plugged in whenever they are in the neighborhood and the controller can use them until the minimum fuel level is reached. It is also similar to the V2G contracts in the literature [32, 33, 37]. Control-based contracts could be attractive in cases when vehicle availability is high without commitment, for example, large fleet of FCEVs that are usually plugged in at regular times, and/or when volume commitment beforehand is not necessary because it is not scheduled ahead.

The three contract types described in this section show different ways for drivers and aggregators to make agreements on the availability and activation criteria of their flexible V2G resources, specifically FCEVs in this case. The main differences are the level of commitment of the plug-in time and the activation criterion: either the energy available (volume) or a minimum price preference. In each case, the aspect over which the driver has control is different. In practice, hybrid forms of contracts could be used by aggregators to ensure a certain level of participation of drivers.

4. Exploring the Role of V2G Contracts Using Agent-Based Models

In this section we demonstrate how V2G contracts can be used for different types of V2G power supply. We present two agent-based models built in Python: one where price-based contracts are used for participation in the day-ahead market and another where volume-based contracts are used to coordinate FCEVs in a microgrid. The models are described following guidelines of the ODD (Overview, Design, concepts, and Details) protocol [42]. In this section we only include the main aspects in summarized form, and more details can be found in the Supplementary Materials (available here). The complete descriptions are also available upon request.

4.1. Conceptual Framework and Approach. We use the complex sociotechnical systems approach to describe the system as a combination of the technical subsystem consisting of the physical units and processes, the social subsystem with the actors involved, and the institutions that guide the interactions [43–45]. The operation of such system is influenced by the interactions between the technology, the involved actors, and the institutional arrangements. In this paper, we focus on the effect of V2G contracts as institutional rules in two systems with heterogeneous actors. We conceptualize the two agent-based models using the three pillars of complex sociotechnical systems, *technology*, *actors*, and *institutions*, in this case the V2G contracts.

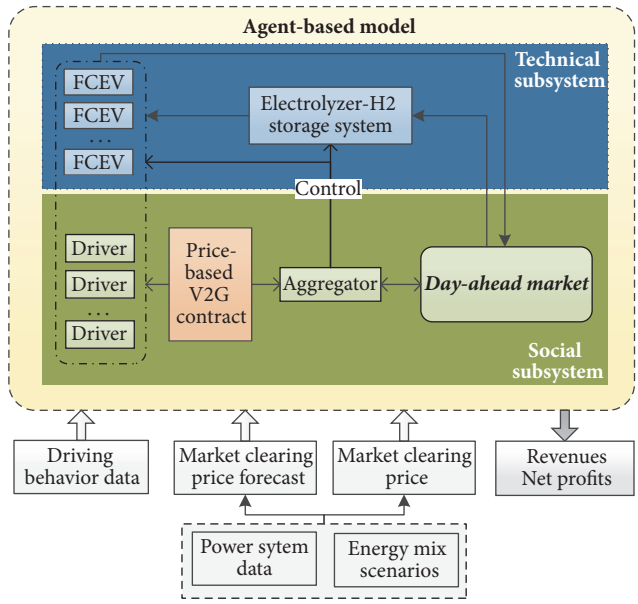

Figure 2: Agent-based model conceptualization: FCEVs in the day-ahead market.

4.2. Model 1: Price-Based Contracts for Participation in the Day-Ahead Market

4.2.1. Model Overview

Purpose. The purpose of this model is to formalize price-based contracts within an agent-based model and to explore the effect of contract parameters. We do this by modeling FCEVs in a car park that are used by an aggregator to sell V2G in the day-ahead market. We model the hourly actions and interactions of the agents, focusing on the role of individual contracts in the amount of V2G sold in the market. The minimum bid volume in the market means that selling power depends also on other drivers' availability and contract parameters. The revenues for the aggregator depend on the aggregated drivers' availability, their contract parameters, and the fluctuating market prices. The revenues for the drivers depend on their own availability and contract, other drivers' behaviors and their contracts, and the changing market prices. With this model, we want to understand these micro-macro-micro relationships to further explore how contract parameters could be used to better understand how to engage drivers to participate in wholesale markets and to design strategies for aggregators.

Figure 2 shows the model concepts, which distinguish the technical and social subsystems. Data sources are used to feed driving schedules to the driver agents and to model future electricity prices and forecasts externally and use them as inputs in the model. The main performance evaluation is based on the net profits and the V2G supplied by the drivers. The model is based on our previous work; please refer to [27] for the description of the day-ahead market model and scenarios.

Table 4: Drivers and V2G contract initialization.

Variable	Value
Driver agents	
Number of drivers	100
Driving schedule	Using distribution derived from [41], weekdays and weekends
Parking profile	50% of drivers with work hours, 50% with home hours
Initial fuel level (kg)	Random from 3.0 to 5.65 (max)
V2G contract	
minPrice (€/MWh)	Cost of V2G ∗ 1.0 [Equal *minPrice*] or cost of V2G ∗ random [1.0–1.5] [Random *minPrice*]
guarFuel (kg)	1.5 ∗ daily driving distance
driverMargin (%)	According to fuel % at arrival: [75–100%]: 75; [50–75%]: 50; [25–50%]: 25; [0–25%]: 10
Remuneration (€)	Calculated using *minPrice* and *driverMargin*

Agents and Objects. In the model there are three types of agents: the drivers, the aggregator, and the day-ahead market agent. Drivers represent both the characteristics of the driver, for example, the driving schedule or V2G contract, and the technical characteristics of the car, for example, the level of hydrogen in the tank. They drive and use the car park to park and plug in their car either during "work" or "home" hours. Driver agents own a price-based V2G contract object that contains the contract parameters. The aggregator agent accesses the information in the V2G contracts to sell V2G in the day-ahead market. It also buys electricity to produce hydrogen using the electrolyzer. It makes forecasts about the predicted market price and predicted availability to make decisions in the market. When V2G is sold, available FCEVs are used, based on the contract between the driver and the aggregator. V2G contracts are built as objects in the model, which contain the contract parameters.

Process Overview. At the beginning, contracts are created between driver agents and the aggregator agent. Every day at 12.00 noon, the aggregator agent uses its forecasts on the next day's expected hourly availability of FCEVs and the hourly market price forecasts for the next day in order to place offers for V2G in the market or bids to buy electricity to produce hydrogen. Given the minimum bid volume of 100 kW in the market and the assumed V2G power of 10 kW, for every 100 kW bid at least 10 vehicles with a minimum price lower than the expected market price are needed. Every day drivers drive cars according to their driving schedule. Based on their parking profile, they use the car park during either "work hours" or "home hours." Once parked, they plug in the vehicle to the grid. When they leave again, they refill if necessary. Based on the volumes of V2G sold in the day-ahead market, plugged in FCEVs with a minimum price lower than the market price are operated to supply V2G. At the end of the simulation run, the revenues for the period are calculated for every driver as well as the aggregator.

Inputs for Simulation. We initialize the agents using the inputs indicated in Table 4. The model is simulated for 8760 steps (one year) for two scenarios: Equal *minPrice* and Random *minPrice*. Since there is no knowledge on how drivers would set this contract parameter in practice, we compare a situation in which all drivers set the price based on the cost of providing V2G and a situation in which some agents increase the minimum price, up to 1.5 times the cost of providing V2G. This is done by using a factor calculated randomly between 1.0 and 1.5. The cost of providing V2G using FCEVs is calculated using (1), where the first part indicates the cost of energy, that is, the cost of purchased energy c_{pe} divided by the fuel cell efficiency and the Higher Heating Value of hydrogen. The second part indicates the degradation cost, which consists of the unit price of the fuel cell c_{FC} divided by its lifetime in hours and multiplied by a factor of 0.5. Similarly, as in [26], the degradation cost of V2G operation is assumed to be 50% of that of the degradation when driving.

$$c_{v2g} = \frac{c_{pe}}{\mathrm{HHV} * \eta_{FC}} + \frac{c_{FC}}{L} * 0.5. \quad (1)$$

The remuneration is calculated by adding the driver margin to the minimum price. The driver margin is the percentage of profit that the driver receives for the difference between the market price and the minimum price. It is assumed that the aggregator will receive the market price for the V2G supplied, and every €/MWh above the minimum price is to be shared between the two. Since there is no reference on how to calculate this margin, we used different levels of margins according to the fuel available at plug-in. Therefore, the driver margin can change every day, and it will reward drivers with fuller tanks.

The day-ahead market prices used in the simulation runs correspond to the "high wind" scenario in [27]. Please refer to Supplementary Materials for more information about the energy scenarios and the data sources used.

4.2.2. Results. The driver agents' and aggregator's results from the two-simulation run are shown in Table 5. As it is expected, the Equal *minPrice* run results in more volume of V2G supplied and higher profits both for drivers and for the aggregator. The potential profits are calculated as the profits that would be realized by the driver if the *driverMargin* had been always the highest, 75%. This value is also higher in the Equal *minPrice* case. The reason is that the minimum price to sell in the market is lower (63.45 €/kWh) in this run. In the Random *minPrice* case, the minimum price is calculated for every agent as the cost of V2G times a random factor between 1.0 and 1.5. In the simulation, the agents have a

Table 5: Simulation results: drivers and aggregator profits.

	Equal *minPrice*	Random *minPrice*
Driver results	Range (average)	
Profits (Eur/year)	18.62–326.09 (146.68)	8.41–248.081 (96.72)
Potential profits (Eur/year)	33.21–362.76 (181.09)	15.24–309.27 (129.73)
V2G supplied (MWh)	1.19–12.65 (6.39)	0.48–7.73 (3.61)
Aggregator results		
Revenues from V2G (Eur/year)	9,477.41	7,625.80

factor between 1.002 and 1.499, and the average is 1.233, which means that the *minPrice* ranges from 64.57 to 95 €/kWh, with an average of 78.24 €/kWh. In the model, the aggregator offers V2G in the market when it expects enough capacity and the expected market price is above the average *minPrice* of all drivers. Due to the high average minimum price, it is possible that some driver agents lose the opportunity to sell. On the other hand, some drivers that have a higher minimum price might sell when the market price is lower, but the aggregator still pays the minimum price. In this case, there could be reduced revenues for the drivers from the difference between the market price and the minimum price. The strategy used by the aggregator to offer V2G in the wholesale market could be different as the one used in the model. The possible bidding strategies of the aggregator and their influence on the drivers' net profits could also be explored using this model.

The purpose of adding randomness in the *minPrice* contract parameter was to illustrate how the actions (availability) and different contract parameters (minimum price) influence the aggregate availability of the vehicles. This in turn affects the profits that individual agents realize in the wholesale market. In the model, the contract parameters and driving schedule of every agent can be changed depending on the availability of data and the purpose of the research.

4.3. Model 2: Volume-Based Contracts in a Microgrid with Fuel Cell Vehicles

4.3.1. Model Overview. The Car as Power Plant microgrid is a community energy system consisting of household loads, renewable generation, conversion to hydrogen and storage, and FCEVs as power plants. In this system, the photovoltaic (PV) panels are used to provide power, and when PV generation is not sufficient, FCEVs are used as power plants. In our previous work [23], cars were assumed to be available for V2G whenever in the neighborhood (similar to control-based contracts). With the introduction of volume-based V2G contracts, drivers are able to reduce the plug-in time and set the maximum amount of energy supplied with their vehicle.

Purpose. The purpose of this model is to show how volume-based contracts can be formulated within an agent-based model and to understand the effect of the contract parameters on the system under study. We model a microgrid with residential households that depends on variable renewable energy sources (V-RES), storage, and FCEVs for the energy supply. Thus, the microgrid operator (aggregator role) depends on FCEV drivers and their availability to supply power to the microgrid. Using the volume-based V2G contracts we want to understand the relationship between self-sufficiency of the microgrid (system performance), the commitment made by the drivers, and the actual use of their vehicles (individual performance). The demand for V2G depends on the renewable generation and the availability of vehicles, and the extent to which a car is used is limited by the contract but depends also on other drivers and their availability. With this model we want to provide insights into designing contract parameters that are more aligned with system goals, for example, self-sufficiency in this case.

Figure 3 shows the concepts of the model, distinguishing the technical and social subsystems. As the figure indicates, households have loads and PV panels, which feed the microgrid at times of surplus to produce hydrogen using an electrolyzer. Whenever PV generation is insufficient, FCEVs are used, and ultimately power is imported if necessary. Wind turbines are also used to produce hydrogen. Data sources are used to input driving schedules to the drivers, for the generation profile of PV panels, and for the electricity consumption in households. The evaluation of the system performance is based on the capacity of self-supply and the amount of power imported. This model is based on our previous work; please refer to [23] for more details on the operation of the microgrid.

Agents and Objects. There are three agent types in the model: the households, the drivers, and the microgrid operator. The households are modeled as simple agents that have no other behavior than updating the electricity consumption and the PV generation. In this model, too, driver agents represent both the characteristics of the driver and the car. In principle they are part of the household agents, but the link is not explored in this model. Drivers drive in and out of the neighborhood according to their driving schedules. Every driver owns a volume-based V2G contract object that contains the parameters. The microgrid operator agent acts like an aggregator and uses the information to know which cars can be operated when needed. The microgrid operator also controls the other technical components of the system, such as the wind turbine and the electrolyzer.

Process Overview. At initialization, volume-based contracts are created. Every hour, drivers either drive, refill, or plug in their vehicle. Households generate electricity using their PV panels and use it for self-consumption. Whenever there is a surplus, it is injected to the local grid. The microgrid operator

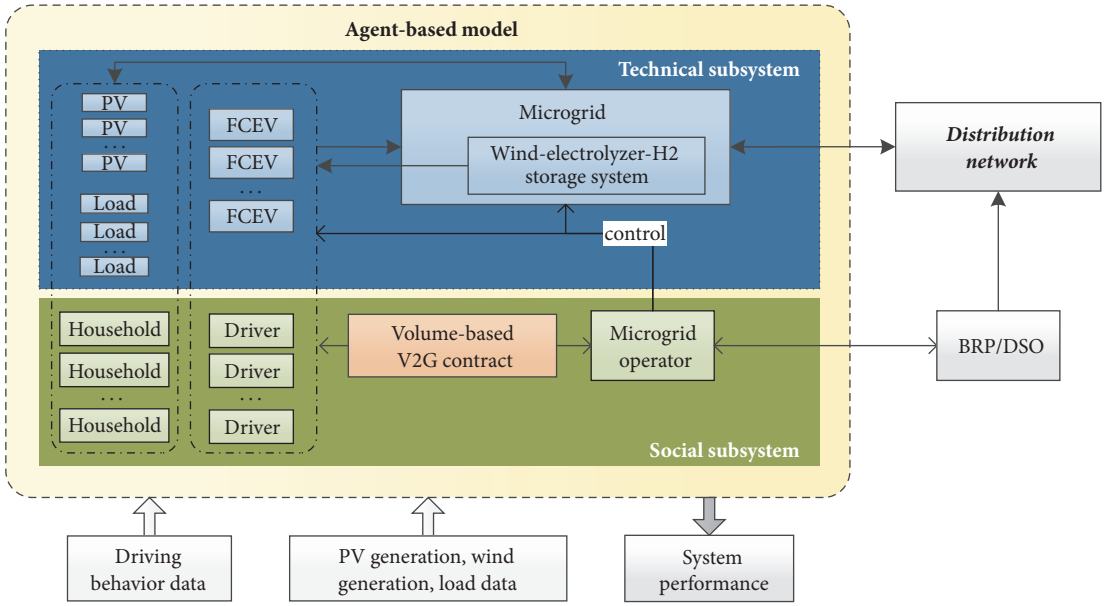

Figure 3: Agent-based model concepts: microgrid with fuel cell vehicles.

Table 6: Drivers and V2G contract initialization.

Variable	Value
Driver agents	
Number of drivers	50
Driving schedule	Using distribution derived from [41], weekdays and weekends
Parking profile	Home hours
Initial fuel level (kg)	Random from 3.0 to 5.65 (max)
V2G contract	
Time: start	Arrival time + random gamma distribution (shape = 3, scale = 0.5)
Time: duration	Random [50–100%] of parked hours
maxVolume	Random [30–90 kWh]

checks the balance in the microgrid: if additional power is needed, it operates available FCEVs, taking into account the limits set by the contract parameters; if there is a surplus from the PV panels and whenever the wind turbine is generating electricity the electrolyzer is used to produce hydrogen, which is stored in the neighborhood. If the microgrid is not capable of supplying enough power or when the electrolyzer capacity is exceeded, power is exchanged with the distribution grid.

Inputs for Simulation. We initialize the agents with the inputs indicated in Table 6. Since we want to represent the possible varying degrees of FCEV availability due to heterogeneous preferences, we randomly initialize the contract parameters within reasonable bounds. For the time interval (start, duration), we define the start by using a random gamma distribution to delay the plug-in time after arrival and choose a duration that ranges from 50 to 100% of the total daily parked time. The maximum volume committed is chosen randomly between 30 and 90 kWh (1.5–4.5 kg hydrogen). In practice, these parameters would be defined by the drivers based on their preferences. The actual distribution of contract parameters in a group of drivers could be very different than the one from this model. Data on driver preferences could be used as input in the V2G contracts of the model, instead of the random values. The model is simulated for 168 steps (one week) for the months of March, June, September, and December, as well as for 8760 steps (one year).

4.3.2. Results. The results in Table 7 show that in the one week periods in June and September the microgrid is self-sufficient and electricity is not imported. The volume of V2G provided on average every day by each car is also the lowest in those months: 13.25 and 17.9 kWh per day. In the weeks in March and December, there is more demand for V2G from FCEVs, but the microgrid still has to import electricity. On a yearly basis, the microgrid needs to import about 8% of the electricity consumption, and on average every car provides about 21 kWh per day. In the yearly simulation run, the average *maxVolume* is 28.36 kWh in weekdays and 29.72 kWh in weekends. This means that on average more volume was committed than actually used. This does not mean that drivers should commit lower volumes, because

Table 7: Results: system and driver performance.

RUN	System performance		Implication for drivers	
	Self-sufficiency %	Total imports (kWh)	Avg. daily plug-in hours/car	Avg. daily volume/car (kWh)
March	97.89%	186.74	7.2	24.79
June	100%	0.0	7.9	13.25
September	100%	0.0	7.5	17.9
December	83.03%	2,003.29	7.0	28.0
Year	92.31%	32,292.77	7.0	21.29

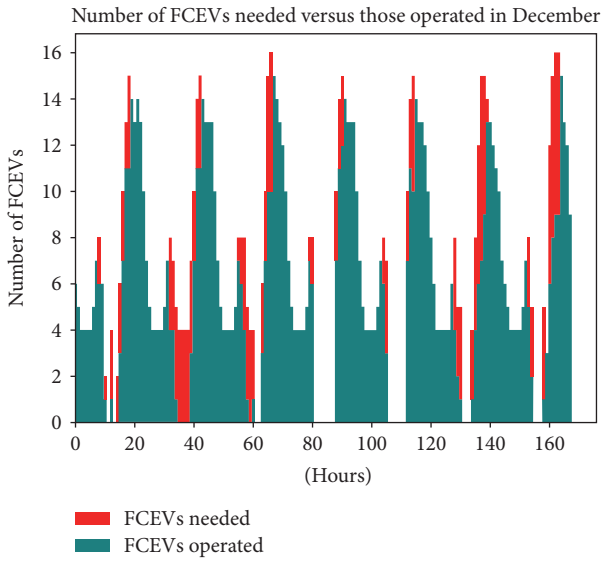

Figure 4: Number of FCEVs needed versus those operated every hour, in a week in December.

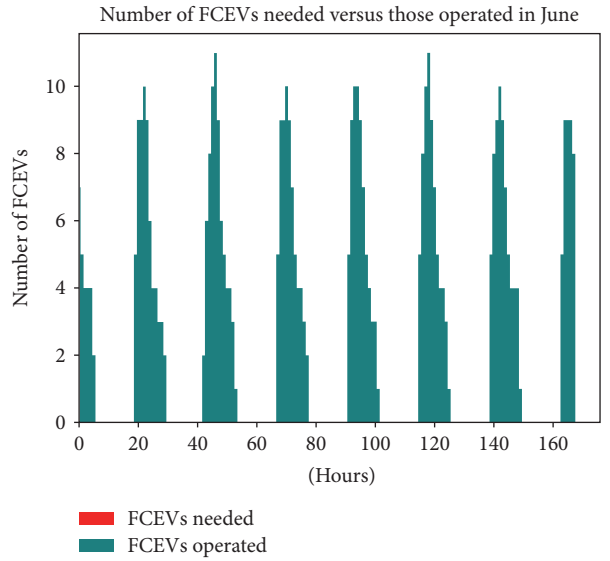

Figure 5: Number of FCEVs needed versus those operated every hour, in a week in June.

there are still moments in which power has to be imported after all available FCEVs are used. The times of demand for V2G also have to match the times when FCEVs are available.

There are two things that these results indicate. First, as the demand for V2G changes with the seasons due to the weather-dependent PV generation, the contract parameters could be adjusted to reduce the commitment from drivers in the summer months and increase it in the winter months. The difference between the average volumes in June versus September or December shows that there is opportunity to reduce contract parameters in summer. Second, with the same level of commitment, self-sufficiency in the system could be improved by adjusting the parameters to increase availability at times it is needed. As Figure 4 shows, there are certain hours where there is a shortage of vehicles (in red). When the potential moments of reduced availability are known, the operator can reward drivers for adjusting their time availability as well as the volume. As shown in Figure 5, in the summer months there is lower demand for FCEVs and there is no shortage. These results, although only illustrative, show that volume-based contracts can be used to allow drivers to participate in a more flexible way while taking into account the system performance.

Although not included in this paper, control-based contracts could also be used in this system. In our previous research, we provide a comparison between volume-based and control-based contracts in the same microgrid [46].

In the model, the contract parameters of every driver agent depend on their driving schedule, which is constant for weekdays and weekends. With the availability of data on drivers' preferences and day-to-day variability of driving behavior, this model could be used to answer different if-then questions.

5. Conclusions

In this paper we discussed the need to explore new types of contracts for the operational coordination of vehicle-to-grid. The current literature presents only one form of contract, but it may not be suitable for all markets and types of V2G supply, as it has been proven that in markets with different characteristics the value of certain parameters is more appropriate than others.

We introduced three different types of contracts, the first two of them being new in the V2G contract literature: price-based, volume-based, and control-based contracts. We also proposed a set of parameters in each contract, which

distinguishes them in terms of availability commitment and the activation criteria, as well as the type of remuneration. We defined these parameters specifically for FCEVs.

To illustrate the use of different contract types for the coordination of V2G, we developed two agent-based models. The V2G contracts were formalized in each model as the set of rules used by the aggregator to control the FCEVs. The models presented in this paper are exploratory, and therefore they can help us gain insights about the relationship between driver needs, contractual agreements, and system or aggregator goals and increase our knowledge on the role of contracts in the implementation of V2G.

In the first model we show how price-based contracts can be used in the participation of FCEVs in the day-ahead market. Using the minimum price in the contract and the market price forecast, aggregators place offers to sell V2G. We compared a scenario with homogeneous and heterogeneous minimum prices, and the results show that when all prices are the same the net profits are higher. When there are differences in the minimum price within a vehicle pool, the aggregator tends to offer V2G at higher prices. As a result, the average revenues per kWh are higher but the total profits are lower due to reduced sales. Some drivers lose the opportunity to sell due to the higher offering prices. The results show that the strategies of an aggregator in the market have to be explored in combination with the drivers' contract parameters, especially when drivers have different preferences.

In the second model we show how volume-based contracts can be used in a microgrid with renewable generation, storage, and FCEVs. We let the drivers choose the contract parameters and see that (1) demand for V2G varies across seasons and (2) the availability pattern does not match the demand pattern at all times, which is especially visible in months of solar generation shortage. This opens up possibilities to adjust contracts to increase participation when it is most critical and to reduce the commitment for drivers whenever V2G demand is relatively low, such as in the summer months. The results show that in such a system where the overall system performance (e.g., self-sufficiency) may be valued, contract parameters can be used to align the system goals and characteristics with the participation and availability of drivers.

In terms of implementation of V2G, the contract types presented in this paper can be used by aggregators to choose a market for V2G and then attract drivers with the characteristics that can be suitable for that market, and vice versa. Moreover, aggregators can use the structure of contracts to design incentives for the participation of drivers, for example, by rewarding availability, energy, or the commitment of time or volume. Although it was not the focus of this paper, the contracts presented here and the agent-based models could be used in the process of designing energy systems with vehicle-to-grid from a complex sociotechnical systems perspective.

Conflicts of Interest

The authors declare that they have no conflicts of interest regarding the publication of this paper.

Acknowledgments

This work is part of the "Car as Power Plant" project, supported by the Netherlands Organisation for Scientific Research (NWO) under the URSES program (Project no. 408-13-001).

Supplementary Materials

The supplementary material contains Appendix that includes more details on the models presented in Section 4, such as the process overview and the input data used. Model 1 is described under Appendix A and Model 2 under Appendix B. The references of data sources are also included. *(Supplementary Materials)*

References

[1] H. Holttinen, A. Tuohy, M. Milligan et al., "The Flexibility Workout: Managing Variable Resources and Assessing the Need for Power System Modification," *IEEE Power & Energy Magazine*, vol. 11, no. 6, pp. 53–62, 2013.

[2] W. Kempton and J. Tomić, "Vehicle-to-grid power fundamentals: calculating capacity and net revenue," *Journal of Power Sources*, vol. 144, no. 1, pp. 268–279, 2005.

[3] J. Tomić and W. Kempton, "Using fleets of electric-drive vehicles for grid support," *Journal of Power Sources*, vol. 168, no. 2, pp. 459–468, 2007.

[4] Z. Lukszo and E. H. Park Lee, "Demand Side and Dispatchable Power Plants with Electric Mobility," in *Smart Grids from a Global Perspective*, A. Beaulieu, J. de Wilde, and M. A. J. Scherpen, Eds., Bridging Old and New Energy Systems, pp. 163–177, Springer International Publishing, 2016.

[5] D. Lauinger, F. Vuille, and D. Kuhn, "A review of the state of research on vehicle-to- grid (V2G): Progress and barriers to deployment," in *Proceedings of European Battery, Hybrid and Fuel Cell Electric Vehicle Congress*, March, 2017.

[6] "Global EV Outlook 2016 Electric Vehicles Initiative," International Energy Agency, 2016, http://www.iea.org/.

[7] A. J. M. van Wijk and L. Verhoef, *Our Car as Power Plant*, 2014, http://www.iospress.nl/book/our-car-as-power-plant/.

[8] E. Sortomme and M. A. El-Sharkawi, "Optimal scheduling of vehicle-to-grid energy and ancillary services," *IEEE Transactions on Smart Grid*, vol. 3, no. 1, pp. 351–359, 2012.

[9] W. Kempton and J. Tomić, "Vehicle-to-grid power implementation: from stabilizing the grid to supporting large-scale renewable energy," *Journal of Power Sources*, vol. 144, no. 1, pp. 280–294, 2005.

[10] S. Vandael, T. Holvoet, G. Deconinck, S. Kamboj, and W. Kempton, "A comparison of two GIV mechanisms for providing ancillary services at the University of Delaware," in *Proceedings of IEEE International Conference on Smart Grid Communications, SmartGridComm*, pp. 211–216, Canada, 2013.

[11] S. Sarabi, A. Davigny, V. Courtecuisse, Y. Riffonneau, and B. Robyns, "Potential of vehicle-to-grid ancillary services considering the uncertainties in plug-in electric vehicle availability and service/localization limitations in distribution grids," *Applied Energy*, vol. 171, pp. 523–540, 2016.

[12] D. M. Hill, A. S. Agarwal, and F. Ayello, "Fleet operator risks for using fleets for V2G regulation," *Energy Policy*, vol. 41, pp. 221–231, 2012.

[13] G. M. Freeman, T. E. Drennen, and A. D. White, "Can parked cars and carbon taxes create a profit? The economics of vehicle-to-grid energy storage for peak reduction," *Energy Policy*, vol. 106, pp. 183–190, 2017.

[14] M. Shafie-Khah, M. P. Moghaddam, M. K. Sheikh-El-Eslami, and J. P. S. Catalão, "Optimised performance of a plug-in electric vehicle aggregator in energy and reserve markets," *Energy Conversion and Management*, vol. 97, article no. 7041, pp. 393–408, 2015.

[15] R. Gough, C. Dickerson, P. Rowley, and C. Walsh, "Vehicle-to-grid feasibility: A techno-economic analysis of EV-based energy storage," *Applied Energy*, vol. 192, pp. 12–23, 2017.

[16] R. Loisel, G. Pasaoglu, and C. Thiel, "Large-scale deployment of electric vehicles in Germany by 2030: An analysis of grid-to-vehicle and vehicle-to-grid concepts," *Energy Policy*, vol. 65, pp. 432–443, 2014.

[17] S. B. Peterson, J. F. Whitacre, and J. Apt, "The economics of using plug-in hybrid electric vehicle battery packs for grid storage," *Journal of Power Sources*, vol. 195, no. 8, pp. 2377–2384, 2010.

[18] W. Kempton, V. Udo, K. Huber et al., "A Test of Vehicle-to-Grid (V2G) for Energy Storage and Frequency Regulation in the PJM System," Tech. Rep., University of Delaware, November 2008.

[19] H. M. Khodr, N. El Halabi, and M. García-Gracia, "Intelligent renewable microgrid scheduling controlled by a virtual power producer: A laboratory experience," *Journal of Renewable Energy*, vol. 48, pp. 269–275, 2012.

[20] C. Battistelli, "Generalized microgrid-to-smart grid interface models for vehicle-to-grid," in *Proceedings of IEEE PES Innovative Smart Grid Technologies Conference (ISGT)*, pp. 1–6, USA, February 2013.

[21] J. Kissock, "Combined heat and power for buildings using fuel-cell cars," in *Proceedings of ASME Int. Solar Energy Conf.*, pp. 121–132, 1998.

[22] T. E. Lipman, J. L. Edwards, and D. M. Kammen, "Fuel cell system economics: comparing the costs of generating power with stationary and motor vehicle PEM fuel cell systems," *Energy Policy*, vol. 32, no. 1, pp. 101–125, 2004.

[23] E. H. P. Lee and Z. Lukszo, "Scheduling FCEVs as power plants in a community microgrid," in *Proceedings of IEEE PES Innovative Smart Grid Technologies Conference (ISGT)*, Slovenia, October 2016.

[24] K. Shinoda, E. P. Lee, M. Nakano, and Z. Lukszo, "Optimization model for a microgrid with fuel cell vehicles," in *Proceedings of IEEE Int. Conf. Networking, Sensing and Control (ICNSC)*, Mexico, April 2016.

[25] F. Alavi, E. Park Lee, N. van de Wouw, B. De Schutter, and Z. Lukszo, "Fuel cell cars in a microgrid for synergies between hydrogen and electricity networks," *Applied Energy*, vol. 192, pp. 296–304, 2017.

[26] V. Oldenbroek, L. A. Verhoef, and A. J. M. van Wijk, "Fuel cell electric vehicle as a power plant: Fully renewable integrated transport and energy system design and analysis for smart city areas," *International Journal of Hydrogen Energy*, vol. 42, no. 12, pp. 8166–8196, 2017.

[27] E. H. Park Lee, Z. Lukszo, and P. Herder, "Aggregated fuel cell vehicles in electricity markets with high wind penetration," in *Proceedings of IEEE International Conference of Networking, Sensing and Control (ICNSC)*, 2018, in Press.

[28] B. K. Sovacool and R. F. Hirsh, "Beyond batteries: an examination of the benefits and barriers to plug-in hybrid electric vehicles (PHEVs) and a vehicle-to-grid (V2G) transition," *Energy Policy*, vol. 37, no. 3, pp. 1095–1103, 2009.

[29] D. B. Richardson, "Encouraging vehicle-to-grid (V2G) participation through premium tariff rates," *Journal of Power Sources*, vol. 243, pp. 219–224, 2013.

[30] UDaily, *UD-developed V2G technology launches in Denmark*, 2016, http://www.udel.edu/udaily/2016/august/vehicle-to-grid-denmark/.

[31] N. Huijts, E. Molin, L. Steg, and A. C. Framework, "Understanding the Public Acceptance of Hydrogen Technologies in Transport," in *Proceedings of 11th International TRAIL Congress "Connecting people, Integrating expertise"*, pp. 1–4, 2010.

[32] C. Guille and G. Gross, "A conceptual framework for the vehicle-to-grid (V2G) implementation," *Energy Policy*, vol. 37, no. 11, pp. 4379–4390, 2009.

[33] G. R. Parsons, M. K. Hidrue, W. Kempton, and M. P. Gardner, "Willingness to pay for vehicle-to-grid (V2G) electric vehicles and their contract terms," *Energy Economics*, vol. 42, pp. 313–324, 2014.

[34] USEF Foundation, *Universal Smart Energy Framework (webpage)*, 2017, https://www.usef.energy.

[35] USEF Foundation, *USEF: The Framework Explained*, 2015, https://www.usef.energy/download-the-framework/.

[36] E. Sortomme and M. A. El-Sharkawi, "Optimal charging strategies for unidirectional vehicle-to-grid," *IEEE Transactions on Smart Grid*, vol. 2, no. 1, pp. 131–138, 2011.

[37] G. Broneske and D. Wozabal, "How Do Contract Parameters Influence the Economics of Vehicle-to-Grid?" *Manufacturing Service Operations Management*, vol. 19, no. 1, pp. 150–164, 2017.

[38] "Smart Energy Demand Coalition, Demand Response: Clarification of the standard processes required between BRPs and independent aggregators," Tech. Rep., July 2015, http://www.smarten.eu/wp-content/uploads/2015/07/SEDC-Standard-processes-required-between-BRPs-and-independent-aggregators1.pdf.

[39] E. Koliou, *Demand Response policies for the implementation of Smart Grids, Ph.D. thesis*, Delft University of Technology, 2016.

[40] X. He, N. Keyaerts, I. Azevedo, L. Meeus, L. Hancher, and J.-M. Glachant, "How to engage consumers in demand response: A contract perspective," *Utilities Policy*, vol. 27, pp. 108–122, 2013.

[41] Centraal Bureau voor de Statistiek (CBS) and Rijkswaterstaat (RWS), "Onderzoek Verplaatsingen in Nederland 2014 (Research on Movements in the Netherlands 2014) - Data Archiving and Networked Services, 2015" (Dutch), http://dx.doi.org/10.17026/dans-x95-5p7y.

[42] V. Grimm, U. Berger, F. Bastiansen et al., "A standard protocol for describing individual-based and agent-based models," *Ecological Modelling*, vol. 198, no. 1-2, pp. 115–126, 2006.

[43] J. Koppenjan and J. Groenewegen, "Institutional design for complex technological systems," *International Journal of Technology, Policy and Management*, vol. 5, no. 3, pp. 240–257, 2005.

[44] P. W. Bots, "Design in socio-technical system development: three angles in a common framework," *Journal of Design Research*, vol. 5, no. 3, p. 382, 2007.

[45] D. Scholten and R. Künneke, "Towards the comprehensive design of energy infrastructures," *Sustainability*, vol. 8, no. 12, article no. 1291, 2016.

[46] E. H. P. Lee, Z. Lukszo, and P. Herder, "Static volume-based and control-based contracts for coordinating vehicle-to-grid supply in a microgrid," in *Proceedings of the 2017 IEEE PES Innovative Smart Grid Technologies Conference Europe (ISGT-Europe)*, pp. 1–6, Torino, Italy, September 2017.

Hindawi
Complexity
Volume 2018, Article ID 3469325, 16 pages
https://doi.org/10.1155/2018/3469325

Research Article

Enabling the Analysis of Emergent Behavior in Future Electrical Distribution Systems Using Agent-Based Modeling and Simulation

Sonja Kolen, Stefan Dähling, Timo Isermann, and Antonello Monti

Institute for Automation of Complex Power Systems, E.ON Energy Research Center, RWTH Aachen University, Mathieustraße 10, 52074 Aachen, Germany

Correspondence should be addressed to Sonja Kolen; skolen@eonerc.rwth-aachen.de

Received 2 June 2017; Revised 6 December 2017; Accepted 22 January 2018; Published 21 February 2018

Academic Editor: Liz Varga

In future electrical distribution systems, component heterogeneity and their cyber-physical interactions through electrical lines and communication lead to emergent system behavior. As the distribution systems represent the largest part of an energy system with respect to the number of nodes and components, large-scale studies of their emergent behavior are vital for the development of decentralized control strategies. This paper presents and evaluates DistAIX, a novel agent-based modeling and simulation tool to conduct such studies. The major novelty is a parallelization of the entire model—including the power system, communication system, control, and all interactions—using processes instead of threads. Thereby, a distribution of the simulation to multiple computing nodes with a distributed memory architecture becomes possible. This makes DistAIX scalable and allows the inclusion of as many processing units in the simulation as desired. The scalability of DistAIX is demonstrated by simulations of large-scale scenarios. Additionally, the capability of observing emergent behavior is demonstrated for an exemplary distribution grid with a large number of interacting components.

1. Introduction

The integration of new technologies enabling the energy transition towards an efficient, environment-friendly, and overall sustainable energy system increases the complexity of distribution systems immensely. New technologies encompass renewable energy sources, storage systems, information and communication infrastructures, and new control approaches. The rise in system complexity is a result of the diversity of these technologies with respect to their individual characteristics, time-wise properties, and level of controllability of their behavior. Considering the growing complexity of the system and the different levels of interaction of components, it can be expected that its overall nature cannot be determined based on the behavior of individual components [1]. The state of the system will no longer be given by the states of the components, but results from their nonlinear cyber-physical interactions. The specific evolution, which is a result of interactions in the system and does not coincide with any of the components' behaviors, is called *emergent behavior* [2].

Emergent behavior is in contradiction with linear system behavior because a linear superposition of subsystems' behaviors results again in a linear system with full predictability and easy calculation. In emergent systems, nonlinear interactions between system components preempt linearization of the system behavior [2], making classical small-signal modeling impossible. To analyze the system behavior of future distribution systems at a meaningful scale prior to their implementation in the real world, a scalable modeling and simulation approach is required which is able to create the emergent system behavior based on nonlinear interactions of the system's components. The tool DistAIX (for DISTributed Agent-based sImulation of compleX power systems) presented in this paper includes the following contributions addressing this requirement:

(i) Components: a system component is modeled as an agent with respect to the component's electrical, communicative, and control behavior.

(ii) Emergent behavior: system behavior results from agents' cyber-physical interactions. Edges between agents model the infrastructures of the system that are used for interactions of components, that is, electrical lines and communication links.

(iii) Scalability: the agent-based model is parallelized using processes with respect to the electrical topology of the system under study. This allows a distributed simulation of the model on multiple computing nodes.

Agent-based modeling is used for the definition of components as autonomous elements of a multiagent system. Other approaches such as metaheuristics have been previously used for analysis and optimization problems in complex energy systems [3]. This approach is not considered here because we do not target a search for the solution of an optimization problem, but the observability of a system behavior that emerges from components' interactions. Agent-based modeling has been proven to be a powerful method for modeling emergent behaviors of complex systems [4, 5]. Specialized simulation tools for agent-based modeling in general [6] and power system modeling and simulation in particular [7] have been proposed in the literature. For example, the tool GridLAB-D is capable of coupling the modeling of the domains power, thermal, control algorithms, and market in an agent-based modeling approach.

DistAIX is not the attempt of a GridLAB-D duplicate, but it aims specifically at improving scalability of agent-based modeling and simulation for distribution systems. GridLAB-D uses a power-flow module with an algebraic solver for the computation of currents and voltages of the system [7]. This limits its scalability to the one of the algebraic power-flow module. A parallelization using POSIX threads has been proposed for GridLAB-D [8]. Parallelization with threads instead of processes limits the number of usable computing nodes to one due to general memory locality restrictions of threads [9].

DistAIX parallelizes the computation of the agent-based model with processes and makes use of multiple distributed computing nodes, for example, as available in computing centers. The memory can be spread over multiple computing nodes as each process has its own memory address space. By using distributed memory and computing architectures, the simulation of large, for example, nation-sized, energy systems is possible [10]. We propose and combine methods that address the arising challenges for distribution system simulation, such as distributed power-flow computation and message handling.

For a combined modeling and simulation of power system, communication system, and control, several cosimulation platforms have been proposed in the literature [11–16] coupling different tools for distribution system, transmission system, communication, or market simulations. In addition to the stand-alone usage, DistAIX also extends the pool of modeling and simulation tools that can be cosimulated with others. A co-simulation of multiple large-scale distribution systems with DistAIX coupled with the simulation of a transmission system using a different tool is a possible use case. For example, the platform GridSpice [14] could be used as scaling interface if a respective interface is added to DistAIX. As we focus on the presentation and analysis of DistAIX, cosimulation with other tools is not considered here and left for further research.

Models of the components' behaviors are required to embed the possibility that emergent behavior, that is, nonlinearity, plays a critical role in the final solution. These models can either be derived from literature or be found experimentally. Especially for the control behavior, DistAIX can serve as a testing environment during development of a future control strategy. New component behavior models can be developed using DistAIX. Despite the individual behaviors of the components, the determination of their electrical as well as communication interactions is vital for an analysis of emergent behavior. Efforts have been made for the identification and formalization of the calculation of interactions on electrical level [17]. Combining electrical with communication interactions and cyber-physical interactions in one scalable modeling and simulation tool is one of the contributions of this work.

Unlike traditional energy system simulation tools, for which [18] provides an overview, DistAIX does not target a system level solution. A fully decentralized implementation of the iterative forward-backward sweep method [19] is used for the determination of voltages and currents at all nodes. For this method, only the local neighbors in the electrical grid need to be known to each node and component [19]. No system level solver for the power-flow calculation is required which eases the distribution of the model to multiple processes. Communication links are modeled based on individual properties such as latencies. Messages are exchanged between components along these links and are routed from one process to another where and when necessary. Thereby, all interactions of components can be calculated by distributed computing resources.

We believe that a simulative study of new control strategies for future distribution systems at large-scale is an essential part on the way towards realization. Distribution systems are the largest part of the electrical supply system with respect to the number of electrical nodes and components. In our opinion, a resilient analysis of emergent behavior of distribution systems requires a model that includes all components and their behaviors. For that reason, modeling and simulation for such systems need to be scalable. We present a simulation tool that finds a useful parallelization of an agent-based model for a given set of computing resources and distributes the computation to these resources. DistAIX is designed to keep the computation time for large-scale simulations of emergent system behavior manageable while at the same time enabling a highly flexible modeling of individual component behaviors in agents.

The paper is organized as follows: Section 2 introduces the challenges and related research in the field of scalable agent-based modeling and simulation of energy systems. In Section 3, DistAIX is presented in detail while Section 4

defines the evaluation methodology. Section 5 discusses the results and Section 6 concludes this work.

2. Scalable Agent-Based Modeling and Simulation of Energy Systems

Modeling and simulation of complex agent-based energy systems face the following challenges when the size of the system under study and/or the number of available computing nodes grows:

(1) Computation of power-flow

(2) Interagent data flow

(3) Result data acquisition.

A scalable modeling and simulation tool needs to address the aforementioned challenges. An outline on solutions found in the literature and how DistAIX makes use of them is discussed in the following subsections.

2.1. Computation of Power-Flow. For the execution of a distribution system model on distributed computation resources it is essential that methods working without a centralized point of knowledge on all system variables are chosen. This is especially important for the calculation of voltages and currents in the system under study. Hence, a decentralized power-flow calculation is needed, which can be formulated in the intended way. This topic has been extensively investigated in recent years, resulting in several decentralized power-flow formulations.

In [20, 21] the grid is divided into a set of subgrids. Two neighboring subgrids share common buses, the so-called boundary buses. For each subgrid, the power-flow is solved independently and the injected power from all neighboring subgrids is calculated subsequently considering the voltage mismatch of boundary buses. This process is repeated iteratively until the power-flow solutions of all subgrids converge. While the overall solution is found in a decentralized way, the power-flow computation within one subgrid is carried out centrally using algorithms such as Newton-Raphson.

Other approaches aim at solving the Gauss-Seidel algorithm in a decentralized way [22]. Each node calculates its voltage using the previously calculated voltage of all neighboring nodes. The new voltage value is passed to the next node which then also updates its own voltage. In this approach the calculation is performed on node level. However, the convergence of Gauss-Seidel can be considered comparatively slow. In [23] an accelerated Gauss-Seidel implementation using FPGAs is presented. Their approach is not compatible with the requirement for a decentralized power-flow calculation as mentioned above.

Another algorithm that can be used for decentralized power-flow calculation of radial power grids is the so-called forward-backward sweep method. It has been used for agent-based smart grid simulation [24, 25] and consists of three iteratively repeated steps [19]:

(1) Calculation of nodal currents: at each node, the current injections into all components connected to a node are calculated for a given nodal voltage. In the first iteration, all nodal voltages are initialized with the rated voltage. The nodal currents are obtained by summing up all component currents of a node.

(2) Backward sweep: starting at the last node of each feeder, the current flows through all branches are calculated by applying Kirchhoff's current law at the nodes.

(3) Forward sweep: starting at the slack node, all node voltages are updated based on the branch impedances and the previously calculated branch currents.

Note that there are also other formulations of the forward-backward sweep method which calculate power-flows instead of current flows in the backward sweep [26]. Forward-backward sweep provides considerable advantages for an agent-based simulation. The most important ones are as follows:

(i) The calculation is performed on node level and is therefore highly decentralized. The electrical system behavior emerges from the electrical interactions of agents.

(ii) The algorithm makes use of the radial structure of distribution grids. As a result, the processing of forward and backward sweep in each feeder can be computed in parallel.

(iii) The electrical behavior of grid components is calculated independently for each component in the first step. Hence, this step can be parallelized.

(iv) Sufficient convergence has been shown for this algorithm [27].

For DistAIX, we choose the forward-backward sweep technique presented in [19] as the given advantages ensure the required scalability feature and allow a system analysis based on the behavior and interactions of single components. Since the algorithm makes use of the structure of a distribution grid it is not able to deal with meshed grids. Extensions described in literature solve this problem for weakly meshed grids [19] such as electrical distribution systems.

2.2. Interagent Data Flow. The separation of a distribution system model into subparts for distributed computation demands an interagent data flow organization that handles the distributed memory architecture in a scalable way. Interagent data flow means the cyber-physical interactions of agents which can take place within a model subpart and between different model subparts. Two approaches addressing this challenge have been identified in existing agent-based modeling and simulation frameworks [28]:

(i) Message boards: Flame [29]

(ii) Agent copy and update: RepastHPC [30].

Both frameworks use the Message Passing Interface (MPI) to parallelize the simulation on multiple computing nodes. Flame uses a message board in each process for the realization

of agent interactions. Agents use the message board in their process to exchange data with other agents and messages are broadcast via MPI either to all or to a set of other agents.

The agent copy and update approach of RepastHPC is illustrated in Figure 1 for a small example with two processes and two agents. The methodology is introduced in [30]. Agent A in process 1 requires data of agent B that belongs to process 2 and vice versa. The required data can be voltage and currents, for example. In RepastHPC, process 1 creates a copy of agent B in its own memory space. Process 2 does the same for agent A. If agent A in process 1 needs to access data of agent B, it reads from the copy in process 1 and not from the original agent. Agent-networks between original and copy agents within the same process (red arrows in Figure 1) are called SharedNetworks in RepastHPC and are maintained in their own data structure. Copies are only created for agent links that go across processes, that is, across subparts of the model. Whenever required, the copies can be updated with the state of the original agents by calling an MPI-based synchronization method of RepastHPC (blue arrows in Figure 1). In contrast to Flame, this method does not use broadcast but asynchronous message sending and receiving via MPI. In the example, the copy of agent B in process 1 is updated with the state of the original agent B and the copy of agent A is updated with the state of the original agent A. The state of the agent copy is never transferred back to the original agent. Thereby, frequent interprocess communication is avoided and the programmer has full control on the points in time when copy updates are necessary.

As has been shown in [28], RepastHPC's scalability outperforms the one of Flame because of this difference in the realization of agent interactions. Also, the memory consumption of RepastHPC stays constant for increasing number of processes used in the simulation while Flame's memory consumption increases [28]. Due to these benefits, RepastHPC is used for the implementation of DistAIX. Two agent network structures (SharedNetworks) are used in each process to organize physical and cyber interactions of agents. For more details on the implementation refer to Section 3.5.

2.3. Result Data Acquisition. Storing of simulation time dependent and independent data should put only minimal stress on the computation resources while at the same time the analysis of result data and postprocessing have to be flexible and convenient. The following two problems need to be solved in an efficient way by a data acquisition solution:

(i) Store huge amounts of data per simulation time step.

(ii) Read specific result data for postprocessing and analysis.

Connecting the simulation to a database system is one possible solution; for example, GridLAB-D offers an interface to a MySQL database [31]. Relational databases such as MySQL and PostgreSQL are useful for storing simulation time independent data, that is, the metadata of the agents and the model. However, they have problems in processing large amounts of data at once in either direction, writing to or reading from the database. Benchmarks have shown that NoSQL databases have a better performance when it comes to fast storing of large amounts of data [32, 33]. For these reasons, DistAIX is interfaced with both a PostgreSQL database for meta information and a NoSQL database cluster based on Cassandra for storing simulation time dependent data in a scalable database system.

With respect to the huge amounts of data that need to be acquired by the database system, serialization of data seems to be a good option. Protocol Buffers [34] have proven to be an efficient method for data serialization and deserialization in other fields of application [35, 36] and are therefore explored here for the decrease of time to write data to the Cassandra database.

3. Modeling and Simulation with DistAIX

DistAIX is presented in this section. Section 3.1 discusses how RepastHPC is used for the parallelization of a simulation and Section 3.2 discusses the distribution of agents to processes. In Section 3.3 we comment on the time step whereas details on the modeling of agent behaviors and all agent types are provided in Section 3.4. Section 3.5 focuses on agent interactions and discusses the computation of communication as well as electrical interactions. Finally, the setup of a simulation is addressed in Section 3.6.

3.1. Parallelization with RepastHPC. RepastHPC uses MPI to parallel a simulation on a high performance computing (HPC) system. A simulation is launched via `mpiexec` with options specifying the hosts to use and the number of processes to start. Each process executes one part of the agent-based distribution system model. In DistAIX, this is reflected by a C++ class `Model` which defines how each process is configured, for which agents it is responsible, and which connections exist among agents in this process and to agents in other processes. The `Model` class also defines the schedule of a process and data that need to be synchronized with other processes.

Figure 2 shows the schedule of a process. The first step is the initialization and encompasses the creation of all agents of the process and all electrical connections between agents in this process. Further, the electrical connections to agents in other processes are established by the creation of copies of these agents in the process. If these copies were not created, electrical connections between agents belonging to different processes would be missing in the simulated model. This would lead to wrong simulation results. The model is kept synchronous and consistent by updating copies with the state of the original agent according to the copy update method explained in Section 2.2. Agent copies are updated between each step of the process schedule (white boxes in Figure 2) and also during the forward-backward sweep step to reach convergence.

After the initialization, a process executes simulation steps for a given simulation step size (loop in Figure 2). The agent messages and individual control behaviors are processed in step 2. This part of the simulation considers

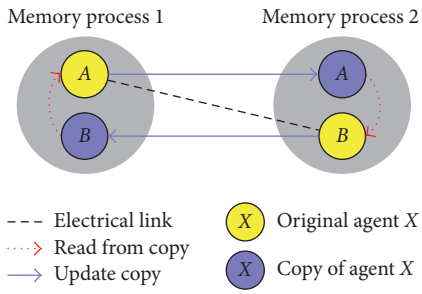

Figure 1: RepastHPC's agent copy and update synchronization.

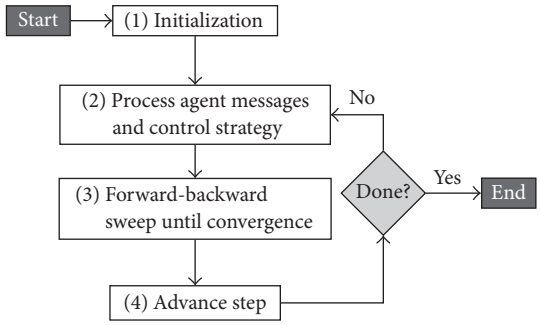

Figure 2: Schedule of each process as defined in `Model` C++ class.

the communication network infrastructure (how communication links are modeled is explained in Section 3.5) as well as the control strategy under study. At the beginning of step 2, agent messages have to be synchronized between processes. After that, a process executes the behaviors of all of its agents independently for each agent. Step 3 of a process is the calculation of current and voltage at each node using the iterative forward-backward sweep method until convergence.

The calculation of the forward-backward sweep algorithm is parallelized according to its three phases as explained in Section 2.1. Similar to the message processing, the calculation of nodal currents is done independently of other agents. The algorithm iterates backward and forward through the grid topology in sweeps. During a sweep, only one node per feeder can be active. After a sweep is completed, an agent copy update is required to synchronize newly computed values of currents and voltages at electrical agent connections spanning over two processes. The three phases of the forward-backward sweep algorithm are repeated until convergence is reached. Step 4 of a process is composed of preparing the next simulation time step, that is, saving results of this step and resetting internal state variables used during forward-backward sweep iterations. This final step is done independently for each agent.

3.2. Distribution of Agents to Processes. Agents need to be distributed to processes in such a way that processes wait for others the least amount of time. The topology of the electrical grid influences a good distribution of agents as only one agent per feeder can be active in the forward-backward sweeping at once. It can be expected that the number of processes beneficial for the parallelization depends on the electrical topology of the system and is therefore limited.

We adapt a node scheduling method [37] to work with contiguous sequences of successive nonbifurcating nodes of the electrical grid, called *workitems* in the following. Workitems are the parts of the grid in which only one node can be active in forward-backward sweeping at once. The electrical topology of the grid under study is analyzed at the start of a simulation. Workitems are determined by parsing the graph topology of the grid under study with a depth-first-search algorithm. The distribution of node agents to processes works in the following steps:

(1) Leaf node agents and their depth in the topology are determined.

(2) If the number of processes available is m, the m deepest leaf node agents are selected (or less if there are less than m leaf nodes in the topology).

(3) The m workitems in which the selected m leaf node agents are included are assigned to one of the m processes so that all m processes are responsible for the nodes contained in one workitem. If $n < m$ leaf node agents were selected in the previous step, the number of workitems and processes in this step is only n.

(4) From now on only the topology of the remaining nodes agents which are not yet assigned to a process is considered. Continue with step 1 if there are still nodes agents to be assigned to a process. Otherwise, all node agents are distributed to processes.

Transformer agents and slack agent are both treated as node agents regarding their distribution to processes. Component agents (load, electric vehicle (EV), photovoltaic (PV), combined heat and power (CHP), wind energy converter (WEC), battery, and compensator) are always created in the process where the node agent they are connected to is located. Note that this procedure does not guarantee the usage of all available processes. The topology of the electrical grid influences the number of processes in use. This is user-friendly as only the maximal available number of processes needs to be known, but not the optimal number with respect to the system under study. If more processes are available than useful, the dispensable processes are idle during the simulation and do not impede the calculations.

3.3. Simulation Time Step. The size of a simulation time step is fixed for one simulation. The main reason for this is that the occurrence of communication events cannot be predetermined due to emergence in the system. A variable time step would increase the chance to miss time steps in which communication occurs. Another aspect to bear in mind is the distributed simulation approach itself. As the time step has to be the same in all processes, additional synchronization would be necessary for the determination of the time step size and the spreading of this information to all processes. The overhead caused by the required synchronization could possibly outweigh the performance improvements of a flexible time step.

However, the number of calculations per time step on agent level can be reduced. For example, the recalculation of nodal currents in step 1 of the forward-backward sweep algorithm can be managed in an event-driven way so that a recalculation is done only when an event has occurred in the signal of the nodal voltage. This can be an attempt to reduce the computational effort for component agents in the future. However, for a first demonstration of DistAIX we have not implemented such a method yet.

3.4. Agent Behaviors. To draw conclusions on emergent behavior of the system, the agent models used in DistAIX are discussed in this section. Equations for the electrical agent models are provided to show their role in the forward-backward sweep iterations. Each agent represents a component of the distribution system and consists of an electrical model, behavior rules for the control, a state and knowledge, and communication capabilities. Figure 3 provides an overview about the interconnection of these parts within the agent model.

The electrical model of an agent and its communication capabilities influence the state of the agent and its knowledge about other components in the system. The control algorithm of an agent is defined by its behavior rules operating based on the current state and knowledge. Behavior rules result in both control signals influencing the electrical model (right side in Figure 3) and triggers for information exchange using the communication capabilities (left side in Figure 3). An agent can be connected to other agents in no more than two ways: via communication and/or electrical network. Detailed descriptions of the electrical steady state models are provided in the following subsections. In the equations below, variables indexed with "ctrl" indicate that this value is a control signal determined by the control behavior rules of an agent.

3.4.1. Slack Agent. In the forward sweep, the nodal voltage of the slack is calculated to be

$$v_{\text{node}} = \frac{V_n}{\sqrt{3}} \cos\left(\vartheta_{\text{slack}}\right) + j \frac{V_n}{\sqrt{3}} \sin\left(\vartheta_{\text{slack}}\right). \tag{1}$$

V_n is the nominal voltage and ϑ_{slack} is the defined voltage angle at the slack node, usually set to zero. In the backward sweep, the output current of the slack node flowing to the next node is

$$i_{\text{out}} = \sum_{n \in N} i_{\text{in},n} + i_{\text{leak},n}, \tag{2}$$

where N is the set of all next nodes, $i_{\text{in},n}$ is the incoming current of node n, and $i_{\text{leak},n}$ is the leakage current of the line connecting the slack node and node n.

3.4.2. Node Agent. In the forward sweep, the nodal voltage is obtained by

$$\begin{aligned} v_{\text{node}} = {} & v_p - i_{\text{out},p}\left(R_l + jX_l\right) \\ & + v_p \frac{\left(G_l + jB_l\right)\left(R_l + jX_1\right)}{2}, \end{aligned} \tag{3}$$

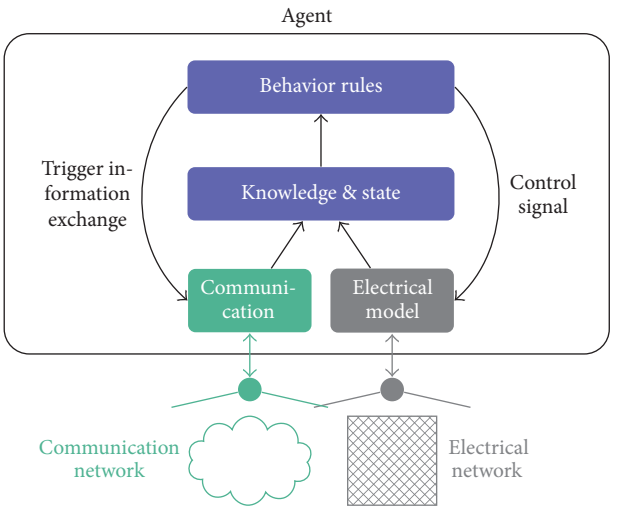

Figure 3: Model of a component agent and its connections to electrical and communication networks.

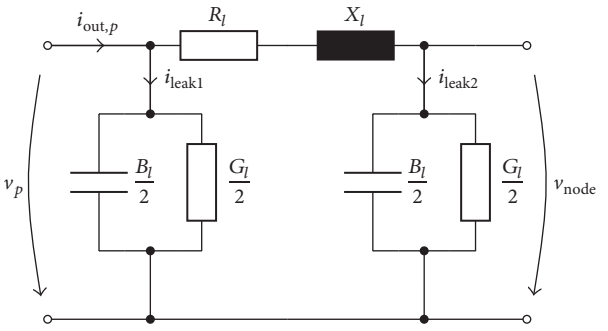

Figure 4: Single-phase reference circuit of a power line.

where v_p is the nodal voltage of the previous node, $i_{\text{out},p}$ is the output current of the previous node, R_l, X_l, G_l, B_l are parameters of the connecting PI-line (see Figure 4). In the backward sweep, the output current from the previous node is

$$i_{\text{out},p} = i_{\text{out}} + i_{\text{leak}} + \sum_{c \in C} i_c, \tag{4}$$

where i_{out} is the output current of the investigated node, i_{leak} is the leakage current of the line connecting this and the previous node, C is the set of all components connected to the node, and i_c is the component current.

3.4.3. Transformer Agent. The transformer model is composed of an RX-line and an ideal transformer as depicted in Figure 5. In the forward sweep, the secondary node voltage is obtained by

$$v_{\text{node}} = \frac{v_{\text{in}} - i_{\text{out},p}\left(R_t + jX_t\right)}{u}, \tag{5}$$

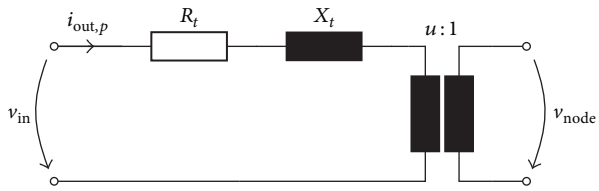

Figure 5: Single-phase reference circuit of a transformer.

with the input current from the previous node $i_{\text{out},p}$, the input voltage at the primary node

$$v_{\text{in}} = v_p - i_{\text{out},p}\left(R_l + jX_l\right) + v_p \frac{\left(G_l + jB_l\right)\left(R_l + jX_l\right)}{2}, \quad (6)$$

the transformer parameters R_t and X_t, and the turns ratio u. R_l, X_l, G_l, and B_l are parameters of the PI-line connecting the transformer with the previous node. In the backward sweep, the output current from the previous node is

$$i_{\text{out},p} = \frac{i_{\text{out}}}{u} + i_{\text{leak}}, \quad (7)$$

where i_{out} is the sum of all currents flowing to the next nodes and i_{leak} is the leakage current of the line between this and the previous node.

In DistAIX we use transformers with an On Load Tap Changer (OLTC) capability. Therefore, the turns ratio can be adjusted within a symmetrical range r around the nominal value u_{nom}. This is done in discrete steps N_{ctrl} where

$$-N \leq N_{\text{ctrl}} \leq N \quad (8)$$

has to be satisfied and N is the number of possible steps. The turns ratio is then calculated as

$$u = u_{\text{nom}} \cdot \left(1 + N_{\text{ctrl}} \frac{r}{N}\right). \quad (9)$$

3.4.4. Load Agent. The load model has an integrated profile providing the active and reactive power demand for each step. The component current is then calculated to

$$i_c = \frac{P + jQ}{3v_{\text{node}}}. \quad (10)$$

3.4.5. Electric Vehicle Agent. An EV is represented by a battery with a capacity C_{el} that is periodically connected to the grid. The connection status is provided by a profile. If the EV is not connected to the grid, it has a certain power consumption P_{con} which is also stored in a profile and leads to a discharge of the EV's battery. For times of disconnection the model output is

$$i_c = 0, \quad (11)$$

with state of charge (SOC) of the battery being

$$\text{SOC} = \text{SOC}_{\text{old}} - \frac{P_{\text{con}} \cdot t_{\text{step}}}{C_{\text{el}}}. \quad (12)$$

If the EV is connected, the battery can be charged with an adjustable active power. Moreover, the EV is able to provide a certain amount of reactive power as it is connected to the grid via a converter. With the control values for active and reactive power P_{ctrl} and Q_{ctrl} the component current is

$$i_c = \frac{P_{\text{ctrl}} + jQ_{\text{ctrl}}}{3v_{\text{node}}}, \quad (13)$$

and the SOC is

$$\text{SOC} = \text{SOC}_{\text{old}} + \frac{P_{\text{ctrl}} \cdot t_{\text{step}}}{C_{\text{el}}}. \quad (14)$$

The EV agent ensures that the component's hardware limitations such as converter capabilities as well as the battery capacity are not violated. Location variability of EV is not considered here as it does not influence the applicability of DistAIX but only the control strategy under study.

3.4.6. Photovoltaic Agent. The model of a PV system is based on a performance prediction model [38] calculating the amount of active power P_{max} that can be generated. It requires the solar irradiance and the temperature as input data. Similar to an EV, PV systems are connected via a converter and can therefore provide reactive power. Furthermore, the active power supply can be curtailed if necessary. This leads to the equation for the component current (see (13)) where the control value for reactive power has to be within the limits of the converter and the control value for active power has to satisfy

$$-P_{\text{max}} \leq P_{\text{ctrl}} \leq 0. \quad (15)$$

Note that P_{ctrl} is negative since active power is produced and not consumed.

3.4.7. Wind Energy Converter Agent. The WEC model makes use of a polynomial relation between wind speed and output power [39]. Hence, the model uses a wind speed profile as input data. Power generation starts when the minimum speed v_s is reached. Up to the rated speed v_r, generation continues following a polynomial relation. Maximum generation P_r is present until the cut off speed v_c is reached. This relation is illustrated by the following equations:

$$\begin{aligned} &P_{\text{max}}(v) = 0, \quad v < v_s, \\ &P_{\text{max}}(v) = a \cdot v^3 + b \cdot v^2 + c \cdot v + d, \quad v_s \leq v \leq v_r, \\ &P_{\text{max}}(v) = P_r, \quad v_r \leq v \leq v_c, \\ &P_{\text{max}}(v) = 0, \quad v > v_c. \end{aligned} \quad (16)$$

Between speeds v_s and v_r, the relationship between wind speed and maximum output power is described by a third-order polynomial with coefficients a, b, c, and d which are found so that a continuous curve is obtained. Similar to the PV and EV, the WEC is connected to a converter, which leads to similar constraints and enables the control of active power P_{ctrl} and reactive power Q_{ctrl}, as shown in (13), while respecting the limits of the generation unit (see (15)).

3.4.8. Combined Heat and Power Agent. The CHP model consists of three main components: combustion engine, synchronous generator, and heat exchanger. In a CHP, mechanical power supplied by a combustion engine is converted to electrical power by a generator. The occurring heat can be used directly for building heating or stored for later use in a thermal storage. Thus, the total fuel input power P_c is composed of the thermal output power Q_{th}, the electrical output power P_{el}, and losses P_{loss}:

$$P_c = Q_{\text{th}} + P_{\text{el}} + P_{\text{loss}}. \tag{17}$$

Thermal and electrical output power are determined considering a thermal and electrical efficiency η_{th} and η_{el}, respectively. With the control value for electrical active power P_{ctrl}, the required fuel input power is

$$P_{\text{c}} = \frac{P_{\text{ctrl}}}{\eta_{\text{el}}}, \tag{18}$$

resulting in the thermal output power

$$Q_{\text{th}} = \eta_{\text{th}} P_c = P_{\text{ctrl}} \frac{\eta_{\text{th}}}{\eta_{\text{el}}}. \tag{19}$$

Moreover, the CHP can produce reactive power, as the power factor of the synchronous machine can be affected by controlling its excitation within the limits of the machine.

To simulate the CHP, a profile is required providing the thermal power demand Q_{dem} for building heating at each time step. The agent considers Q_{dem} and the currently stored thermal energy E_{th} and controls P_{ctrl} and Q_{ctrl} of the CHP model which returns the actual i_c to the simulation analogously to (13). The SOC of the thermal storage with capacity C_{th} is updated accordingly to

$$\text{SOC} = \text{SOC}_{\text{old}} + \frac{(Q_{\text{th}} - Q_{\text{dem}})\, t_{\text{step}}}{C_{\text{th}}}, \tag{20}$$

for the next time step. One constraint of the operation of the CHP agent is the satisfaction of limits of the thermal storage.

3.4.9. Battery Agent. Similar to the EV agent, the battery agent controls a battery system. Its battery can be charged/discharged with an adjustable active power and is connected to the grid via a converter. This enables the control of P_{ctrl} and Q_{ctrl} (see (13)). With respect to the loads of nearby consumers, the battery agent releases power to or stores power from the grid when necessary. Meanwhile, it ensures that the battery's operation boundaries will not be exceeded in terms of (14).

3.4.10. Compensator Agent. The compensator can provide capacitive reactive power to the grid to neutralize inductive reactive power caused by most loads. Reduction of grid losses is the main reason for the utilization of a compensator. To counter losses, the compensator is operated through N stages of switchable shunt capacitors with a nominal susceptance of B_{nom}. The agent controls the step size N_{ctrl} of the shunt banks resulting in the grid connected susceptance

$$B = B_{\text{nom}} \frac{N_{\text{ctrl}}}{N}. \tag{21}$$

The output current i_c is calculated as follows:

$$i_c = jBv_{\text{node}}. \tag{22}$$

3.5. Agent Interactions. As interactions play a major role in emergent systems, they have to be modeled accurately. RepastHPC's SharedNetwork structure is used to model the electrical network, where the agents are the nodes and components in the network and cable models represent the edges between them. A cable model includes an equation system and parameters of a cable (see PI-line in Figure 4). Each process stores the excerpt of the electrical network involving its own agents and boundary agents to other processes in a SharedNetwork object. This object is a part of the `Model` class introduced in Section 3.1. The electrical interactions are calculated based on the forward-backward sweep method as explained in Section 2.1 and the SharedNetwork objects in the processes.

A generic modeling of communication interactions and communication edges requires a different approach. Assuming that a control strategy may require flexible communication connections, communication between all agents in all processes has to be possible. As the system under study is emergent, it may be unknown in advance which communication links will be used, that is, which agents communicate with each other. If a SharedNetwork was used for the modeling of communication links similar to electrical edges, copies of all agents in all processes would have to be synchronized. Hence, the SharedNetwork is not a scalable method for explicit modeling of communication edges, especially when only a small subset of all available communication links is used.

For this reason, one message router is introduced in each process (Figure 6). A message router does not represent a hardware component of the distribution system but is a method to implement the simulation of communication between agents. In step 2 of a process schedule (see Figure 2), the task of the message router is the collection of messages to be sent from all agents in their process (orange in Figure 6). For each message to be sent, the message router checks the model of the communication link used by the message transfer, for example, the latency or packet error rate of the link. In case no specific communication link properties are available, the user can define default values for all links. The message router applies the communication link model to determine whether or not a message has to be transmitted in the current simulation time step. If the latency of a link requires delaying a message, it will stay in a pending queue of the message router and will be checked again in the next simulation time step. If a message has to be transmitted to the target agent, two cases have to be distinguished:

(1) If the target of a message is an agent in the process of the message router, it will route the message to the inbox of this agent.

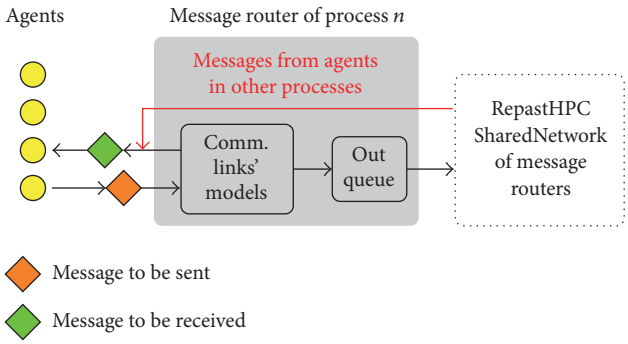

Figure 6: Modeling of communication infrastructure with message routers in process n.

(2) If the target of a message is an agent in a different process, the message is added to the out queue of the message router.

Each process has a RepastHPC SharedNetwork in which its own message router is connected to the message routers of all other processes. Once all messages to be transmitted are treated according to cases 1 or 2, the out queues of all message routers are synchronized between all processes via the SharedNetwork of message routers. Afterwards, each process has an up-to-date copy of the out queue of each message router. Each message router checks the others' out queues for messages that target an agent in its process and routes messages accordingly (red arrow in Figure 6). This way of communication interaction modeling allows an individual modeling of communication links and an efficient routing of agent messages in the distributed simulation.

3.6. Simulation Setup. Figure 7 shows the setup of a simulation with DistAIX. The simulation time step size and the number of time steps to simulate can be freely chosen. However, they should be selected in a meaningful way for the scenario and component models under study regarding the desired resolution of electrical dynamics and message exchange. Time series are used as input data for component agents that require profile information. If a time step smaller than the time step of the profile data is chosen, the profiles can be either linearly interpolated using the respective functionality of the GNU Scientific Library or the last value of the profile is held until the next value of the profile is reached by the simulation time. The user may choose between these options when configuring a simulation.

The simulation scenario is configured by lists of the nodes and components to be simulated and the electrical lines. Furthermore, the properties of communication links (e. g., package drop rates, latency) can be added as input for the simulation if these parameters are relevant for the scenario under study. It would also be possible to extend the interfaces of the simulator so that scenarios available in a Common Information Model (CIM) representation can be used as input for the simulation tool. A method for the automated transformation of CIM representations of distribution systems to C++ classes has already been presented

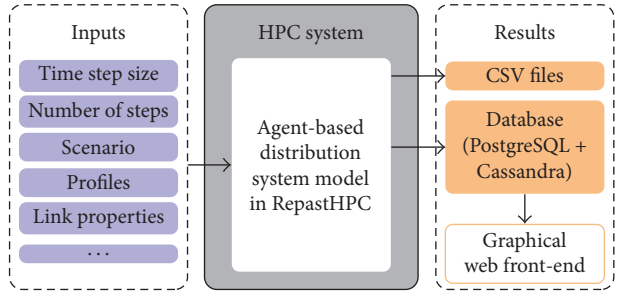

Figure 7: Simulation setup of DistAIX with inputs and results.

by our research group in [40]. For an initial demonstration of DistAIX, we choose a less complex method of scenario reading.

The user can choose between a simulation result output in a PostgreSQL and Cassandra database system, comma separated value (CSV) files, or both. Simulation results in CSV test simulations have proven to be useful during development of DistAIX due to their simplicity. Database output is integrated into the simulator because it allows a structured and efficient storage of large amounts of simulation data. It also enables a resource saving of the computing resources as database queries can be sent to the databases via a computer network and do not need to be handled by the executing computer system.

If the database is selected as result storage option, all simulation parameters, such as configuration of the simulation and constant agent properties, are stored as metadata in a PostgreSQL database. The result data of all agents for each simulation time step is stored in a Cassandra database system which currently consists of three nodes. The Cassandra cluster is horizontally scalable according to user demands. The three Cassandra nodes handle the storing of results into the database during simulation and split the workload automatically in a fair manner. For the database output, a graphical web front-end is available enabling an easy and efficient inspection and evaluation of simulation results. To further reduce the time it takes to send the result data of each simulation time step to the database, the data is serialized using Protocol Buffers and sent in a binary format. For the extraction of data from the database, the Protocol Buffers need to be applied again for deserialization.

4. Evaluation Methodology

For the evaluation of correctness and performance of DistAIX, we address three aspects: correctness of the distributed forward-backward sweep implementation, observability of emergent behavior, and the scalability of the simulator on an HPC system. The methodology used to address these three aspects is discussed in the following subsections.

4.1. Correctness of Distributed Power-Flow Calculation. The utilized method for the calculation of electrical interactions is the forward-backward sweep method. Convergence of this method has already been shown in [27]. DistAIX implements

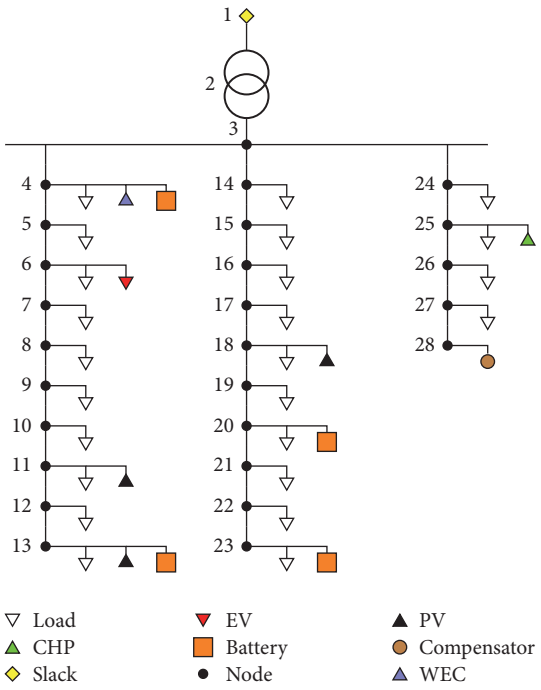

Figure 8: Low voltage distribution system for evaluation of correctness of distributed forward-backward sweep implementation.

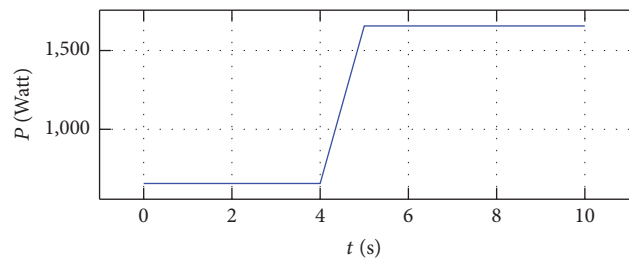

Figure 9: Profile of single family household load.

the algorithm in a distributed way. To demonstrate that our implementation with processes provides numerically correct results we select a small scenario and compare results to those obtained from Modelica modeling and simulation of the same scenario. Modelica is chosen for this demonstration, due to its flexible use and free availability as OpenModelica. As a metric to evaluate the correctness, we use the absolute differences Δ between node voltages and line currents obtained with DistAIX and Modelica as well as the number of occurrences of such differences. From the voltage and line current differences we derive conclusions on the correctness of our implementation.

To obtain comparable results, the electrical components are modeled according to Sections 3.4.1–3.4.10 in Modelica. Further, the same profile data are used as input for the electrical component models in both simulation environments. Control values for all components are found without communication interactions by simple rules as presented in the reference scenario in [41]. The distribution system scenario used as reference is shown in Figure 8. All agent types are used to ensure a general correctness of the presented approach. For the Modelica simulation, we use the DASSL solver with a tolerance of 10^{-6} and a time step of 60 s. The same time step is applied to our simulator. Convergence of simulation results is detected when all nodal voltages change less than a certain ϵ between two iterations. The ϵ is set to the value of the DASSL solver tolerance 10^{-6}. The simulation is executed for a complete day.

4.2. Observability of Emergent Behavior. Methods to detect and characterize emergent behavior in complex systems are discussed in the literature, for example, [42–44]. Such methods are always dependent on the application and system under study. In order to analyze emergent behavior characteristics of different control applications for distribution systems, DistAIX enables observability of emergent behavior in large-scale simulations. We demonstrate this functionality by selecting one control application called SwarmGrid [41]. SwarmGrid is expected to result in emergent behavior of the distribution system due to its bottom-up, decentralized control strategy. In the SwarmGrid control concept, the system level target is voltage stability of the system. Power producers and consumers (agents) negotiate the amount of power they supply or consume in a self-organized way. Their main objective is the usage of flexibilities for the local balancing of power production and consumption. Agents form so-called swarms, that is, groups of agents that need to interact with one another in order to achieve their goal.

The formulation of such a bottom-up heuristic control as one complete analytical model is infeasible. However, DistAIX allows the system behavior to emerge from the definition of the individual component behaviors. The agent-based concept and the need to simulate electrical and communicative interactions as well as component control together make the presented simulation tool suitable for an evaluation of SwarmGrid control. Furthermore, due to the vast number of components in the distribution grid that can be utilized in control approaches such as SwarmGrid, the system can be described as highly complex with various possible interactions among agents.

For a demonstration of observability of emergent behavior, we use the rural low voltage grid of 177 nodes as described in Section 4.3 and the electrical models given in Sections 3.4.1–3.4.10. In order to provoke emergent behavior, all input profiles have constant values except for the ones of single family household loads. These profiles feature a ramp up of 1 kW within 1 s as depicted in Figure 9. The ramps happen simultaneously, start at 4 s, and end at 5 s. As the total number of single family households in the grid is 140, the aggregated change in the total power exchange of the grid is 140 kW. The time step size of this assessment is set to 10 ms and 1000 time steps (10 s) are simulated. The communication link latency for all links is set to 100 ms to consider delays caused by message transmission. Thereby, the system behavior before, during, and after the household load ramp can be analyzed.

We determine (a) the aggregated active power behavior based on a reference simulation without self-organizing

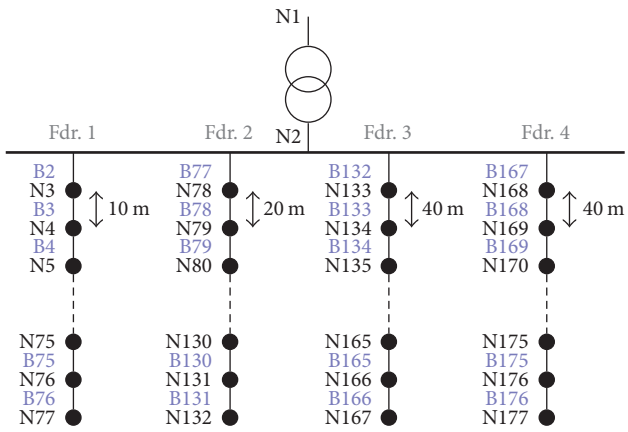

Figure 10: Low voltage grid with 177 nodes used in emergent behavior and scalability methodologies; figure taken from [41].

control and (b) the aggregated active power behavior of a simulation with SwarmGrid enabled. By comparing the results for (a) and (b), we can conclude on how emergent behavior appeared in the system and changed the overall behavior of specific component types and the system itself. As the emergent behavior results from the interactions of agents, the number of exchanged messages is evaluated as an additional indicator. Due to the individual and heterogeneous control behaviors of the system components (agents) and their situation-dependent interactions, it is virtually impossible to anticipate their behavior as a group or swarm. Even if their controls are designed to achieve a particular system level result, such a control cannot possibly have targets for all internal system variables. DistAIX enables the observation of even these internal variables and understanding their relation to the system level target.

4.3. Scalability. For the performance assessment of DistAIX with respect to scalability, a rural low voltage grid containing 177 nodes and 310 components (i.e., a total of 487 agents) is chosen. The low voltage grid is shown in Figure 10. It is identical to the one used by the authors in [41] and consists of four feeders with 75, 55, 35, and 10 nodes with different distances between single nodes. While two of the feeders are equipped with overhead lines the other two are built with cables. The installed power is listed in Table 1. The total installed producer power is 503.5 kVA and consumer power is 448.6 kVA. Moreover, it contains 275.2 kWh battery capacity and 60 kvar reactive power compensation. The low voltage grid is connected to a medium voltage feeder as many times as needed to upscale the system. This means the number of agents N_{agents} in the system is

$$N_{\text{agents}} = N_{\text{LV}} \cdot 487 - (N_{\text{LV}} - 1), \tag{23}$$

where N_{LV} is the amount of low voltage grids connected to the medium voltage feeder and $(N_{\text{LV}} - 1)$ is subtracted as there is only one slack bus.

This methodology is used to analyze the execution time of the simulation for different quantities of agents. In order to evaluate the impact of communicative and electrical interactions, two simulations are executed for each grid size:

(1) With agent communication: SwarmGrid [41] is enabled.

(2) Without agent communication: components behave in an uncoordinated manner based on currently valid guidelines for Germany (same as reference case in [41]).

Table 1: Installed power in scenario of 177 nodes; table adapted from [41].

Component	Number	Installed power/capacity
Load	175	282.6 kVA
EV	35	166 kVA
PV (peak power)	30	220 kVA (165 kW)
WEC (peak power)	5	84 kVA (69 kW)
CHP	25	199.5 kVA
Storage	35	275.2 kWh
Compensator	4	60 kvar

The simulation execution time $T(p)$ for a number of p processes is measured and serves as scalability metric. The fastest execution time and the respective number of processes are used in the evaluation. The number of simulation time steps to execute is set to 1000 with a time step size of 1 s. All component profiles consist of two different values (one for $t = 0$ and one for $t = 1000$). The intermediate steps are linearly interpolated between these two values so that there is a power demand or generation change in each time step. Hence, the communicative interactions caused by SwarmGrid are representative for a case where the power system conditions change dynamically. Each simulation was carried out several times to ensure stable results for the execution time.

The available computation resources are four computing nodes. Each node includes 24 physical cores of type Intel Xeon E5-2658 v3 at 2.20 GHz. One computing node is used for simulations with 1–24 processes, two nodes for 25–48 processes, three nodes for 49–72 processes, and four nodes for 73–96 processes. Processes are always split equally among computing nodes. Each computing node has 126 GB RAM and all four nodes are connected via an Ethernet network for the benchmarks. They all run a CentOS 7.3 operating system using a 3.10.0 Linux kernel. The MPI implementation used on all computing nodes is the high performance MPI library ParaStation MPI [45]. Since the base grid for the scalability investigations has four feeders and our methodology duplicates this grid N_{LV} times to generate larger grids, $N_{\text{LV}} = 25$ is the largest scenario for the scalability study. This scenario has 100 feeders, that is, workitems, which can be optimally parallelized by the available computation resources. Additionally, the execution times of three scenarios containing considerably more feeders than available processors are investigated to give an impression of the examinable scenario sizes.

In practice, DistAIX can use separate computer networks (Ethernet and InfiniBand) for the interprocess communication and saving the result to the database. The database server

Table 2: Number and magnitude of absolute deviations Δ among node voltages and line currents (unit of Δ is V for voltages and A for currents).

Δ	Re $\{v_{\text{node}}\}$	Im$\{v_{\text{node}}\}$	Re$\{i_{\text{line}}\}$	Im$\{i_{\text{line}}\}$
$= 0$	37440	37431	35939	35987
$\in (0, 10^{-6}]$	0	6	50	2
$\in (10^{-6}, 10^{-5}]$	0	3	10	7
$\in (10^{-5}, 10^{-4}]$	0	0	1	4

is located on a resource different from the four computing nodes. Thereby, the simulation execution itself and the storage of result data are decoupled. The time required to initiate the savings to the database is regarded as a steady component of the simulation runtime and is therefore not considered here. Simulation results presented in the following section were obtained from a simulation setup without any result saving (except for runtime of the simulation) with no loss of generality.

5. Evaluation

The methodologies defined in the previous section are used for an evaluation of DistAIX. The results are discussed in this section.

5.1. Correctness of Distributed Power-Flow Calculation. Table 2 provides the number of deviations Δ between node voltages and line currents of the two simulations in four intervals. The total number of current and voltage values differs because there are more busses than lines in the grid. As both simulations have an accuracy of 10^{-6}, smaller deviations are not discovered and are set to zero. Especially the difference between nodal voltages is small. While all Δ for node voltages are below or equal to 10^{-5} V for the line currents, some Δ are between 10^{-5} and 10^{-4} A. The reason for this is the application of the convergence criteria of the forward-backward sweep method to the node voltages. As the current is calculated by each component, this value can be considered the electrical interaction variable of agents. Hence, for a demonstration of correctness it is important to consider the line currents as well. For the imaginary part of the line currents only 4 values differ by more than 10^{-5} A. Experiments have been repeatedly carried out for different numbers of processes always yielding the same results. Therefore, the overall correctness of the implemented forward-backward sweep calculation is demonstrated and deviations to the reference simulation are negligible.

5.2. Observability of Emergent Behavior. Figure 11 shows the active power behavior of the whole grid at the slack bus for the reference simulation without a communicative control approach and for the SwarmGrid control approach. The different starting values of the two simulation results are caused by the way flexibility is used in the SwarmGrid approach. The starting conditions for the two simulations are identical. However, in SwarmGrid components negotiate immediately for a local balancing of production and

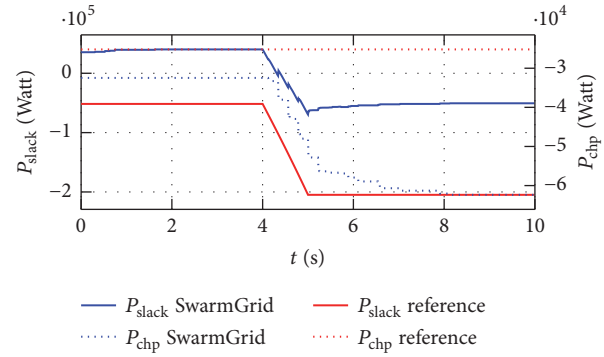

Figure 11: Active power behavior of slack bus and CHPs.

consumption resulting in a smaller load at the slack bus compared to the reference case due to more efficient usage of storage. When the load starts to increase at $t = 4$ s the active power behavior at the slack bus in the reference simulation follows. The difference between the end and start value of active power at the slack bus is 153.2 kW, which corresponds to the change of load power (140 kW) plus losses in the grid due to higher currents. Therefore, the behavior of the whole grid in the reference simulation can be determined from the behavior of the single components, namely, in this case the single family household loads.

The difference between the end and start value in the SwarmGrid simulation is 90.1 kW which equals only 64.4% of the change of load power. Moreover, the shape of the active power at the slack bus indicates that the overall grid behavior does not follow the behavior of the loads. Instead, the change of load power is partly compensated. This is a dynamic process continuing after the single family household loads have reached their final value at 5 s. To find the cause for this behavior difference, the results for internal variables of single component types have to be investigated. Notice that the load change compensation is done by flexible components such as CHP. The total power production of all CHP is also depicted in Figure 11. In the reference case, the CHP determines the required power production according to the thermal demand, which is constant during the simulation time. In SwarmGrid control, the CHP utilizes thermal storage capacity to offer flexibility. As a result, the power production changes after the load power starts to increase.

Note that there is no centralized controller or optimization driving CHP towards this behavior. Instead, agents interact and determine their control values autonomously

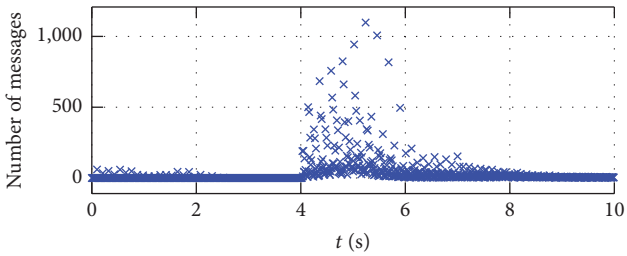

Figure 12: Number of messages sent between agents.

Table 3: Execution time results for different grid sizes.

SwarmGrid on/off	N_{LV}	p	$T(p)$ in sec
On	1	4	20.02
On	5	19	31.74
On	10	39	42.27
On	15	59	55.68
On	20	61	69.25
On	25	96	87.84
Off	1	3	10.66
Off	5	20	20.00
Off	10	39	27.58
Off	15	44	39.04
Off	20	61	51.27
Off	25	44	61.88

according to behavior rules. The overall system behavior, that is, the power behavior at the slack bus, emerges from the behavior of the single components and cannot be predetermined as in the reference case. Since the communication of agents plays a critical role in this process, Figure 12 shows the number of messages that are generated per time step. A large amount of interactions takes place during the change of load behavior and also afterwards. The number of messages decreases again when the system reaches a stable end value. The intensity of communication depends on the operating conditions and evolution of the physical system and can therefore not be anticipated precisely. Overall, these results demonstrate that emergent behaviors of distribution systems can be observed with DistAIX.

5.3. Scalability. The results of simulation benchmarks with respect to scalability are shown in Table 3. The minimal simulation execution time $T(p)$ scales almost linearly with the number of agents in the scenario for both cases with and without SwarmGrid control enabled. This result can also be observed in Figure 13 and is achieved by using more processes and spreading the simulation across multiple computing nodes; for example, for $N_{LV} = 10$ the simulation execution time is minimal for 39 processes. The simulation is spread across 2 computing nodes running 19 and 20 processes, respectively. The gradient of the $T(p)$ scaling factor is considerably lower than 1, indicating that the parallelization

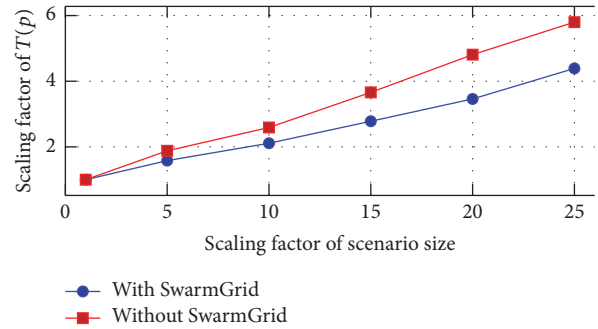

Figure 13: Scaling factors of scenario size in relation to scaling factors of minimal simulation execution time $T(p)$.

with processes is able to exploit computation resources efficiently for growing scenario sizes.

Linear scalability means that large electrical grids plus agent-based control can be simulated efficiently by an appropriate number of processes. It also indicates that the computation of communicative agent interactions adds an offset to the simulation execution time but does not change the scalability behavior in essence. Another aspect taken from Figure 13 is that the scaling for the case with communication is better than without. Keeping in mind that the benchmark scenarios were chosen in such a way as to require an extensive amount of agent communication, this leads to the conclusion that the message router concept is an effective method to parallelize the computational burden of agent message processing. However, the results presented here are only valid for the specific agent-based control strategy under study [41]. The experiments have to be repeated for different strategies resulting in potentially different communication link usages of agents to draw more general conclusions.

In most cases, the number of processes p of the minimal execution time $T(p)$ correlates well with the number of feeders in the electrical grid. This demonstrates the benefits of the proposed agent distribution methodology (see Section 3.2) for the simulation execution time and scalability. As the chosen benchmarking methodology uses grids with repetitive electrical topology with only a few workitems compared to the number of agents, it provides a worst case scenario for agent distribution. In more realistic grids of similar size containing more bifurcation nodes as considered here, the number of workitems will increase and the size (length) of each workitem will decrease. Hence, the execution time for a grid with a similar number of agents but more branched electrical topology can be expected to be equal to or smaller than the presented results.

Figure 14 shows the decrease of execution time with increasing number of processes for the $N_{LV} = 10$ scenario. The execution time decreases rapidly up to 10 processes and is close to the minimal value afterwards. DistAIX enables an efficient simulation even if less than the optimal number of processes for the given electrical topology is available. We observed this behavior for other scenario sizes as well. Future investigations on how to recommend a reasonable minimal number of processes to the user for a given electrical topology

Table 4: Execution time results for large grid sizes generated with 96 processes on 4 computational nodes.

SwarmGrid on/off	N_{LV}	Grid nodes	N_{agents}	$T(p)$ in sec
On	50	8,850	24,301	196.69
On	100	17,700	48,601	481.89
On	250	44,250	121,501	2019.86
Off	50	8,850	24,301	155.78
Off	100	17,700	48,601	401.05
Off	250	44,250	121,501	1824.61

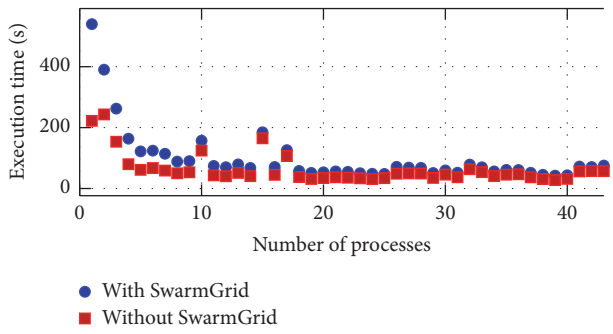

Figure 14: Execution time results of scenario with $N_{LVgrid} = 10$.

are necessary to exploit computation resources even more efficiently.

The results include only scenarios in which agents are assigned to all processes. Experiments with small testing scenarios such as the 27-node low voltage grid used for power-flow demonstrations showed that the influence of dispensable processes on the simulation execution time is negligible. Due to limitations of the hardware used for the benchmark simulations, only scenarios up to $N_{LV} = 25$ can be reasonably analyzed here with respect to scaling. The results for three additional scenarios are shown in Table 4. They demonstrate that even for grids exceeding the 40,000 nodes the presented approach provides a solution in a reasonable amount of time—even if not the optimal number of processes but only a maximum of 96 processes is available. Due to the memory limits of our computing nodes we do not provide results for larger scenarios here. It should be noted that the increase in execution time for the large scenarios is mainly caused by initialization procedures for the communication network setup which are specific for the control strategy used here and can be improved in the future.

6. Conclusion

This paper introduces DistAIX, an agent-based modeling and simulation approach for electrical distribution systems. It is designed to study emergent behavior of such systems at large scale. The simulation is parallelized by processes enabling the distribution of computations to multiple computing nodes with distributed memory. The distribution system components are modeled as agents in the required level of detail. No model simplifications or restrictions are needed for scalability. The properties of communication links between agents, such as latencies, can be modeled. DistAIX facilitates the design and analysis of agent-based bottom-up control concepts for distribution systems. Due to nonlinear cyber-physical interactions of the agents, such concepts may result in emergent system behavior. The emergent behavior can be observed in simulations with DistAIX. Process-based parallelization and linear scalability properties of DistAIX enable the study of models at nation scale if appropriate computation resources are used.

Conflicts of Interest

The authors declare that there are no conflicts of interest regarding the publication of this paper.

Acknowledgments

This work was supported by the German Federal Ministry of Education and Research in the project SwarmGrid (Grant no. 03EK3568A).

References

[1] C. E. Hmelo-Silver and R. Azevedo, "Understanding complex systems: Some core challenges," *Journal of the Learning Sciences*, vol. 15, no. 1, pp. 53–61, 2006.

[2] T. El-Mezyani, R. Wilson, M. Sattler, S. K. Srivastava, C. S. Edrington, and D. A. Cartes, "Quantification of complexity of power electronics based systems," *IET Electrical Systems in Transportation*, vol. 2, no. 4, pp. 211–222, 2012.

[3] S. Ikeda and R. Ooka, "Metaheuristic optimization methods for a comprehensive operating schedule of battery, thermal energy storage, and heat source in a building energy system," *Applied Energy*, vol. 151, pp. 192–205, 2015.

[4] W. K. V. Chan, Y.-J. Son, and C. M. Macal, "Agent-based simulation tutorial - Simulation of emergent behavior and differences between agent-based simulation and discrete-event simulation," in *Proceedings of the 2010 43rd Winter Simulation Conference, WSC'10*, pp. 135–150, USA, December 2010.

[5] P. Ringler, D. Keles, and W. Fichtner, "Agent-based modelling and simulation of smart electricity grids and markets - A literature review," *Renewable & Sustainable Energy Reviews*, vol. 57, pp. 205–215, 2016.

[6] A. Pokahr, L. Braubach, and W. Lamersdorf, "Jadex: A BDI Reasoning Engine," in *Multi-Agent Programming*, vol. 15 of *Multiagent Systems, Artificial Societies, and Simulated Organizations*, pp. 149–174, Springer US, Boston, Ma, 2005.

[7] D. P. Chassin, J. C. Fuller, and N. Djilali, "GridLAB-D: An agent-based simulation framework for smart grids," *Journal of Applied Mathematics*, vol. 2014, Article ID 492320, 2014.

[8] S. Jin and D. P. Chassin, "Thread group multithreading: Accelerating the computation of an agent-based power system modeling and simulation tool - GridLAB-D," in *Proceedings of the 47th Hawaii International Conference on System Sciences, HICSS 2014*, pp. 2536–2545, USA, January 2014.

[9] A. Tanenbaum and H. Bos, *Modern Operating Systems, , Pearson*, 4th edition, 2015.

[10] C. Kuschel and U. Rüde, "High-performance simulation of nation-sized smart grids," *International Journal of Parallel, Emergent and Distributed Systems*, vol. 32, no. 6, pp. 647–668, 2016.

[11] P. Oliveira, T. Pinto, H. Morais, and Z. Vale, "MASGriP a multi-agent smart grid simulation platform," in *Proceedings of the 2012 IEEE Power and Energy Society General Meeting, PES 2012*, USA, July 2012.

[12] J. C. Fuller, S. Ciraci, J. A. Daily, A. R. Fisher, and M. Hauer, "Communication simulations for power system applications," in *Proceedings of the 2013 Workshop on Modeling and Simulation of Cyber-Physical Energy Systems, MSCPES 2013*, USA, May 2013.

[13] M. Stifter, E. Widl, F. Andren, A. Elsheikh, T. Strasser, and P. Palensky, "Co-simulation of components, controls and power systems based on open source software," in *Proceedings of the 2013 IEEE Power and Energy Society General Meeting, PES 2013*, Canada, July 2013.

[14] K. Anderson, J. Du, A. Narayan, and A. E. Gamal, "GridSpice: A distributed simulation platform for the smart grid," *IEEE Transactions on Industrial Informatics*, vol. 10, no. 4, pp. 2354–2363, 2014.

[15] R. Bottura and A. Borghetti, "Simulation of the volt/var control in distribution feeders by means of a networked multiagent system," *IEEE Transactions on Industrial Informatics*, vol. 10, no. 4, pp. 2340–2353, 2014.

[16] J. Vaubourg, Y. Presse, B. Camus et al., "Multi-agent Multi-Model Simulation of Smart Grids in the MS4SG Project," in *Advances in Practical Applications of Agents, Multi-Agent Systems, and Sustainability: The PAAMS Collection*, vol. 9086 of *Lecture Notes in Computer Science*, pp. 240–251, Springer International Publishing, Cham, 2015.

[17] M. Cvetkovic and M. Ilic, "Interaction variables for distributed numerical integration of nonlinear power system dynamics," in *Proceedings of the 53rd Annual Allerton Conference on Communication, Control, and Computing, Allerton 2015*, pp. 560–566, USA, October 2015.

[18] K. Mets, J. A. Ojea, and C. Develder, "Combining Power and Communication Network Simulation for Cost-Effective Smart Grid Analysis," *IEEE Communications Surveys Tutorials*, vol. 16, no. 3, pp. 1771–1796, 2014.

[19] D. Shirmohammadi, H. W. Hong, A. Semlyen, and G. X. Luo, "A compensation-based power flow method for weakly meshed distribution and transmission networks," *IEEE Transactions on Power Systems*, vol. 3, no. 2, pp. 753–762, 1988.

[20] Z. Haibo, Z. Boming, S. Hongbin, and A. Ran, "A new distributed power flow algorithm between multi-control-centers based on asynchronous iteration," in *Proceedings of the 2006 International Conference on Power System Technology*, pp. 1–7, Chongqing, China, October 2006.

[21] H. Sun and B. Zhang, "Distributed power flow calculation for whole networks including transmission and distribution," in *Proceedings of the Transmission and Distribution Exposition Conference: 2008 IEEE PES Powering Toward the Future, PIMS 2008*, USA, April 2008.

[22] J. M. Gonzalez de Durana, O. Barambones, E. Kremers, and L. Varga, "Agent based modeling of energy networks," *Energy Conversion and Management*, vol. 82, pp. 308–319, 2014.

[23] J.-H. Byun, A. Ravindran, A. Mukherjee, B. Joshi, and D. Chassin, "Accelerating the gauss-seidel power flow solver on a high performance reconfigurable computer," in *Proceedings of the IEEE Symposium on Field Programmable Custom Computing Machines, FCCM 2009*, pp. 227–230, USA, April 2009.

[24] C. P. Nguyen and A. J. Flueck, "A Novel Agent-Based Distributed Power Flow Solver for Smart Grids," *IEEE Transactions on Smart Grid*, vol. 6, no. 3, pp. 1261–1270, 2015.

[25] X. Zhang, A. J. Flueck, and C. P. Nguyen, "Agent-Based Distributed Volt/Var Control with Distributed Power Flow Solver in Smart Grid," *IEEE Transactions on Smart Grid*, vol. 7, no. 2, pp. 600–607, 2016.

[26] M. Wolter, H. Guercke, T. Isermann, and L. Hofmann, "Multi-agent based distributed power flow calculation," in *Proceedings of the IEEE PES General Meeting, PES 2010*, USA, July 2010.

[27] R. D. Zimmerman, *Comprehensive distribution power flow: modeling, formulation, solution algorithms and analysis [Ph.D. thesis]*, Cornell University, 1995, https://pdfs.semanticscholar.org/a1b6/eb1871701538ce2147523e8753a218ff0894.pdf.

[28] A. Rousset, B. Herrmann, C. Lang, and L. Philippe, "A survey on parallel and distributed multi-agent systems for high performance computing simulations," *Computer Science Review*, vol. 22, pp. 27–46, 2016.

[29] S. Coakley, M. Gheorghe, M. Holcombe, S. Chin, D. Worth, and C. Greenough, "Exploitation of high performance computing in the FLAME agent-based simulation framework," in *Proceedings of the 14th IEEE International Conference on High Performance Computing and Communications, HPCC-2012 - 9th IEEE International Conference on Embedded Software and Systems, ICESS-2012*, pp. 538–545, gbr, June 2012.

[30] N. Collier and M. North, "Parallel agent-based simulation with Repast for High Performance Computing," *Simulation*, vol. 89, no. 10, pp. 1215–1235, 2013.

[31] D. P. Chassin, K. Schneider, and C. Gerkensmeyer, "GridLAB-D: An open-source power systems modeling and simulation environment," in *Proceedings of the Transmission and Distribution Exposition Conference: 2008 IEEE PES Powering Toward the Future, PIMS 2008*, USA, April 2008.

[32] J. S. van der Veen, B. van der Waaij, and R. J. Meijer, "Sensor data storage performance: SQL or NoSQL, physical or virtual," in *Proceedings of the IEEE 5th International Conference on Cloud Computing (CLOUD '12)*, pp. 431–438, IEEE, June 2012.

[33] T. Rabl, M. Sadoghi, H.-A. Jacobsen, S. Gómez-Villamor, V. Muntés-Mulero, and S. Mankovskii, "Solving big data challenges for enterprise application performance management," pp. 1724–1735.

[34] K. Varda, "Protocol Buffers: Google's Data Interchange Format," 2008, https://opensource.googleblog.com/2008/07/protocol-buffers-googles-data.html.

[35] J. Feng and J. Li, "Google protocol buffers research and application in online game," in *Proceedings of the 2013 IEEE Conference Anthology*, pp. 1–4, China, January 2013.

[36] S. Popić, D. Pezer, B. Mrazovac, and N. Teslić, "Performance evaluation of using Protocol Buffers in the Internet of Things communication: Protobuf vs. JSON/BSON comparison with a

focus on transportation's IoT," in *Proceedings of the 1st IEEE International Conference on Smart Systems and Technologies, SST 2016*, pp. 261–265, Croatia, October 2016.

[37] T. C. Hu, "Parallel sequencing and assembly line problems," *Operations Research*, vol. 9, pp. 841–848, 1961.

[38] W. Zhou, H. Yang, and Z. Fang, "A novel model for photovoltaic array performance prediction," *Applied Energy*, vol. 84, no. 12, pp. 1187–1198, 2007.

[39] M.-R. Haghifam and S. Soltani, "Reliability models for wind farms in generation system planning," in *Proceedings of the 2010 IEEE 11th International Conference on Probabilistic Methods Applied to Power Systems, PMAPS 2010*, pp. 436–441, Singapore, June 2010.

[40] L. Razik, M. Mirz, D. Knibbe, S. Lankes, and A. Monti, "Automated deserializer generation from CIM ontologies: CIM++—an easy-to-use and automated adaptable open-source library for object deserialization in C++ from documents based on user-specified UML models following the Common Information Model (CIM) standards for the energy sector," *Computer Science - Research and Development*, pp. 1–11, 2017.

[41] S. Kolen, T. Isermann, S. Dähling, and A. Monti, "Swarm behavior for distribution grid control," in *Proceedings of the 2017 IEEE PES Innovative Smart Grid Technologies Conference Europe (ISGT-Europe)*, pp. 1–6, Torino, Italy, September 2017.

[42] W. K. Chan, "Interaction metric of emergent behaviors in agent-based simulation," in *Proceedings of the 2011 Winter Simulation Conference - (WSC 2011)*, pp. 357–368, 2011.

[43] C. Szabo and Y. M. Teo, "An integrated approach for the validation of emergence in component-based simulation models," in *Proceedings of the Winter Simulation Conference*, pp. 2412–2423.

[44] E. O'Toole, V. Nallur, and S. Clarke, "Towards Decentralised Detection of Emergence in Complex Adaptive Systems," in *Proceedings of the 2014 8th IEEE International Conference on Self-Adaptive and Self-Organizing Systems, SASO 2014*, pp. 60–69, UK, September 2014.

[45] C. Clauss, T. Moschny, and N. Eicker, "Dynamic Process Management with Allocation-internal Co-Scheduling towards Interactive Supercomputing," in *Proceedings of the 1st COSH Workshop on Co-Scheduling of HPC Applications, 2016*.

Hindawi
Complexity
Volume 2017, Article ID 1967645, 23 pages
https://doi.org/10.1155/2017/1967645

Review Article

Creating Agent-Based Energy Transition Management Models That Can Uncover Profitable Pathways to Climate Change Mitigation

Auke Hoekstra, Maarten Steinbuch, and Geert Verbong

Eindhoven University of Technology, Eindhoven, Netherlands

Correspondence should be addressed to Auke Hoekstra; a.e.hoekstra@tue.nl

Received 6 June 2017; Revised 17 October 2017; Accepted 12 November 2017; Published 28 December 2017

Academic Editor: Ettore Bompard

The energy domain is still dominated by equilibrium models that underestimate both the dangers and opportunities related to climate change. In reality, climate and energy systems contain tipping points, feedback loops, and exponential developments. This paper describes how to create realistic energy transition management models: quantitative models that can discover profitable pathways from fossil fuels to renewable energy. We review the literature regarding agent-based economics, disruptive innovation, and transition management and determine the following requirements. Actors must be detailed, heterogeneous, interacting, learning, and strategizing. Technology should be represented as a detailed and heterogeneous portfolio that can develop in a bottom-up manner, using endogenous feedback loops. Assumptions about discount rates and the social cost of carbon should be configurable. The model should contain interactions between the global, national, local, and individual level. A review of modelling techniques shows that equilibrium models are unsuitable and that system dynamics and discrete event simulation are too limited. The agent-based approach is found to be uniquely suited for the complex adaptive sociotechnical systems that must be modelled. But the choice for agent-based models does not mean a rejection of other approaches because they can be accommodated within the agent-based framework. We conclude with practical guidelines.

1. Introduction

Scientists are "95% certain that humans are the main cause of global warming [which] will lead to high to very high risk of severe, widespread and irreversible impacts globally" [1]. They advise "stabilizing temperature increase to below 2°C relative to pre-industrial levels" but note that "this will require an urgent and fundamental departure from business as usual" [1]. Politicians in 194 countries signed the "Paris Agreement" that pledges to keep global warming below the 2°C mark [2]. Anthropogenic greenhouse gasses are largely caused by humanity's use of fossil fuels to power energy intensive machinery. Electricity and heat are responsible for 25%, and it is tightly connected to transportation (which might become electrified) with 14%, industry with 21%, and other energy related greenhouse gasses with 10% [1]. We need models that help us to uncover quick and preferably profitable pathways to a renewable energy system [3].

Since our industrial civilization is built on fossil energy that now permeates every aspect of it, switching to renewables is a fundamental and integral transition that is not easy to model. Renewable energy is also decentralized and intermittent with a larger role for *prosumers* (consumers who are also producers) and demand-response and storage, which makes the entire energy system fundamentally different. Current models cannot cope with the magnitude of this transition and offer ineffective and myopic perspectives. But the reality is less pessimistic: renewable technologies are on track to be cheaper than fossil alternatives [4, 5], even more so if we phase out fossil fuel subsidies [6, 7] and internalize risk calculations [8]. Renewables promise economic growth [9], jobs [10], and energy security [11] while reducing geopolitical tensions [12].

So why not take a more positive approach and try to take advantage of the opportunities that renewables offer?

In this paper we build on theories found in *agent-based economics, disruptive innovation*, and *transition management*. We formulate requirements and make practical recommendations for models that can not only make better predictions but also empower us to *actively manage* the transition to renewable energy. We call them *energy transition management models* and define them as *quantitative models that can discover profitable pathways from fossil fuels to renewable energy.*

This paper brings together a wide review of both theory and practice in order to show how such models could be constructed. It consists of five parts:

(1) "Clinging to Equilibrium" functions as a problem statement, showing that most current models are unsuitable for transitions.

(2) "Theories of Disruption" reviews *agent-based economics, disruptive innovation*, and *transition management*.

(3) "Modelling Requirements" builds on the theories and focusses on *actors*, *technologies*, and *carbon pricing*.

(4) "Modelling Methods" evaluates *system dynamics* and *discrete event simulations* before concluding that modelling *complex adaptive systems* requires *agent-based models*.

(5) "Building a Model" contains practical advice.

2. Clinging to Equilibrium

Currently, most predictions regarding the energy transition come from equilibrium models that are simply not suited to dealing with transitions.

> *Imagine how hard physics would be if electrons could think (Murray Gell-Mann)*

2.1. Equilibrium Models Still Dominate. Economics became a science in the period that most social scientists tried to emulate Newtonian physics, requiring humans to be just as predictable as, say, electrons. Adam Smith's *Wealth of Nations* (1776) [13] was inspired by Newton's *Principia*. Leon Walras translated Smith's ideas into "Newtonian" economic models called *general equilibrium models* [14]. Computing them was first done in 1967 and such models were called *Applied General Equilibrium* (AGE) models [15]. Since the mid-1980s an implementation called *Computable General Equilibrium* (CGE) models came to dominate economics [16–18] and their newest incarnation called *Dynamic Stochastic General Equilibrium Models* (DSGE) dominates economics now [19].

"The concept of equilibrium … is one of the central pillars of the Great Borrowing from physics … Voluntary exchange matches up buyers and sellers, prices float until everyone is content, and all markets clear. The similarity to the ideal gas law of physics is not at all accidental" [20]. A generally accepted definition does not exist [21] but an often used one is as follows [18]: [CGE models] "describe the allocation of resources in a market economy as the result of the interaction of supply and demand, leading to equilibrium prices. The building blocks of these models are equations representing the behavior of the relevant economic agents: consumers, producers, the government, etc. Each of these agents demands or supplies goods, services and factors of production, as a function of their prices."

Proponents of CGE argue that the models are complex enough to capture the essential features of an economic situation yet simple enough to be tractable [22]. Other claimed advantages are accounting consistency due to the use of a closed accounting system and an accurate measurement of changes in wealth (as defined in macroeconomics) and they are widely used in economics because they "ensure policy-making is guided by a correct theoretical understanding of how economies function" [23]. They also provide a "solid microeconomic foundation" [18] so "CGE analysis constitutes a powerful scientific method for the comprehensive ex-ante simulation of adjustment effects induced by exogenous policy interference" [24].

According to Fagiolo and Roventini [19]: "at the dawn of 2008 – just before the financial crisis unexpectedly hit – a new consensus emerged: the New Neoclassical Synthesis, … grounded upon Dynamic Stochastic General Equilibrium (DSGE) models." Proponents claimed that monetary and even economic policy was finally becoming science [25–27]. Currently most energy models are still largely equilibrium models, for example, the World Energy Model (used by the IEA for its influential "Energy Outlook" series), POLES (used by Enerdata), and PRIMES (used by the European Commission) [28]. Stanton et al. [29] also review the following integrated assessment models using CGE: JAM; IGEM; IGSM/EPPA (MIT); SMG; WORLDSCAN (CPB); ABARE-GTEM; G-CUBED; MS-MRT; AIM; IMACLIM-R; WIAGEM; MiniCAM; and GIM.

2.2. Equilibrium Models Are Precisely Wrong. It is better to be partly right than precisely wrong [30] and notwithstanding their dominance and mathematical precision, equilibrium models have a long list of problems. They are essentially static: they assume that external shocks can take the system from one equilibrium to another but that the transition itself is irrelevant [17]. Furthermore they are top-down models based on "the holy trinity of rationality, selfishness, and equilibrium" [31]. They assume *"rational" actors* that can be represented by a couple of "representative" aggregated agents [19]. These "rational" actors only strive for utility maximization. They immediately know the utility of every product and price on the market. They are impervious to status, strategizing, populism, idealism, tribalism, hearsay, or marketing. They do not empathize with future generations (see "discount rate" in this paper) or people in other countries (see "Negishi welfare weights" in this paper). Furthermore, the actors function in *"ideal" markets*. This means, among other things, no bankers with perverse incentives, no lobbyists, no political games, no idealists, no monopolistic tendencies, no network effects, no incumbent resistance to change, and so on.

Each of the above simplifications has been falsified, both within economics and by findings from other social sciences like psychology, sociology, and political science [20]. But in equilibrium models they endure, hence the accusation that

users of equilibrium models display "a steadfast refusal to face facts" [32].

But we are beginning to see some change. For many economists, the 2008 economic crisis was the last straw. It laid bare the crisis in economic theory itself [33–36]. Utility theory became mocked as a "fetish" [37]. Fagiolo and Roventini survey the update of CGE to DSGE in detail and conclude it is "patches on torn clothes" [19].

Ackerman observes [38]: "The mathematical dead end reached by general equilibrium analysis is not due to obscure or esoteric aspects of the model, but rather arises from intentional design features, present in neoclassical theory since its beginnings. Modification of economic theory to overcome these underlying problems will require a new model of consumer choice, nonlinear analyses of social interactions, and recognition of the central role of institutional and social constraints."

Nobel laureate Krugman adds [35]: "As I see it, the economics profession went astray because economists, as a group, mistook beauty, clad in impressive-looking mathematics, for truth. ... Economists need to abandon the neat but wrong solution of assuming that everyone is rational and markets work perfectly. The vision that emerges as the profession rethinks its foundations may not be all that clear; it certainly won't be neat; but we can hope that it will have the virtue of being at least partly right."

2.3. Specific Problems with Energy Models. State-of-the-art integrated assessment models (IAMs) usually embed equilibrium models that treat climate policy as an additional constraint while predicting and factoring in climate-related damage [39]. But there is growing consensus in the literature that this conveys a false sense of control and underestimates both the damage of climate change and profits reaped when implementing renewable energy [8, 40–46]. For more, see the discussion on "Pricing Climate Change" in this paper.

Most models also underestimate the potential of technologies that diverge from the status quo and we want to give one example to illustrate the magnitude of the problem. We will use the photovoltaic (PV) predictions of the World Energy Model (WEM) in the World Energy Outlook (WEO) of the International Energy Agency (IEA). Although it is only a partial equilibrium model, we take it as an example because it is probably the most influential energy model in the policy domain [48].

The output of the WEM is shown in Figure 1. NPS stands for "New Policy Scenario" which assumes that a realistic amount of commitments (e.g., to the Paris accord) are implemented into new policies stimulating PV. The thick black line shows that annual additions of solar have been steeply increasing (meaning new or bigger factories for solar panels). We can see that each WEO accepts this past reality because each new scenario has a higher starting point. However, we also see that the WEO essentially predicts that no new factories will be build. This stagnation of the solar industry is predicted over and over again, in every WEO PV scenario since 2002 [47].

Since the WEM is a proprietary model, it hard to pinpoint the cause of the problem. Johnsen points to erroneously high

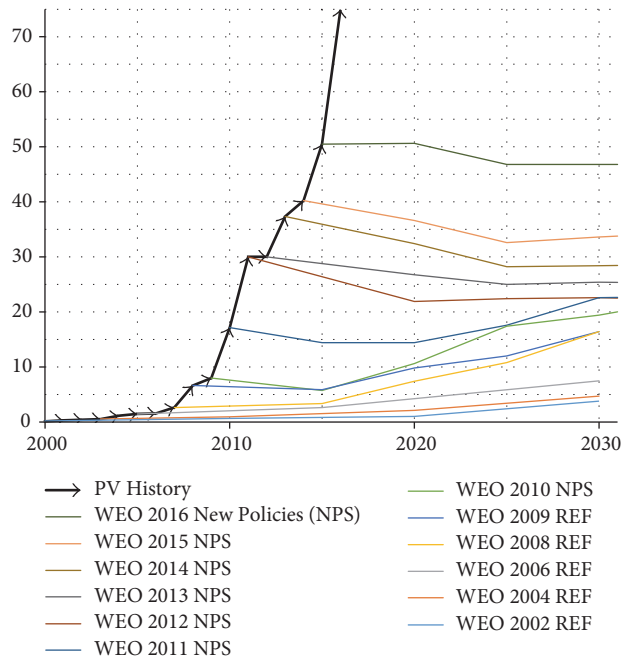

Figure 1: Reality versus IEA predictions: annual PV additions. In gigawatt peak. Data from IEA WEO 2002-2016 NPS and REF scenarios [47].

prices; little learning due to little growth; and assumptions about the absence of flexibility that reduce the value of PV [49]. In 2017 the IEA conducted a study together with IRENA [50]. Page 80 shows that WEM NPS predicts that utility-scale PV will cost USD 1/W in 2030. However, NREL reports that this price was already reached in 2017 (in the US) and that prices have been falling with 19% per year for the last 7 years [34]. If that were to continue the price per watt in 2030 would be seven cents instead of one dollar, and although that is probably too optimistic, there is a big difference with IEA expectations. Furthermore, the IEA acknowledges that PV has grown *exponentially* with—on average—43.3% per year over the last 26 years. However, page 74 shows that WEM NPS predicts *linear* growth from 228 GW in 2015 to 1800 GW in 2050. A yearly production of well under 50 GW would suffice to accommodate this growth. In reality, there was already over 75 GW annual production capacity in 2016 and healthy growth is expected in 2017 [50]. The IEA, once again, implies that the PV sector will collapse instead of continuing its exponential growth.

This disconnection from reality could be due to, for example, sponsor requirements or mental biases like confirmation bias [51], status quo bias [52], or system justification bias [53] but the way the model works could also be a factor. We would argue that, looking at Tables 1 and 2, most of the energy transition management model requirements that we deduce from the literature are implemented partially or not at all. The result is a model that is unable to envision and leverage the exponential developments in solar energy.

Table 1: Overview of requirements for energy transition management models.

	Agents are detailed, heterogeneous, and strategizing. They learn in interaction with each other and the environment. Behavior is defined through interviews and surveys. Exceptional individuals and institutions can drive innovation.		Global level with technological innovation through science, R&D, and economies of scale. Also, climate impacts and policies. Ability for rich nations to invest in climate mitigation in poorer nations (e.g., rainforests).
	Technology is detailed, disaggregated, decentralized, and validated by domain experts. Agent adoption drives endogenous, possibly exponential, bottom-up feedback loops for, for example, solar, wind, storage, and EVs.		National level with energy related policy, subsidy, and taxes. Also, large scale energy production/use, high voltage grids, and mobility patterns. Important level for modelling regime resistance.
	Ability to price externalities differently for different actors. Underlying assumptions are explicit and user adjustable, for example, discount rates, Negishi welfare weights, chance of catastrophe, and value of health/ecosystems.	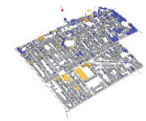	Local level with actors that drive adoption and use of new energy technology. Constrained by spatially modelled physical infrastructure, connecting subsystems like grids, roads, buildings, machines, and people.

Table 2: Characteristics of different types of systems and accompanying simulation techniques.

	Equilibrium	Dynamic systems	Complex adaptive systems
Model characterization	*Static*	*Dynamic*	*Adaptive*
System creation	*Top-down*	*Top-down*	*Bottom-up*
Transition & resistance	*Invisible*	*Observed as aggregate*	*Can be traced back to individual agents*
Dynamic parts of model	*Inputs*	*Relationships & inputs*	*Actors, behaviors, relationships & inputs*
Dominant paradigm	*Equilibrium (CGE)*	*SD and DES*	*Agent based modelling (ABM)*
Simulated system	*No simulation*	*Predefined system*	*System emerges during runtime*
Strong feedback loops	*No*	*Yes (especially SD)*	*Yes*
Spatial awareness	*Hard*	*Yes (especially DES)*	*Yes*
Heterogeneous actors	*Hard*	*Yes (especially DES)*	*Yes*
Emergent behavior	*No*	*No*	*Yes*
Actors can interact	*No*	*No*	*Yes*
Actors can learn	*No*	*No*	*Yes*

3. Theories of Disruption

We have determined that equilibrium theory is not a useful basis for transition management. What technologies are more appropriate? We start with agent-based economics that is quickly growing into a mature field within economics. We expand that with theories on disruptive technological innovation. Finally, we look at transition management: a body of literature with a focus on accelerating the energy transition. Thus, we try to capture the perspectives of economists, engineers, and social/political scientists.

> *The Mecca of the economist lies in economic biology ... But biological conceptions are more complex than those of mechanics (Alfred Marshall, 1907)*

3.1. Agent-Based Computational Economics. After the fundamental problems of equilibrium models became clear, some economists started looking for new paradigms. They found inspiration in biology and natural evolution where path dependency is just as important (if not more so) than equilibrium. An overview is found in Nelson [54]. Evolutionary economics was then combined with a new approach from the social sciences that took advantage of modern computing power: agent-based modelling (ABM). The result was a very different, post-Walrasian, branch of economics called Agent-Based Computational Economics (ACE) that uses ABM instead of equilibrium models [55]. ACE is based on the complex adaptive systems paradigm and grows economies from the bottom-up, thereby bridging the divide separating micro- and macroeconomics [56–58]. It extends evolutionary economics in four ways: agents are heterogeneous with

individual memories and large autonomy; new interactions are possible (e.g., predatory or cooperative instead of just based on price and quality); evolutionary pressure acts on individuals instead of entire populations which drives individual behavior; and, finally, the implementation is a virtual economic world in the computer that functions without intervention by the modeller [59]. Balint et al. [39] show that ACE is making an especially pronounced contribution in the areas of energy and climate change.

ABMs are used to find the most effective policies to mitigate the macroeconomic effects of climate change. They show that it is effective in combining an approach using sticks (carbon taxes) with one using carrots (incentives to technology adoption) [60]. ABM enables us to reframe climate change from a zero-sum game to a coordination problem offering win-win solutions [61]. Dosi and Nelson show that it is important to endogenize the Schumpeterian diffusion of low-carbon innovation [62]. When ABMs take that into account, they show that subsidizing R&D into carbon-free technologies leads to a swift transition and higher economic growth [63, 64]. Isley et al. [65] show how ABM can be used to compare market-based emission reduction policies with some having surprising and transformative results. Determining storage needed in schemes with more intermittency is also an ideal candidate for ABM studies (e.g., [66]). And when it comes to cap defining policies for financing green innovation ABMs are also proving increasingly useful [67].

ABMs also give us a better picture of the costs of climate change in a networked world [68]. They show how the burden hits parts of the population especially hard [69]. They use catastrophes like the flooding of Louisiana after Hurricane Katrina to show that losses increase nonlinearly due to propagation effects [70]. Propagation effects are also studied globally [71, 72]. Combining costs and mitigation into agent-based integrated assessment models (IAMs) is a new field. One of the first examples of combining complex economies with climate models comes from the LAGOM model family that is able to deal with different timescales for modules and spatially distributed energy production and pollution [73–75] but it is not yet an IAM. The first fully fledged agent-based IAM might be the Dystopian Schumpeter meeting Keynes (DSK) model from Lamperti et al. [76].

Climate negotiation and coalition formation is an interesting new field of study for which ABMs are especially well suited [77–79]. Realistic ABMs that take different perspectives into account produce very different result than equilibrium-based models with rational actors [80] and the way the negotiations are structured have a large impact on the results [81, 82]. Policies that return part of a carbon tax back to conforming companies are found to survive longer [83]. As we will see in the discussion on "Energy Transition Management," individual (instead of highly aggregated) actors and technologies and new ways of interacting are vital for models that aspire to explore novel energy transition pathways and they can also increase stakeholder participation because the model is a closer representation of the reality the stakeholders recognize.

ABMs are now ubiquitous when modelling the electricity sector [84–86] because of their higher explanatory power in general [87, 88] and better ability to explore the effects of increasing amounts of renewable energy in the mix [89–91]. Multiagent systems can also be used to actually run a decentralized power grid [92, 93].

An application of ABMs in ACE that is closely related to the next section on Disruptive Technological Innovation is predicting technology diffusion [94], especially of renewable technology [95–99]. The agent-heterogeneity that ABM facilitates is a central factor in technology diffusion in general [100], and environmentally benign technology specifically, with "eco warriors" and early adopters functioning as launching customers [101]. While some income inequality speeds up adoption, too much hampers it [102, 103]. The interplay between customers and firms is also important [99]. Finally, the diffusion of knowledge among consumers is crucial for the spread of diffusion (contrary to the rational actor model). An interesting side is that ABM gives a result that we have observed in reality: moral persuasion is ineffective [104] at taking away this barrier while graded eco-labels are very effective [105].

3.2. Disruptive Technological Innovation. Burning organic matter has brought humanity hitherto unfathomable energy [78] and prosperity [79] but now we are making the transition to renewable energy [80]. This will not be an incremental upgrade but a transformative system level change in the Schumpeterian tradition of creative destruction [106] with superior technologies replacing inferior ones [107]. The basic reason is simple: while fossil technology is hardly improving anymore [108], there are increasing [109] or even accelerating [110–112] returns for renewable innovations regarding solar, wind, batteries, and synthetic fuels [113].

This improvement is usually modelled using learning curves. Originally the concept was confined to learning inside factories [114, 115] but they are now deployed in a wider context [116]: many technologies exhibit a relatively predictable exponential trajectory that is a more reliable predictor of its development than mere (expert) opinions because human beings (experts too) have a tendency to assume linear trends.

The most famous example is probably Moore's law [117], but, in energy, it is solar panels that steal the show. We have seen that their price drops 21% for every doubling of production [118]. This has already resulted in a more than *hundredfold* price decrease in the past 35 years. The price of wind energy has decreased *tenfold* in the same time [90]. Lithium batteries for electric vehicles do not go that far back but their price has decreased *tenfold* in the last 17 years alone [93]. So, the technology advantage is tilting dramatically towards renewable technology. Will this continue?

Availability of energy is not the problem: the sun gives us thousands of times more energy (through radiation) than we need [81, 82] and the first derivative (wind energy) is also abundant [83]. The raw materials we need are not really scarce either and since we can recycle—we are not burning stuff—we could continue with renewable energy until the sun runs out. The price reductions will also continue since we have many, many doublings to go and renewable energy uses much less raw material than fossil energy. For example, wind

needs between 2 grams (airborne wind energy [85]) and 10 grams of material per kWh [86, 87] while a coal fired power plant burns about 300 grams per kWh [88, 89]. And electric vehicles running on this renewable energy use only 400 kg of battery (falling to 100–200 kg) to replace over 15 tons of crude oil over the lifetime of the car [91, 92]. So, if human civilization continues it is likely that fossil technology will be displaced.

However, in many areas renewable technology is still *inferior*. How do we make sure the disruption does not stall? Christensen et al. have put forward the theory of disruptive technology to explain how an inferior new technology can beat an incumbent one [119–121]. They posit that the new technology might be inferior from the vantage point of mainstream criteria, customers or firms, but for some customers there may be *performance oversupply*: they get more performance along the traditional criteria than they are willing to pay for. Since consumers often experience decreasing marginal utility [122], performance oversupply could even be the rule. Competing firms can continue to increase performance oversupply as a form of nonprice differentiation [123]. But the performance oversupply makes customers attracted to products that give more attention to price or to new criteria that have so far been considered secondary. Incumbents often react too slow to this shift because they are *resource dependent* [124] on high-value customers that will not accept the inferior new technology yet.

Adner extends disruptive innovation with a demand based and emergent perspective [125]. He introduces *functional thresholds* below which a consumer will not consider the product and *net utility thresholds* that specify the highest price consumers will pay and may be based on the customers internal resources [126], capabilities [127], or human capital [128]. Adner also develops a formal model describing how technology A in market segment X will more easily disrupt market segment Y if there is a large preference overlap between the market segments. Adner states that he would have liked to include asymmetries in firm capabilities, market segment size, and economies of scale.

A final dynamic we must mention is the lock-in to interior technological development trajectories. Arthur points out that this has happened to, for example, our keyboard and electricity grid and the type of nuclear reactors we use [109]. It uses the same dynamic of increasing returns but now has the effect of giving an incumbent an ever-increasing advantage, effectively creating a monopoly for a product (e.g., Google or Facebook) or technology (e.g., gasoline cars). Most important in the context of this paper is humanity's *carbon lock-in* towards the use of more fossil fuels [129, 130]. Even though we know it is destroying our habitat, the lock-in of fossil technologies is maintained by subsidies and the absence of carbon pricing [131]. It is also spreading to developing countries [132]. We must be able to model innovative ways to break such lock-ins.

Let us give an example touching upon most of these issues to show what we mean. For over a hundred years the only practical rechargeable battery was a lead acid battery. But when the laptop and mobile phone came along, research into lightweight batteries intensified and soon the lithium battery was born. This enables people to build electric sports cars like the Tesla Roadster that changed the image of electric vehicles for the better.

Tesla went on to produce the model S: an upmarket electric car with good looks, range, and specs. The Model S has now started to displace many conventional car types in the upper car segment. It is inferior in the sense that it has limited range (450 km per charge), takes longer to recharge (about 250 km in 30 min), and offers a less premium finish. But customers—especially people interested in new technology with access to either private parking or a public charger close to their house—liked that it had unparalleled acceleration (faster than the fastest production sports car) and was silent and clean [133]. Once they owned the vehicle they noticed how they loved charging at home (which they did more than 90% of the time) and how the range was not really an issue [133].

The price of the batteries was still too high to make a mid-level car but the success of the Model S enabled Tesla to build a Gigafactory for batteries (together with Panasonic) that brought prices down [134]. Government subsidies and charging infrastructure are currently also vital [135]. But prognoses show that electric vehicles will soon be cheaper to own due to falling battery prices, low energy use, and low maintenance [135, 136] after which displacement will continue without subsidies. This example contains a number of dynamics that an energy transition management model should be able to capture.

3.3. Transition Management. In our view, transition management enriches theories on agent-based economics and disruptive innovation with political and sociological insights. It also specifically addresses lock-in of fossil technologies. Energy transition management was born from the observation that transitions to new technologies often fail to materialize, even if they are beneficial to society. In order to change this, transition management researchers aim to "develop appraisal and valuation techniques that could inform a choice between different technologies" from the vantage point of societal benefit [137]. Later this technology focus was extended to "interconnected systems of artefacts, institutions, rules and norms" and especially on how to make systems transition in response to environmental signals [138].

Recent overviews of the field are given by Sengers et al. [139], Li et al. [140], and Holtz et al. [141]. According to Li et al.: "Today's most influential body of innovation-focused transition research originates in the Netherlands, and is often called the "Dutch approach". Approaches that descended from the Dutch school are transition management (TM), strategic niche management (SNM), technological innovation systems (TIS), and the multilevel perspective (MLP)." These approaches are particularly suited for investigating sociotechnical transitions in the energy supply, buildings, and transport sectors, as they focus on means of supplanting the incumbent system with radical alternatives, disruption of the status quo, and the initiation of rapid change.

If this paper refers to transition management, this is meant to include SNM, MLP, and TIS. All these approaches focus on regime resistance from incumbents and how

protected niches can function as incubators for beneficial innovation [142–144]. SNM [145, 146] draws on evolutionary economics [147, 148] and had high ambitions (although the originators concede that "we were certainly over-optimistic about the potential of SNM as a tool for transition" [149]). MLP [150] focusses on the fact that change is required at multiple levels at the same time. As the name implies, the study of technological innovation systems (TIS) [151] is focused on technology instead of on the energy transition as a whole [152, 153]. However, since the energy transition is driven in part by these technological innovation systems, their integration into transition management yields powerful synergies [154, 155].

Transition management sets out to explore radically new ways to meet societal needs for, for example, energy or mobility [156, 157] and draws heavily on the ideas of Malina and Kauffman [158] regarding complexity [159]. It combines many of the aspects of the other approaches and gives special focus to individuals and organizations that are aligned to both the innovative technology and the societal goal (e.g., sustainability) since it is them (and not members of the incumbent regime) that will drive the change [160, 161]. However, this requires "multiple explicit actors with differentiated selection criteria and behavioral parameters that possess agency to shape transitions" [140]. An intriguing new idea is to use the transition management perspective in conjunction with crises to create "game changers" [162].

Currently, transition management models are usually qualitative in nature. Drawing on Holtz et al. [141] we conclude that quantified transition management models are needed because they improve internal consistency [163–165] and enable validation of theory [166–168]. Models can also enhance participatory processes [169, 170] while challenging incorrect narratives [171] and bringing relevant factors into scope [172, 173]. Finally, quantified models would increase the use of transition management by policy-makers which is needed because currently it is used only rarely [141].

4. Modelling Requirements

In this section we present the requirements for energy transition management modelling that we deduce from the theory in the previous section first about modelling actors, then about modelling technologies, and finally about carbon pricing.

4.1. Requirements for Actors

4.1.1. Detailed and Heterogeneous Actors. According to transition management (esp. MLP), there is a range of transition pathways. Geels et al. [174–176] identify the following:

(1) Transformation: incumbents adjust some regime rules under pressure of, for example, social movements, for example, the adoption of carbon capture and storage (CCS).

(2) Technological substitution: novelties are developed before incumbents act and they are replaced within the regime, for example, electric vehicles and large scale solar.

(3) Reconfiguration: a range of novelties is adopted by incumbents and this deeply changes the regime, for example, self-driving vehicles, supergrids, and smart grids.

(4) De- and realignment: landscape pressure, uncertainty, and multiple novelties lead to a new regime, for example, solar plus storage replaces centralized energy systems with autarkic micro grids.

We find that models that strongly aggregate and simplify actors mostly capture the first type of pathway. Transition management can capture all pathways by viewing transitions as driven by *specific innovators* that are part of a *niche* and resisted by *specific incumbents* that are part of a *regime*. But this requires heterogeneous actors that are modelled in detail.

Furthermore, the actors possess *agency.* The transition management view of *agency* could be characterized as follows: "Never doubt that a small group of thoughtful committed citizens can change the world. Indeed, it is the only thing that ever has" [177]. In transition management it is the actor that goes against the grain that is the nucleus for change (together with technological breakthroughs), whether at the global level (e.g., Henry Ford, Steve Jobs, or Elon Musk) or at the local level (e.g., a community organizer or buyer of solar panels and electric vehicles). At first the *innovator* is part of a *niche.* A niche is created when the innovator is joined by a group of actors that are open to the innovation. After a while the bottom-up innovation can grow out of the niche to become a new incumbent. The implication of this idea is that change is caused by (groups of) actors that diverge from the mainstream. So actors especially that might act as innovators or early adopters must be modelled in detail.

But not all actors are individuals. Important actors in the energy transition are governments, knowledge institutions, corporations, and NGOs [178, 179].

Different stages of the transition see different innovators as its drivers. For example, solar cells were first developed for satellites, then adopted for buoys and ships, then adopted by households in sunny countries with high electricity prices, and only now are they becoming the cheapest form of energy in wholesale installations. In each phase the innovator was a different actor.

The importance of bottom-up modelling can also be illustrated by the way we have adopted new technologies like PCs, the Internet, mobile phones, and digital cameras. Every one of these trends surprised incumbents [180] and such trends are typically underpredicted by economic (top-down) models [181]. A similar underestimation is currently happening regarding PV, EV, and wind. If we switched our perspective to the actors actually adopting the new technology—because they perceive a benefit—this would remove the problem of underestimating change.

A way to gather the relevant actors and behaviors suitable to transition management could be to conduct interviews, focus groups, and surveys among human actors and organizations that could be instigators for change and to make sure that the diversity of their behaviors and interactions is captured in the model. An example would be smart-grid users [182]. Representation and aggregation would only be

acceptable if a valid line of reasoning suggests it does not diminish the ability of nonstandard actors to instigate or resist change. When the model is ready the modeller should preferably return to the flesh and blood versions of the actors represented in the model and gather their feedback on how well they are represented.

4.1.2. Interacting and Learning Actors. A characteristic of particular interest is how actors interact with each other and the physical infrastructure.

In sociotechnical systems interrelations are important and determine, for example, the success of innovative entrepreneurs [183]. Innovation is spread by actors interacting and learning from each other [184, 185]. Interactions with the physical environment are just as important. For example, people cannot put solar panels on their roof if they do not have a roof and for some countries the adoption of land based wind power is easy (like the USA) while for others off-shore wind is more logical (like the UK and the Netherlands). In transportation the importance of geographical locations and infrastructure is even more obvious. For example, adoption of electric vehicles is less for actors that depend on public charging infrastructure that does not materialize. Finally, actors can learn. An example of this is that people seem to like electric vehicles better with experience [186].

An approach we would recommend is to copy a representative set of environments of interest (e.g., neighborhoods) in which actors can "live" and interact in a realistic fashion. For example, when modelling electric vehicle charging you would model houses, parking places, and charging stations and give actors realistic buying, charging, and driving behaviors. Realistic computerized neighborhoods can provide a scaffold for scenarios in which the modeller is forced to "face reality" and it is beneficial in interactions with domain experts and policy-makers because it provides them a recognizable interface.

4.1.3. Actors with Foresight and Strategizing. Transition management actors need foresight and strategy. For example, Karl Benz had the foresight to develop the internal combustion engine (but would have gone bankrupt if his wife had not had the foresight that he needed buyers so she kidnapped the prototype to make the world's first "long distance car trip" [187]). Henry Ford faced customers who had no idea what an automobile was but he foresaw the age of the automobile. Elon Musk has claimed at several occasions that he started Tesla because he thought he could prove that electric cars were cool, even though he considered the chances of success for the company to be less than 10%.

A more statistically relevant example is investment in solar panels. The investment is now more than hundreds of billions of euros which is only rational if the investors have considered a longer time frame and exponential developments.

Regime actors can also use foresight to stave off challenges to the status quo, for example, by sponsoring scientists that support their view and by paying lobbyists and politicians that help to keep/make the playing field uneven.

4.2. Requirements for Technologies

4.2.1. Realistic, Disaggregated with Endogenous Learning. Transition management models require a "disaggregated portfolio of technology options with different price and performance characteristics that function within operational boundaries and face resource constraints" [140]. In practical terms, each individual technology should be modelled as a separate bottom-up contender for adoption, including all the characteristics determining its adoption such as the space practically available and the measures needed to overcome intermittency (like storage and smart charging of electric vehicles).

Especially important is the inclusion of learning curves as detailed in the previous theory section. Learning curves can be exogenous or endogenous. An example is the analysis of learning curves of batteries by Nykvist and Nilsson [188]. They present an exogenous feedback loop where the costs of battery production are declining by 8–14% *per year*. Then his endogenous feedback loop shows battery prices declining at 6–9% per *doubling of production capacity*. The second curve is called an endogenous feedback loop because it feeds on itself *within* the model: an increase in battery sales would lead to a corresponding decrease in the price of batteries which could lead to an increase in battery sales, and so on. Models that assume endogenous technical change frequently recommend much more aggressive carbon abatement policies and see a much quicker and less costly replacement of fossil fuels by sustainable alternatives. A review of 25 well known models concludes that the impact is significant [189].

Feedback loops can be negative (dampening the reaction of the system) or positive (quickly taking the system to new states). Positive feedback loops are important because "they generate a much richer variety of trajectories which the system may follow" [190]. One objective of transition management models is to enable policy-makers to spot and then accelerate positive feedback they deem beneficial, for example, by protecting niches (when they have the potential to provide powerful positive feedback) from regime resistance until they are self-propelling.

Another aspect is the facilitation of bottom-up adoption that leads to the emergence of new pathways. Top-down models "tend to be more pessimistic than bottom-up models about the costs of energy policies. This is related to the difference in the scope and potential for energy efficiency improvements as well as the treatment of technological change" [181]. Verbong and Geels [175] describe how different pathways can lead to different solutions, for example, either to micro grids, smart grids, or supergrids [176, 191]. By allowing new pathways to emerge in a bottom-up manner, transition models allow us to find better ways forward.

4.2.2. Use of Real World Technological Experts. When translating the real world into a model it is valuable to do it in such a way that the model is easy to understand for real world experts. Then modellers (e.g., economists) and experts (e.g., engineers) could work together. Let us take PV as an example.

PV production is comprised of many subprocesses with different rates of learning. In the case of PV, traditional

cells benefit from our ability to slice ever thinner silicon wafers in an ever more efficient fashion while thin film technologies benefit from breakthroughs in printing cells on a flexible substrate. Experts could help us judge those different learning curves. They could also double-check them based on predicted raw material usage. In the case of PV, a silicon wafer that makes up a solar cell has a minimum thickness and can never become cheaper than the silicon it is made off. The fragile wafers also require a rigid (e.g., glass) encapsulation of a certain thickness. That is why many experts predict that thin flexible film will win out over silicon wafers in the long run. But things can change: when the price of silicon skyrocketed a few years ago the PV industry developed newer and simpler processes specifically for PV (instead of borrowing from the processes used to make CPUs) that now produce solar silicon significantly cheaper than before. So, we have to keep monitoring and updating our models. Using models that closely resemble reality makes it possible to interact with domain experts that can help us with that.

This leads us to R&D. One could argue that Einstein's Nobel prize winning explanation of the photoelectric effect paved the way and that our current computer models of quantum gaps and the way we apply machine learning to the simulation of digital composites are an important factor in the constant PV breakthroughs. R&D has the advantage of being relatively cheap (compared to scaling up production) but the disadvantage of being relatively slow (especially fundamental research at universities). Thus, investing in more PV R&D might be a very cost-effective way to increase learning rates in the long run but it requires foresight. Experts could help us to incorporate the possible impact of R&D in our models.

But although domain experts are vital, there is a catch. Experts are just as critical of paradigm changing feedback loops as ordinary humans and can have a stronger than average status quo bias [52] and system justification bias [53]. Maybe that is why science is said to progress "one funeral at the time" and why the science fiction writer Clarke proclaimed his "first law" to be as follows: "When a distinguished scientist states that something is possible, he is almost certainly right. When he states that something is impossible, he is very probably wrong" [192]. These biases can combine with groupthink that exacerbates confirmation bias [51] and are in turn exacerbated by shared information bias [193], especially when the group is seeking consensus [193]. In short: experts tend to be conservative, especially in groups.

For this reason, the model should follow the knowledge of experts when capturing the dynamics and constraints of the technology but predictions about the future should be based on where the model leads us, and that will probably surprise both us and the experts.

4.2.3. Externalities of Imperfect Markets. Externalities are costs or benefits (usually costs) that are not internalized in the transaction under review. For example, we know that burning coal fuel and eating meat contributes to climate change but the costs of climate change are not incorporated in the price of coal or meat. This means that producers can offer fossil fuels and meat at low prices and that society as a whole picks up the tab.

Governments could remove these market imperfections by levying taxes, using a principle often called *the polluter pays*. But this causes regime resistance, for example, from the producers and consumers of fossil fuels and meat. We also face a prisoner's dilemma in the sense that industries in the first country to adopt taxes would find it hard to compete with industries from other countries that did not adopt the taxes. So, taxes that are beneficial on a global level can be detrimental on the national level if some countries opt out.

Transition management models looking for beneficial pathways should assume neither a continuing status quo nor perfect markets. Instead they should focus on the overall costs and benefits of realistic interventions. These costs should be attributed to individual actors on different levels (e.g., the planet, individual nations, and individual producers and consumers) so that resistance and gain are visible on the level of the relevant decision-makers. This holds true for all parts of a transition management model but is especially relevant when modelling technological pathways.

For example, a pathway that assumes erasing subsidies for meat or forcing people not to eat it is highly unrealistic. But subsidizing tasty meat replacement products might be achievable, especially in the early stages when production volume is still low. Investing in R&D towards meat replacements might be even more cost-effective and have a higher chance of collecting the ROI locally. Such a pathway is especially promising if the meat replacement technology has the potential to become cheaper and tastier through the existence of a positive feedback loop. Then it would be able to replace regular meat, even in an imperfect market where the costs to society are not internalized.

Thus, well-crafted transition management models have the potential to shift the dialogue from ideological trench warfare around bland win-lose solutions to an intellectual game where the goal is to discover an achievable win-win pathway. And because the pathway is constructed in a bottom-up manner using recognizable building blocks (instead of impenetrable mathematics) it could also be used to create broader support for the investment opportunities that are involved. It might even convince the meat producer to enter the meat replacement business.

4.3. Requirements for Carbon Pricing. The last set of requirements for models that guide the transition to renewable energy pertain to pricing the damage done by fossil technologies. This section should make the transition management modeller aware of the most important assumptions regarding what is often called the social cost of carbon (SCC).

We propose transition management models should be able to use a different SCC, depending on the actor, for example, a high price for actors focused on the state of the art in science, a medium price for economists, a low price for policy-makers based on what is politically palatable, and a negligible price for companies that have the power to lobby for exemptions. Incidentally this could also be a realistic way to model regime resistance. In an ideal model (not an ideal world), discount rates should be context sensitive and all assumptions should be user configurable. We will illustrate the importance of these points below.

4.3.1. Economists versus Climate Scientists. A meta-analysis of 800 estimates showed a "bias-corrected" SCC of between 0 and 134 dollars while "uncorrected" prices are often much higher [194]. But narrowing it down shows that most economists agree that 37 dollars is a safe lower bound and this is what many policy-makers strive for [195]. The actual price on the EU ETS market at the time of writing was 4 dollars. Why this is important can be illustrated by a simple example. Producing one kWh of electricity from a coal fired power plant emits around one kg of CO_2 [196]. A CO_2 price of 37 dollars per ton would thus lead to a SCC of 3.7 cents per kWh. This would almost double the wholesale price of electricity from coal.

And, actually, the economists are probably underestimating the SCC. Nordhaus (possibly the most influential economist in the field) noticed a deep divide between climate scientists and economists regarding the SCC. He conducted a survey [197] and concluded that "At one extreme are mainstream economists who view the prospect of greenhouse warming with little concern, confident that human societies will adapt handily to such changes. At the other extreme, natural scientists worry about irreversible impacts on natural systems. They warn of unpredictable extreme events, such as shifting ocean currents or migrating monsoons. [Concerning damage] natural scientists' estimates were 20 to 30 times higher."

Climate scientists include tipping points and other nonlinear relationships in their analysis [198] which creates a discontinued risk profile akin to what is used to calculate the fire insurance for a house [8, 40]. This, combined with the limited availability of data, leads statisticians like Ikefuji et al. to apply Weitzman's "Dismal Theorem" [199] which gives the risk profile a relatively "fat tail" like a Student's t distribution [200]. The result is an SCC of hundreds of dollars [201–203]. Economists like Nordhaus dispute the applicability of the Dismal Theorem [204] and treat climate change as a continuous cost subject to cost-benefit analysis (e.g., the price of electricity) to arrive at a much lower SCC. So, the question becomes: who do we trust to estimate the risks of climate change: climate scientists or economists? If we trust the climate scientists or even if we choose a middle ground between them and the economists, the SCC would be so high that fossil fuels would instantly be prohibitively expensive.

4.3.2. Discounting the Future, Hardwiring Inequality, and Pricing the Priceless. The extent to which future damage is taken into account depends on the discount rate [205]. The impact is most easily demonstrated by an example. Assume a damage of *a hundred euros* to people living one hundred years from now. How much should we invest today to prevent that future damage? Many important economists [206–208] argue that we should not burden future generations with our excesses. They thus argue for a discount rate of 0% and want to invest *a hundred euros* now. Stern [8] would advocate for a compromise at 1.4% (higher than what governments pay for a loan but much lower than what banks ask of a company) leading to an investment of *twenty-five euros*. Nordhaus [209] argues that this is an ordinary market transaction and that a prudent rate is 4.3%, which would mean investing little more than *one dollar*. Some consensus seems to be building towards distinguishing between the interest rate on risk capital and a social-welfare-equivalent (e.g., the 1% rate on obligations) for use in SCC [210, 211]. This last approach would validate Stern's *SCC of roughly two hundred euros*. If you look at the previous illustration you will see that this would make electricity from coal five times more expensive. We concur with Kaplow et al. [212] that the discount rate is too important to leave to the modeller because this one assumption can completely alter the output of the model. We contend that the discount rate should be user configurable and in the case of static output (like a paper report) there should at least be a sensitivity analysis present that shows readers what happens when different discount rates are applied.

Another obscure part of SCC calculations is *Negishi welfare weights*. This mechanism basically assures that money cannot leave rich countries to be put to work in poor countries where it would save more lives [213]. Although this corresponds to political reality it is good that the user of the model is aware of this, for example, because it can alert her or him to cost-effective win-win solutions that are now routinely forgotten like protecting ecosystems in their country of origin.

The problem of pricing goes beyond the discounting of poor and future people and ignoring catastrophes. Economics primarily deals with putting a price on goods humans produce and consume and in those cases pricing is relatively clear. But how to put a price on the destruction of ecosystems, loss of biodiversity, depletion of aquifers, desertification of fertile ground, and the relocation of people? Are pandas worth more than bees? Are European woods worth more than rainforests? Must the calculation be based on tourist industry earnings or can things have an intrinsic *dignity* as Immanuel Kant proposed? How many km^2 of rainforest have to disappear before we admit to a link between biofuels and land use change? These are fundamental questions that relate to norms and values that can only be judged subjectively but are currently decided by modellers that hide them from the policy discussion.

Table 1 summarizes the requirements that have been established so far in the paper.

5. Modelling Methods

So far, we have denounced equilibrium models, reviewed theories, and deduced requirements. Now it is time to describe how better models actually work.

There are myriad ways to characterize what is happening in energy modelling [28, 214–216]. Even the classification of the underlying simulation methods is diverse [217, 218]. We will take the perspective of Borshchev and others [218–220] to create a narrative describing how modelling techniques for sociotechnical systems has become more realistic over time with the help of computers.

5.1. From Static to Dynamic Systems. Energy transition management models focus on "transition pathway dynamics: assessment of normative goals; radical alternatives to incumbent status quo technology or behavior options; time

horizons sufficient for exploring long-term sociotechnical change; and path dependencies" [140]. We saw that equilibrium models cannot produce such pathways. System dynamics (SD) offers a big step forward. SD models consist of an ordered set of differential and algebraic equations that model stocks (also called states) connected by flows (signals: inputs and outputs) [221]. This approach became practical after the advent of computers. Originally SD was implemented on analog computers where op-amps represented the differential equations but it soon turned to digital computers [222].

As described under technologies, some of the most interesting dynamics in transition management occur when the model contains endogenous learning curves for technology. For example, the adoption of PV leads to economies of scale that make it cheaper, which leads to more adoption, and so on. In static modelling this is a problem because it can lead to so-called algebraic loops for which an analytical solution can only be found using nonlinear optimization. This problem often occurs in energy models [223]. If time derivatives are added to the model, as is the case with SD models, the feedback mechanisms can easily be incorporated.

SD models are widely used in biology, chemistry, and engineering [224] with notable examples in mechatronics [225], multibody vehicle dynamics [226], and the spread of disease [227] and also in the social sciences with notable examples being marketing [228]; policy analysis [229]; project management [230]; and learning [231, 232]. Many people know SD from the study "Limits of Growth" that drew attention to the ecological problems caused by humanities ever-increasing use of natural resources [233, 234]. SD has also been widely applied to energy models [235–241]. Within transition management it is mainly used in the context of technical innovation systems [152, 155, 242–245]. But uptake is lagging behind original expectations. In 2007 Forrester—one of the founders of SD—sketched a picture in which SD had to leave its current plateau and climb new mountains. He was especially disappointed by the lack of use in economics and the public sector [246].

A relevant characteristic for transition management is that SD models contain stocks. For example, in a country the existence of roads, houses, fertile ground, and aquifers that provide sweet water can be modelled as stocks that represent value. Even soft factors like a shared culture and trust in government and democracy are stocks vital to wealth that could in theory be modelled. Monitoring stocks is especially important for environmental models. For example, the build-up of pollutants or greenhouse gasses, the depletion of aquifers, or the effects of land use change due to the use of biomass.

After adding the dynamic of time, we should add the dynamic of space. In energy systems the spatial distribution of energy production, transportation, and use is highly relevant [139, 247–250]. For example, electricity is produced by power plants, windmills, and solar panels at certain locations, transported by a geographically distributed power grid that poses practical costs and constraints and used by agent and machines like residents and electric vehicles that can all be a bit different.

If this was all the dynamism we were after we could use discrete event simulations (DES). As the name implies, DES processes the simulation one event at a time [251] and it is well known for things like complex and spatially distributed queuing problems and Goldratt's *theory of constraints* [252]. Simply put: if you want to model an assembly line or airport, DES is probably your first choice.

DES is more recent than SD because it is even more dependent on computers: calculating every event and constantly updating the state and position of every product is computationally intensive, especially since models can no longer be reduced.

In most developed countries the geographic layout of these subsystems has been described and is now publicly available in the form of shapefiles. We can create a spatial environment with many layers that connect events in space. Let us give an example. Electric vehicles can use the road layer to determine how long they have to travel. The building layer tells us where the residents live and we choose a parking place close to that location. The grid layer gets activated as soon as the electric vehicle starts charging, and so on. In this way a many-layered GIS file enables us to create complex, realistic, integral models with relative ease.

Realistic geographic environments are also valuable when the modeller interacts with domain experts or policy-makers. Running the model on a recognizable geographical substrate is visually stimulating, makes it easier to understand what is happening in the model, supports the detection of unrealistic behaviors, and creates trust in the model results.

5.2. From Dynamic to Complex Adaptive Systems. But this is still not enough. Researchers now know that many domains, and certainly energy and mobility, need to be studied as complex adaptive systems (CAS) [253]. The first thing to understand about CAS is that the system itself is constantly adapting. You must model the system in a bottom-up manner using autonomous actors and their behaviors in space and time, and as the actors interact with each other and their physical environment, systemic order *emerges*. (This cannot be modelled in system dynamics or discrete event simulation [254].) Although top-down control of this order is absent, it is *adaptive* in the sense that individual and collective behavior can *mutate* and *self-organize* in order to create a system that can be more *robust* [255] and *resilient* [256] than comparable systems with top-down control. The Internet is a good example [257].

Biology was among the early adopters since CAS was able to portray ecologies with complex behavior emerging from simple rules. Wilson used it to popularize sociobiology [258], Dawkins to explain selfish genes [259], and Goodwin and Saunders to improve developmental biology [260]. In chemistry Prigogine used CAS to increase our understanding of dissipative structures and irreversibility [261]. In particle physics, famous adherents were Feynman and Gell-Mann [262]. CAS was even used successfully in philosophy [263]. Holland and Reitman used CAS to create genetic algorithms [264] while Holland also wrote one of the best introductions to CAS [265, 266] and created the often used definition of "systems that have a large number of components, often called agents, that interact and adapt or learn" [267].

Although early ideas pointing to CAS can be found in sociology [268] the uptake in the social sciences was slow [269] and it took until 1996 for it to be applied to social systems by Epstein and Axtell [270] and Axelrod [271, 272]. In economics Tesfatsion played a pivotal role from 1998 onwards [59] while 2006 was a "golden year" with the handbook on Agent-Based Computational Economics [55] and powerful arguments by Foster [58] and Beinhocker [273].

Properties of complex systems that *emerge* from the interplay between underlying processes [274] are highly relevant to transition models [174]. Transition management, SNM, and MLP view the transition to renewable energy and sustainable transportation as "a radical, structural change of a societal (sub)system that is the result of a coevolution of economic, cultural, technological, ecological, and institutional developments at different scale levels" [159] which require a complex adaptive multilevel multidimensional systems approach [158, 275, 276].

Complex adaptive systems can change their ontology. In transition management this is indicated by the term deep uncertainty [277–279]. Examples are the introduction of a radically new technology (e.g., electric vehicles) that replaces an old technology or the rise of a new kind of actor (e.g., prosumers). This is something that is relatively easy to model in agent-based simulation but (almost) impossible to do using other methods.

5.3. Agent-Based Modelling. We already spoke at length about Agent-Based Computational Economics. But how do agent-based models work exactly?

First it is good to appreciate that complex adaptive systems are counterintuitive for primate brains due to nonlinearity, feedback, time delays, and interdependencies [231]. Various empirical studies have demonstrated the severity of the problem [280–284]. Fortunately, there are ways to simulate complex adaptive systems using a computer [270, 285, 286] so now we can begin to understand them [287].

Models that accomplish this are called *agent-based models* (ABMs). Although one could theoretically trace ABM back to the Von Neumann machine, the first real ABM (using coins on a board) was Schelling's segregation model from 1969 [288]. After some experiments in the 80s by, among others, Axelrod and Reynolds it was Holland and Miller who used the term "agent" for the first time in 1991 [289] and it was only in 1996 that Epstein and Axtell [270] and Axelrod [271] explicitly introduced ABMs to the social sciences. Axelrod and Epstein both called it a third way of doing science [272, 290]: generative and bottom-up and distinct of the usual inductive or deductive approaches. In recent years an increasing number of reviews note their promise for advancing the social sciences [291, 292]. And, as we already saw, ABM is increasingly used in economics.

ABM is now well accepted in empirical social research [293] and the preferred modelling method for sociotechnical systems [294, 295]. Recent reviews note that ABM is now widely used, for example, in health [296] and more specifically oncology [297]; epidemiology [298]; chronic [299] and noncommunicable diseases [300]. Other reviews look at their use in organizational science [301]; emergency response [302]; land use [303, 304]; manufacturing [305]; ecosystem management [306]; and marketing [228, 307].

Energy systems are a particularly fertile area for ABM with reviews in the fields of energy modelling in general [253, 308–310], smart grids [311–313], electricity markets [314–316], distributed generation [317], and transportation [318–321]. A recent review of transition management models found one DES, six SDs, and seven ABMs [140] which is remarkable considering that in the modelling world at large DES and SD are still much more common than ABM.

The reasoning of these agents is becoming increasingly complex. In most cases we find task oriented actors to be the most efficient and easy to understand implementation but many authors advocate explicitly programming different agent states [219] and some like to rely on the belief-intent-desire model [322–324]. Niches, incumbents, and regime resistance can be modelled with relative ease but should ideally not be represented by aggregates but by the individual actors that they consist of in reality. It is also relatively easy to model disaggregate technologies (including endogenous learning curves) and radical innovation, driven by entrepreneurs and policy-makers with strategy and foresight but slowed down with regime actors possessing the same.

5.4. Multilevel Agent-Based Models. Finally transition management models need to be multilevel. In the multilevel perspective (MLP) that we already described, the upper level is often called *the landscape*, the intermediate level *the regime,* and the bottom level the *niche* [150, 191, 325, 326].

On the global level we have issues like climate change, the Paris treaty, and technological developments. The latter are of special interest to transition management models, for example, price developments in silicon solar cells, off-shore wind, heat pumps, NCM batteries, and electric vehicles. We also have R&D breakthroughs about to get out of the laboratory like metal-air batteries, solar fuels, airborne wind energy, and the application of "wonder materials" like graphene. All these developments have the power to shape what happens at other levels by making renewable technologies more attractive to actors on lower levels.

There are many possible intermediate levels, for example, a cooperation that together buys solar panels and heat pumps; or an industry site or municipality that decides to develop an integral energy plan for dealing with heat, electricity, a wind park, and electric mobility, making the combined business case much easier; or a country that decides to promote EVs and change rules and regulations to enable self-driving vehicles.

On the bottom level we have, for example, small companies, households, and persons that can develop, buy, and use solar panels, heat pumps, and electric vehicles. They can also invest or divest in technologies. Their decisions drive the energy transition on all levels but are influenced by developments on higher levels.

We could theoretically model every actor in the world but that would be impossible to program and compute. By choosing a multilevel approach we can choose representative actors on every level and scale, for example, with one actor per global policy and technology, a couple of countries

and municipalities on the intermediate level, and maybe a thousand individuals on the bottom level.

In Table 2 we give an overview of the types of systems and their characteristics as discussed in this paper.

6. Building a Model

We have shown the requirements and methods needed for transition models, but how do you actually build them? This question might appear too practical for a scientific paper, until you realize how little valuable advice is available in the literature and how important this step is for the successful development of a model. This chapter aims to make the knowledge gap in the literature a little smaller.

6.1. Learn from Professional Programmers. Every scientist has a habit of undertaking rigorous literature study but the tools and development trajectories are often chosen less rigorously. We think that, in this respect, modellers should learn from people who are able to work in large teams to develop models containing millions of lines of codes: professional programmers. There are strong similarities between object oriented (OO) programming and ABM and it is no coincidence that the dozens of ABM frameworks we know are all written in OO languages. Terms in an OO language like Java often have an equivalent in ABM, for example, object/agent, class/species, and method/action [327]. That is fortunate because OO is now the de facto standard in large software projects because it makes code manageable and does not create "spaghetti code" [328]. We would suggest that, similarly, ABM is optimal for most modelling challenges because it does not produce "spaghetti models." So, ABM might be the right approach not only for modelling complex adaptive systems but also for other large modelling projects. Using ABM as an organizing principle akin to OO makes it easier to divide the model into independent agents (akin to objects) and to hide their inner workings (using *encapsulation*). One could even encapsulate entire models. Agents can be hotlinked and used in cosimulations.

Choosing your agents is similar to choosing your objects in object oriented programming. The right choice depends on the modelling situation and/or question. However, we feel we can provide some general guidelines, especially since we advocate the use of ABM as a container for other modelling approaches. From a modelling perspective agents should make independent decisions [271, 329, 330]. Humans (e.g., consumers) and institutions or organizations (e.g., households, governments, or energy producers) are logical choices. But agents do not have to be self-conscious. For example, an electric power line could be an agent that "decides" when it is overloaded, thus causing a blackout. From a programming perspective, agents should be viewed as chunks of code that can be developed independently. Using OO principles such agents should have well defined interfaces that are used to initiate behaviors. In this way new agents can be added to the model without impacting the other code in the model.

Of course, it is important to choose a good programming framework and because agent-based modelling (ABM) is such a recent phenomenon, those frameworks are still immature. There are literally dozens of competing ABM frameworks in which the modeller is basically programming directly in an object oriented (OO) language like Java [331]. However, we found that using a dedicated language developed specifically for ABM can greatly enhance productivity [332] (we estimate a factor of ten) and make ABM more accessible to modellers without a computer science background. A language developed for a specific application is called a "domain specific language." MATLAB and R are examples of tools (but not ABM tools) that use a domain specific language. The best-known framework using a language especially developed for ABM is called Netlogo. However, we chose the GAMA-platform because it combines the ease of use of Netlogo with the maturity of Java (e.g., building on Eclipse). It also has advanced spatial capabilities (e.g., read and "agentify" shapefiles). Like Netlogo it is free and open source which enables users to extend the domain specific language. Some ABM frameworks are specialized even further (e.g., for smart grids [333]) but we would warn against their use because it inhibits the development of integral models [176].

A key lesson from open source projects is that making the underlying code directly downloadable provides much better error detection and makes it much easier to collaborate on models. For scientific projects and public policy, especially in the important and often politicized case of energy models, the transparency provided by open source models might be even more important [334]. We would go as far as to say that downloadable models are like peer-review for the 21st century. Combining agent-based and their inherent modularity with open source also makes it much easier to create large integrative models. It is worrisome that policy recommendations are often provided by consulting firms that do not disclose their funding or provide their underlying model. If transition management modellers are serious about unleashing bottom-up change and governing the energy transition [335] they should lead by example and share their code online.

6.2. Create Hybrid Models When Needed. Many authors point to the added capabilities from ABM over equation based models [298, 336] and more specifically equilibrium models [20, 55, 217, 337]. Simply put: complex systems can be implemented in ABMs but not in equilibrium models. However, it *is* possible to include equilibrium models in ABMs. That it is *possible* does not mean it is *advisable* and making an ABM that expresses the equilibrium paradigm is probably just a bad idea [19]. However, comodelling simulations are increasingly common [338, 339] and we could imagine scenarios where equilibrium driven agents are part of a larger complex adaptive model [55, 337, 340].

Implementing the stocks and flows of system dynamics (SD) in an agent-based model (ABM) is much more straightforward: simply create an agent for every stock and flow. In most cases you could also model just the stocks and include the flows as behaviors of the agent minding the stock. Heterogeneity can now be added by splitting up stocks into separate agents. For example, instead of one agent representing a shoal of fishes we might create separate agents that represent a single fish. Some fishes might then

be different than others and might be differently processed (e.g., by releasing accidentally netted dolphins). Even more realism can be added by giving each agent a unique location in space. For example, instead of one "flow agent" signifying "fishing" the model could contain multiple agents signifying "fishing boats." The amount of fish caught could depend on the concentration of fish in that part of the ocean. One application where SD and ABM can be combined is integrated assessments [341, 342].

Similarly implementing discrete event stimulation (DES) in an ABM is easy. Both are inherently location based and can work with maps on which the entities in the simulation have a clearly defined position. In DES the events are implemented using active entities that have a fixed position in space. Instead of theoretically continuous flows of SD, DES uses discrete passive entities that are processed by the active entities. Products that are processed by humans and machines at an assembly line is a typical example. When implementing DES in ABM you would simply instantiate each active entity as an agent with behaviors and each passive entity as an agent without behaviors. However, in ABM the passive entities could also be made active. For example, when modelling a queue of people, an ABM would enable you to give some of them behavior like walking away, talking to each other, or starting a row.

The idea of combining SD, DES, and ABM is so logical that the firm Anylogic markets its product as a tool that can use all three paradigms [286] but as we showed this is possible in any ABM.

6.3. Create Quantified Narratives. Agent-based models make it easy to add geographic layers, agents, behaviors, and variables. The advantage is that we can avoid the falsified simplifications of equilibrium theory but it also creates a confusing amount of freedom. We think the solution is the use of clear *quantified narratives*. Narratives can contain a rich tapestry of variables in a way that is meaningful and memorable to the human brain, and transition management already has a tendency to tell stories [146]. We propose combining the narrative approaches used in the famous Shell scenario studies [343] with the quantitative transition management models as described in this paper that clarify, validate, and quantify the narrative.

Another reason to use the quantified narrative approach is that it enables us to explain what the model is doing to experts and policy-makers. That is needed because the integral and multidisciplinary models that we have to create in order to find the best pathways and interventions towards renewable energy require a *lot* of expertise. Fortunately, ABMs represent reality in a way that is easy to understand for domain experts and with quantified narratives it is also possible to explain what the model is doing. We think every ABM should be checked by experts to get *face validity*. This might not seem like a rigorous test but as we have seen with the example of the IEA prediction of solar power this is a test that many of the most influential models cannot pass.

7. Outlook

The transition from fossil fuels to renewable energy is a complex global challenge. Technologies like off-shore solar, airborne wind, battery storage, smart grids, and shared self-driving electric vehicles are developing quickly. They are driven by R&D, investors with foresight, users that function as early adopters, and learning curves that can become self-sustaining. Transition theory also draws attention to the ways in which innovators in niches compete with incumbent regimes and how this can lead to entirely different system configurations.

Such developments might lead to a range of very different pathways. Global warming might accelerate and this might either unite or divide humanity. Realistic carbon pricing or the price reduction of renewables might lead to stranded fossil assets and an early collapse of the fossil system. The energy system could become local and decentralized with users becoming producers that share energy and storage on demand. Mobility might become a service that replaces fossil cars by small, shared, self-driving vehicles. Developing countries without existing infrastructure might leapfrog developed countries and so on.

The modelling approach described in this paper should—at least in theory—be able to capture these dynamics in quantitative models. The agent-based modelling paradigm could also facilitate comodelling, where multidisciplinary teams of experts work together using a suite of new or existing models. Combined with object oriented programming techniques—that already allow us to collaborate on millions of lines of code—we might be able to create powerful models that uncover pathways towards a sustainable energy future that is both more realistic and more interesting than what is currently offered. We hope this paper will inspire some students, teachers, researchers, policy-makers, and entrepreneurs to do just that.

Conflicts of Interest

The authors declare that there are no conflicts of interest regarding the publication of this paper.

Acknowledgments

Auke Hoekstra gratefully acknowledges the sponsoring for this research from the ElaadNL foundation.

References

[1] R. K. Pachauri and L. Mayer, "Intergovernmental panel on climate change," in *Climate Change 2014: Synthesis Report*, Intergovernmental Panel on Climate Change, Geneva, Switzerland, 2015.

[2] Paris Agreement, Wikipedia, 2017.

[3] Energy Modeling, Wikipedia, 2017.

[4] "Lazard's Levelized Cost of Energy Analysis".

[5] P. Dowling and M. Gray, "End of the Load for Coal and Gas? Challenging Power Technology Assumptions," *Carbon Tracker*, 2016.

[6] D. Coady, I. Parry, L. Sears, and B. Shang, "How large are global fossil fuel subsidies?" *World Development*, vol. 91, pp. 11–27, 2017.

[7] L. Merrill, *Tackling Fossil Fuel Subsidies And Climate Change: Levelling the Energy Playing Field*, Nordic Council of Ministers, 2015.

[8] N. Stern, "The economics of climate change: the stern review," *The Economics of Climate Change: The Stern Review*, pp. 1–692, 2007.

[9] J. Blazejczak, F. G. Braun, D. Edler, and W.-P. Schill, "Economic effects of renewable energy expansion: a model-based analysis for Germany," *Renewable & Sustainable Energy Reviews*, vol. 40, pp. 1070–1080, 2014.

[10] D. Connolly, H. Lund, and B. V. Mathiesen, "Smart energy europe: the technical and economic impact of one potential 100% renewable energy scenario for the european union," *Renewable & Sustainable Energy Reviews*, vol. 60, pp. 1634–1653, 2016.

[11] G. Escribano Francés, J. M. Marín-Quemada, and E. San Martín González, "RES and risk: Renewable energy's contribution to energy security. a portfolio-based approach," *Renewable & Sustainable Energy Reviews*, vol. 26, pp. 549–559, 2013.

[12] D. Scholten and R. Bosman, "The geopolitics of renewables; exploring the political implications of renewable energy systems," *Technological Forecasting & Social Change*, vol. 103, pp. 273–283, 2016.

[13] N. S. Hetherington, "Isaac newton's influence on adam smith's natural laws in economics," *Journal of the History of Ideas*, vol. 44, no. 3, pp. 497–505, 1983.

[14] D. A. Walker, "Walrasian economics," *Walrasian Economics*, pp. 1–357, 2006.

[15] J. B. Shoven and J. Whalley, "A general equilibrium calculation of the effects of differential taxation of income from capital in the U.S.," *Journal of Public Economics*, vol. 1, no. 3-4, pp. 281–321, 1972.

[16] R. A. Chumacero and K. S. Hebbel, "General equilibrium models: an overview," *Doc. Trab. Banco Cent. Chile*, vol. 307, 2004.

[17] M. E. Burfisher, *Introduction to Computable General Equilibrium Models*, Cambridge University Press, 2017.

[18] A. M. Borges, "Applied general equilibrium models: an assessment of their usefulness for policy analysis," *OECD Econ. Stud*, vol. 1986, p. 43, 1986.

[19] G. Fagiolo and A. Roventini, "Macroeconomic policy in DSGE and agent-based models redux: New developments and challenges ahead," *JASSS*, vol. 20, no. 1, article no. 1, 2017.

[20] V. Mosini, *Equilibrium in Economics: Scope and Limits*, Routledge, 2008.

[21] L. Bergman, "Chapter 24 CGE modeling of environmental policy and resource management," in *Handbook of Environmental Economics*, M. K.-G and J. R. Vincent, Eds., vol. 3, pp. 1273–1306, Elsevier, 2005.

[22] P. J. Kehoe and T. J. Kehoe, "A primer on static applied general equilibrium models," *Fed. Reserve Bank Minneap. Q. Rev.-Fed. Reserve Bank Minneap*, vol. 18, no. 2, p. 2, 1994.

[23] A. S. Hosny, "Survey of recent literature on CGE trade models: with special reference to the case of egypt," *Journal of World Economic Research*, vol. 2, no. 1, p. 9, 2013.

[24] C. Böhringer, T. F. Rutherford, and W. Wiegard, "Computable general equilibrium analysis: Opening a black box," *ZEW - Zentrum für Europäische Wirtschaftsforschung/Center for European Economic Research, ZEW Discussion Paper*, pp. 3–56, 2003.

[25] F. S. Mishkin, "Will monetary policy become more of a science?" *The Science and Practice of Monetary Policy Today: The Deutsche Bank Prize in Financial Economics 2007*, pp. 81–103, 2010.

[26] M. Goodfriend, "How the world achieved consensus on monetary policy," *Journal of Economic Perspectives (JEP)*, vol. 21, no. 4, pp. 47–68, 2007.

[27] J. Galí and M. Gertler, "Macroeconomic modeling for monetary policy evaluation," *Journal of Economic Perspectives (JEP)*, vol. 21, no. 4, pp. 25–45, 2007.

[28] A. Herbst, F. Toro, F. Reitze, and E. Jochem, "Introduction to energy systems modelling," *Swiss Journal of Economics and Statistics*, vol. 148, no. 2, pp. 111–135, 2012.

[29] E. A. Stanton, F. Ackerman, and S. Kartha, "Inside the integrated assessment models: four issues in climate economics," *Climate and Development*, vol. 1, no. 2, pp. 166–184, 2009.

[30] C. Read, *Logic, Deductive and Inductive*, Grant Richards, 1st edition, 1898.

[31] D. Colander, R. P. F. Holt, and J. B. Rosser Jr., "The changing face of mainstream economics," *Review of Political Economy*, vol. 16, no. 4, pp. 485–499, 2004.

[32] C. A. E. Goodhart, "The continuing muddles of monetary theory: A steadfast refusal to face facts," *Economica*, vol. 76, no. 1, pp. 821–830, 2009.

[33] A. Kirman, "The economic crisis is a crisis for economic theory," *CESifo Economic Studies*, vol. 56, no. 4, Article ID ifq017, pp. 498–535, 2010.

[34] D. Colander et al., The financial crisis and the systemic failure of academic economics, 2009.

[35] P. Krugman, *How Did Economists Get It So Wrong?* The New York Times, 2009.

[36] R. J. Caballero, "Macroeconomics after the crisis: time to deal with the pretense-of- knowledge syndrome," *Journal of Economic Perspectives (JEP)*, vol. 24, no. 4, pp. 85–102, 2010.

[37] G. Dosi and A. Roventini, "The irresistible fetish of utility theory: from "pleasure and pain" to rationalising torture," *Intereconomics*, vol. 51, no. 5, pp. 286-287, 2016.

[38] F. Ackerman, "Still dead after all these years: interpreting the failure of general equilibrium theory," *Journal of Economic Methodology*, vol. 9, no. 2, pp. 119–139, 2002.

[39] T. Balint, F. Lamperti, A. Mandel, M. Napoletano, A. Roventini, and A. Sapio, "Complexity and the economics of climate change: a survey and a look forward," *Ecological Economics*, vol. 138, pp. 252–265, 2017.

[40] F. Ackerman, *Can We Afford the Future?: the Economics of a Warming World*, Zed Books, 2009.

[41] R. S. Pindyck, "Climate change policy: what do the models tell us?" *Journal of Economic Literature*, vol. 51, no. 3, pp. 860–872, 2013.

[42] K. Arrow, M. Cropper, C. Gollier et al., "Determining benefits and costs for future generations," *Science*, vol. 341, no. 6144, pp. 349-350, 2013.

[43] R. L. Revesz, P. H. Howard, K. Arrow et al., "Global warming: improve economic models of climate change," *Nature*, vol. 508, no. 7495, pp. 173–175, 2014.

[44] S. Dietz and N. Stern, "Endogenous growth, convexity of damage and climate risk: How Nordhaus' framework supports deep cuts in carbon emissions," *Economic Journal*, vol. 125, no. 583, pp. 574–620, 2015.

[45] J. D. Farmer, C. Hepburn, P. Mealy, and A. Teytelboym, "A third wave in the economics of climate change," *Environmental and Resource Economics*, vol. 62, no. 2, pp. 329–357, 2015.

[46] N. Stern, "Economics: current climate models are grossly misleading," *Nature*, vol. 530, no. 7591, pp. 407–409, 2016.

[47] B. Fatih, *World Energy Outlook 2016*, International Energy Agency, 2016.

[48] International Energy Agency, *World Energy Model Documentation*, International Energy Agency, 2016.

[49] K. Johnsen, *Solar Power, Electricity Grids, Energy Models and the World Energy Model - Why Is Solar Underestimated in the WEM of the IEA*, The University of Bergen, 2016.

[50] Perspectives for the Energy Transition, xOECD/IEA and IRENA, 2017.

[51] R. S. Nickerson, "Confirmation bias: a ubiquitous phenomenon in many guises," *Review of General Psychology*, vol. 2, no. 2, pp. 175–220, 1998.

[52] W. Samuelson and R. Zeckhauser, "Status quo bias in decision making," *Journal of Risk and Uncertainty*, vol. 1, no. 1, pp. 7–59, 1988.

[53] J. T. Jost, M. R. Banaji, and B. A. Nosek, "A decade of system justification theory: accumulated evidence of conscious and unconscious bolstering of the status quo," *Political Psychology*, vol. 25, no. 6, pp. 881–919, 2004.

[54] R. R. Nelson, "Recent evolutionary theorizing about economic change," *Journal of Economic Literature*, vol. 33, no. 1, pp. 48–90, 1995.

[55] L. Tesfatsion and K. L. Judd, Eds., *Handbook of Computational Economics Volume 2: Agent-Based Computational Economics*, vol. 13 of *Handbooks in Economics*, Elsevier/North-Holland, 2006.

[56] L. Tesfatsion, "Agent-based computational economics: growing economies from the bottom up.," *Artificial Life*, vol. 8, no. 1, pp. 55–82, 2002.

[57] J. D. Farmer and D. Foley, "The economy needs agent-based modelling," *Nature*, vol. 460, no. 7256, pp. 685-686, 2009.

[58] J. Foster, "Why is economics not a complex systems science?" *Journal of Economic Issues*, vol. 40, no. 4, pp. 1069–1091, 2006.

[59] L. Tesfatsion, *Agent-Based Computational Economics: A Brief Guide to the Literature*, Iowa State Univ., 1998.

[60] D. A. Robalino and R. J. Lempert, "Carrots and sticks for new technology: abating greenhouse gas emissions in a heterogeneous and uncertain world," *Integrated Assessment*, vol. 1, no. 1, pp. 1–19, 2000.

[61] C. C. Jaeger, K. Hasselmann, G. Leipold, D. Mangalagiu, and J. D. Tàbara, "Reframing the problem of climate change: from zero sum game to win-win solutions," *Reframing the Problem of Climate Change: From Zero Sum Game to Win-Win Solutions*, pp. 1–258, 2013.

[62] G. Dosi and R. R. Nelson, "Technical change and industrial dynamics as evolutionary processes," *Handbook of the Economics of Innovation*, vol. 1, no. 1 C, pp. 51–127, 2010.

[63] M. D. Gerst, P. Wang, A. Roventini et al., "Agent-based modeling of climate policy: an introduction to the ENGAGE multi-level model framework," *Environmental Modeling and Software*, vol. 44, pp. 62–75, 2013.

[64] B. Rengs, M. Scholz-Wäckerle, A. Gazheli, M. Antal, J. van den Bergh, and M. Scholz-Wäckerle, "Testing innovation, employment and distributional impacts of climate policy packages in a macro-evolutionary systems setting," 2015, http://www.foreurope.eu/fileadmin/documents/pdf/Workingpapers/WWWforEurope_WPS_no080_MS19.pdf.

[65] S. C. Isley, R. J. Lempert, S. W. Popper, and R. Vardavas, "An Evolutionary Model of Industry Transformation and the Political Sustainability of Emission Control Policies," 2013, https://www.rand.org/pubs/technical_reports/TR1308.html.

[66] D. W. Bunn and J. I. Muñoz, "Supporting the externality of intermittency in policies for renewable energy," *Energy Policy*, vol. 88, pp. 594–602, 2016.

[67] M. Raberto, B. Ozel, L. Ponta, A. Teglio, and S. Cincotti, "From financial instability to green finance: the role of banking and monetary policies in the Eurace model, 2016".

[68] D. Helbing, "Globally networked risks and how to respond," *Nature*, vol. 497, no. 7447, pp. 51–59, 2013.

[69] L. Brouwers, K. Hansson, H. Verhagen, and M. Boman, "Agent models of catastrophic events," in *Modelling Autonomous Agents in a Multi-Agent World, 10th European workshop on Multi Agent Systems*, 2001.

[70] S. Hallegatte, "An adaptive regional input-output model and its application to the assessment of the economic cost of Katrina," *Risk Analysis*, vol. 28, no. 3, pp. 779–799, 2008.

[71] R. Bierkandt, L. Wenz, S. N. Willner, and A. Levermann, "Acclimate—a model for economic damage propagation. Part 1: basic formulation of damage transfer within a global supply network and damage conserving dynamics," *Environment Systems and Decisions*, vol. 34, no. 4, pp. 507–524, 2014.

[72] L. Wenz, S. N. Willner, R. Bierkandt, and A. Levermann, " Acclimate—a model for economic damage propagation. Part II: a dynamic formulation of the backward effects of disaster-induced production failures in the global supply network," *Environment Systems and Decisions*, vol. 34, no. 4, pp. 525–539, 2014.

[73] A. Haas and C. Jaeger, "Agents, bayes, and climatic risks - A modular modelling approach," *Advances in Geosciences*, vol. 4, pp. 3–7, 2005.

[74] A. Mandel, S. Fürst, W. Lass, F. Meissner, C. Jaeger, and S. Fürst, "Lagom generic: an agent-based model of growing economies," in *European Climate Forum, Working Paper*, vol. 1, 2009.

[75] S. Wolf, S. Fürst, A. Mandel et al., "A multi-agent model of several economic regions," *Environmental Modelling & Software*, vol. 44, pp. 25–43, 2013.

[76] F. Lamperti, G. Dosi, M. Napoletano, A. Roventini, and A. Sapio, "Faraway, so close: coupled climate and economic dynamics in an agent-based integrated assessment model," 2017.

[77] R. Smead, R. L. Sandler, P. Forber, and J. Basl, "A bargaining game analysis of international climate negotiations," *Nature Climate Change*, vol. 4, no. 6, pp. 442–445, 2014.

[78] M. A. Janssen and E. Ostrom, "Chapter 30 governing social-ecological systems," in *Handbook of Computational Economics*, L. Tesfatsion and K. L. Judd, Eds., vol. 2, pp. 1465–1509, 2006.

[79] R. Lempert, J. Scheffran, and D. F. Sprinz, "Methods for long-term environmental policy challenges," *Global Environmental Politics*, vol. 9, no. 3, pp. 106–133, 2009.

[80] M. Janssen and B. De Vries, "The battle of perspectives: a multi-agent model with adaptive responses to climate change," *Ecological Economics*, vol. 26, no. 1, pp. 43–65, 1998.

[81] D. C. Earnest, "Coordination in large numbers: an agent-based model of international negotiations," *International Studies Quarterly*, vol. 52, no. 2, pp. 363–382, 2008.

[82] S. Greeven, O. Kraan, É. J. L. Chappin, and J. H. Kwakkel, "The emergence of climate change mitigation action by society: an agent-based scenario discovery study," *JASSS*, vol. 19, no. 3, article no. 9, 2016.

[83] S. C. Isley, R. J. Lempert, S. W. Popper, and R. Vardavas, "The effect of near-term policy choices on long-term greenhouse gas transformation pathways," *Global Environmental Change*, vol. 34, pp. 147–158, 2015.

[84] J. Sun and L. Tesfatsion, "Dynamic testing of wholesale power market designs: an open-source agent-based framework," *Computational Economics*, vol. 30, no. 3, pp. 291–327, 2007.

[85] A. Weidlich and D. Veit, "A critical survey of agent-based wholesale electricity market models," *Energy Economics*, vol. 30, no. 4, pp. 1728–1759, 2008.

[86] E. Guerci, M. A. Rastegar, and S. Cincotti, "Agent-based modeling and simulation of competitive wholesale electricity markets," in *Handbook of Power Systems II*, pp. 241–286, Springer, Berlin, Germany, 2010.

[87] M. Saguan, N. Keseric, P. Dessante, and J.-M. Glachant, "Market power in power markets: Game theory vs. agent-based approach," in *Proceedings of the 2006 IEEE PES Transmission and Distribution Conference and Exposition: (TDC'06)*, August 2006.

[88] E. Guerci and S. Sapio, "Comparison and empirical validation of optimizing and agent-based models of the Italian electricity market," in *Proceedings of the 2011 8th International Conference on the European Energy Market, EEM 11*, pp. 849–856, May 2011.

[89] G. Sáenz de Miera, P. del Río González, and I. Vizcaíno, "Analysing the impact of renewable electricity support schemes on power prices: the case of wind electricity in Spain," *Energy Policy*, vol. 36, no. 9, pp. 3345–3359, 2008.

[90] A. Banal-Estañol and A. Rupérez Micola, "Behavioural simulations in spot electricity markets," *European Journal of Operational Research*, vol. 214, no. 1, pp. 147–159, 2011.

[91] O. Browne, S. Poletti, and D. Young, "How does market power affect the impact of large scale wind investment in 'energy only' wholesale electricity markets?" *Energy Policy*, vol. 87, pp. 17–27, 2015.

[92] J. K. Kok, C. J. Warmer, and I. G. Kamphuis, "Powermatcher: multiagent control in the electricity infrastructure," in *Proceedings of the Fourth International Joint Conference on Autonomous Agents and Multiagent Systems*, pp. 75–82, New York, NY, USA, July 2005.

[93] P. Vytelingum, T. D. Voice, S. D. Ramchurn, A. Rogers, and N. R. Jennings, "Agent-based micro-storage management for the smart grid," in *Proceedings of the 9th International Joint Conference on Autonomous Agents and Multiagent Systems 2010 (AAMAS '10)*, pp. 39–46, 2010.

[94] E. Kiesling, M. Günther, C. Stummer, and L. M. Wakolbinger, "Agent-based simulation of innovation diffusion: a review," *Central European Journal of Operations Research*, vol. 20, no. 2, pp. 183–230, 2012.

[95] N. Schwarz and A. Ernst, "Agent-based modeling of the diffusion of environmental innovations - an empirical approach," *Technological Forecasting & Social Change*, vol. 76, no. 4, pp. 497–511, 2009.

[96] A. Faber, M. Valente, and P. Janssen, "Exploring domestic micro-cogeneration in the Netherlands: an agent-based demand model for technology diffusion," *Energy Policy*, vol. 38, no. 6, pp. 2763–2775, 2010.

[97] T. Zhang, S. Gensler, and R. Garcia, "A study of the diffusion of alternative fuel vehicles: an agent-based modeling approach," *Journal of Product Innovation Management*, vol. 28, no. 2, pp. 152–168, 2011.

[98] E. Karakaya, A. Hidalgo, and C. Nuur, "Diffusion of eco-innovations: a review," *Renewable & Sustainable Energy Reviews*, vol. 33, pp. 392–399, 2014.

[99] M. A. Janssen and W. Jager, "Stimulating diffusion of green products - Co-evolution between firms and consumers," *Journal of Evolutionary Economics*, vol. 12, no. 3, pp. 283–306, 2002.

[100] G. Silverberg, G. Dosi, and L. Orsenigo, "Innovation, diversity and diffusion: a self-organisation model," *The Economic Journal*, vol. 98, no. 393, p. 1032, 1988.

[101] P. Windrum, T. Ciarli, and C. Birchenhall, "Consumer heterogeneity and the development of environmentallyfriendly technologies," *Technological Forecasting & Social Change*, vol. 76, no. 4, pp. 533–551, 2009.

[102] A. Tavoni, A. Dannenberg, G. Kallis, and A. Löschel, "Inequality, communication, and the avoidance of disastrous climate change in a public goods game," *Proceedings of the National Acadamy of Sciences of the United States of America*, vol. 108, no. 29, pp. 11825–11829, 2011.

[103] F. Vona and F. Patriarca, "Income inequality and the development of environmental technologies," *Ecological Economics*, vol. 70, no. 11, pp. 2201–2213, 2011.

[104] B. Maya Sopha, C. A. Klöckner, and E. G. Hertwich, "Exploring policy options for a transition to sustainable heating system diffusion using an agent-based simulation," *Energy Policy*, vol. 39, no. 5, pp. 2722–2729, 2011.

[105] M. Bleda and M. Valente, "Graded eco-labels: A demand-oriented approach to reduce pollution," *Technological Forecasting & Social Change*, vol. 76, no. 4, pp. 512–524, 2009.

[106] J. Schumpeter, *Capitalism, Socialism and Democracy*, Routledge, 2013.

[107] R. N. Foster, *Innovation: The Attackers Advantage*, Summit Books, New York, NY, USA, 1986.

[108] J. M. Utterback and W. J. Abernathy, "A dynamic model of process and product innovation," *Omega* , vol. 3, no. 6, pp. 639–656, 1975.

[109] W. B. Arthur, "Competing technologies, increasing returns, and lock-in by historical events," *The Economic Journal*, vol. 99, no. 394, p. 116, 1989.

[110] V. Vinge, *Marooned in Realtime*, Bluejay Books, 1986.

[111] R. Kurzweil, *Age of Spiritual Machines: When Computers Exceed Human Intelligence*, Penguin, New York, NY, USA, 1st edition, 1999.

[112] R. Kurzweil, "The Law of Accelerating Returns," in *Alan Turing: Life and Legacy of a Great Thinker*, C. Teuscher, Ed., pp. 381–416, Springer, Berlin, Germany, 2004.

[113] J. A. Mathews and E. S. Reinert, "Renewables, manufacturing and green growth: energy strategies based on capturing increasing returns," *Futures*, vol. 61, pp. 13–22, 2014.

[114] L. E. Yelle, "The learning curve: historical review and comprehensive survey," *Decision Sciences*, vol. 10, no. 2, pp. 302–328, 1979.

[115] A. B. Atkinson and J. E. Stiglitz, "A new view of technological change," *The Economic Journal*, vol. 79, no. 315, pp. 573–578, 1969.

[116] M. J. Anzanello and F. S. Fogliatto, "Learning curve models and applications: literature review and research directions," *International Journal of Industrial Ergonomics*, vol. 41, no. 5, pp. 573–583, 2011.

[117] C. A. Mack, "Fifty years of moore's law," *IEEE Transactions on Semiconductor Manufacturing*, vol. 24, no. 2, pp. 202–207, 2011.

[118] A. J. C. Trappey, C. V. Trappey, H. Tan, P. H. Y. Liu, S.-J. Li, and L.-C. Lin, "The determinants of photovoltaic system costs: an evaluation using a hierarchical learning curve model," *Journal of Cleaner Production*, vol. 112, pp. 1709–1716, 2016.

[119] J. L. Bower and C. M. Christensen, "Disruptive technologies: catching the wave," *Long Range Planning*, vol. 28, no. 2, p. 155, 1995.

[120] C. M. Christensen, *The Innovators Dilemma*, Harvard Business School Press, 1997.

[121] C. M. Christensen, M. E. Raynor, and R. McDonald, "What Is Disruptive Innovation?" *Harvard Business Review*, 2015, https://hbr.org/2015/12/what-is-disruptive-innovation.

[122] R. Meyer and E. J. Johnson, "Empirical generalizations in the modeling of consumer choice," *Marketing Science*, vol. 14, no. 3_supplement, pp. G180–G189, 1995.

[123] R. Adner and D. Levinthal, "Demand heterogeneity and technology evolution: implications for product and process innovation," *Management Science*, vol. 47, no. 5, pp. 611–628, 2001.

[124] R. N. Stern, J. Pfeffer, and G. Salancik, "The external control of organizations: a resource dependence perspective," *Social Science Research Network, Rochester*, vol. 8, no. 4, p. 612, 1978.

[125] R. Adner, "When are technologies disruptive? a demand-based view of the emergence of competition," *Strategic Management Journal*, vol. 23, no. 8, pp. 667–688, 2002.

[126] J. B. Barney, "Strategic factor markets: expectations, luck, and business strategy," *Management Science*, vol. 32, no. 10, pp. 1231–1241, 1986.

[127] R. Amit and P. J. H. Schoemaker, "Strategic assets and organizational rent," *Strategic Management Journal*, vol. 14, no. 1, pp. 33–46, 1993.

[128] G. S. Becker, "Investment in human capital :a theoretical analysis," *Journal of Political Economy*, vol. 70, pp. 9–49, 1962.

[129] G. C. Unruh, "Understanding carbon lock-in," *Energy Policy*, vol. 28, no. 12, pp. 817–830, 2000.

[130] G. C. Unruh, "Escaping carbon lock-in," *Energy Policy*, vol. 30, no. 4, pp. 317–325, 2002.

[131] D. G. Victor, "The politics of fossil-fuel subsidies," *Social Science Research Network, Rochester*, 2009.

[132] G. C. Unruh and J. Carrillo-Hermosilla, "Globalizing carbon lock-in," *Energy Policy*, vol. 34, no. 10, pp. 1185–1197, 2006.

[133] A. Hoekstra, Characteristics of Dutch EV drivers, 2017.

[134] E. Musk, *The Secret Tesla Motors Master Plan (just between you and me [Master, thesis]*, 2006.

[135] A. Hoekstra, Modelling the Total Cost of Ownership of Electric Vehicles in the Netherlands, 2017.

[136] Bloomberg Finance, *Electric Vehicle Outlook 2017*, Bloomberg New Energy Finance, 2017.

[137] B. Elzen, F. Geels, and K. Green, *System Innovation and the Transition to Sustainability*, Edward Elgar Publishing, 2004.

[138] F. Berkhout, A. Smith, and A. Stirling, "Socio-technological regimes and transition contexts," *Syst. Innov. Transit. Sustain. Theory Evid. Policy Edw. Elgar Chelten*, vol. 44, no. 106, pp. 48–75, 2004.

[139] F. Sengers, A. J. Wieczorek, and R. Raven, "Experimenting for sustainability transitions: a systematic literature review," *Technological Forecasting & Social Change*, 2015.

[140] F. G. N. Li, E. Trutnevyte, and N. Strachan, "A review of socio-technical energy transition (STET) models," *Technological Forecasting & Social Change*, vol. 100, pp. 290–305, 2015.

[141] G. Holtz, F. Alkemade, F. De Haan et al., "Prospects of modelling societal transitions: position paper of an emerging community," *Environmental Innovation and Societal Transitions*, vol. 17, pp. 41–58, 2015.

[142] I. Bailey and G. A. Wilson, "Theorising transitional pathways in response to climate change: Technocentrism, ecocentrism, and the carbon economy," *Environment and Planning A*, vol. 41, no. 10, pp. 2324–2341, 2009.

[143] S. Jolly, R. Raven, and H. Romijn, "Upscaling of business model experiments in off-grid PV solar energy in India," *Sustainability Science*, vol. 7, no. 2, pp. 199–212, 2012.

[144] A. Smith and R. Raven, "What is protective space? reconsidering niches in transitions to sustainability," *Research Policy*, vol. 41, no. 6, pp. 1025–1036, 2012.

[145] R. Kemp, J. Schot, and R. Hoogma, "Regime shifts to sustainability through processes of niche formation: the approach of strategic niche management," *Technology Analysis and Strategic Management*, vol. 10, no. 2, pp. 175–195, 1998.

[146] J. Schot and F. W. Geels, "Strategic niche management and sustainable innovation journeys: theory, findings, research agenda, and policy," *Technology Analysis and Strategic Management*, vol. 20, no. 5, pp. 537–554, 2008.

[147] G. Dosi, "Technological paradigms and technological trajectories. a suggested interpretation of the determinants and directions of technical change," *Research Policy*, vol. 11, no. 3, pp. 147–162, 1982.

[148] R. R. Nelson and S. G. Winter, *An Evolutionary Theory of Economic Change, Digitally Reprinted*, The Belknap Press of Harvard Univ. Press, Cambridge, UK, 2004.

[149] R. Hoogma, R. Kemp, and J. Schot, "Experimenting for sustainable transport," *The Approach of Strategic Niche Management*, 2002.

[150] F. W. Geels, "Technological transitions as evolutionary reconfiguration processes: A multi-level perspective and a case-study," *Research Policy*, vol. 31, no. 8-9, pp. 1257–1274, 2002.

[151] B. Carlsson and R. Stankiewicz, "On the nature, function and composition of technological systems," *Journal of Evolutionary Economics*, vol. 1, no. 2, pp. 93–118, 1991.

[152] A. Bergek, M. Hekkert, and S. Jacobsson, "Functions in innovation systems: a framework for analysing energy system dynamics," in *Innovation for a Low Carbon Economy: Economic*, Edward Elgar Publishing, 2008.

[153] F. W. Geels, M. P. Hekkert, and S. Jacobsson, "The dynamics of sustainable innovation journeys," *Technology Analysis and Strategic Management*, vol. 20, no. 5, pp. 521–536, 2008.

[154] T. Meelen and J. Farla, "Towards an integrated framework for analysing sustainable innovation policy," *Technology Analysis and Strategic Management*, vol. 25, no. 8, pp. 957–970, 2013.

[155] J. Markard and B. Truffer, "Technological innovation systems and the multi-level perspective: towards an integrated framework," *Research Policy*, vol. 37, no. 4, pp. 596–615, 2008.

[156] S. van den Bosch and J. Rotmans, Deepening, Broadening and Scaling up: a Framework for Steering Transition Experiments, 2008.

[157] F. Alkemade, M. P. Hekkert, and S. O. Negro, "Transition policy and innovation policy: friends or foes?" *Environmental Innovation and Societal Transitions*, vol. 1, no. 1, pp. 125–129, 2011.

[158] R. F. Malina and S. Kauffman, *At Home in the Universe: The Search for Laws of Self-organization and Complexity*, Oxford University Press, 1995.

[159] J. Rotmans and D. Loorbach, "Complexity and transition management," *Journal of Industrial Ecology*, vol. 13, no. 2, pp. 184–196, 2009.

[160] J. Schot, L. Kanger, and G. Verbong, "The roles of users in shaping transitions to new energy systems," *Nature Energy*, vol. 1, no. 5, p. 16054, 2016.

[161] S. van den Bosch, "Transition Experiments: Exploring societal changes towards sustainability," 2010.

[162] D. Loorbach, F. Avelino, A. Haxeltine et al., "The economic crisis as a game changer? Exploring the role of social construction in sustainability transitions," *Ecology and Society*, vol. 21, no. 4, article no. 15, 2016.

[163] J. W. Eising, T. van Onna, and F. Alkemade, "Towards smart grids: identifying the risks that arise from the integration of energy and transport supply chains," *Applied Energy*, vol. 123, pp. 448–455, 2014.

[164] H. de Haan, "The dynamics of functioning investigating societal transitions with partial differential equations," *Computational and Mathematical Organization Theory*, vol. 14, no. 4, pp. 302–319, 2008.

[165] A. Van Der Vooren and F. Alkemade, "Managing the diffusion of low emission vehicles," *IEEE Transactions on Engineering Management*, vol. 59, no. 4, pp. 728–740, 2012.

[166] N. Bergman, L. Whitmash, J. Köhler, M. Schilperoord, and J. Rotmans, "Modelling Socio-Technical Transition Patterns and Pathways," 2008, http://jasss.soc.surrey.ac.uk/11/3/7.html.

[167] G. Holtz and C. Pahl-Wostl, "An agent-based model of groundwater over-exploitation in the Upper Guadiana, Spain," *Regional Environmental Change*, vol. 12, no. 1, pp. 95–121, 2012.

[168] G. Yücel, "Analyzing Transition Dynamics: The Actor-Option Framework for Modelling Socio-Technical Systems," 2010.

[169] K. A. West, "Mediated Modeling: A Systems Approach to Environmental Consensus Building Marjan van den Belt . Mediated Modeling: A Systems Approach to Environmental Consensus Building. Island Press. Washington D.C. 339 paper. 2004. ISBN: 1-55963-961-X.," *Natural Areas Journal*, vol. 26, no. 2, pp. 221-222, 2006.

[170] J. Vennix, *Group Model Building: Facilitating Team Learning Using System Dynamics*, Wiley, New York, NY, USA, 1 edition, 1996.

[171] E. Trutnevyte, J. Barton, Á. O'Grady, D. Ogunkunle, D. Pudjianto, and E. Robertson, "Linking a storyline with multiple models: a cross-scale study of the UK power system transition," *Technological Forecasting & Social Change*, vol. 89, pp. 26–42, 2014.

[172] T. Hansen and L. Coenen, "The geography of sustainability transitions: review, synthesis and reflections on an emergent research field," *Environmental Innovation and Societal Transitions*, vol. 17, pp. 92–109, 2015.

[173] E. Trutnevyte, M. Stauffacher, M. Schlegel, and R. W. Scholz, "Context-specific energy strategies: coupling energy system visions with feasible implementation scenarios," *Environmental Science & Technology*, vol. 46, no. 17, pp. 9240–9248, 2012.

[174] F. W. Geels and J. Schot, "Typology of sociotechnical transition pathways," *Research Policy*, vol. 36, no. 3, pp. 399–417, 2007.

[175] G. P. J. Verbong and F. W. Geels, "Exploring sustainability transitions in the electricity sector with socio-technical pathways," *Technological Forecasting & Social Change*, vol. 77, no. 8, pp. 1214–1221, 2010.

[176] G. Verbong and F. Geels, "Future electricity systems: visions, scenarios and transition pathways," in *Governing the Energy Transition: Reality, Illusion or Necessity?* pp. 203–219, 2012.

[177] M. Mead and M. Margaret, https://en.wikiquote.org/wiki/Margaret_Mead.

[178] T. Piketty, *Capital in the Twenty-First Century*, Harvard University Press, 2017.

[179] M. Mazzucato, *The Entrepreneurial State: Debunking Public Vs. Private Sector Myths*, Anthem Press, 2015.

[180] T. Seba, *Clean Disruption of Energy and Transportation: How Silicon Valley Will Make Oil, Nuclear, Natural Gas, Coal, Electric Utilities and Conventional Cars Obsolete by 2030*, 2014.

[181] Neil Strachan, "UKERC Energy Research Landscape: Energy Systems Modelling," 2011, http://ukerc.rl.ac.uk/Landscapes/Modelling.pdf.

[182] G. P. J. Verbong, S. Beemsterboer, and F. Sengers, "Smart grids or smart users? involving users in developing a low carbon electricity economy," *Energy Policy*, vol. 52, pp. 117–125, 2013.

[183] B. Walrave, K. S. Podoynitsyna, M. Talmar, G. P. Verbong, and A. G. L. Romme, *Technology Ventures And Their Ecosystem within the Socio-Technical Settings: A Systemic Framework*, Catania Italy Univ., Catania, Italy, 2013.

[184] E. M. Rogers, *Diffusion of Innovations*, Simon and Schuster, 4th edition, 2010.

[185] S. O. Negro, F. Alkemade, and M. P. Hekkert, "Why does renewable energy diffuse so slowly? a review of innovation system problems," *Renewable & Sustainable Energy Reviews*, vol. 16, no. 6, pp. 3836–3846, 2012.

[186] F. Schmalfuß, K. Mühl, and J. F. Krems, "Direct experience with battery electric vehicles (BEVs) matters when evaluating vehicle attributes, attitude and purchase intention," *Transportation Research Part F: Traffic Psychology and Behaviour*, vol. 46, pp. 47–69, 2017.

[187] Bertha Benz Memorial Route, Wikipedia, 2017.

[188] B. Nykvist and M. Nilsson, "Rapidly falling costs of battery packs for electric vehicles," *Nature Climate Change*, vol. 5, no. 4, pp. 329–332, 2015.

[189] K. Gillingham, R. G. Newell, and W. A. Pizer, "Modeling endogenous technological change for climate policy analysis," *Energy Economics*, vol. 30, no. 6, pp. 2734–2753, 2008.

[190] G. Dosi and Y. Kaniovski, "On "badly behaved" dynamics - Some applications of generalized urn schemes to technological and economic change," *Journal of Evolutionary Economics*, vol. 4, no. 2, pp. 93–123, 1994.

[191] G. P. J. Verbong and F. W. Geels, "Pathways for sustainability transitions in the electricity sector: multi-level analysis and empirical illustration," in *Proceedings of the 2008 1st International Conference on Infrastructure Systems and Services: Building Networks for a Brighter Future, INFRA 2008*, November 2008.

[192] A. C. Clarke, *Profiles of the Future*, Warner Books Inc, New York, NY, USA, 1985.

[193] T. Postmes, R. Spears, and S. Cihangir, "Quality of decision making and group norms," *Journal of Personality and Social Psychology*, vol. 80, no. 6, pp. 918–930, 2001.

[194] T. Havranek, Z. Irsova, K. Janda, and D. Zilberman, "Selective reporting and the social cost of carbon," *Energy Economics*, vol. 51, pp. 394–406, 2015.

[195] O. US EPA, "The Social Cost of Carbon," 2017, https://www.epa.gov/climatechange/social-cost-carbon.

[196] Frauenhofer Institute, "Levelized Cost of Electricity, Fraunhofer Institute for Solar Energy Systems ISE," 2013, http://www.ise.fraunhofer.de/en/publications/studies/cost-of-electricity.html.

[197] W. D. Nordhaus, "Expert opinion on climatic change," *AM.SCI*, vol. 82, no. 1, pp. 45–51, 1994.

[198] T. M. Lenton, H. Held, E. Kriegler et al., "Tipping elements in the Earth's climate system," *Proceedings of the National Adacemy of Sciences of the United States of America*, vol. 105, no. 6, pp. 1786–1793, 2008.

[199] M. Ikefuji, R. J. Laeven, J. Magnus, and C. Muris, "Expected Utility and Catastrophic Risk," *SSRN Electronic Journal*, 2013.

[200] M. L. Weitzman, "Fat tails and the social cost of carbon," *American Economic Review*, vol. 104, no. 5, pp. 544–546, 2014.

[201] J. Pycroft, L. Vergano, C. Hope, D. Paci, and J. C. Ciscar, "A tale of tails: uncertainty and the social cost of carbon dioxide," *Social Science Research Network*, 2011.

[202] I. C. Hwang, R. S. J. Tol, and M. W. Hofkes, "Fat-tailed risk about climate change and climate policy," *Energy Policy*, vol. 89, pp. 25–35, 2016.

[203] S. Dietz and N. Stern, "Endogenous growth, convexity of damage and climate risk: how Nordhaus' framework supports deep cuts in carbon emissions, 2014".

[204] W. D. Nordhaus, "An Analysis of the Dismal Theorem," *Social Science Research Network*, 2009.

[205] R. S. Tol, "The social cost of carbon: trends, outliers and catastrophes," *Social Science Research Network*, 2008.

[206] R. F. Harrod, *Towards a Dynamic Economics*, Macmillan, London, UK, 1948.

[207] A. C. Pigou, *The Economics of Welfare*, Macmillan, London, UK, 1932.

[208] F. P. Ramsey, "A mathematical theory of saving," *The Economic Journal*, vol. 38, no. 152, p. 543, 1928.

[209] W. D. Nordhaus, "A review of the stern review on the economics of climate change," *Journal of Economic Literature (JEL)*, vol. 45, no. 3, pp. 686–702, 2007.

[210] L. H. Goulder and R. C. Williams, "The choice of discount rate for climate change policy evaluation," *Climate Change Economics*, vol. 3, no. 4, p. 1250024, 2012.

[211] R. B. Howarth, "Discounting, uncertainty, and revealed time preference," *Land Economics*, vol. 85, no. 1, pp. 24–40, 2009.

[212] L. Kaplow, E. Moyer, and D. A. Weisbach, "The social evaluation of intergenerational policies and its application to integrated assessment models of climate change," *B.E. Journal of Economic Analysis and Policy*, vol. 10, no. 2, article no. 7, 2010.

[213] E. A. Stanton, "Negishi welfare weights in integrated assessment models: the mathematics of global inequality," *Climatic Change*, vol. 107, no. 3, pp. 417–432, 2011.

[214] C. Spataru, *Whole Energy System Dynamics: Theory, modelling and Policy*, Routledge, 2017.

[215] S. C. Bhattacharyya and G. R. Timilsina, "A review of energy system models," *International Journal of Energy Sector Management*, vol. 4, no. 4, pp. 494–518, 2010.

[216] N. Neshat, M. R. Amin-Naseri, and F. Danesh, "Energy models: methods and characteristics," *J. Energy South. Afr*, vol. 25, no. 4, pp. 101–111, 2014.

[217] C. F. Nicholson, "Review of methods for modelling systems evolution , ILRI," *Working Paper*, 2007.

[218] S. Sumari, R. Ibrahim, N. H. Zakaria, and A. H. Ab Hamid, "Comparing three simulation model using taxonomy: system dynamic simulation, discrete event simulation and agent based simulation, discrete event simulation and agent based simulation," *International Journal of Management Excellence*, vol. 1, no. 3, pp. 54–59, 2013.

[219] A. Borshchev, "The Big Book of Simulation Modeling," 2015, https://www.amazon.com/Big-Book-Simulation-Modeling-Multimethod-ebook/dp/B00YO0K1ZQ/ref=sr_1_2?ie=UTF8&qid=1483289768&sr=8-2&keywords=Borshchev.

[220] R. Maidstone, "Discrete event simulation, system dynamics and agent based simulation: discussion and comparison," *System*, pp. 1–6, 2012.

[221] D. H. Meadows, *Thinking in Systems: A Primer*, Chelsea Green Publishing, 2008.

[222] J. W. Forrester, "The beginning of system dynamics," in *Banquet Talk at the international meeting of the System Dynamics Society*, vol. 13, Stuttgart, Germany, 1989.

[223] J. Köhler, M. Grubb, D. Popp, and O. Edenhofer, "The transition to endogenous technical change in climate-economy models: a technical overview to the innovation modeling comparison project," *Energy*, vol. 27, pp. 17–55, 2006.

[224] S. H. Strogatz, *Nonlinear Dynamics and Chaos: With Applications to Physics, Biology, Chemistry, and Engineering*, Westview Press, 2014.

[225] D. C. Karnopp, D. L. Margolis, and R. C. Rosenberg, *System Dynamics: Modeling, Simulation, and Control of Mechatronic Systems*, John Wiley & Sons, 2012.

[226] W. K. DLR, "Review of Multibody Computer, Codes for Vehicle System Dynamics," *Veh. Syst. Dyn*, vol. 22, pp. 3–31, 1993.

[227] B. C. Dangerfield, "System dynamics applications to european health care issues," *Journal of the Operational Research Society*, vol. 50, no. 4, pp. 345–353, 1999.

[228] G. P. Richardson and P. Otto, "Applications of system dynamics in marketing: editorial," *Journal of Business Research*, vol. 61, no. 11, pp. 1099–1101, 2008.

[229] Y. Barlas, "System dynamics: systemic feedback modeling for policy analysis," *System*, vol. 1, p. 59, 2007.

[230] J. M. Lyneis and D. N. Ford, "System dynamics applied to project management: a survey, assessment, and directions for future research," *System Dynamics Review*, vol. 23, no. 2-3, pp. 157–189, 2007.

[231] J. D. Sterman, "Learning in and about complex systems," *System Dynamics Review*, vol. 10, no. 2-3, pp. 291–330, 1994.

[232] J. D. Sterman, "System dynamics modeling: tools for learning in a complex world," *California Management Review*, vol. 43, no. 4, pp. 8–25, 2001.

[233] D. H. Meadows, D. L. Meadows, J. Randers, and W. W. Behrens, *The Limits to Growth: A report for the Club of Rome's Project on the Predicament of Mankind*, Universe Books, New York, NY, USA, 1972.

[234] G. M. Turner, "A comparison of the limits to growth with 30 years of reality," *Global Environmental Change*, vol. 18, no. 3, pp. 397–411, 2008.

[235] J. Sterman, *The Energy Transition and the Economy: A System Dynamics Approach*, Massachusetts Institute of Technology, 1982.

[236] R. F. Naill, "A system dynamics model for national energy policy planning," *System Dynamics Review*, vol. 8, no. 1, pp. 1–19, 1992.

[237] R. F. Naill, "Managing the energy transition: a system dynamics search for alternatives to oil and gas," *Use of COAL2 Model*, 1977.

[238] A. Ford, "System dynamics and the electric power industry," *System Dynamics Review*, vol. 13, no. 1, pp. 57–85, 1997.

[239] I. Dyner, R. A. Smith, and G. E. Pena, "System dynamics modelling for residential energy efficiency analysis and management," *Journal of the Operational Research Society*, vol. 46, no. 10, pp. 1163–1173, 1995.

[240] A. Aslani, P. Helo, and M. Naaranoja, "Role of renewable energy policies in energy dependency in Finland: system dynamics approach," *Applied Energy*, vol. 113, pp. 758–765, 2014.

[241] K. Chyong Chi, W. J. Nuttall, and D. M. Reiner, "Dynamics of the UK natural gas industry: system dynamics modelling and long-term energy policy analysis," *Technological Forecasting & Social Change*, vol. 76, no. 3, pp. 339–357, 2009.

[242] B. Walrave and R. Raven, "Modelling the dynamics of technological innovation systems," *Research Policy*, vol. 45, no. 9, pp. 1833–1844, 2016.

[243] A. Bergek, S. Jacobsson, B. Carlsson, S. Lindmark, and A. Rickne, "Analyzing the functional dynamics of technological innovation systems: a scheme of analysis," *Research Policy*, vol. 37, no. 3, pp. 407–429, 2008.

[244] V. de Gooyert, E. Rouwette, H. van Kranenburg, E. Freeman, and H. van Breen, "Sustainability transition dynamics: towards overcoming policy resistance," *Technological Forecasting & Social Change*, vol. 111, pp. 135–145, 2016.

[245] T.-H. Kwon, "Strategic niche management of alternative fuel vehicles: a system dynamics model of the policy effect," *Technological Forecasting & Social Change*, vol. 79, no. 9, pp. 1672–1680, 2012.

[246] J. W. Forrester, "System dynamics - The next fifty years," *System Dynamics Review*, vol. 23, no. 2-3, pp. 359–370, 2007.

[247] P. Krugman, "What's new about the new economic geography?" *Oxford Review of Economic Policy*, vol. 14, no. 2, pp. 7–17, 1998.

[248] C. Karlsson, M. Andersson, and T. Norman, *Handbook of Research Methods and Applications in Economic Geography*, Edward Elgar Publishing, 2015.

[249] H. A. Bulkeley, V. C. Broto, and G. A. S. Edwards, *An Urban Politics of Climate Change: Experimentation and the Governing of Socio-Technical Transitions*, Routledge, 2014.

[250] B. Truffer, "The geography of sustainability transitions: Think/act, globally/locally," 2016.

[251] J. Banks, J. S. Carson, and L. Barry, *Discrete-event system simulation*, Pearson, 2005.

[252] E. M. Goldratt and J. Cox, *The Goal: A Process of Ongoing Improvemen*, North River Press, Great Barrington, Mass, USA, 30th edition, 2014.

[253] C. S. Bale, L. Varga, and T. J. Foxon, "Energy and complexity: new ways forward," *Applied Energy*, vol. 138, pp. 150–159, 2015.

[254] T. Lorenz, "Abductive fallacies with agent-based modeling and system dynamics," *Lecture Notes in Computer Science (including subseries Lecture Notes in Artificial Intelligence and Lecture Notes in Bioinformatics): Preface*, vol. 5466, pp. 141–152, 2009.

[255] B. Visser, "Complexity, robustness, and performance: trade-offs in organizational design," *Social Science Research Networ*, 2002.

[256] F. Berkes, J. Colding, and C. Folke, *Navigating Social - Ecological Systems: Building Resilience for Complexity and Change*, Cambridge University Press, Cambridge, UK, 2008.

[257] G. W. Klau and R. Weiskircher, "Robustness and resilience," in *Network Analysis*, U. Brandes and T. Erlebach, Eds., vol. 3418 of *Lecture Notes in Computer Science*, Springer, Berlin,Germany, 2005.

[258] E. O. Wilson, *The Insect Societies*, Harvard University Press, Cambridge, UK, 1971.

[259] R. Dawkins, *The Selfish Gene*, Oxford University Press, 1976.

[260] B. Goodwin and P. Saunders, *Theoretical Biology: Epigenetic and Evolutionary Order from Complex Systems*, Edinburg University Press, 1989.

[261] I. Prigogine, *Introduction to Thermodynamics of Irreversible Processes*, 1967.

[262] M. Gell-Mann, *The Quark and the Jaguar: Adventures in the Simple and the Complex*, 1995.

[263] P. Cilliers and D. Spurrett, "Complexity and post-modernism: understanding complex systems," *South African Journal of Philosophy*, vol. 18, no. 2, pp. 258–274, 1999.

[264] J. H. Holland and J. S. Reitman, "Cognitive Systems Based on Adaptive Algorithms," *SIGART Bull*, no. 63, p. 49, 1977.

[265] F. Fukuyama and J. H. Holland, "Hidden order: how adaptation builds complexity," *Foreign Affairs*, vol. 75, no. 4, p. 137, 1996.

[266] J. H. Holland, *Complexity: A Very Short Introduction*, Oxford University Press, New York, NY, USA, 2014.

[267] J. H. Holland, "Studying complex adaptive systems," *Journal of Systems Science & Complexity*, vol. 19, no. 1, pp. 1–8, 2006.

[268] T. Parsons, É. Durkheim, A. Marshall, and V. Pareto, "The Structure of Social Action. A Study in Social Theory with Special Reference to a Group of Recent European Writers," *Max Weber*, 1937.

[269] R. J. Eidelson, "Complex adaptive systems in the behavioral and social sciences," *Review of General Psychology*, vol. 1, no. 1, pp. 42–71, 1997.

[270] J. Epstein and R. Axtell, *Growing Artificial Societies: Social Science From the Bottom Up (Complex Adaptive Systems)*, Brookings Institution Press, 1996.

[271] R. M. Axelrod, *The Complexity of Cooperation: Agent-Based Models of Competition And Collaboration*, Princeton University Press, Princeton, NJ, USA, 1997.

[272] R. Axelrod, "Advancing the Art of Simulation in the Social Sciences," in *Simulating Social Phenomena*, D. R. Conte, P. D. R. Hegselmann, and P. D. P. Terna, Eds., vol. 456 of *Lecture Notes in Economics and Mathematical Systems*, pp. 21–40, Springer, Berlin, Germany, 1997.

[273] E. D. Beinhocker, *The Origin of Wealth: The Radical Remaking of Economics and What it Means for Bu*, Harvard Business School Press, London, UK, 2007.

[274] D. Elder-Vass, *The Causal Power of Social Structures: Emergence, Structure and Agency*, Cambridge University Press, 2010.

[275] J. Grin, J. Rotmans, and J. Schot, *Transitions to Sustainable Development: New Directions in the Study of Long Term Transformative Change*, Routledge, New York, NY, USA, 1st edition, 2011.

[276] A. Rip and R. Kemp, "Technological change," in *Human Choice and Climate Change*, S. Rayner and E. L. Malone, Eds., pp. 327–399, Battelle Press, 1998.

[277] J. H. Kwakkel, W. E. Walker, and V. A. W. J. Marchau, "Classifying and communicating uncertainties in model-based policy analysis," *International Journal of Technology, Policy and Management*, vol. 10, no. 4, pp. 299–315, 2010.

[278] R. J. Lempert, *Shaping the Next One Hundred Years: New Methods for Quantitative, Long-Term Policy Analysis*, Rand Corporation, 2003.

[279] W. E. Walker, M. Haasnoot, and J. H. Kwakkel, "Adapt or perish: a review of planning approaches for adaptation under deep uncertainty," *Sustainability*, vol. 5, no. 3, pp. 955–979, 2013.

[280] P. W. B. Atkins, R. E. Wood, and P. J. Rutgers, "The effects of feedback format on dynamic decision making," *Organizational Behavior and Human Decision Processes*, vol. 88, no. 2, pp. 587–604, 2002.

[281] B. Brehmer, "Dynamic decision making: human control of complex systems," *Acta Psychologica*, vol. 81, no. 3, pp. 211–241, 1992.

[282] E. Diehl and J. D. Sterman, "Effects of feedback complexity on dynamic decision making," *Organizational Behavior and Human Decision Processes*, vol. 62, no. 2, pp. 198–215, 1995.

[283] D. N. Kleinmuntz, "Information processing and misperceptions of the implications of feedback in dynamic decision making," *System Dynamics Review*, vol. 9, no. 3, pp. 223–237, 1993.

[284] J. D. Sterman, "Modeling managerial behavior: misperceptions of feedback in a dynamic decision making experiment," *Management Science*, vol. 35, no. 3, pp. 321–339, 1989.

[285] M. A. Bedau, "Weak Emergence," *Noûs*, vol. 31, pp. 375–399, 1997.

[286] A. Borshchev, *The Big Book of Simulation Modeling: Multimethod Modeling with Anylogic 6*, AnyLogic, 2013.

[287] J. D. Sterman, "All models are wrong: reflections on becoming a systems scientist," *System Dynamics Review*, vol. 18, no. 4, pp. 501–531, 2002.

[288] T. C. Schelling, "Models of Segregation," *American Economic Review*, vol. 59, no. 2, pp. 488–493, 1969.

[289] J. H. Holland and J. H. Miller, "Artificial adaptive agents in economic theory," *Am. Econ. Rev*, vol. 81, no. 2, pp. 365-71, 1991.

[290] J. M. Epstein, "Agent-based computational models and generative social science," *Complexity*, vol. 4, no. 5, pp. 41–60, 1999.

[291] E. Bonabeau, "Agent-based modeling: methods and techniques for simulating human systems," *Proceedings of the National Acadamy of Sciences of the United States of America*, vol. 99, no. 3, pp. 7280–7287, 2002.

[292] S. De Marchi and S. E. Page, "Agent-based models," *Annual Review of Political Science*, vol. 17, pp. 1–20, 2014.

[293] E. Bruch and J. Atwell, "Agent-based models in empirical social research," *Sociological Methods & Research*, vol. 44, no. 2, pp. 186–221, 2015.

[294] K. H. Van Dam, *Capturing socio-technical systems with agent-based modelling [Ph.D. thesis]*, Delft University of Technology, 2009.

[295] K. H. van Dam, I. Nikolic, and Z. Lukszo, *Agent-Based Modelling of Socio-Technical Systems*, Springer Publishing Company, 2014.

[296] R. Hilscher, "Review of A Spatial Agent-Based Simulation Modeling in Public Health: Design, Implementation, and Applications for Malaria Epidemiology (Wiley Series in Modeling and Simulation)," 2017, http://jasss.soc.surrey.ac.uk/20/1/reviews/2.html.

[297] Z. Wang, J. D. Butner, V. Cristini, and T. S. Deisboeck, "Integrated PK-PD and agent-based modeling in oncology," *Journal of Pharmacokinetics and Pharmacodynamics*, vol. 42, no. 2, pp. 179–189, 2015.

[298] S. R. Sukumar and J. J. Nutaro, "Agent-based vs. equation-based epidemiological models: A model selection case study," in *Proceedings of the 2012 ASE International Conference on BioMedical Computing, BioMedCom 2012*, pp. 74–79, December 2012.

[299] Y. Li, M. A. Lawley, D. S. Siscovick, D. Zhang, and J. A. Pagán, "Agent-based modeling of chronic diseases: a narrative review and future research directions," *Preventing Chronic Disease*, vol. 13, no. 5, article no. E69, 2016.

[300] R. A. Nianogo and O. A. Arah, "Agent-based modeling of noncommunicable diseases: a systematic review," *American Journal of Public Health*, vol. 105, no. 3, pp. e20–e31, 2015.

[301] G. Fioretti, "Agent-based simulation models in organization science," *Organizational Research Methods*, vol. 16, no. 2, pp. 227–242, 2013.

[302] G. I. Hawe, G. Coates, D. T. Wilson, and R. S. Crouch, "Agent-based simulation for large-scale emergency response: a survey of usage and implementation," *ACM Computing Surveys*, vol. 45, no. 1, article no. 8, 2012.

[303] R. B. Matthews, N. G. Gilbert, A. Roach, J. G. Polhill, and N. M. Gotts, "Agent-based land-use models: a review of applications," *Landscape Ecology*, vol. 22, no. 10, pp. 1447–1459, 2007.

[304] D. C. Parker, S. M. Manson, M. A. Janssen, M. J. Hoffmann, and P. Deadman, "Multi-agent systems for the simulation of land-use and land-cover change: a review," *Annals of the Association of American Geographers*, vol. 93, no. 2, pp. 314–337, 2003.

[305] W. Shen, Q. Hao, H. J. Yoon, and D. H. Norrie, "Applications of agent-based systems in intelligent manufacturing: an updated review," *Advanced Engineering Informatics*, vol. 20, no. 4, pp. 415–431, 2006.

[306] F. Bousquet and C. Le Page, "Multi-agent simulations and ecosystem management: a review," *Ecological Modelling*, vol. 176, no. 3-4, pp. 313–332, 2004.

[307] A. Negahban and L. Yilmaz, "Agent-based simulation applications in marketing research: an integrated review," *Journal of Simulation*, vol. 8, no. 2, pp. 129–142, 2014.

[308] T. Ma and Y. Nakamori, "Modeling technological change in energy systems - From optimization to agent-based modeling," *Energy*, vol. 34, no. 7, pp. 873–879, 2009.

[309] E. J. L. Chappin and G. P. J. Dijkema, "Agent-based modelling of energy infrastructure transitions," *International Journal of Critical Infrastructures*, vol. 6, no. 2, pp. 106–130, 2010.

[310] V. Rai and A. D. Henry, "Agent-based modelling of consumer energy choices," *Nature Climate Change*, vol. 6, no. 6, pp. 556–562, 2016.

[311] P. Ringler, D. Keles, and W. Fichtner, "Agent-based modelling and simulation of smart electricity grids and markets - A literature review," *Renewable & Sustainable Energy Reviews*, vol. 57, pp. 205–215, 2016.

[312] R. Roche, B. Blunier, A. Miraoui, V. Hilaire, and A. Koukam, "Multi-agent systems for grid energy management: A short review," in *Proceedings of the 36th Annual Conference of the IEEE Industrial Electronics Society, IECON 2010*, pp. 3341–3346, November 2010.

[313] P. Vrba, V. Marik, P. Siano et al., "A review of agent and service-oriented concepts applied to intelligent energy systems," *IEEE Transactions on Industrial Informatics*, vol. 10, no. 3, pp. 1890–1903, 2014.

[314] F. Sensuß, M. Genoese, M. Ragwitz, and D. Möst, *Energy Sources, Part A: Recovery, Utilization, and Environmental Effects*, Working paper sustainability and innovation, 2007.

[315] R. Marks, "Chapter 27 market design using agent-based models," in *Handbook of Computational Economics*, K. L. Judd, Ed., vol. 2, pp. 1339–1380, Elsevier, 2006.

[316] J. Babic and V. Podobnik, "A review of agent-based modelling of electricity markets in future energy eco-systems," in *Proceedings of the 1st International Multidisciplinary Conference on Computer and Energy Science, SpliTech 2016*, pp. 1–9, July 2016.

[317] J. G. Veneman, M. A. Oey, L. J. Kortmann, F. M. Brazier, and L. J. De Vries, "A review of agent-based models for forecasting the deployment of distributed generation in energy systems," in *Proceedings of the 2011 Grand Challenges on Modeling and Simulation Conference*, pp. 16–21, Vista, CA, USA, June 2011.

[318] B. Chen and H. H. Cheng, "A review of the applications of agent technology in traffic and transportation systems," *IEEE Transactions on Intelligent Transportation Systems*, vol. 11, no. 2, pp. 485–497, 2010.

[319] A. L. C. Bazzan and F. Klügl, "A review on agent-based technology for traffic and transportation," *The Knowledge Engineering Review*, vol. 29, no. 3, pp. 375–403, 2014.

[320] US Department of Transportation, "A Primer for Agent-Based Simulation and Modeling in Transportation Applications," https://www.fhwa.dot.gov/advancedresearch/pubs/13054/13054.pdf.

[321] N. Ronald, R. Thompson, and S. Winter, "Simulating demand-responsive transportation: a review of agent-based approaches," *Transport Reviews*, vol. 35, no. 4, pp. 404–421, 2015.

[322] G. B. Rens, A belief-desire-intention architechture with a logic-based planner for agents in stochastic domains, 2010.

[323] P. Taillandier, E. Amouroux, D. A. Vo, and A.-M. Olteanu-Raimond, "Using belief theory to formalize the agent behavior: application to the simulation of avian flu propagation," in *Principles and Practice of Multi-Agent Systems*, N. Desai, A. Liu, and M. Winikoff, Eds., vol. 7057, pp. 575–587, Springer, Berlin, Germany, 2010.

[324] P. Taillandier, O. Therond, and B. Gaudou, "A new BDI agent architecture based on the belief theory. Application to the modelling of cropping plan decision-making," in *Proceedings of the 6th Biennial Meeting of the International Environmental Modelling and Software Society: Managing Resources of a Limited Planet, iEMSs 2012*, pp. 2463–2470, July 2012.

[325] R. Walz, J. H. Köhle, C. Lerch, and J. H. Köhler, "Towards modelling of innovation systems: An integrated TIS-MLP approach for wind turbines," *Fraunhofer Institute for Systems and Innovation Research (ISI)*, 2016.

[326] L. Coenen, R. Raven, and G. Verbong, "Local niche experimentation in energy transitions: a theoretical and empirical exploration of proximity advantages and disadvantages," *Technology in Society*, vol. 32, no. 4, pp. 295–302, 2010.

[327] GAMA User Manual, 2017, http://gama-platform.org/.

[328] B. Eckel, *Thinking in Java*, Prentice Hall, 4th edition, 2006.

[329] K. H. van Dam, I. Nikolic, and Z. Lukszo Springer Science & Business Media, 2012.

[330] A. Drogoul, D. Vanbergue, and T. Meurisse, "Multi-agent based simulation: where are the agents?" in *Multi-agent-based simulation II*, vol. 2581, pp. 1–15, Springer, 2003.

[331] "Comparison of agent-based modeling software," Wikipedia, 2017.

[332] D. B. Borenstein, "A composite constraints approach to declarative agent-based modeling," 2015, https://arxiv.org/abs/1503.08880.

[333] G. Basso, N. Gaud, F. Gechter, V. Hilaire, and F. Lauri, "A framework for qualifying and evaluating smart grids approaches: focus on multi-agent technologies," *Smart Grid and Renewable Energy*, vol. 4, no. 4, pp. 333–347, 2013.

[334] Leopoldina - Nationale Akademie der Wissenschaften, acatech - Deutsche Akademie Technikwissenschaften, and Union der Deutschen Akademien der Wissenschaften, Consulting with energy scenarios: requirements for scientific policy advice, 2016.

[335] G. Verbong and D. Loorbach, *Governing the Energy Transition*, 2012.

[336] H. V. D. Parunak, R. Savit, and R. L. Riolo, "Agent-Based Modeling vs. Equation-Based Modeling: A Case Study and Users' Guide," in *Multi-Agent Systems and Agent-Based Simulation*, J. S. Sichman, R. Conte, and., and N. Gilbert, Eds., pp. 10–25, Springer, Berlin, Germany, 1998.

[337] M. Lengnick, "Agent-based macroeconomics: a baseline model," *Journal of Economic Behavior & Organization*, vol. 86, pp. 102–120, 2013.

[338] N. Q. Huynh, H. X. Huynh, A. Drogoul, and C. Cambier, "Co-modeling: an agent-based approach to support the coupling of heterogeneous models," in *Nature of Computation and Communication*, P. C. Vinh, E. Vassev, and M. Hinchey, Eds., vol. 144, pp. 156–170, Springer International Publishing, 2014.

[339] A. Drogoul, N. Q. Huynh, and Q. C. Truong, "Coupling environmental, social and economic models to understand land-use change dynamics in the mekong delta," *Frontiers in Environmental Science*, vol. 4, 2016.

[340] A. Caiani, A. Russo, A. Palestrini, and M. Gallegati, *Economics with Heterogeneous Interacting Agents: A Practical Guide to Agent-Based Modeling*, Springer, 2016.

[341] R. A. Kelly et al., "Selecting among five common modelling approaches for integrated environmental assessment and management," *Environ. Model. Softw*, vol. 47, pp. 159–181, 2013.

[342] B. de Vries, "Interacting with complex systems: models and games for a sustainable economy," 2017, http://dspace.library.uu.nl/handle/1874/203530.

[343] P. J. Schoemaker and C. A. van der Heijden, "Integrating scenarios into strategic planning at Royal Dutch/Shell," *Planning Review*, vol. 20, no. 3, pp. 41–46, 1992.

Hindawi
Complexity
Volume 2017, Article ID 7494313, 24 pages
https://doi.org/10.1155/2017/7494313

Research Article

Assessing the Plurality of Actors and Policy Interactions: Agent-Based Modelling of Renewable Energy Market Integration

Marc Deissenroth, Martin Klein, Kristina Nienhaus, and Matthias Reeg

German Aerospace Center, Institute of Engineering Thermodynamics, Department of Systems Analysis and Technology Assessment, Pfaffenwaldring 38-40, 70569 Stuttgart, Germany

Correspondence should be addressed to Marc Deissenroth; marc.deissenroth@dlr.de

Received 2 June 2017; Revised 1 September 2017; Accepted 31 October 2017; Published 10 December 2017

Academic Editor: Liz Varga

The ongoing deployment of renewable energy sources (RES) calls for an enhanced integration of RES into energy markets, accompanied by a new set of regulations. In Germany, for instance, the feed-in tariff legislation for renewables has been successively replaced by first optional and then obligatory marketing of RES on competitive wholesale markets. This paper introduces an agent-based model that allows studying the impact of changing energy policy instruments on the economic performance of RES operators and marketers. The model structure, its components, and linkages are presented in detail; an additional case study demonstrates the capability of our sociotechnical model. We find that changes in the political framework cannot be mapped directly to RES operators as behaviour of intermediary market actors has to be considered as well. Characteristics and strategies of intermediaries are thus an important factor for successful RES marketing and further deployment. It is shown that the model is able to assess the emergence and stability of market niches.

1. Introduction

Electricity and heat production are the main sources of worldwide CO_2eq emissions and hence one of the main drivers of anthropogenic climate change [1]. In order to ensure a successful transition of these sectors to carbon-free or low-carbon, a further expansion of the usage of renewable energy sources (RES) is needed [2]. To initiate the necessary investments and changes in technical, organizational, and financial regimes, various policy approaches are being discussed and implemented. In 2016, most countries in the world had RES targets or support policies in place [3].

As one of the earliest examples, the German government has adopted targets for the installation of renewables: by 2025, the share of renewable energy in the electricity sector shall be expanded to 40–45% and to 55–60% by the year 2035 [4]. The most important policy instrument to achieve these targets is the Renewable Energy Sources Act (German: "Erneuerbare Energien Gesetz") (EEG), which was enacted in 2000 [5]. Its longevity and structural stability make it a fruitful case study to investigate energy policy in the field. In its original state, it mainly operated as a feed-in tariff (FiT) law which guaranteed a fixed remuneration for renewable energy sources for electricity (RES-E). It has been effective in fostering the deployment of RES-E [6]. Several amendments and revisions have been undertaken, such as, in 2012, when the German government introduced, for example, a monthly adjustment of feed-in tariffs for solar panels and an optional variable market premium to support the marketing from RES-E at the power exchange [7, 8] (see "The Market Premium" in the appendix).

The main intention of the EEG is to have a regulatory impact on the market conditions and the technoeconomic regime, as well as on the involved market actors who play a key role in the energy system's transition, as they provide the necessary investments in RES-E technologies. However, the invoked investment dynamics were not stable under all circumstances. With the fall of system prices and the accompanying relative sluggish adjustments of incentives, the deployment of solar plants in Germany went up from roughly 2.0 GW in 2008 to 7.5 GW/a in the years 2010–2012. The deployment went back to 1.9 GW in 2014 [9], which created

considerable market distortions and unstable investment behaviour.

The deployment and integration of RES can only be reliably regulated, as long as policy instruments do consider the interdependencies and interactions with and of the involved actors as well as the resulting market interplay on the investment dynamics. The motivation for the development of the agent-based model AMIRIS is therefore to study the adequacy of policy measures which affect the entities that comprise the electricity system; the aim is to examine the impact of policy on the involved market actors on the microlevel (e.g., income situation of renewable power plant operators) as well as their effects on the macrolevel (e.g., power exchange prices and market structure) [10].

The remainder of the paper is structured as follows. In Section 2, we will elaborate on the complexity of the energy system transition, and our motivation to choose an agent-based model (ABM) approach to address our research questions. Section 3 will give a brief overview of the AMIRIS model. For further detail, the technically interested reader can refer to Section 4, which describes the agents and their behaviours in detail. To exemplify the model's capabilities and questions to be addressed, Section 5 presents a case study on the marketing of RES-E at the power exchange and how an amendment of the policy regime affects market actors in different ways. Here we will show how the heterogeneity of agents, for example, different portfolios, affects the income and behaviour of the represented renewable electricity marketers and power plant operators. Section 6 discusses the case study and gives an overview of the lessons learned from the use of the ABM approach. Section 7 concludes with lessons learned from both the case study and the modelling approach in general.

2. Modelling the Complexity of Energy Transitions

2.1. Challenges of Modelling the Impact of Energy Policy Measures on the Behaviour of Actors. The pathway of the development of the global energy system, namely, the anticipated shift of supply from centralized fossil-fuelled power plants towards a decarbonised and RES dominated regime, is uncertain; many possible energy futures are conceivable [12]. Part of the uncertainty of which energy future will materialize results from the unexplored behaviour of the market actors who implement new technologies, as their relationships and intentions remain understudied. Bale et al. [13] state that "Energy systems can be understood as complex adaptive systems in that they have interrelated, heterogeneous elements (agents and objects). In addition, there is no autonomous control over the whole system, and, in that sense, self-organized emergent behaviour arises that cannot be predicted by understanding each of the component elements separately." As such, the result of markets at the macrolevel of the system is based on a variety of individual actions on the microlevel [14].

In Germany, individual options of choices and the number of actors in the system have increased substantially since the liberalization of electricity markets and the introduction of the EEG and its several amendments [17]. They decide under the influence of cognitive biases [18, 19] and inherent uncertainty and are therefore only bounded rational [20]. Policies are directed towards those actors to induce a desired collective behaviour and are uncertain in their effect as well.

Electricity is different to most other commodities, for at least two reasons: it is not storable at low costs, and the demand side is only marginally elastic. Hence, it is necessary to balance supply and demand on short notice at all times in order to ensure system stability. This situation got more challenging with the large-scale integration of RES-E into the system. Due to inherent output forecast limitations and their nondispatchability, RES-E can always be subjected to high balance energy cost due to day-ahead forecast errors and cannot hedge risks on future markets [21–24]. As such, additional intermediary market actors which specialize in forecasting and dispatching variable renewable energy (VRE) emerged. These intermediary market actors increased the order of complexity in the market.

Additionally complicating is the fact that diverse electricity markets, like spot and futures, control energy as well as CO_2 certificates markets interacting with and influencing each other [25]. As a result, the heterogeneous power plant and marketing actors can react very differently to energy policy adjustments and the development of the electricity system as a whole can follow diverse pathways [26]. This is a tremendous challenge from a modelling perspective.

2.2. Overview of Agent-Based Models in Energy System Modelling. Given the challenges mentioned above, we have chosen an agent-based modelling (ABM) approach, which addresses these questions by placing the actors, their interrelationships, and their influencing environment in the centre of the modelling exercise [14]. The origin of the ABM approach is found in the field of artificial intelligence and cellular automata research and has been used for analysing complex and interrelated systems in such various research domains as ecology, social sciences, and software engineering [27]. The ABM approach enables the modeller to describe the complex relationships of the systems entities by identifying a set of attributes, behavioural rules, adaptations of those behavioural rules in response to the behaviour of others and the environment, and an environment itself [28]. The analysis is executed step by step and allows for developing these relationships on an evolutionary path in an artificial laboratory-like environment [29, 30]. Agent-based models are therefore particularly suitable for the simulation of multiply linked and complex systems with autonomous actors. The system's behaviour is not centrally determined but evolves bottom-up from the actions taken by the individual agents to a complex system with emergent structures.

The ABM approach has been successfully applied in the energy sciences. Recent publications have investigated the role of certain technologies, like the market diffusion of PV [31, 32] and biomass power plants [33], or the value of storage technologies [34]. Others have put their focus on certain aspects of the demand side of the energy system, as this aspect is associated with a need for a more "human" modelling and preference depiction: their works focus on demand response

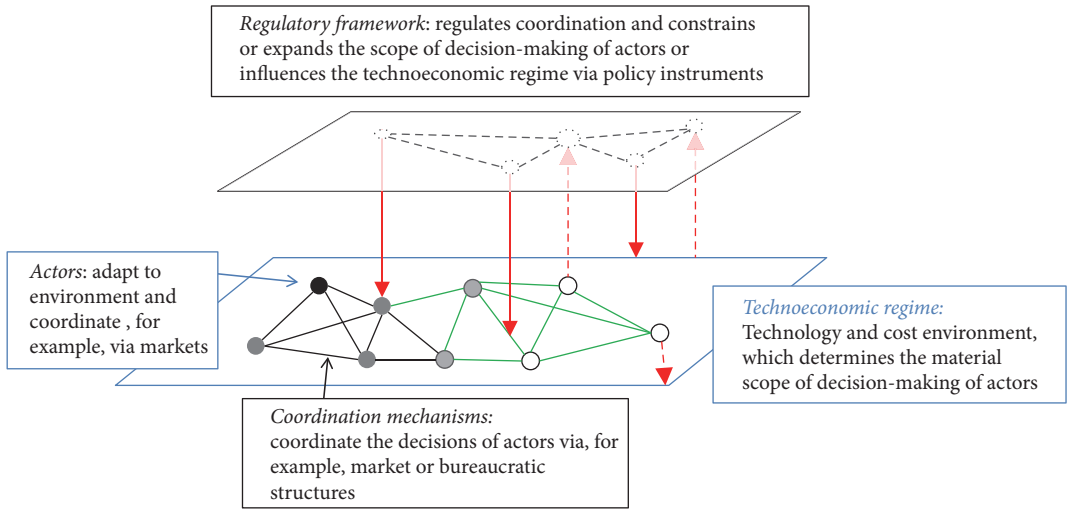

Figure 1: A sketch of the system that is represented by the AMIRIS model.

[35–37], adoption of dynamic tariffs [38], price elasticities [39], and smart meter diffusion [40], among others. Another branch focuses on energy trading on the balancing market [41], the merit order effect [42], emission trading and investment decisions [43], and forecasting [44, 45]. For a comprehensive review of energy market applications, the reader might want to refer to [25, 46] and to [47] for a special focus on newly emerging market structures.

2.3. Conceptual Approach of the AMIRIS Model. Figure 1 depicts the model's scope of analysis; it shows components and interrelations between actors, regulatory frameworks, technologies, and markets which are addressed by the simulation. The technoeconomic layer represents technologies and corresponding costs that are available to the actors of the energy system. It is characterized by technical parameters like efficiencies and durability values and cost parameters. In this sense, the technoeconomic layer determines what is technically feasible. Actors sketched as dots in the technoeconomic layer coordinate themselves, for example, via markets, like the spot market and balancing energy markets. They may set up contracts to invest in technologies and sell or buy energy.

The technoeconomic layer is influenced in several ways by the overlying regulatory framework layer, which may change the apparent costs of technologies by, for example, increase of research and development in certain technologies, deployment incentives like feed-in tariffs, or the financial promotion of RES-E direct marketing. The term *direct marketing* here refers to selling RES-E at market places for electricity via the market premium model under the EEG (see "The Market Premium" in the appendix). Furthermore, this layer may as well enhance or reduce actors action space by regulating markets or by setting up rules that prohibit certain decisions and behaviours of actors.

Solid arrows represent possible vectors of analysis, while dashed arrows are not explicitly incorporated in the model. More influences may appear in such a system that are not subject to the actual implementation, like, for example, feedback from actors to the regulatory level or impacts from actors onto the technoeconomic layer itself.

With the ambition to model the agents and the impact of policy framework adoptions in the process of market integration of RES-E, knowledge about the relevant actors and their expectations, motivations, and strategies is required. To depict the qualitative differences among market actors, systematic actors analysis has been carried out. The actors characteristics of RES-E power plant operators and direct marketers have been developed on the basis of document analysis and expert interviews [10, 48]. These two agents types are modelled in detail compared to other (system) relevant actors of the power system (see Sections 3 and 4). The assumptions were then tested and reassessed in semistructured expert interviews with representatives from the most important actor groups, as well as in the context of an actor workshop. An exemplified version of the typecast of actors into agents is given in the case study in Section 5. The current state of the model will be presented in the following two sections.

3. AMIRIS Model Overview

3.1. Agent Topology. The model comprises two different types of agents: (a) agents with scope of decision-making and (b) agents without scope of decision-making. Type (a) agents are able to adapt to changed circumstances and may decide which action to perform. Contrary to this, type (b) agents have strictly defined tasks to perform during simulation from which they cannot deviate. The model covers the following type (a) and type (b) agents:

(i) Wind, solar, and biomass power plant operator agents as well as the thermal power plant operators generate electricity with their plants (type (a)).

(ii) Direct marketer agents trade electricity from RES on the power exchange market and control power market (type (a)).

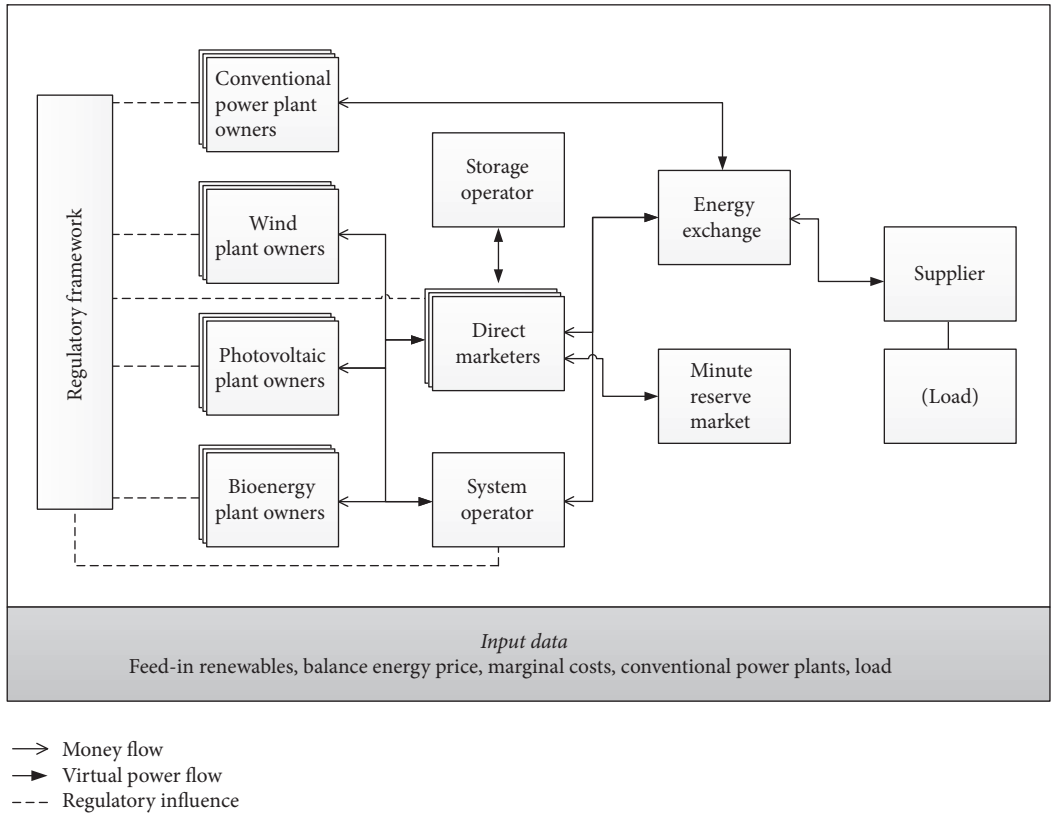

Figure 2: The AMIRIS model.

(iii) Optionally, a storage operator agent can be associated with a direct marketer that in turn can improve the operation and coordination of plants in her portfolio (type (a)).

(iv) The day-ahead power exchange market agent determines the wholesale power market price via a merit order model (its implementation is discussed in Section 4.3.2) (type (b)).

(v) The negative minute reserve market allows offering control power provision (type (b)).

(vi) The grid operator agent manages the generated electricity from wind, solar, and biomass which is not traded by direct marketers. It is sold mandatorily on the day-ahead power exchange market (type (b)).

(vii) The total load of the German power system serves as a static demand sink (type (b)).

(viii) The regulatory framework agent holds information about the total installed power in the system, the remuneration schemes, and undertakes calculations according to the EEG (type (b)).

The agents interact in a changing environment influenced by the energy policy framework of the Renewable Energy Sources Act (EEG) and its corresponding RES-E support scheme as well as the Energy Industry Act [49] and grid regulations. Figure 2 gives a schematic overview of the model interconnections. Boxes represent agents in the model; multilayered boxes indicate that these agent types have multiple instances during the course of simulation. Solid lines represent money and power flows, which are differentiated by open and closed arrows, respectively. Regulatory influence is depicted with dashed lines. Wind, PV, and biomass power plant operators (PPOs) can sell electricity either to the direct marketer or to the grid operator.

As the focus of the AMIRIS model is to investigate the effects of the market integration process of renewable energy sources on the involved actors, the cost and revenue structure of marketers that trade electricity from RES-E PPOs are implemented in detail and will be discussed in Section 4.2.1. PPOs can sign contract with direct marketers and switch contracts at the beginning of each year if a better offer is received (see also Section 4.2.2).

3.2. Process Overview and Scheduling. The model has a one-hour time resolution and is usually run over the course of 8–20 calculative years. Computation time on a conventional desktop computer is in the order of minutes. Internal time is set by the regulatory framework class. The following steps are calculated each time frame, which equals one calculative hour:

(i) Generated electricity and its virtual distribution to direct marketers or to grid operator are determined.

(ii) The residual load, the merit order, and corresponding wholesale power market price are calculated.

Table 1: External input parameters for the AMIRIS model. l indicates the type of the primary product as follows: $l = 1$: uranium, $l = 2$: lignite, $l = 3$: coal, and $l = 4$: gas. Index i defines the power plant type with $i = 1$: nuclear, $i = 2$: lignite, $i = 3$: coal, $i = 4$: combined cycle gas turbine (CCGT), $i = 5$: open cycle gas turbine (OCGT), $i = 6$: offshore wind, $i = 7$: onshore wind, $i = 8$: photovoltaics, and $i = 9$: biomass.

Parameter	Description	Unit
$C^l_{\text{prim}}(t)$	Time series of costs of the primary products used for the calculation of the stock market prices	[€/MWh]
$C_{\text{carb}}(t)$	Time series of cost for carbon dioxide emission certificates	[€/t_{CO2}]
$C^i_{\text{var}}(t)$	Time series of variable costs of conventional power plant of type $i = 1$–5	[€/MWh]
$\eta^i_{\text{min}}(t)$	Time series of minimal efficiency of conventional power plant of type $i = 1$–5	[%]
$\eta^i_{\text{max}}(t)$	Time series of maximal efficiency of conventional power plant of type $i = 1$–5	[%]
$w^i(t)$	Normalized generation potential time series for $i = 6, 7, 8$	[%]
α^i	Availability factor to regard shut-down periods ($\alpha^1 = 0.8$, $\alpha^2 = 0.8$, $\alpha^3 = 0.7$, $\alpha^4 = 0.7$, and $\alpha^5 = 1.0$)	-
$\text{PR}_{\text{bal}}(V)$	Histogram of 2011 prices for balancing energy	[€/MWh]
c_{mark}	Costs for marketing	[€]
c_{IT}	Costs for IT	[€/a]
$c_{\text{trade,var}}$	Costs of charges for trading at the exchange market	[€/MWh]
$c_{\text{trade,fix}}$	Costs for permission of trading at the exchange market	[€/a]
c_{liab}	Costs for the liability of equity to be able to trade at the exchange market, payed once	[€]
$c_{\text{pers,spec}}(V)$	Specific costs for personnel depending on traded volume	[€/MWh]
$c_{\text{fcst}}(\mathscr{P})$	Costs for forecast of electricity generation volume dependent on installed capacity	[€/MW]
$M(t)$	Time series of management premium according to the EEG	[€/MWh]
$R(t)$	Time series of remuneration for renewable energy power plants according to the German Renewable Energy Act	[€/MWh]
$P^i_{\text{inst}}(t)$	Time series of installed power of corresponding technology i	[MW]
$D(t)$	Time series of demand for Germany	[MW/h]
$G^i(t)$	Power generation in t from technology i	[MWh]

(iii) The grid operator calculates the marginal capacity price for the control power provision of the negative minute reserve market by a regression model.

(iv) With an appropriate portfolio, marketers can offer firm capacity at the control power market.

(v) Revenues and costs are assigned to the marketers and the power plant operators.

(vi) Marketers forecast the electricity production of their portfolio and estimate the market price at $t + 24$ h and decide on curtailment of contracted RES-E power plants.

3.3. Modelling Framework. AMIRIS uses the free and open source agent-based modelling and simulation development framework Repast Simphony, which facilitates model design, execution, and data export and serves as an initial context builder for our model. Repast Simphony has been conjointly developed by the University of Chicago and Argonne National Laboratory [50]. It is available directly from the web (http://repast.sourceforge.net/ (last accessed: 23.09.2015)) and licensed under "new BSD" ("New BSD" is a BSD 3-Clause License; see https://opensource.org/licenses/BSD-3-Clause (last accessed: 23.09.2015)). The model is implemented in the Java programming language (http://www.oracle.com/technetwork/java/index.html (last accessed: 23.09.2015)).

4. Agents and Input Data

4.1. Input Data. At initialization of the program several data files are read according to the scenario under investigation. The files contain time series and lists as shown in Table 1 that can be categorized as input for (a) the electricity generation from renewable and conventional power plants, (b) the calculation of marginal costs of conventional power plants, (c) the direct marketers' typecast, and (d) the regulatory framework. The total installed power in the system $P_{\text{inst}}(t)$ for all types of technologies is based on a study for the Federal Ministry of Environment, Nature Conservation, Building and Nuclear Safety covering long term scenarios of renewable energy plant deployments in Germany [51]. For conventional power plants, the installed power is multiplied by an availability factor to take shut-down periods into account. In order to represent the electricity generation of fluctuating renewable power plants, normalized generation potential time series $w(t)$ for wind and solar are used. These generation time series are derived by the EnDat module of the energy system model REMix [52, 53]. EnDat uses a historic weather time series containing wind speeds and solar radiation of the year 2006 that is processed with characteristic system curves for wind and photovoltaic power plants in Germany [52]. In the model, the shape of the demand curve $D(t)$ is represented by the total German electricity demand of 2011 [16]. The scale can be varied according to the underlying scenario study. Marginal costs are determined regarding fuel specific costs and additional variable costs as well as costs for carbon dioxide emission certificates. Fuel specific costs are calculated by primary product costs and efficiencies for correspondent technologies. The calculations' underlying scenarios are found in [51], and details on the applied values are given in [10].

Costs c for various marketing services for compensations are represented in Table 1 and used for a typecast of the cost structure of actors. The use of the various cost parameters is described further in Section 4.2.1.

The input for the regulatory framework is given by a time series $M(t)$ containing the management premium and its decrease over time [54] (compare also "Revenue" in Section 4.2.1). The Renewable Energy Sources Act [4] and its remuneration schemes for different technologies are represented by time series $R(t)$.

4.2. Agents with Scope of Decision-Making

4.2.1. The Direct Marketing Agents. In the process of simulation, the direct marketer agents have the possibility of basing their decisions on the current market conditions. The marketer's business is to profitably sell renewable electricity at the power exchange market. Success or failure of their businesses is evaluated by the profits $p(t)$, which is the difference between revenues $i(t)$ and costs $c(t)$:

$$p(t) = i(t) - c(t). \quad (1)$$

The typecast parameters shown in Table 2 allow a representation of the real market actors heterogeneity. Different types of marketers with diverse revenue and cost structures (compare Section 5) are implemented in the model. The forecast quality of a marketer, described by σ and μ, is crucial for a successful business. By reducing forecast errors, balancing energy procurement costs can be minimised.

Revenue. Revenues can be generated by the support scheme as well as on two markets: the power exchange market and the control energy market, with revenues i_{XM} and i_{CE}, respectively. In reality the control energy market consists of the primary, secondary, and minute reserve markets. On these pay-as-bid markets, participants can offer control power to the system operator for grid stability requirements. The balancing energy market determines the cost (or incomes) for a trader or supplier that deviates from their day-ahead schedule within its corresponding balancing region. Balancing market prices are determined by control energy demand requirements of the system operator. Hence, it is rather an accounting system than a market.

Additional regulated revenues are derived from payouts of the management premium $M(t)$ for direct marketing. Within the implementation of the market premium scheme in the year 2012, the management premium has been introduced as additional entity for compensating for the costs associated with direct marketing duties compared to the FiT scheme (see "The Market Premium" in the appendix). The more efficiently direct marketers fulfill their marketing services for RES-E power plant operators (PPO), the higher the decision scope for either increasing their own profits or the bonus payments to their associated PPOs (see also "Bonus Payments" below).

Whereas the power exchange market represents the marketer's primary source of revenue, participation in the control energy market is optional. The model allows for the participation in the negative minute reserve market (due to opportunity costs with the day-ahead spot market biddings and the required curtailed operation mode, positive reserve provision is financially not attractive for RES-E plant operators and is therefore not modelled). The marginal capacity price at which bids of the direct marketing agents are accepted is determined by the grid operator agent every fourth simulated time step by a multiple linear regression model (compare Section 4.3.1).

Table 2: Variables describing properties of direct marketers. Variations of variable values are used to define the type of marketer and to reflect heterogeneity of actors.

Variable	Unit	Description
σ_{price}		Uncertainty of price forecast of direct marketer, depending on the traded volume V with values 0.15, 0.2, or 0.25
σ_{power}		Uncertainty of power forecast of direct marketer with values 0.15, 0.2, or 0.25
μ_{power}		Estimated value of power forecast of direct marketer with values 0.05, 0.1, or 0.15
$\mathscr{P}$	[MW]	Power generation portfolio of marketer, that is, $\mathscr{P} = \sum_{\tau,\mathrm{rc}} \mathscr{P}_{\tau,\mathrm{rc}}$ of technologies τ in remuneration classes rc
$\mathscr{C}$	[€]	Initial capital of marketer

The direct marketing agents can follow two bidding strategies to maximize profits:

(i) "Low-Risk-Strategy": with this strategy marketers offer a capacity price on the pay-as-bid market corresponding to the median of the preceding month's 180 4 h-price-blocks. This way acceptance of a bid is very likely but only at a relative low capacity price Π_{CE}.

(ii) "High-Risk-Strategy": with this strategy marketers offer a capacity price on the pay-as-bid market corresponding to the median of the preceding month's 180 4 h-price-blocks plus the standard deviation of these prices. This way acceptance of a bid is less likely but in case of acceptance a relatively high capacity price Π_{CE} is ensured.

Further revenue $i_{\mathrm{bal}}(t)$ can originate in case the own local imbalance can reduce the imbalances of the corresponding balancing grid region.

Costs. Both fixed and variable costs are considered in the total cost determination. For yearly fixed costs c_{fix}, IT and trading permission are regarded. Further, upon starting the direct marketing business, the marketer has to provide a liable equity. The different positions of variable costs depend primarily on the amount of electricity traded by the direct marketer. Trading fees are to be paid for each traded MWh,

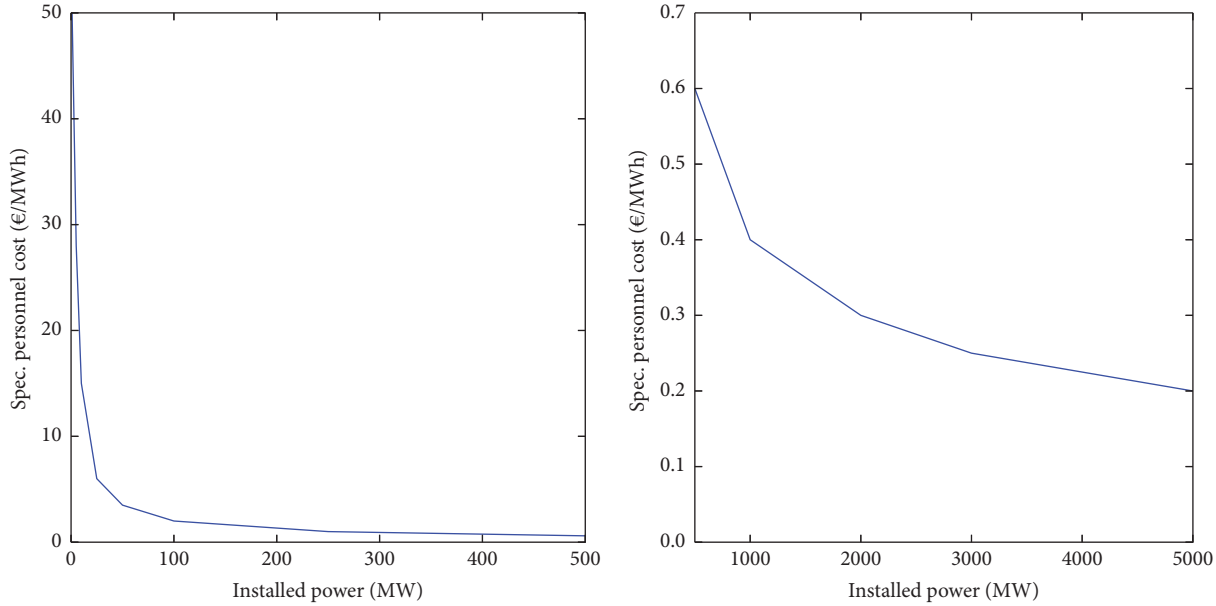

Figure 3: Specific personnel costs $c_{\text{pers,var}}$ per installed capacity of the marketers in the model. Data from [11].

whereas costs for balancing energy depend on the deviation between the forecast and actual VRE generation.

The balancing energy price is determined at each time step by the grid operator by uniform random selection out of a price histogram based on balancing energy prices of the year 2011 in Germany. The balancing price as well as the balancing volume may take negative and positive values; thus balancing costs can contribute to the marketers' revenue for $c_{\text{bal}}(t) < 0$ and $i_{\text{bal}}(t) = -c_{\text{bal}}(t)$ (see also (A.1) in the appendix).

Payments for balancing energy and expenses for the staff and IT are the largest cost positions for direct marketers [11]. The specific personnel costs reveal substantial economies of scale and range from several €/MWh for portfolios smaller than 50 MW to only €cents/MWh for +500 MW of contracted VRE capacities (compare Figure 3). Additionally, expenses for the power output forecast c_{fcst} affect the profit calculation. As direct marketers mainly manage a generation portfolio and do not own the corresponding plants, a competition for acquisition of generation plants follows. To bind customers and to be financially attractive to potential new customers, marketers make bonus payments for the contracted power plant operators, another cost factor described in the following section.

Bonus Payments. At the start of the simulation, the bonus is defined to be half of the management premium of the corresponding year; that is, $c_{\text{bonus}}(t = 0) = (1/2)M(t = 0)$. In order to guarantee the direct marketer flexibility and control over costs, bonus payments can be adopted at the end of each simulated year. Within each adoption process the specific operating results $\beta(\text{OR}_{\text{spec}})$ are evaluated. Further, the ratio of capital to operating results may additionally adjust the bonus payouts by $\beta'(\text{OR}_{\text{capital}})$ in case of negative operating results.

Table 3: Definition of bonus parameters β and β' depending on operating results (OR); that is, $\text{OR}_{\text{capital}} = \mathscr{C}/\text{OR}$.

OR_{spec} [€/MWh]	β	$\text{OR}_{\text{capital}}$	β'
≥1.0	1.1	0	0.0
[0.6, 1.0[	1.05	]0-1]	0.5
[0.4, 0.6[	1.00	]1-2]	0.7
[0.2, 0.4[	0.95	]2-3]	0.8
<0.2	0.90	]3-4]	0.875
		]4-5]	0.95

The values for the bonus adjustments are given in Table 3. The bonus does not merely increase the profit margins of the marketers; instead, they will invest their surpluses to increase the bonus payouts for the PPOs if the specific operational results are larger than 0.5 euro/MWh. This definition ensures a competition between the marketers seeking to attract new PPOs. In the model, bonus costs are thus calculated by

$$c_{\text{bonus}}(t) = \begin{cases} c_{\text{bonus}}(t-1) \cdot \beta\left(\text{OR}_{\text{spec}}\right) \cdot \beta'\left(\text{OR}_{\text{capital}}\right) & \text{for OR} < 0, \\ c_{\text{bonus}}(t-1) \cdot \beta\left(\text{OR}_{\text{spec}}\right) & \text{for OR} \geq 0. \end{cases} \quad (2)$$

Curtailment. The AMIRIS model allows for a market-driven curtailment of RES-E according to the incentives of the implemented policy instrument. In case of potentially high renewable electricity generation and low demand, the marketer may decide to switch off plants of her portfolio to avoid payments due to negative wholesale electricity prices

(compare Section 4.3.2). The marketer's decision is based on a price forecast, given by

$$\Pi_{\text{fcst}}(t) = \Pi_{\text{perf}}(t+24) \cdot \left(1 + \sigma_{\text{price}} \cdot g\right), \quad (3)$$

with the random error variable g drawn from a normal distribution times the perfect foresight price $\Pi_{\text{perf}}(t+24)$. Plant specific opportunity costs for curtailment determine whether RES-E generation is being curtailed. The estimation of these costs depends on the variable market premium $F(t)$ and the management premium $M(t)$ according to

$$\left|\Pi_{\text{fcst}}(t)\right| \geq F(t) + M(t) \quad \text{for } \Pi_{\text{fcst}}(t) < 0. \quad (4)$$

In case the sum of both premiums is lower than or equal to the absolute value of the forecast wholesale power market price $\Pi_{\text{fcst}}(t)$, the direct marketer will advise the corresponding PPOs to shut-down generation.

4.2.2. The RES-E Power Plant Operator Agents. The potential generation of electricity from renewables is given by the plant operator's installed capacity $\mathscr{P}_{\text{rc},\tau}$ multiplied by a normalized weather time series $w^i(t)$:

$$G_{\text{rc},\tau}(t) = \mathscr{P}_{\tau,\text{rc}}(t) \cdot w^i(t), \quad (5)$$

with $i = \tau$ in this case.

Plant operator agents are distinguished primarily by the generation technology τ in operation, that is, plants using wind, solar radiation, or biomass, as well as by the corresponding remuneration class rc the technology is assigned to (see also Section 4.3.4). The height of the remuneration class rc is calculated from empirical data about historical developments of FiTs and so-called "values to be applied" (replacing the FiT in the direct marketing regime) [55]. Each RES-E technology is subdivided in four representative remuneration classes, since the remuneration for a specific plant depends on the year of installation, the resource site, the type and size of the technology, and the energy carrier in use (the resource site is taken into account for wind power plants; the type and size of technology is relevant for PV and biomass plants and the energy carrier in use for biomass plants only). Table 4 lists all characterizing parameters for the renewable power plant agents. Their revenue is based on the remuneration of the fed-in electricity as well as on the bonus payments i_{bonus} they receive from the direct marketers. The value of i_{bonus} corresponds to the costs of the marketer c_{bonus}. PPOs opting for direct marketing receive new bonus offers at the beginning of each year from different direct marketing agents (see also "Bonus Payments" in Section 4.2.1). To capture transaction costs when switching the partnering agent, the difference between the old and new bonus offer must at least exceed a certain threshold x_{min}. This threshold increases with the height of the remuneration class rc, as the relative attractiveness of additional bonus payments correlates directly with the height of remuneration an agent is already receiving (see also Section 5).

4.3. Agents without Scope of Decision-Making. Figure 2 shows all agents in the AMIRIS model. Direct marketers and power plant operators are implemented with heterogeneous characteristics. They have several options for decision-making. Nevertheless, other agents without scope of decision-making are inevitable to complete the electricity systems representation. Hence, they hold important information for the hole systems functionality. They perform model endogenous calculations that are not subject to their own pursuit of strategic goals like revenue maximization.

Table 4: Variables that characterize the type of renewable power plant agents.

Variable	Unit	Description
τ	-	RES-E technology of the power plant operator
rc	-	Remuneration class this agent is assigned to
$\mathscr{P}_{\tau,\text{rc}}(t)$	[MW]	Installed capacity of this technology in the corresponding remuneration class
x_{min}	[€/MWh]	Threshold which needs to be exceeded by a new bonus offer in order to switch contracts with direct marketers

4.3.1. Grid Operator Agent. According to the Ordinance on a Nationwide Equalisation Scheme (German: "Ausgleichsmechanismusverordnung") [56], the grid operator is responsible for the settlement of the support schemes in place and the payouts of FiTs and market premiums to the PPOs or direct marketers, respectively. He calculates ex post the height of the market premium for each remuneration class rc. For this, he receives the past months market values MV_τ of the VREs from the wholesale power market agent.

The agent also determines the balance energy price by uniform random selection of PR_{bal}. Additionally, the grid operator conducts the auctions for the negative minute reserve market. The marginal capacity price MCP_{CE} is determined by a multiple linear regression model with the independent variables of the wholesale power market price x_1, the load x_2, and the onshore wind feed-in x_3:

$$\text{MCP}_{\text{CE}}(t) = -\alpha_1 \cdot \frac{\sum_{t=h}^{t+4} x_{1,h}}{4} - \alpha_2 \cdot \frac{\sum_{t=h}^{t+4} x_{2,h}}{4} + \alpha_3 \cdot \frac{\sum_{t=h}^{t+4} x_{3,h}}{4} + \beta \quad (6)$$

with $\alpha_1 = 0.5304$, $\alpha_2 = 0.0029$, $\alpha_3 = 0.0005$, and $\beta = 154.1$.

The estimation of the regression parameters α has been derived from the negative minute reserve prices of the year 2011 [10].

4.3.2. Wholesale Power Market Agent. The agent representing the power exchange market defines the wholesale power price every time step and disburses the market revenue to the corresponding agents according to the uniform market clearing

Table 5: Associated residual loads, RL, and wholesale power prices according to analysis of market situations with low (0–20 €/MWh) and negative (<0 €/MWh) prices in Germany 2011 [15, 16].

Power price [€/MWh]	20	10	5	0	−5	−10	−30	−50	−75	−100
RL intervals [GW]	29.6	27.1	26.6	26.1	25.7	20.7	15.7	11.7	8.7	6.7

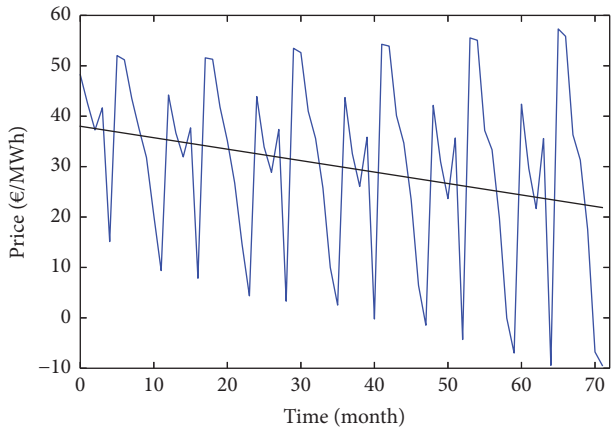

Figure 4: Average monthly wholesale power market prices generated by the model (the underlying data input is given in the case study Section 5). The line represents a linear fit to the data.

price $\mathrm{MCP}_{\mathrm{XM}}$. For the calculation of the $\mathrm{MCP}_{\mathrm{XM}}$ a merit order model is implemented. The merit order calculation is based on the residual load and the marginal costs of the conventional power plants $\mathrm{MC}_{\mathrm{PPconv}}$. Marginal costs of each power block q of 200 MW are set by (see also Table 1)

(i) fixed and variable costs of primary products $C_{\mathrm{prim}}(t)$ (including fuel transportation or shipping);

(ii) certificate costs of carbon dioxide emissions $C_{\mathrm{carb}}(t)$;

(iii) efficiencies $\eta(t)$ of the power plants;

(iv) other variable costs $C_{\mathrm{var}}(t)$ (i.e., for insurance, etc.).

Once these costs are determined, they are ordered from the lowest to the highest value. The $\mathrm{MCP}_{\mathrm{XM}}$ is set by the last 200 MW power bloc q needed to satisfy the residual load:

$$\mathrm{MCP}_{\mathrm{XM}}(t) = \min\left(\mathrm{MC}_{\mathrm{PPconv}} \mid \sum_{i=1}^{n} q_i \leq \mathrm{RL}\right). \quad (7)$$

Simulated average monthly clearing prices are shown in Figure 4 for the years 2014 to 2019. Over the course of the simulation the price-spread increases due to rising CO_2-certificate and fossil fuel prices but the average price decreases due to the increased VRE feed-in with marginal costs of approximately 0 €/MWh. The general structure of the price curve reoccurs annually because only one representative weather year and load profile are used.

Conventional must-run (must-run capacities are due to power plants that offer complementary goods on other markets (like ancillary services or heat) and therefore need to be present in the wholesale market at all times, irrespective of very low or negative wholesale market prices) capacity is included via the definition of so-called "residual load intervals." The residual load intervals have been derived from the analysis of market conditions in which wholesale market prices have dropped below 20 €/MWh (reference year 2011, [10]). If the lower-bound of an interval boundary is exceeded in a specific hour, the regular $\mathrm{MCP}_{\mathrm{XM}}$ calculation mechanism described above is replaced by the associated price of the corresponding residual load interval. Table 5 gives the residual load reference values and its associated wholesale power prices of the year 2011 in Germany. Over the course of the simulation, the interval boundaries decrease from year to year according to the development of the retirement of conventional base-load capacities in [51].

The calibration of the power exchange model is conducted by markups and markdowns of the conventional power plant agents, which are added to or subtracted from the $\mathrm{MC}_{\mathrm{PPconv}}$ values. The validation of the merit order model can be found in [10].

4.3.3. Demand Side Agent. The model's demand side is represented by a time series comprising total load values for each simulation step. The annual total energy consumption is scaled according to scenario A values from [51].

4.3.4. Regulatory Framework Agent. The regulatory framework agent holds all the energy policy information necessary for simulating the market integration process of RES-E. The law differentiates the remuneration for PPOs dependent on the general type of the RES-E technology installed, the potential full-load-hours at the installation site for wind onshore plants, the size of the plant for PV plants, and the chosen technology of biomass plants as well as on the corresponding biomass substrate in use [4]. In addition, as remunerations decrease over the years (since 2012 the decrease of remunerations for wind onshore and PV plants is carried out on a quarterly or even monthly basis) a complicated payout structure has evolved in reality since 2000. As a consequence, by the year 2017, there are over 5.000 different remuneration categories within the EEG support scheme and about 1.5 Mio. RES-E power plants in place [55].

A mapping of plants to actors in every detail would require knowledge about each owner, plant type, and remuneration for each plant. Besides the fact that such information is, if at all, not easy to access, mapping of all PPOs individually would lead to a multiagent system (MAS) with over a million agents to be parametrized.

Therefore, four different remuneration classes are defined for each year and each renewable technology type τ. This more homogeneous assignment allows for a transparent handling of the remuneration schemes in the model. Each class contains information about the remuneration, the technology, and the corresponding installed power.

Table 6: Table representing the direct marketers' initial portfolios.

Direct marketer	BM [MW]	PV [MW]	Wind [MW]
Big utility	522	1697	14145
Municipal utility	904	3394	8492
Small municipal utility	395	3394	1619
Green electricity provider	930	1697	3237
Startup	2602	23759	6873

The regulatory framework agent saves and updates this information at the beginning of each year and remits the relevant data to the grid operator agent, who is in charge for the payouts of the support instrument in place (see also Section 4.3.1). Further, the agent calculates the reference market values $MV_{\tau,ref}$ on a monthly basis and governs the height of the management premium (compare "The Market Premium" in the appendix).

5. Case Study

5.1. Model Setup and Agent Parametrization. In this section a case study shall demonstrate the model's basic working mode and give an example for possible fields of analyses. The case study examines the effects of a change in the regulatory framework, taking into account the interplay of the power plant owners and their possibility of changing their contracted direct marketers.

The regulatory framework refers to the market premium under the German Renewable Energy Sources Act (EEG) in its version of 2012 [7], when the market premium scheme has been introduced. Two variations of the correspondent management premium are analysed. In "Scenario 1," the level of the management premium $M(t)$ for variable (VRE) and dispatchable renewables is set to 3.7 €/MWh and 1.125 €/MWh, respectively, in accordance with the initial values of the EEG 2012. In "Scenario 2," $M(t)$ for VRE is reduced by 50% to 1.85 €/MWh; for dispatchable renewables no changes are assumed. This decrease of the management premium for VRE reflects the decision of policymakers in 2012 when figuring out that the original height of $M(t)$ has led to considerable windfall profits for wind PPOs.

On the basis of an actor analysis [10, 48] (compare Section 4.2.1), five different types of direct marketers were aggregated for this case study: (1) big utility, representing big and medium power supply companies; (2) municipal utility; (3) small municipal utility; (4) green electricity provider; and (5) startup. The technology specific size of the portfolios is linearly growing each month according to the underlying time series of installed power of each technology. These numbers are based on empirical data on the number of plant operators receiving FiTs or market premiums published by the grid operators in Germany [55]. In the simulation, yearly changes in portfolio sizes and composition might take place due to the marketers' competition for PPOs. The simulation period for the case study is set to 2014 to 2019.

The initial technology specific composition of the portfolios for the starting year 2014 is displayed in Table 6. A more detailed resolution disclosing corresponding remuneration classes can be found in Table 9. Other important differentiation factors are the direct marketers' specific forecast capabilities as well as their capital resources (compare Section 4.2.1 and the appendix). Their initial parametrization is given in Table 7.

In Section 4.2.1, we describe how the bonus payments of marketers are changing throughout the simulation. The PPOs can cancel their contract at the end of each simulation year and enter into a new contract with another direct marketer offering higher bonus payments if the corresponding threshold value of x_{min} is exceeded (compare Section 4.2.2). The threshold x_{min} depicts transaction costs and is parametrized according to the power plants' remuneration classes. It is assumed that contracts for plants in lower remuneration classes have lower thresholds as they gain proportionally higher revenues (compare Section 4.2.2). Values have been derived by taking the height of the starting bonus, rounding it to an integer, and dividing it by four. The corresponding x_{min} values per remuneration class are displayed in Table 8.

5.2. Results

Scenario 1. In this scenario, the height of the management premium is set according to the EEG 2012. Overall good operating results are achieved by all marketers in this case, except for the small municipal utility (see Figure 5(a)). This marketer shows a nonprofitable operation for 5 of the 6 simulated years and operates with constantly decreasing bonus payouts. The big municipal utility and the green electricity provider start with the highest operating results of about 1.2 €/MWH and 1.8 €/MWh, respectively. Their average results show a decrease in the following years and a convergence to 0.5 €/MWh. Both marketers increase their bonus payouts accordingly reaching a maximum of up to 2.5 €/MWh in the last year of simulation. The operating results of startups and big utilities exhibit a slow but steady growth for the first-mentioned marketer and a nearly constant income on average for the big utilities. Both fluctuate around a profit of 0.5 €/MWh and decrease or increase their bonus payouts over the years according to their operational results.

The specific balance energy cost (compare Figure 5(c)) of the small municipal utility is between double and triple the costs of its competitors. This cost factor does not change significantly over time and therefore poses a constant burden for the marketer.

The switch of power plant owners to other marketers offering a higher bonus payment starts after year two of the simulation. At this moment the gap between lowest and highest bonus offered is large enough to encourage plant owners with a small threshold to switch the marketing partner. The small municipal utility is the first to lose clients to the green electricity provider, as the difference of the bonus payouts is the largest between these two; see Figure 5(b). In the following years, a part of the clients of all other marketers switch to the green electricity provider as well, except for clients from the big municipal utility. Over the course of the simulation, the big utilities portfolio is reduced by about 5 GW, the one of the small municipal utility is reduced by about 2.7 GW, and the startup loses

Table 7: Table representing the direct marketers' initial forecast uncertainties and capital resources.

Direct marketer	σ_{price}	σ_{power}	μ_{power}	M€
Big utility	0.15	0.15	0.05	100
Municipal utility	0.15	0.15	0.05	50
Small municipal utility	0.25	0.25	0.15	20
Green electricity provider	0.2	0.15	0.05	20
Startup	0.15	0.2	0.1	20

Table 8: Table representing the power plant owners' changing thresholds x_{min}.

Remuneration class	WAB [€/MWh]	PV [€/MWh]	BM [€/MWh]
1	0.5	0.5	0.5
2	1.0	1.0	2.0
3	1.5	1.5	1.5
4	2.0	2.0	1.0

Table 9: Installed capacity per remuneration class as assigned to the marketers at the beginning of simulation.

Direct marketer	BM [MW]	PV [MW]	Wind [MW]
Big utility			
RC 1	360	881	1648
RC 2	22	567	5342
RC 3	125	29	5960
RC 4	15	220	1195
Municipal utility			
RC 1	719	1761	1030
RC 2	45	1134	3339
RC 3	125	59	3725
RC 4	15	440	398
Small municipal utility			
RC 1	240	1761	206
RC 2	15	1134	668
RC 3	125	59	745
RC 4	15	440	-
Green electricity provider			
RC 1	479	881	412
RC 2	30	567	1336
RC 3	375	29	1490
RC 4	46	220	-
Startup			
RC 1	599	12329	824
RC 2	37	7940	2671
RC 3	1750	412	2980
RC 4	216	3077	398

about 2 GW. The sum of them is added to the portfolio of the green electricity provider doubling its portfolio size; see Figure 7(a).

Scenario 2. In the scenario with a 50% reduced management premium for VRE, the simulation shows a different development of the marketers business success as can be seen in Figure 6. The "big municipal utility" and green electricity provider start with positive operating results; the other marketers' results are negative. Whereas the green electricity provider can assure his income throughout the simulation and increases his bonus payouts, the "big municipal utility" earns about 0.5 €/MWh until year four hardly changing the bonus. In this year the gap between own bonus payouts and the highest payouts of the green electricity provider is large enough to lose wind and biomass power plants. The loss of biomass plants especially reduces the high profitable income from the reserve market and, accordingly, the bonus

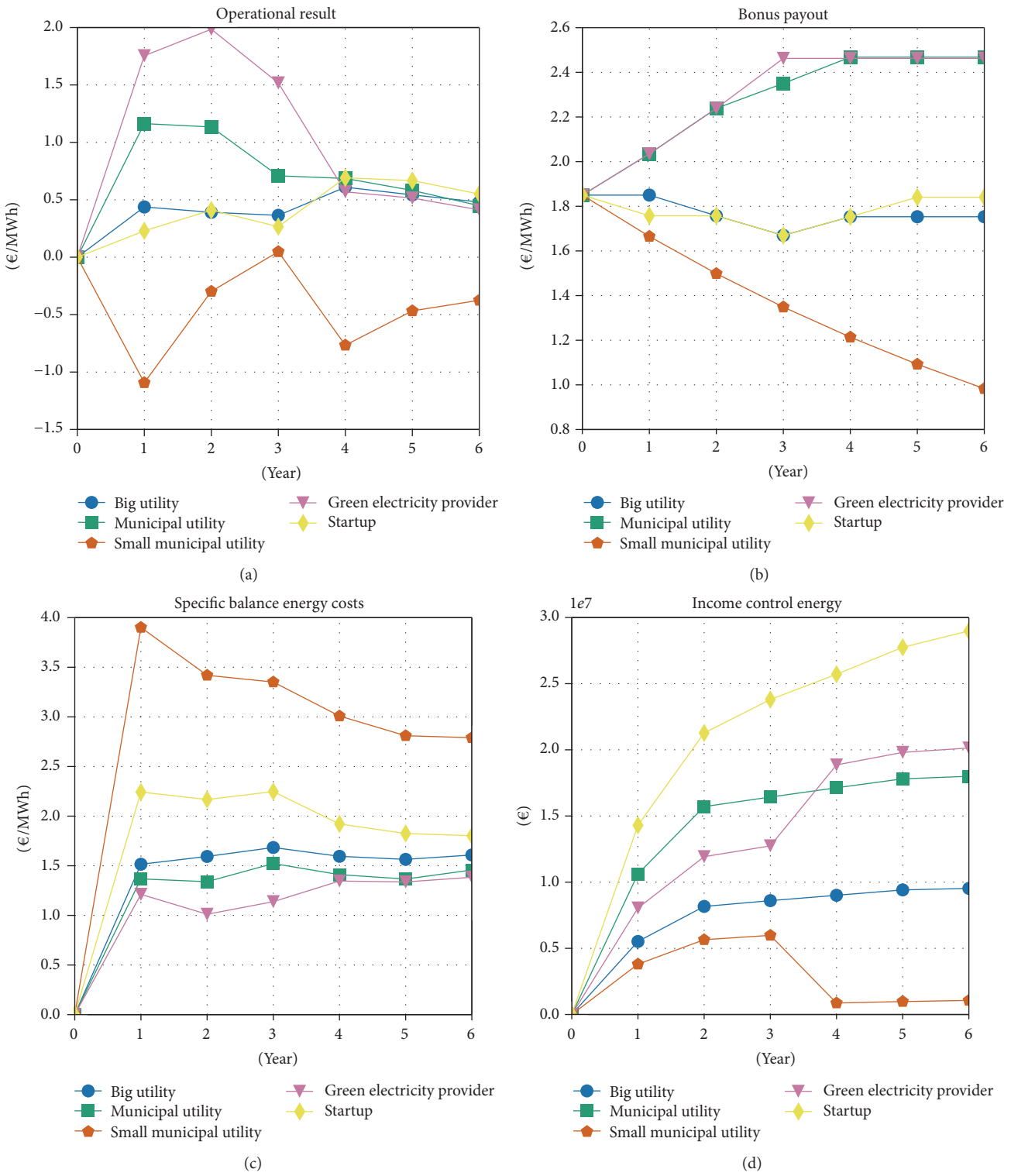

Figure 5: Specific operational results, bonus payouts, balance energy costs, and income from the control energy market for all 5 marketers in the first scenario.

is reduced in the following years with negative results of about −0.8 €/MWh.

The startup has an operational result of just below zero, depletes all its available capital until the fourth year, and reduces its bonus payout to 0 €/MWh. Already after the second year, the bonus difference to the green electricity provider is too large, losing a part of its biomass power plants to this competitor. Accordingly, the income of the reserve

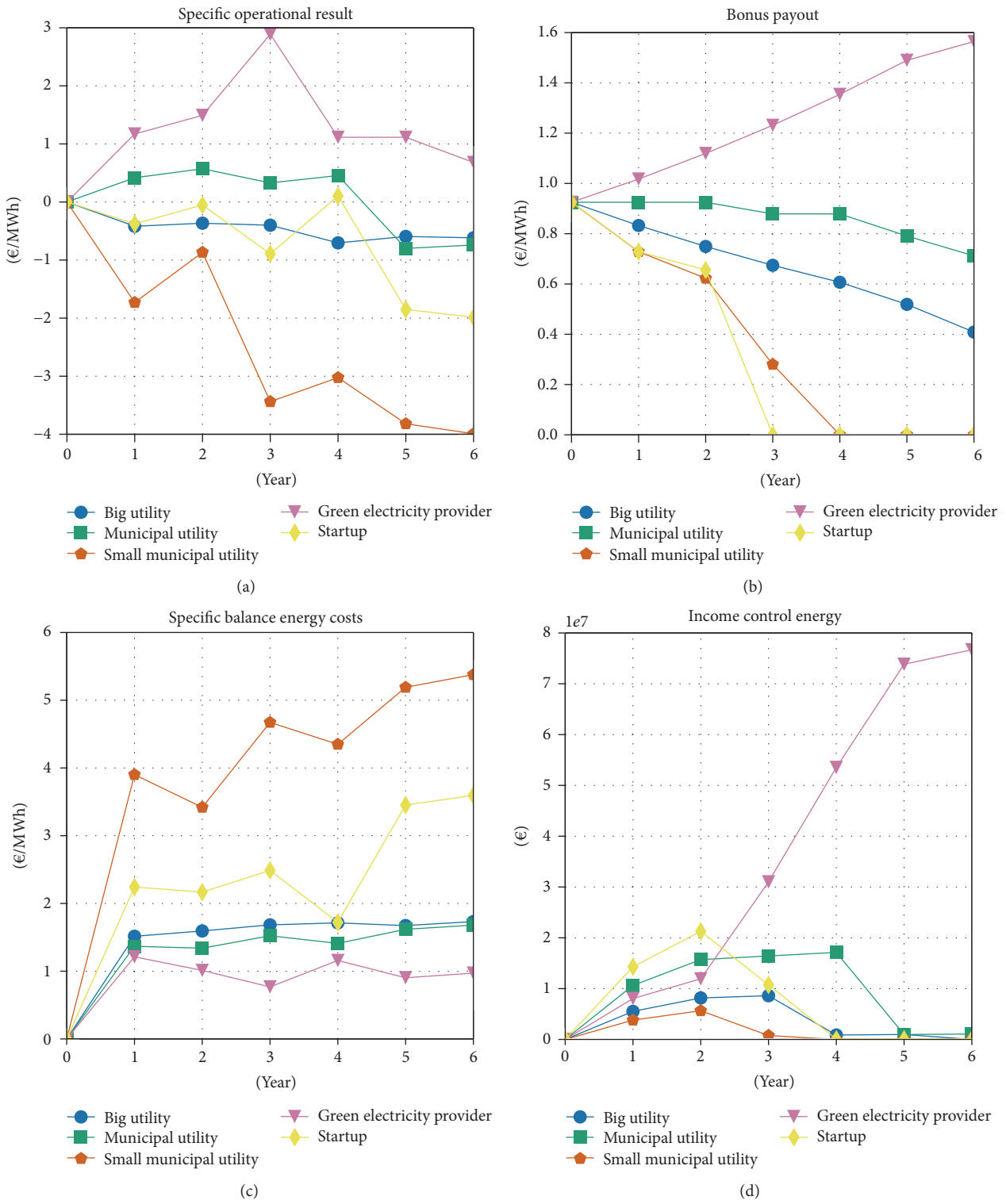

FIGURE 6: Specific operational results, bonus payouts, balance energy costs, and income from the control energy market for all 5 marketers in the second scenario with reduced management premium.

market decreases while the cost for balance energy increases. The specific operational result drops to about −1 €/MWh in year three. The capital of the startup is used up and bonus payments are stopped. Biomass, wind, and photovoltaic power plant operators switch to the green electricity provider that offers the highest bonus payouts. The new portfolio implies a reduction of balance energy costs leading to a positive operational result in year four. Yet the capital stock remains

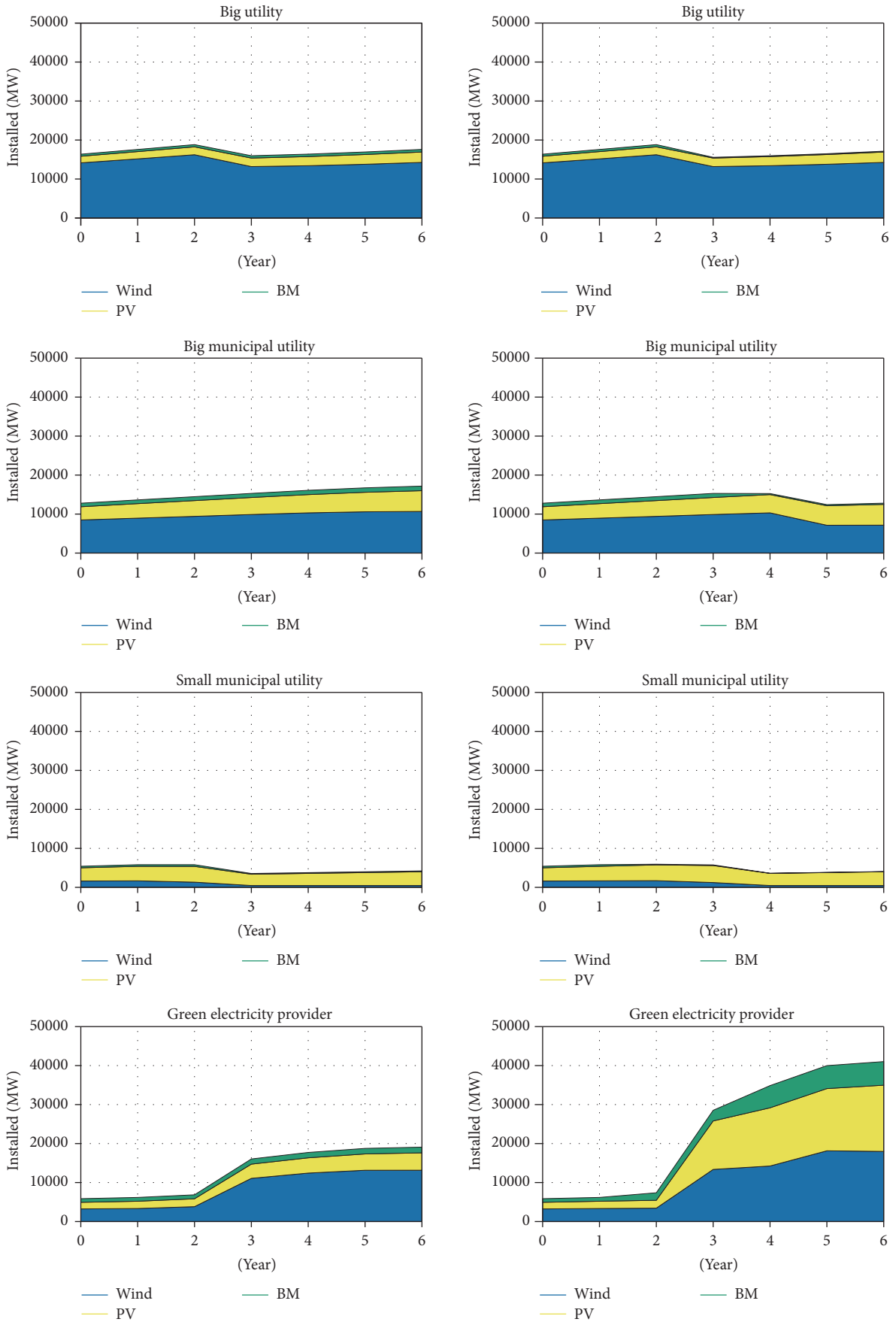

Figure 7: Continued.

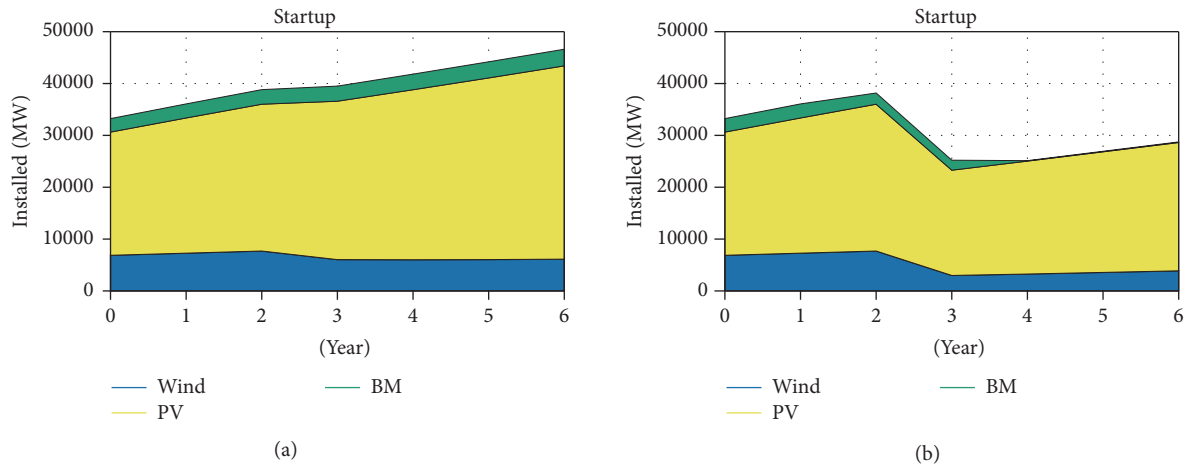

Figure 7: Evolution of the marketers' portfolios for Scenario 1 (a) and Scenario 2 (b).

negative and bonus payouts are still ceased. A large fraction of the remaining biomass plants leave the startup, resulting in increased balance energy costs and negative operational results of up to −2 €/MWh in the following years.

With an operational result of about −0.6 €/MWh over the years, the big utility gradually reduces its bonus payout without hardly any effect on its results. The only slow decrease of bonus is due to the operational result to capital ratio; compare Table 3 and Figure 8. The small municipal utility loses money for every MWh produced. On average, this marketer is losing every year 0.6 €/MWh more than in the previous year. After the fourth year, it stops bonus payouts and most of its portfolio's wind and biomass plants switch to another marketer. At the end of simulation, it is the green electricity provider that increases its portfolio by about 4.5 GW from the big utility, 3.5 GW from "big municipal utility," 3 GW from small municipal utility, and 17 GW from the startup, Figure 7(b).

6. Discussion

6.1. Discussion of Case Study Results. The case study reveals valuable insights concerning the income and portfolio dynamics of different RES-E marketer actor classes. Scenario 1 shows that incumbent marketers such as big utilities that focus on a large wind power portfolio-share can benefit due to economies of scale from lower specific operational costs and better forecast qualities. On absolute levels, their economic success is among the best (see Figures 8 and 9). However, we also identify a mediating disutility of scale. As described earlier, marketers can profit by trading electricity on different electricity markets, namely, the wholesale power market and the negative minute reserve market. Yet, only the electricity of biomass plants has been allowed to participate in the control power market in the model (since 2017 also wind power plant operators are allowed to bid firm capacity on the control power market if certain prequalifying conditions are fulfilled in a pilot phase). Trading electricity of these controllable plants implies less balancing costs and improves overall operational results. The access to this dispatchable resource is limited and unevenly distributed among the marketers' portfolios. However, the actors analysis revealed that upcoming small marketers often have better access to biomass PPOs through personal connections to local farmers and thus comparatively more biomass contracted in their portfolio. Having access to this dispatchable energy source can mitigate the disadvantages of small portfolio sizes. In combination with an adequate forecast quality, this can lead to financially successful marketing of RES-E, as the results of the green electricity provider depict, allowing a niche of new market entrants to survive next to incumbent marketers.

Additionally, the model allows the investigation of how the market structure changes if marketers are enabled to compete for new PPOs to complement their portfolio. The bonus payout follows a simple adjustment rule: the higher the operational result is, the higher the bonus marketers pay to their contracted PPOs. This leads to a convergence towards a common specific operational result for all marketers in Scenario 1 (except for the small municipal utility) and ensures a strong competition concerning the bonus payout and the attraction of new PPOs. In this scenario, the bonus adjustments and the contract switches of PPOs to other marketers are only moderately dynamic. Comparatively small gaps between bonus heights arise, and plant capacities of only about 10 GW in total switch marketers. Except for the small municipal utility, the system stabilizes to a state in which four successful marketers coexist.

Slight changes in the regulatory framework (a reduction of the management premium for VRE) lead to completely changed income and portfolio dynamics; compare Figures 10 and 11. In Scenario 2, only one marketer manages to trade the electricity profitably and to increase bonus heights. All other marketers have to decrease their bonus payouts and thus a large difference in payouts exists between the marketers even in an early stage of simulation. Startups, for example, struggle in the first four years with their operational result just below zero. During this time, they reduce the bonus height to be profitable. In year four, the startup manages to have a positive result but at the same time its bonus payouts ceased and a large difference in bonus height to

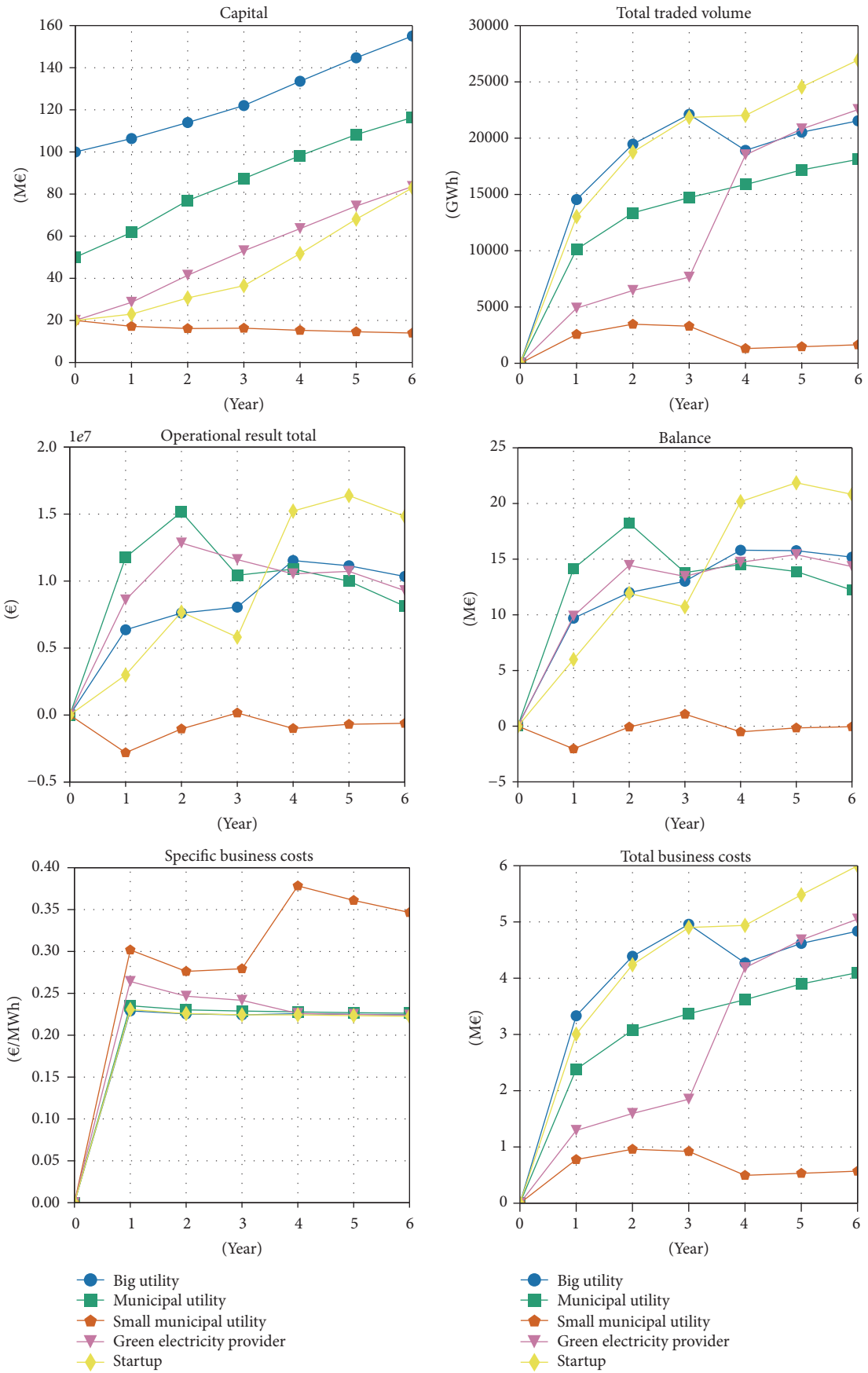

Figure 8: Scenario 1 results. The balance reflects all income and expenses at the market, including payments for balance energy, excluding the business costs. Business costs are considered in the operational result.

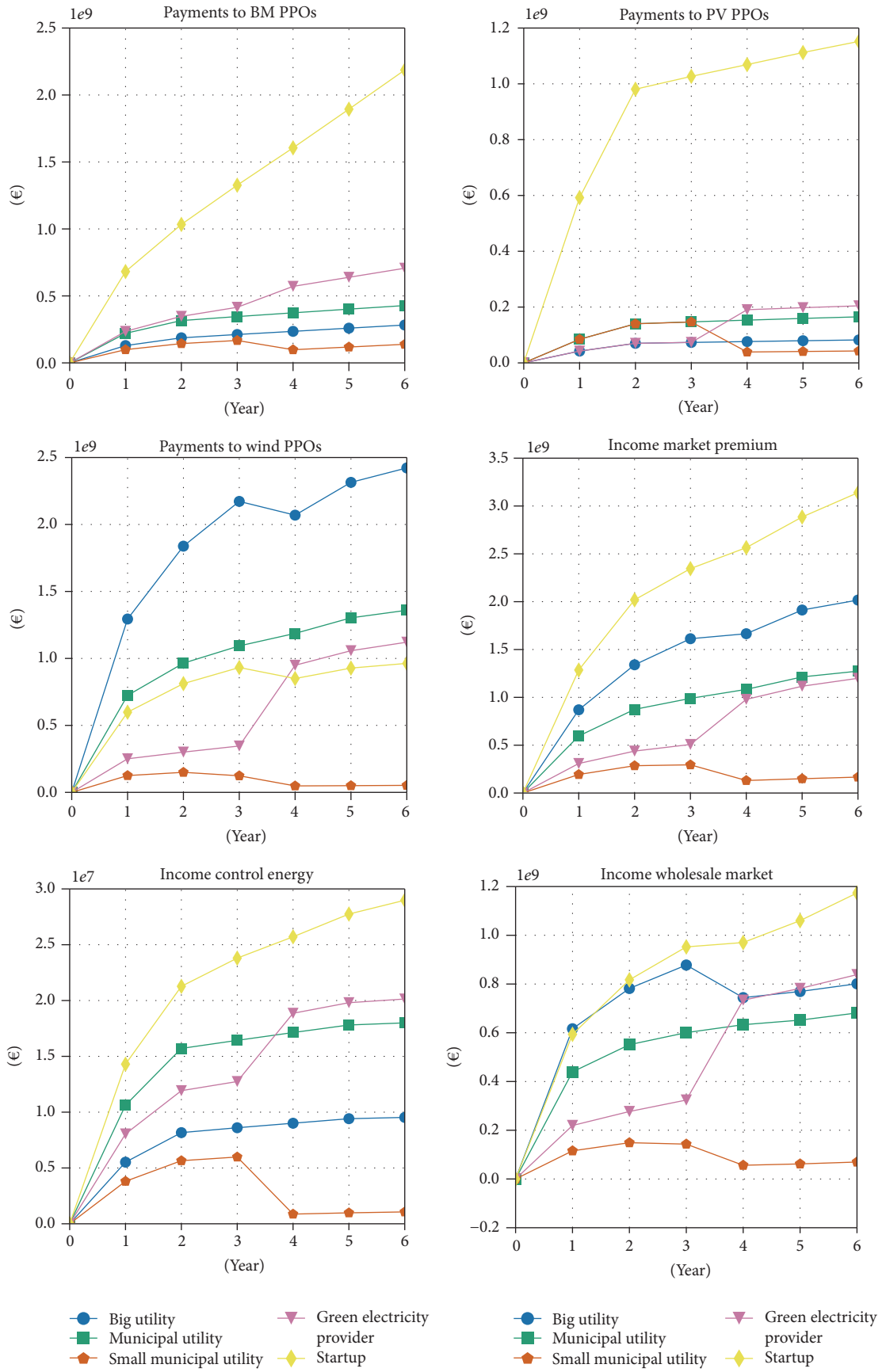

Figure 9: Scenario 1 results. Income and expenses of the marketers.

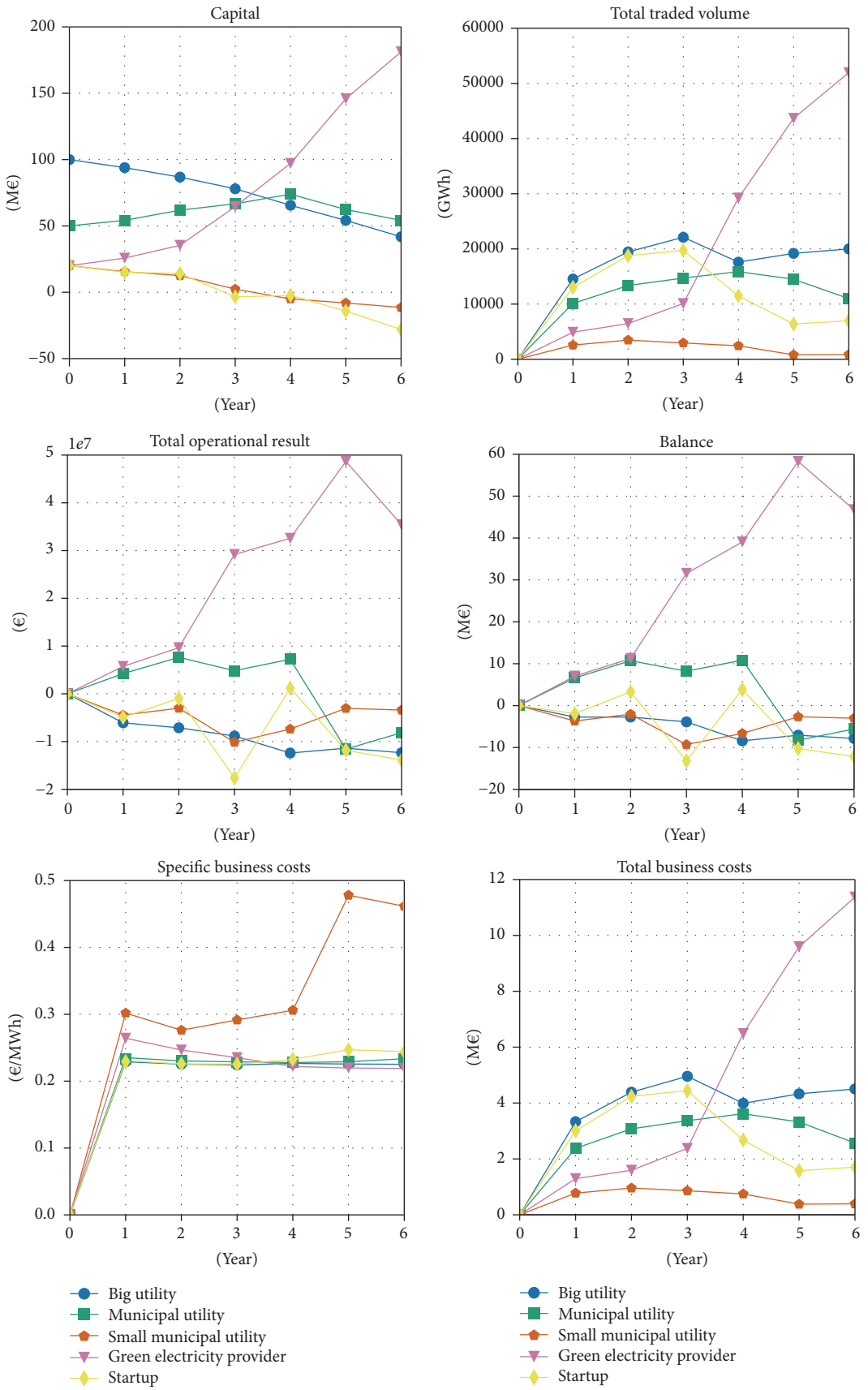

FIGURE 10: Scenario 2 results. The balance reflects all income and expenses at the market, including payments for balance energy and excluding the business costs. Business costs are considered in the operational result.

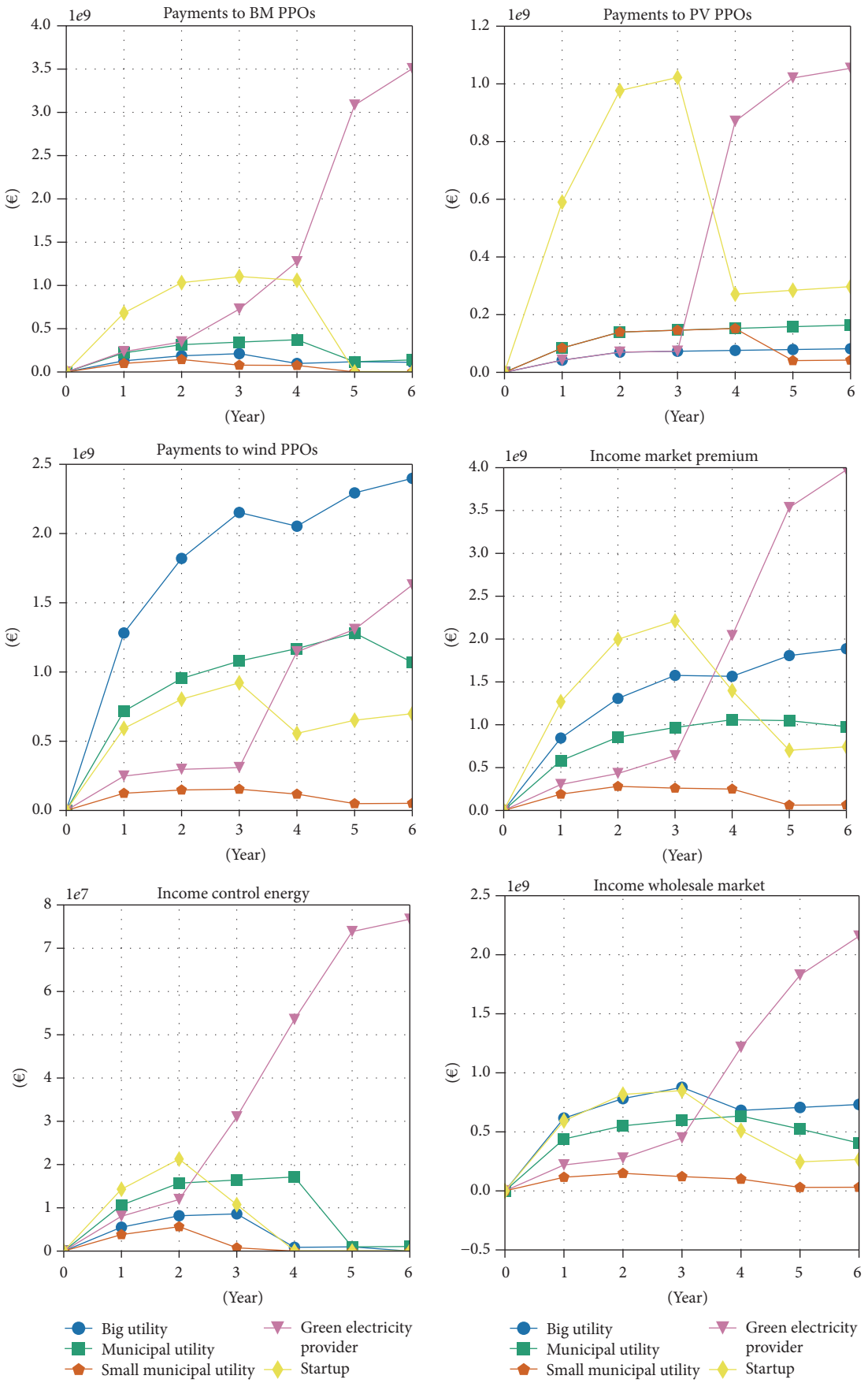

Figure 11: Scenario 2 results. Income and expenses of the marketers.

the other marketers has emerged. Even with a well balanced portfolio with a relatively large share of biomass plants, they cannot offer bonus payouts and lose the biomass plants to competitors. With the remaining variable renewables in their portfolio and forecasts of minor quality, it is impossible for the startup to trade profitably.

Clearly, the observed effect of a changed management premium depends on the initial parametrization of the studied marketers as well as on the behaviour of the power plant owners. It is therefore important that an rigorous and profound actors analysis is performed to gain parameter values from empirical actors data. A relative comparison between two scenario variants as presented here should be uncritical, however. The question of parameter choice is discussed in the upcoming subsection.

6.2. Model Outlook: Overcoming Current Weaknesses. In agent-based modelling, the complexity of the modelled systems inevitably hampers the reporting of results as well as the policy advice. However, for some years now, attempts have been made to establish standards for the model description [57], model calibration and validation [58], and the setting up of simulation experiments [59].

In this line of reasoning, some of the used parameter assumptions should be systematically elaborated in further studies. Only an automated sensitivity analysis of a broad set of parameters would offer the required confidence intervals for a comprehensive quantitative evaluation. For example, the setting of a starting bonus for all marketers is not very realistic. Starting conditions should be adapted to the actors according to their capabilities in order to avoid skewed results in the beginning of the simulation. The threshold parameter $x_{x\min}$ and the capital of the marketers can only be based on educated guesses so far. Individual decisions and confidentiality limit the information flow in these cases.

Likewise, the decision-making of actors has to be studied and implemented with sufficient accuracy. The presented bonus adjustment rules are grounded on the assumption that marketers aim for an operational result of 0.5 €/MWh (stated as "typical margin" in power trading in general in the interviews) and adapt the bonus payouts according to the budgetary surplus. An alternative approach would assign different goals for the operational results to different marketers. However, it would be hard to estimate the marketers aim for the operational results individually as those numbers would be handled confidentially in real-world examples in most cases. An even more sophisticated approach would optimize the marketer's profit in dependence on the choice of bonus height.

Improvements of the presented bonus adjustment rules would certainly address the current myopic decision rules, as they are only based on operational results and the capital of the last year. Additional learning from previous years would improve the adoption of decision thresholds.

In general, the adaptability of AMIRIS' agents—how they change behaviours during the simulation—needs to be enhanced. In this context, an important development goal is the model endogenous expansion of installed RES-E capacity. This would allow for an estimation of the possible height of incentives to reach certain deployment goals and to study potential barriers for RES-E investments. Developments for this are currently carried out.

Further model enhancements consider the use of flexibility options, the analysis of the demand side, and the modelling of additional support mechanisms. This way, further relevant dimensions in the future energy system's complexity are represented.

Besides the use as a standalone model, AMIRIS may complement studies done with traditional energy system optimization models in order to enhance insights for the electricity system transformation from a market-based perspective (for a recent example, see, e.g., [60]). This way, the so-called "efficiency gap" between optimal and real market outcomes could be analysed. Additionally, conclusions might be drawn from such complementary studies about why decisions of heterogeneous actors on the microlevel might not necessarily result in a cost-optimal system configuration at the macrolevel and likewise on necessary policy instruments design to achieve a cost-optimal system configuration.

6.3. Lessons Learned Using an Agent-Based Model Approach. In a recent study, Macal presented a classification of agent-based modelling approaches, namely, individual, autonomous, interactive, and adaptive ABMs, in increasing order of sophistication [61]. In adaptive ABMs, agents change behaviours during the simulation. In comparison, an interactive agent-based model offers individuality of the agents with a diverse set of characteristics, endogenous and autonomous behaviours, and direct interactions between agents and the environment [61]. AMIRIS falls under the interactive category. The agents are modelled with particular scopes in decision-making, for example, the marketers' decisions regarding the adjustment of bonuses. The agents' interactions such as the one between marketer and plant operator or between marketer and market determine their success on the microlevel of actors. Nevertheless, agents do not change behaviours during simulation.

For the purpose of the model, however, this adaptability is not necessary in order to study complex system interrelations. With the case study, we present evidence for the existence of economic niches that arise for smaller, upcoming marketers and which can prevent a market concentration towards the biggest marketers with best forecast qualities and lowest specific operational incomes. We thus show that specific agent attributes like portfolio composition and size are decisive for the evolutionary economic success of marketers. This shows that sophisticated behavioural modelling is not always necessary in an ABM to make claims about emergent phenomena in systems and the complexity of agent interactions. Likewise, it would be hard to gain these insights about portfolio effects from other simulation methods but ABM.

The modelled market modules have been validated with classical "history friendly" methods (compare [10]). Results of AMIRIS depend on the interplay between several implemented modules generating a macrooutcome that remains hard to validate due to missing empirical data about market structure developments. Therefore, model results are to be interpreted as possible and plausible tendencies of the system

development—an interpretation that is suitable for most models with explorative character including ABMs.

AMIRIS allows importing changes in the regulatory framework as input parameters for explorative scenarios, considering that no normative system targets are to be achieved by individual actors. Specific policy interventions can be dynamically traced in the model. According to the classification of intervention modelling carried out by Chappin [62], this level should be aimed for when assessing interventions in a model context. In this way, our approach allows examining the impact of policy instruments considering the complex interplay between the regulatory framework, the actors, and the technoeconomic regime (see also Figure 1).

7. Conclusion

The agent-based model AMIRIS has been developed in order to analyse the impact of policy instruments regulating renewable energy market integration. The model depicts the electricity system as a complex sociotechnical system and focuses on the interdependencies between the regulatory framework, actors, and markets. The model contributes to the scientific literature in several ways.

AMIRIS offers configurations of scenarios under different external input parameters like RES-E policy support mechanisms. While there are other energy related ABMs that explore the impact of policy instruments on energy markets (see, e.g., [42, 43]), the focus on RES-E in a high temporal resolution and the typecast of actor groups is unique in the field of energy systems analysis to our best knowledge.

Different agent specifications enable defining the degree of uncertainty and bounded rationality of the actors and modelling heterogeneous system entities. Marketers especially can be defined in detail by specifying, for example, their portfolios and cost structures and their capitalization and forecast uncertainties. The specification of agents is crucial for the right interpretation of simulation results, so actor analyses have been conducted prior to model implementation and simulations. The gained insights from such analyses are used to map agent decision rules and to characterize the actors and to configure corresponding parameters in AMIRIS. It is shown that many market dynamics can be unraveled if heterogeneous agent attributes are taken into consideration.

The case study demonstrated how only minor policy changes can have a considerable effect on the agent population. This indicates how well-prepared and parametrized a transition of regulatory framework conditions has to be in order to further ensure the functioning of the system and the survival of particular actor classes. In Scenario 2, for example, the economic survival of the startup and further marketers might have been possible in case the regulatory framework would have been changed by more circumspect planning. We thus show that the intermediary market actors have to be considered in case amendments of RES-E policy instruments are planned as new interdependencies between plant operators and marketers arise.

Niches play a vital role in innovation formation in sociotechnical systems and are a fundamental driver of system transition [63]. With AMIRIS, the emergence and stability of energy market niches can be depicted without prior knowledge about their prospect of success. Their economic success would be hard to identify and trace in other, more traditional modes of simulation. The model is thus also business relevant if the results are viewed from an actors perspective. For instance, the case study revealed that competition and related changes of actors' portfolios may lead to bankruptcy of otherwise successful marketers.

To sum up, the paper demonstrates that agent-based models are suitable in multiple dimensions to study the dynamics of electricity systems under transition which are driven by a diverse set of heterogeneous actors. While there is still many open development goals (see Section 6.2), we do not regard any of these issues raised as a fundamental concern impossible to overcome.

Studying the energy system transition demands methods that are able to capture the system's complexity and dynamics. An important property of ABM approaches is their ability to flexibly use models in the model, enabling the researcher to represent the system in multiple layers. We conclude that agent-based modelling approaches like AMIRIS have the ability to enhance the knowledge that is required to ensure a successful energy system transition while preventing system breakages.

Appendix

The revenue calculation is described in detail in the following section. Revenue can be generated at the wholesale (XM) and control energy market (CE); balancing energy (bal) can add to the revenue if circumstances are favourable. The total revenue is given by

$$i(t) = i_{\mathrm{XM}}(t) + i_{\mathrm{CE}}(t) + i_{\mathrm{bal}}(t). \tag{A.1}$$

The sold volume $V_{\mathrm{XM}}(t)$ traded at the power exchange market is refunded with the management premium $M(t)$ and allows earnings of

$$i_{\mathrm{XM}}(t) = V_{\mathrm{XM}}(t) \cdot \left(\Pi_{\mathrm{XM}}(t) + M(t)\right), \tag{A.2}$$

with the wholesale power market price $\Pi_{\mathrm{XM}}(t)$. Likewise, revenues from the control energy market equate to

$$i_{\mathrm{CE}}(t) = V_{\mathrm{CE}}(t) \cdot \Pi_{\mathrm{CE}}(t). \tag{A.3}$$

The revenue from balancing energy equals negative balancing costs of the marketer; that is,

$$i_{\mathrm{bal}}(t) = -c_{\mathrm{bal}}(t). \tag{A.4}$$

The fix costs are calculated as

$$c_{\mathrm{fix}} = c_{\mathrm{IT}} + c_{\mathrm{trade,fix}}. \tag{A.5}$$

Variable costs equate to

$$\begin{aligned} c_{\mathrm{var}}(t) = {} & c_{\mathrm{XM,trading}}(t) + c_{\mathrm{pers,var}}(t) + c_{\mathrm{bal}}(t) \\ & + c_{\mathrm{fcst}}(t) + c_{\mathrm{bonus}}(t). \end{aligned} \tag{A.6}$$

Trading costs are based on the fees at the exchange market for every traded MWh with

$$c_{\mathrm{XM,trading}}(t) = c_{\mathrm{trade,var}} \cdot V(t). \tag{A.7}$$

In case balancing energy is required, the corresponding volume $V_{\mathrm{bal}}(t)$ must be procured for a price $\mathrm{PR}_{\mathrm{bal}}$ and costs are defined as

$$c_{\mathrm{bal}}(t) = \mathrm{PR}_{\mathrm{bal}} \cdot V_{\mathrm{bal}}(t). \tag{A.8}$$

According to the actors analysis the prices $\mathrm{PR}_{\mathrm{fcst}}$ per MW typically decrease with larger portfolio sizes, so

$$c_{\mathrm{fcst}}(t) = c_{\mathrm{fcst}}(\mathscr{P}) \cdot \mathscr{P}(t). \tag{A.9}$$

The size of $V_{\mathrm{bal}}(t)$ is the difference between the real actual $V(t)$ and the forecast $V_{\mathrm{fcst}}(t)$ electricity feed-in at time t:

$$V_{\mathrm{bal}}(t) = V(t) - V_{\mathrm{fcst}}(t), \tag{A.10}$$

where the latter has been forecast by the marketer $24h$ before and is determined by

$$V_{\mathrm{fcst}}(t + 24\,\mathrm{h}) = V(t + 24\,\mathrm{h}) \cdot \left(1 + \mu_{\mathrm{power}} + \sigma_{\mathrm{power}} \cdot g\right), \tag{A.11}$$

with g representing a random variable from a normal distribution. $V(t + 24\,\mathrm{h})$ denotes the actual feed-in volume 24 h ahead. The revenue of the RES operator agents is based on the remuneration and the bonus payments from the direct marketer; that is,

$$i(t) = V_{\mathrm{el}} \cdot \left(\Pi_{\mathrm{rc}}(t) + i_{\mathrm{bonus}}(t)\right). \tag{A.12}$$

The Market Premium. The aim of the market premium under the EEG is to integrate renewable energy sources into the energy market system by fostering direct marketing. Producers receive a financial compensation for the difference between energy-source-specific values to be applied (replacing the fixed feed-in tariff) as a calculation basis and the market value. This is the average energy-source-specific monthly value of the hourly contracts on the spot market for electricity (Part 3, Division 1 and Annex 1 EEG 2017). Compensating for occurring costs from direct marketing the values to be applied are higher than the replaced feed-in tariffs. The difference is set to 2 €/MWh for dispatchable renewables and 4 €/MWh for intermittent renewables (Section 53 EEG 2017). Under EEG 2012 such a difference has been separately disclosed as a management premium (Section 33g EEG 2012).

Conflicts of Interest

The authors declare that there are no conflicts of interest regarding the publication of this article.

Acknowledgments

The authors are grateful to Wolfram Krewitt who originally conceived the development of an agent-based simulation model for the analysis of the market integration of renewables. They would also like to show their gratitude to Ulrich Frey, Benjamin Fuchs, Eva Hauser, Wolfgang Hauser, Thomas Kast, Uwe Klann, Uwe Leprich, Tobias Naegler, Nils Roloff, Christoph Schimeczek, Yvonne Scholz, Bernd Schmidt, Sandra Wassermann, Rudolf Weeber, and Wolfgang Weimer-Jehle for their expert advice and contributions to the development of AMIRIS. They are thankful to all colleagues of their department for numerous fruitful discussions on AMIRIS's development and application. For the recent and ongoing funding they are much obliged to the German Ministry for the Environment, the German Ministry for Economic Affairs, the German Ministry for Research, and internal funding by the DLR within several research projects (Grant nos. BMU FKZ 0325015, BMU FKZ 0325182, BMWi FKZ 03ET4020A, BMWi FKZ 03SIN108, BMWi FKZ 03ET4032B, BMWi FKZ 03ET4025B, and BMBF FKZ 03SFK4D1).

References

[1] IPCC, *Mitigation of Climate Change. Contribution of Working Group III to the Fifth Assessment Report of the Intergovernmental Panel on Climate Change. Summary for Policymakers*, Cambridge University Press, Cambridge, UK, 2014.

[2] IEA, "World Energy Outlook 2015," Digestive Endoscopy, 2015, http://dx.doi.org/10.1787/weo-2015-en.

[3] REN21, Renewables 2016 Global Status Report, REN21 Secretariat, Paris, 2016, http://www.ren21.net/GSR-2016-Report-Full-report-EN.

[4] J. Scheffler, "Gesetz für den Vorrang Erneuerbarer Energien – EEG," in *Die gesetzliche Basis und Förderinstrumente der Energiewende*, essentials, pp. 5–31, Springer Fachmedien Wiesbaden, Wiesbaden, 2014.

[5] J. Scheffler, "Gesetz für den Vorrang Erneuerbarer Energien – EEG," in *Die gesetzliche Basis und Förderinstrumente der Energiewende*, essentials, pp. 5–31, Springer Fachmedien Wiesbaden, Wiesbaden, 2000.

[6] U. Büsgen and W. Dürrschmidt, "The expansion of electricity generation from renewable energies in Germany," *Energy Policy*, vol. 37, no. 7, pp. 2536–2545, 2009, http://dx.doi.org/10.1016/j.enpol.2008.10.048.

[7] EEG, "Gesetz für den Vorrang Erneuerbarer Energien (Erneuerbare-Energien-Gesetz)," 2012, https://www.erneuerbare-energien.de/EE/Redaktion/DE/Gesetze-Verordnungen/eeg_2012_bf.html.

[8] M. Klobasa, M. Ragwitz, F. Sensfuß et al., "Nutzenwirkung der Marktprämie," Working Paper Sustainability and Innovation No. S 1/2013, Fraunhofer Institut für System- und Innovationsforschung ISI.

[9] Federal Ministry for Economic Affairs, "Energy, Renewable Energy Sources in Figures," *National and International Development*, 2014.

[10] R. Matthias, K. Nienhaus, N. Roloff et al., "Weiterentwicklung eines agentenbasierten Simulationsmodells (AMIRIS) zur Untersuchung des Akteursverhaltens bei der Marktintegration von Strom aus erneuerbaren Energien unter verschiedenen Fördermechanismen," Deutsches Zentrum für Luft- und Raumfahrt e.V. (DLR), 2013, http://elib.dlr.de/82808/.

[11] R. Schemm and B. Daniel, "Make oder Buy," *Erneuerbare Energien*, vol. 10, no. 2014, pp. 40–43, 2014.

[12] A. Grunwald, "Energy futures: Diversity and the need for assessment," *Futures*, vol. 43, no. 8, pp. 820–830, 2011, http://dx.doi.org/10.1016/j.futures.2011.05.024.

[13] C. S. Bale, L. Varga, and T. J. Foxon, "Energy and complexity: New ways forward," *Applied Energy*, vol. 138, pp. 150–159, 2015.

[14] L. Tesfatsion, "Chapter 16 Agent-Based Computational Economics: A Constructive Approach to Economic Theory," *Handbook of Computational Economics*, vol. 2, pp. 831–880, 2006.

[15] EEX, "EEX Spot-price data from the year 2011," https://www.eex.com/de/marktdaten/strom/spotmarkt.

[16] ENTSO-E, "ENTSO-E load and consumption data," https://www.entsoe.eu/db-query/consumption/monthly-consumption-of-a-specific-country-for-a-specific-range-of-time.

[17] L. Matthias and L. Annette, "The 2014 German Renewable Energy Sources Act revision - from feed-in tariffs to direct marketing to competitive bidding," *Journal of Energy and Natural Resources Law*, vol. 33, no. 2, pp. 131–146, 2015, http://dx.doi.org/10.1080/02646811.2015.1022439.

[18] D. Kahneman, *Thinking, Fast and Slow*, Penguin Books, London, UK, 2011.

[19] A. Tversky and D. Kahneman, "Judgent Under Uncertainty: Heuristics and Biases," *Science*, vol. 185, pp. 1124–1131, 1974.

[20] W. Brian Arthur, "Inductive Reasoning and Bounded Rationality," *The American Economic Review*, vol. 84, no. 2, pp. 406–411, 1994, http://www.jstor.org/stable/2117868.

[21] M. G. De Giorgi, A. Ficarella, and M. Tarantino, "Error analysis of short term wind power prediction models," *Applied Energy*, vol. 88, no. 4, pp. 1298–1311, 2011.

[22] M. Lange, *Analysis for the Uncertainty of Wind Power Prediction, [Ph.D. thesis]*, Carl von Ossietzky University of Oldenburg, Germany, 2003.

[23] S. Rentzing, "Im Schatten der Photovoltaik," *Neue Energie*, vol. 10, pp. 48–51, 2011.

[24] O. Tietjen, *Analyses of Risk Factors in Conventional and Renewable Energy Dominated Electricity Markets, [Ph.D. thesis]*, Masterarbeit an der Freien Universiterlin (FU) und Potsdam Institute for Climate Impact Research (PIK), 2014.

[25] A. Weidlich, *Engineering Interrelated Electricity Markets - An agentbased computational Approach [Ph.D. thesis]*, Disseration - Universitat Karlsruhe TH - Faculty of Economics, 2008.

[26] G. Gallo, "Electricity market games: How agent-based modeling can help under high penetrations of variable generation," *The Electricity Journal*, vol. 29, no. 2, pp. 39–46, 2016, http://dx.doi.org/10.1016/j.tej.2016.02.001.

[27] B. Wooldrige, *An Introduction to Multi-Agent Systems*, John Wiley and Sons, Chichester, UK, 2002.

[28] C. M. MacAl and M. J. North, "Tutorial on agent-based modelling and simulation," *Journal of Simulation*, vol. 4, no. 3, pp. 151–162, 2010, http://dx.doi.org/10.1057/jos.2010.3.

[29] J. M. Epstein and R. L. Axtell, *Growing artificial societies: Social science from the bottom up*, Massachusetts Institute of Technology, Cambridge, USA, 1996.

[30] J. H. Holland and J. H. Miller, "Artificial adaptive agents in economic theory," *The American Economic Review*, vol. 81, pp. 365–370, 1991.

[31] V. Rai and S. A. Robinson, "Agent-based modeling of energy technology adoption: Empirical integration of social, behavioral, economic, and environmental factors," *Environmental Modelling and Software*, vol. 70, pp. 163–177, 2015, http://www.sciencedirect.com/science/article/pii/S1364815215001231?via%3Dihub.

[32] J. Palmer, G. Sorda, and R. Madlener, "Modeling the diffusion of residential photovoltaic systems in Italy: An agent-based simulation," *Technological Forecasting & Social Change*, vol. 99, pp. 106–131, 2015.

[33] G. Sorda, Y. Sunak, and R. Madlener, "An agent-based spatial simulation to evaluate the promotion of electricity from agricultural biogas plants in Germany," *Ecological Economics*, vol. 89, pp. 43–60, 2013.

[34] F. Genoese and M. Genoese, "Assessing the value of storage in a future energy system with a high share of renewable electricity generation," *Energy Systems*, vol. 5, no. 1, pp. 19–44, 2014.

[35] S. Yousefi, M. P. Moghaddam, and V. J. Majd, "Optimal real time pricing in an agent-based retail market using a comprehensive demand response model," *Energy*, vol. 36, no. 9, pp. 5716–5727, 2011.

[36] M. Zheng, C. J. Meinrenken, and K. S. Lackner, "Agent-based model for electricity consumption and storage to evaluate economic viability of tariff arbitrage for residential sector demand response," *Applied Energy*, vol. 126, pp. 297–306, 2014.

[37] Z. Zhou, F. Zhao, and J. Wang, "Agent-based electricity market simulation with demand response from commercial buildings," *IEEE Transactions on Smart Grid*, vol. 2, no. 4, pp. 580–588, 2011.

[38] A. Kowalska-Pyzalska, K. Maciejowska, K. Suszczyński, K. Sznajd-Weron, and R. Weron, "Turning green: Agent-based modeling of the adoption of dynamic electricity tariffs," *Energy Policy*, vol. 72, pp. 164–174, 2014.

[39] P. R. Thimmapuram and J. Kim, "Consumers' price elasticity of demand modeling with economic effects on electricity markets using an agent-based model," *IEEE Transactions on Smart Grid*, vol. 4, no. 1, pp. 390–397, 2013.

[40] T. Zhang and W. J. Nuttall, "Evaluating Government's Policies on Promoting Smart Metering Diffusion in Retail Electricity Markets via Agent-Based Simulation*," *Journal of Product Innovation Management*, vol. 28, no. 2, pp. 169–186, 2011.

[41] R. A. C. van der Veen, A. Abbasy, and R. A. Hakvoort, "Agent-based analysis of the impact of the imbalance pricing mechanism on market behavior in electricity balancing markets," *Energy Economics*, vol. 34, no. 4, pp. 874–881, 2012.

[42] F. Sensfuß, M. Ragwitz, and M. Genoese, "The merit-order effect: A detailed analysis of the price effect of renewable electricity generation on spot market prices in Germany," *Energy Policy*, vol. 36, no. 8, pp. 3076–3084, 2008.

[43] J. C. Richstein, E. J. L. Chappin, and L. J. de Vries, "Cross-border electricity market effects due to price caps in an emission trading system: An agent-based approach," *Energy Policy*, vol. 71, pp. 139–158, 2014.

[44] G. Li and J. Shi, "Agent-based modeling for trading wind power with uncertainty in the day-ahead wholesale electricity markets of single-sided auctions," *Applied Energy*, vol. 99, pp. 13–22, 2012.

[45] L. A. Wehinger, G. Hug-Glanzmann, M. D. Galus, and G. Andersson, "Modeling electricity wholesale markets with model predictive and profit maximizing agents," *IEEE Transactions on Power Systems*, vol. 28, no. 2, pp. 868–876, 2013.

[46] F. Sensuß, M. Genoese, M. Ragwitz, and D. Möst, "Agent-based Simulation of Electricity Markets -A Literature Review," *Energy Studies Review*, vol. 15, no. 2, 2007.

[47] P. Ringler, D. Keles, and W. Fichtner, "Agent-based modelling and simulation of smart electricity grids and markets - A literature review," *Renewable & Sustainable Energy Reviews*, vol. 57, pp. 205–215, 2016.

[48] S. Wassermann, M. Reeg, and K. Nienhaus, "Current challenges of Germany's energy transition project and competing strategies of challengers and incumbents: The case of direct marketing of electricity from renewable energy sources," *Energy Policy*, vol. 76, pp. 66–75, 2015.

[49] ENWG, "Gesetz über die Elektrizitäts- und Gasversorgung," Bundesanzeiger des Bundesministerium fr Justiz, 2005, https://www.gesetze-im-internet.de/enwg_2005/.

[50] M. J. North, N. T. Collier, J. Ozik et al., "Complex adaptive systems modeling with Repast Simphony," *Complex Adaptive Systems Modeling*, vol. 1, no. 1, p. 3, 2013.

[51] N. Joachim, T. Pregger, T. Naegler et al., "Long-term scenarios and strategies for the deployment of renewable energies in Germany in view of European and global developments," DLR Portal, 2012, http://elib.dlr.de/76044/.

[52] Y. Scholz, *Renewable energy based electricity supply at low costs: development of the REMix model and application for Europe [Ph.D. thesis]*, Universität Stuttgart, Germany, 2012.

[53] D. Stetter, *Enhancement of the REMix energy system model: Global renewable energy potentials, optimized power plant siting and scenario validation [Ph.D. thesis]*, Universität Stuttgart, Germany, 2014.

[54] MaPrV, Verordnung über die Höhe der Managementprämie für Strom aus Windenergie und solarer Strahlungsenergie, 2012, https://www.clearingstelle-eeg.de/maprv.

[55] Übertragungsnetzbetreiber, https://www.netztransparenz.de/EEG/Verguetungs-und-Umlagekategorien.

[56] AusglMechV., "Verordnung zur Weiterentwcklung des bundesweiten Ausgleichmechanismus," *Bundesanzeiger des Bundesministerium für Justiz*, 2010.

[57] V. Grimm, U. Berger, D. L. DeAngelis, J. G. Polhill, J. Giske, and S. F. Railsback, "The ODD protocol: A review and first update," *Ecological Modelling*, vol. 221, no. 23, pp. 2760–2768, 2010.

[58] P. Windrum, G. Fagiolo, and A. Moneta, "Empirical Validation of Agent-Based Models: Alternatives and Prospects," *Journal of Artificial Societies and Social Simulation*, vol. 10, no. 2, 2007, http://jasss.soc.surrey.ac.uk/10/2/8.html.

[59] I. Lorscheid, B.-O. Heine, and M. Meyer, "Opening the "black box" of simulations: increased transparency and effective communication through the systematic design of experiments," *Computational and Mathematical Organization Theory*, vol. 18, no. 1, pp. 22–62, 2012, https://doi.org/10.1007/s10588-011-9097-3.

[60] O. Weiss, D. Bogdanov, K. Salovaara, and S. Honkapuro, "Market designs for a 100% renewable energy system: Case isolated power system of Israel," *Energy*, vol. 119, pp. 266–277, 2017.

[61] C. M. Macal, "Everything you need to know about agent-based modelling and simulation," *Journal of Simulation*, vol. 10, no. 2, pp. 144–156, 2016.

[62] E. J. L. Chappin, *Simulating Energy Transitions [Ph.D. thesis]*, TU Delft, 2011, http://resolver.tudelft.nl/uuid.

[63] F. W. Geels, "Technological transitions as evolutionary reconfiguration processes: A multi-level perspective and a case-study," *Research Policy*, vol. 31, no. 8-9, pp. 1257–1274, 2002.

Hindawi
Complexity
Volume 2017, Article ID 5031505, 26 pages
https://doi.org/10.1155/2017/5031505

Research Article

A Stability Analysis of Thermostatically Controlled Loads for Power System Frequency Control

Ellen Webborn[1] and Robert S. MacKay[1,2]

[1]*Centre for Complexity Science, University of Warwick, Coventry, UK*
[2]*Mathematics Institute, University of Warwick, Coventry, UK*

Correspondence should be addressed to Ellen Webborn; ellen.webborn@warwickgrad.net

Received 30 June 2017; Accepted 10 October 2017; Published 6 December 2017

Academic Editor: Paul Hines

Thermostatically controlled loads (TCLs) are a flexible demand resource with the potential to play a significant role in supporting electricity grid operation. We model a large number of identical TCLs acting autonomously according to a deterministic control scheme to provide frequency response as a population of coupled oscillators. We perform stability analysis to explore the danger of the TCL temperature cycles synchronising: an emergent phenomenon often found in populations of coupled oscillators and predicted in this type of demand response scheme. We take identical TCLs as it can be assumed to be the worst case. We find that the uniform equilibrium is stable and the fully synchronised periodic cycle is unstable, suggesting that synchronisation might not be as serious a danger as feared. Then detailed simulations are performed to study the effects of a population of frequency-sensitive TCLs acting under real system conditions using historic system data. The potential reduction in frequency response services required from other providers is determined, for both homogeneous and heterogeneous populations. For homogeneous populations, we find significant synchronisation, but very minimal diversity removes the synchronisation effects. In summary, we combine dynamical systems stability analysis with large-scale simulations to offer new insights into TCL switching behaviour.

1. Introduction

To operate the electricity grid reliably and securely requires controlling a number of factors, one of which is the electricity grid frequency. The AC frequency continually varies close to its nominal value (50 Hz in Europe) and is kept there by the System Operator (SO) in order to respect regulations and prevent network instabilities and blackouts. This is mainly done by employing flexible power generators, such as gas turbines, to vary their output in response to imbalance between supply and demand. This type of service is often known as frequency response, or frequency regulation. With the arrival of large numbers of wind and solar farms, smart meters, and thousands of domestic solar panels, uncontrolled and largely invisible to the System Operator, new challenges and opportunities have arisen. Rather than relying on a few large (typically fossil-fuelled) power plants to provide system balancing, there is the potential, and perhaps a need, for consumers to play a role. However, for a large number of very small players to participate would require a modelling approach capable of incorporating the complexities of such a system and foreseeing emergent phenomena that may arise as a result of the interactions involved. In this article we explore the potential for certain types of domestic appliances to provide frequency response through simple deterministic rules and consider the possibility of (potentially harmful) demand synchronisation.

Thermostatically controlled loads (TCLs) are well-suited for the provision of demand-side response (DSR), due to their simple temperature set point operating rules and ubiquity in society. Examples include fridges, freezers, air-conditioners, hot-water tanks, heat pumps, and swimming pool pumps. Research into the possibility of using TCLs for grid balancing services began in the 1980s with key papers such as [1–4]. Despite the existence of technology for creating frequency-sensitive TCLs for nearly 40 years, implementation remains limited to a relatively small number of trials [5–9]. There are a number of reasons for the absence of large roll-outs of

Table 1: Comparison of centralised and decentralised TCL control strategies. Informed by, for example, [19, 38].

	Centralised control	Decentralised control
Key features	(i) TCLs instructed by a central controller (ii) 2-way communication in all TCLs	(i) Autonomous local control (ii) Control scheme established once, may be updated periodically
Advantages	(i) Highly controllable (ii) Reasonably predictable	(i) No communications infrastructure required (ii) No security risks (iii) Very fast response possible
Disadvantages	(i) Establishing and maintaining a secure communications network are very expensive (ii) Response time limited by communication speed (iii) Vast amounts of data to manage (iv) Data and appliance control security risks (v) Negative public perceptions of external control of home appliances	(i) Response is less predictable than with centralised control (ii) Synchronisation and instability effects possible and not yet fully understood (iii) Errors and noise in local frequency measurements more likely

highly distributed DSR schemes [10, 11]. Historically, control paradigms from both technical and economic perspectives have been established for service provision from a (relatively) small number of large power plants. Understandably, the critical nature of electricity grid operation and security deters potentially risky changes and experimentation, and so a great deal of motivation is required for shifts away from traditional approaches. Service availability and reliability can be improved by splitting a service between a multitude of providers, compared to a single unit which will become completely unavailable in the event of a fault or scheduled repair [9, 12]. Yet there is also inherent complexity and potentially reduced predictability in procuring services from thousands of very small demand-side resources if they act autonomously, which is undoubtedly an obstacle to be overcome. Effects on consumers and their appliances will also be of concern to potential participants. Finally, it will be crucial for the success of any scheme, to adequately address the requirements for minimum participation numbers and develop the right business models that ensure fair rewards and effective incentives.

The changing energy landscape in the 21st century has brought a new focus to the use of TCLs for electricity grid support and a wealth of literature on the topic [5, 9–11, 13–37]. Work has varied in nature from mathematical frameworks to numerical simulations and real-world trials. Most of the theory can be applied to any type of TCL, and simulations have covered many different possible TCL technologies. A variety of control schemes have been proposed, many of which are discussed and compared in [10, 19, 35]. There are two main classes into which these types of TCL control schemes can be divided: *centralised* and *decentralised* control (with a spectrum in between). Their key features and comparative advantages and disadvantages are summarised in Table 1. It is widely accepted that if millions of TCLs could be used for frequency response they could potentially provide a valuable resource for the system. However, if each device needed constant communication with a central controller, sending data about its temperature and switching history and receiving operation instructions, then the economics and security risks would severely outweigh the benefits of the service. Public perception of the service is also vital for the implementation of any control scheme that involves appliances in people's homes. For these reasons we choose to focus on decentralised control for our research. A better understanding, however, of the potential undesirable side-effects of decentralised control, is required before any control strategy could be put in place.

The challenges of implementing a decentralised control scheme largely centre around the propensity for TCL temperature cycling to become synchronised. A number of simulations in the literature indicate TCL synchronisation following a frequency disturbance, for example, [13, 21, 22, 25, 30–32]. As a result, various control schemes have been proposed that aim to prevent such behaviour. A popular choice is some form of stochastic temperature set point control [11, 13, 33, 34, 39, 40]. For example, [11] simulates a heterogeneous population of electric heaters in the Nordic power grid, with deterministic control to respond to sudden frequency fluctuations followed by randomised switch times as the system returns to normal. Domestic fridges are modelled in [13] as Markov-jump linear systems where the on/off switching is governed by transition probability rates rather than temperature set points. These rates are determined by choosing the desired population average temperature or duty cycle, and the temperature probability density is steered towards a desired distribution. While stochastic control schemes do offer solutions to the potential for demand synchronisation, they are typically accompanied by two disadvantages. Firstly, naive stochastic switching can involve a TCL switching twice (or more) within a short time frame, which is detrimental to serving its purpose, and can cause wear on the device (though non-Markovian approaches can avoid this). Secondly, learning that home appliances will

randomly switch on and off could cause negative public perceptions of a DSR scheme. We believe further study of potential deterministic schemes would be beneficial before putting attention on stochastic schemes, particularly given the natural diversity in TCL populations that could prevent synchronisation phenomena.

An alternative to direct instructions and frequency signals is the use of a price signal that TCLs could respond to. The advantages of price signals are that it is possible to measure the financial benefits to consumers of DSR participation, and individual consumers could potentially make their own choices about the value they place on service disruption at, say, given times of day. However, current price signals typically change on half-hourly or at least several-minute time scales, which makes them ill-suited for dynamic frequency response. Reviews on the use of price signals for demand response can be found in [41–43]. A related approach proposed in [44] involves each device calculating the price directly from the grid frequency, and the authors argue that a well-chosen design for the controller and frequency-price coupling may prevent possible oscillations and instabilities. However, the drawbacks of price-based demand response, as remarked upon in [27], are the potential for synchronisation and the exposure of customers to price volatility, which could prevent sufficient participation for success.

In [13] Angeli and Kountouriotis offer theoretical arguments for the long-term tendency of the system towards TCL synchronisation. It is reasoned that any "small periodic ripples in power system frequency will gradually entrain oscillations of refrigerators that have similar frequencies of oscillation, thus reinforcing the frequency ripple and eventually leading to an even larger number of entrained refrigerators." We concur with the mathematical reasoning presented. However, we believe that further reasoning and inquiry are required for a more complete understanding of this phenomenon.

A population of TCLs responding to frequency through preset deterministic rules with no other communications or control can be thought of as a system of coupled oscillators. Synchronisation phenomena emerging from systems of coupled oscillators have been studied in many contexts, from neural signals in the brain to flashing fireflies [45]. The Kuramoto framework was developed [46, 47] which elegantly describes basic features of such systems and allows for stability analysis. Inspired by results for the Kuramoto model, in this article we explore the stability of a system of TCLs and grid frequency using techniques from dynamical systems and agent-based modelling.

We study the potential for a population of TCLs to support grid frequency and explore the possibilities for frequency-sensitive TCLs to cause instabilities due to cycle synchronisation. We use techniques from dynamical systems stability analysis along with simulations that incorporate data from the British power grid. In Section 2 we introduce our model for a population of TCLs and the electricity grid frequency and explain our choices of parameter values. In Section 3.1 we present a stability analysis of the nominal frequency in the presence of a uniformly distributed population of TCLs. Section 3.2 solves the behaviour of a fully synchronised TCL population and analyses the stability of the population under a split into two groups. Section 4.1 describes our simulations of a large population of TCLs using the model in Section 3.1. Section 4.2 describes our simulations of a population of TCLs acting on the system in the presence of other frequency response providers and naturally occurring frequency fluctuations, including simulations of a heterogeneous population. Section 5 contains our final discussion and conclusions.

2. Modelling TCLs and Electricity Grid Frequency

The modelling is kept appliance-neutral where possible, but it is set up for cooling devices such as fridges, (fridge-)freezers, and air-conditioners and would need to be altered in minor ways for other appliances such as heat pumps and hot-water tanks. We make the following assumptions:

(i) Electricity grid frequency is the same everywhere on the network and there are no inter-area oscillations [48] (therefore all machines on the power grid are assumed to rotate in synchrony).

(ii) All TCLs sense frequency deviations with negligible measurement delay or measurement error.

(iii) All system parameters remain constant over time.

(iv) Fridges and freezers are not affected by the fridge/freezer door being opened, or by the addition or removal of food (in effect we assume this never occurs).

(v) TCLs have continuous thermostat control (in temperature and time) and can therefore sense and implement temperature/set point changes with infinite precision.

(vi) TCLs consume constant power when on and zero power when off and are controlled only by the rules outlined in the model.

These assumptions allow us to create a tractable model for analytic study. Assumptions (iii) and (iv) are probably the easiest and most natural to relax first and could be relaxed by adding time-dependent forcing effects. For most of the paper we consider a population of identical TCLs, but our formulation can be extended easily to an inhomogeneous population and we believe the effects of sufficient diversity will be stabilising, as supported by our final simulation.

2.1. Individual TCLs. For the temperature cycling of a TCL we adopt the linear model and notation presented in [13]. Let the temperature of a TCL at time t be denoted by $T(t)$, the cooling/heating coefficient by α, and the asymptotic temperatures that the TCL would reach if left on and off indefinitely by T_{ON} and T_{OFF}, respectively. Then

$$\dot{T}(t) = \begin{cases} \alpha\left(T_{\mathrm{ON}} - T(t)\right) & \text{when the TCL is on} \\ \alpha\left(T_{\mathrm{OFF}} - T(t)\right) & \text{when the TCL is off.} \end{cases} \quad (1)$$

A (cooling) TCL will switch off when the temperature reaches its lower temperature set point T_- and switch on when it reaches its upper temperature set point T_+. We choose to make these set points sensitive to system frequency deviations away from 50 Hz, denoted $f(t)$ (i.e., $f(t)$ = Frequency(t) − 50 Hz). Insufficient generation to meet demand causes $f < 0$ and so we need the TCLs to reduce their power consumption to bring f back to zero. We implement this by increasing the temperature set points so that the TCLs switch off sooner/stay off for longer. Oversupply of electricity to the grid causes $f > 0$, and so in this case we decrease the temperature set points to increase overall power consumption. Thus we define our frequency-sensitive temperature set points,

$$T_-\left(f\left(t\right)\right) \coloneqq T_-^0 - \beta_- f\left(t\right) \quad \text{lower (switch off) set point} \tag{2a}$$

$$T_+\left(f\left(t\right)\right) \coloneqq T_+^0 - \beta_+ f\left(t\right) \quad \text{upper (switch on) set point,} \tag{2b}$$

where β_-, β_+ are positive constants that determine the sensitivity of the lower and upper temperature set points to frequency deviations. T_-^0 and T_+^0 are the uncoupled (a fridge is "uncoupled" from the grid frequency if $\beta_- = \beta_+ = 0$) temperature set points, which we typically take to be 2°C and 7°C, respectively. This framework is very similar to that suggested in [30], although we allow the upper and lower temperature set points to have different sensitivities to the frequency (β_- and β_+).

We can solve (1) for the temperature of a TCL at time t. If a TCL has temperature T_0 at time t_0 and does not switch on or off before time t then the temperature $T(t)$ is given by

$$T\left(t\right) = \left(T_0 - T_{\mathrm{ON}}\right) e^{-\alpha\left(t-t_0\right)} + T_{\mathrm{ON}} \quad \text{when on} \tag{3a}$$

$$T\left(t\right) = \left(T_0 - T_{\mathrm{OFF}}\right) e^{-\alpha\left(t-t_0\right)} + T_{\mathrm{OFF}} \quad \text{when off.} \tag{3b}$$

We can rearrange (3a) and (3b) and solve for the on and off durations τ_{ON} and τ_{OFF}, respectively, assuming constant grid frequency:

$$\tau_{\mathrm{ON}}\left(f\right) = \frac{1}{\alpha}\log\left(\frac{T_+\left(f\right) - T_{\mathrm{ON}}}{T_-\left(f\right) - T_{\mathrm{ON}}}\right) \tag{4a}$$

$$\tau_{\mathrm{OFF}}\left(f\right) = \frac{1}{\alpha}\log\left(\frac{T_{\mathrm{OFF}} - T_-\left(f\right)}{T_{\mathrm{OFF}} - T_+\left(f\right)}\right). \tag{4b}$$

These variables will be useful when we consider the equilibrium of the system, in which the temperature set points become fixed. In the traditional case when TCLs are uncoupled from the grid (or the special case $f \equiv 0$) their "natural" on and off cycle durations, τ_{ON}^0 and τ_{OFF}^0, are given by

$$\tau_{\mathrm{ON}}^0 = \frac{1}{\alpha}\log\left(\frac{T_+^0 - T_{\mathrm{ON}}}{T_-^0 - T_{\mathrm{ON}}}\right) \tag{5a}$$

$$\tau_{\mathrm{OFF}}^0 = \frac{1}{\alpha}\log\left(\frac{T_{\mathrm{OFF}} - T_-^0}{T_{\mathrm{OFF}} - T_+^0}\right). \tag{5b}$$

In order for the TCLs to operate properly they need to cycle on and off, and so we require that

$$T_{\mathrm{ON}} < T_-\left(f\left(t\right)\right) < T_+\left(f\left(t\right)\right) < T_{\mathrm{OFF}} \quad \forall t. \tag{6}$$

We also need a TCL to respond "appropriately" to a change in frequency, that is to say, for the average power consumption over one cycle to increase when the frequency increases and decrease when the frequency decreases. It is shown in Appendix A that a sufficient condition to ensure this is

$$\frac{\beta_+}{\beta_-} \in \left(\frac{T_{\mathrm{OFF}} - T_+}{T_{\mathrm{OFF}} - T_-}, \frac{T_+ - T_{\mathrm{ON}}}{T_- - T_{\mathrm{ON}}}\right) \tag{7}$$

which is a nonempty interval (notably containing {1}).

2.2. Electricity Grid Frequency. A simplified equation for the frequency F of a power system can be determined by Newton's 2nd Law of Motion or the derived equation for energy. If we let $f \coloneqq F - F_0$, where F_0 is the nominal grid frequency (50 Hz in Europe) and linearise about F_0, then we obtain [26]

$$M\frac{\mathrm{d}f}{\mathrm{d}t} + Df\left(t\right) = \Delta P_g - \Delta P_l \tag{8}$$

and for brevity we introduce new variables along with explicit consideration of TCL power consumption

$$\frac{\mathrm{d}f}{\mathrm{d}t}\left(t\right) = c\left(\Delta P - \rho\left(t\right) P_c\right) - \gamma f\left(t\right), \tag{9}$$

where

$M \coloneqq 4\pi^2 I F_0$ stands for 2π times nominal angular momentum of the rotating masses in the system,

I stands for total inertia of the rotating masses of the system,

D stands for damping factor representing the natural frequency dependence of the load alongside the damping provided by synchronous generator damper windings,

ΔP_g stands for change in total active power generation, compared to a reference level,

ΔP_l stands for change in total active power load, compared to a reference level,

$c \coloneqq 1/M$ stands for inverse nominal angular momentum, introduced for brevity,

ΔP stands for "surplus power generation for the TCLs;" total system active power generation minus total system active power load, excluding TCL power consumption,

ρ stands for proportion of TCLs switched on,

P_c stands for power consumed by TCL population when all switched on,

$\gamma \coloneqq D/M$ is a variable introduced for brevity.

We make the simplifying assumption in Sections 2 and 3 that the "surplus" power generation on the system for TCL consumption ΔP is a constant. We use the "$*$" notation to denote equilibrium values. In equilibrium

$$c\left(\Delta P - \rho^* P_c\right) - \gamma f^* = 0, \tag{10}$$

hence

$$f^* = \frac{c}{\gamma}\left(\Delta P - \rho^* P_c\right), \tag{11}$$

and therefore we can rewrite our equation for $\dot{f}$ in terms of deviations from equilibrium values:

$$\dot{\tilde{f}}(t) = cP_c\left(\rho^* - \rho(t)\right) - \gamma\tilde{f}, \tag{12}$$

where

$$\tilde{f} \coloneqq f - f^*. \tag{13}$$

2.3. Parameter Choices. We take as reference the Great Britain (GB) electricity system. This covers England, Scotland, and Wales. In 2015 approximately 10.4 m households in the UK, which also includes Northern Ireland, owned a fridge and 19.1 m households owned a fridge-freezer [49]. In the same year approximately 2.8% of the population lived in Northern Ireland [50]. If we assume that the average number of people per household is the same in Northern Ireland and in GB and an even distribution of fridge and fridge-freezer ownership, then approximately 10.1 m and 18.6 m households in GB owned a fridge and fridge-freezer, respectively. If using TCLs for frequency response became standard practice, that would mean that a very large number of appliances could participate in frequency response. We model the case of 1 million fridges participating in frequency response, which corresponds to roughly 10% of fridges in GB. We take the power consumed by an individual fridge when switched on, p, to be 70 W, as assumed in [32, 33]. This means that we let $p = 7 \times 10^{-5}$ MW and the total power consumption if all fridges were switched on, $P_c = 7\times10^{-5}\times10^6 = 70$ MW. Using our approximation for $\dot{f}(t)$ [51], $c = 50/(2E_k)$. Our GB system data (discussed later) gives an approximate average value for total stored kinetic energy E_k; $E_k = 2.5 \times 10^5$ MVAs (note that MVAs = MJ), and so $c = 1 \times 10^{-4}$. We let ρ^* vary between 0 and 1 by changing ΔP. Our parameters are summarised in Table 2, and throughout this paper take these values unless stated otherwise.

Table 2: Parameter values assumed, unless stated otherwise.

Parameter	Value	Units
T_{OFF}	20	°C
T_{ON}	−26	°C
T_-^0	2	°C
T_+^0	7	°C
α	1.808×10^{-4}	s^{-1}
β_+	2.4	°C·Hz^{-1}
β_-	2.4	°C·Hz^{-1}
c	1×10^{-4}	Hz(MVAs)$^{-1}$
γ	0	s^{-1}
p	7×10^{-5}	MW
P_c	70	MW
ΔP	0.3355	MW

3. Stability Analysis

Concerns that frequency-responsive TCLs controlled by deterministic rules will exhibit herding behaviour and create frequency oscillations have been raised in various previous works, either by predictions or examples from simulations [13, 21, 22, 25, 30–32]. The simplicity of our model allows for a rigorous mathematical treatment of the stability of a population of TCLs responding according to the scheme introduced above. In the first part of this section we model a TCL population as a continuum on the temperature cycle and linearise about the equilibrium discussed in Section 2.2. In the second part of this section we consider the opposite extreme for a TCL distribution (one or two Dirac delta distributions), solving for the behaviour of a fully synchronised population of TCLs and studying the dynamics of two synchronised groups.

3.1. Uniform Distribution of TCLs. We begin by studying the stability of a population of TCLs uniformly distributed in phase (meaning the time since last switch on). This means that under constant temperature set point conditions the TCLs would switch on at a constant rate and switch off at a (possibly different) constant rate (note that since TCLs heat (or cool) at different rates depending on their current temperature, uniformly distributing the TCLs within each part of the cycle does not correspond to uniformly distributing the population over the temperature scale). In the context of the Kuramoto model this is usually referred to as the "incoherent solution," for example [47, 52]. Just as in Strogatz and Mirollo's treatment of the Kuramoto model [52], we model the infinite-N limit of a population of TCLs as a continuum of TCLs distributed over an interval with periodic boundary conditions.

In order to obtain a tractable model, comparable to the Kuramoto model, three key challenges must be addressed. Firstly, the TCL temperature cycling is described by the piecewise-smooth nonlinear function (see (3a) and (3b)), with nondifferentiability at each temperature set point. Secondly, these set points are continuously changing with grid frequency, and so any map to a periodic regime must be sufficiently flexible to accommodate this. Finally, in order to know a TCL's rate of change of temperature at any time, one needs to know both its current temperature and its current (on/off) state. We therefore propose a new modelling framework to overcome these challenges and permit stability analysis for the model.

We map each TCL with temperature and on/off state to a point θ on the interval $[-1, 1)$, in such a way that θ dictates both the temperature and the state of a TCL. The switched off TCLs are mapped to the interval $[-1, 0)$ and the switched on TCLs are mapped to $[0, 1)$. Then we define the position

$\theta(t)$ of a TCL at time t with temperature $T(t)$ and state on or off by

$$\theta(t) = \begin{cases} \theta_{\mathrm{ON}}(t) = \dfrac{1}{\alpha\tau_{\mathrm{ON}}(f(t))}\log\left(\dfrac{T_+(f(t)) - T_{\mathrm{ON}}}{T(t) - T_{\mathrm{ON}}}\right) \in [0,1) & \text{if on} \\ \theta_{\mathrm{OFF}}(t) = \dfrac{1}{\alpha\tau_{\mathrm{OFF}}(f(t))}\log\left(\dfrac{T_{\mathrm{OFF}} - T_+(f(t))}{T_{\mathrm{OFF}} - T(t)}\right) \in [-1,0) & \text{if off.} \end{cases} \tag{14}$$

Note that the model implicitly assumes that the temperature set points never change fast enough to leave a TCL outside of the interval $[T_-(f(t)), T_+(f(t))]$. Since in this paper we use this model for only linear stability analysis about the equilibrium, we consider this to be a reasonable assumption. Our choice of θ means that uniformly distributing a population of TCLs over each part of the temperature cycle (as discussed above) corresponds to a uniform distribution of on and off TCLs in their respective halves of θ-space.

As in [52], we consider the population density in θ-space; let $u(\theta,t)\mathrm{d}\theta$ denote the fraction of TCLs that lie between θ and $\theta+\mathrm{d}\theta$ at time t. Then u is nonnegative, with period length 2 in θ, and satisfies the normalisation

$$\int_{-1}^{+1} u(\theta,t)\,\mathrm{d}\theta = 1 \tag{15}$$

for all t. The evolution of u is governed by the continuity equation [53]

$$\frac{\partial u}{\partial t} + \frac{\partial}{\partial\theta}(uv) = 0, \tag{16}$$

where v is the velocity of a TCL in θ-space, $v(\theta,t) \coloneqq \dot{\theta}(t)$. Differentiating (14) gives

$$v_{\mathrm{ON}}(\theta,t) = \frac{1}{\tau_{\mathrm{ON}}(f(t))}\left(1 + \frac{1}{\alpha}\left[\phi_{\mathrm{ON}}(f(t))\,\theta - \frac{\beta_+}{T_+(f(t)) - T_{\mathrm{ON}}}\right]\dot{f}(t)\right) \tag{17a}$$

$$v_{\mathrm{OFF}}(\theta,t) = \frac{1}{\tau_{\mathrm{OFF}}(f(t))}\left(1 + \frac{1}{\alpha}\left[\phi_{\mathrm{OFF}}(f(t))\,\theta + \frac{\beta_+}{T_{\mathrm{OFF}} - T_+(f(t))}\right]\dot{f}(t)\right), \tag{17b}$$

where

$$\phi_{\mathrm{ON}}(f) \coloneqq \frac{\beta_+}{T_+(f) - T_{\mathrm{ON}}} - \frac{\beta_-}{T_-(f) - T_{\mathrm{ON}}} \tag{18a}$$

$$\phi_{\mathrm{OFF}}(f) \coloneqq \frac{\beta_+}{T_{\mathrm{OFF}} - T_+(f)} - \frac{\beta_-}{T_{\mathrm{OFF}} - T_-(f)}. \tag{18b}$$

Note that, for β_+/β_- satisfying (7), $\phi_{\mathrm{ON}}(f) < 0$ and $\phi_{\mathrm{OFF}}(f) > 0$. Under a constant grid frequency, $\dot{\theta}_{\mathrm{ON}}$ and $\dot{\theta}_{\mathrm{OFF}}$ are constants. In equilibrium u^* we have $\dot{u}^* = 0$, and therefore (16) implies

$$u^*_{\mathrm{ON}}(\theta) = \frac{k_0}{v^*_{\mathrm{ON}}(\theta)}; \qquad u^*_{\mathrm{OFF}}(\theta) = \frac{k_0}{v^*_{\mathrm{OFF}}(\theta)}, \tag{19}$$

for some constant k_0. Since $\dot{f}^* = 0$, from (17a) and (17b) we have

$$v^*_{\mathrm{ON}} = \frac{1}{\tau^*_{\mathrm{ON}}}; \qquad v^*_{\mathrm{OFF}} = \frac{1}{\tau^*_{\mathrm{OFF}}}. \tag{20}$$

Then for all $\theta \in [-1,0), [0,1)$, respectively,

$$u^*_{\mathrm{ON}}(\theta) = k_0\tau^*_{\mathrm{ON}} \qquad u^*_{\mathrm{OFF}}(\theta) = k_0\tau^*_{\mathrm{OFF}} \tag{21}$$

and k_0 is determined by the normalisation criterion (15),

$$k_0 = \frac{1}{\tau^*_{\mathrm{ON}} + \tau^*_{\mathrm{OFF}}}. \tag{22}$$

The proportion of TCLs switched on, $\rho(t)$, is given by

$$\rho(t) = \int_0^1 u(\theta,t)\,\mathrm{d}\theta. \tag{23}$$

In equilibrium $\rho(t) = \rho^*$ (12),

$$\rho^* = \int_0^1 u^*(\theta,t)\,\mathrm{d}\theta = \frac{\tau^*_{\mathrm{ON}}}{\tau^*_{\mathrm{ON}} + \tau^*_{\mathrm{OFF}}}. \tag{24}$$

We introduce the notation "$\bullet$" to imply that an equation holds for the variable with either of two values, "on" or "off." Our approach is to perturb the system about the equilibrium (u^*, f^*) by a small amount $\tau^*_\bullet\eta(\theta,t)$ and to consider the evolution of the perturbation. By (15) the perturbation satisfies

$$\int_{-1}^{+1} \eta(\theta,t)\,\mathrm{d}\theta = 0. \tag{25}$$

We write

$$u_\bullet = \left(k_0 + \eta\left(\theta, t\right)\right)\tau_\bullet^* \tag{26}$$

$$v_\bullet = \frac{1}{\tau_\bullet^*}\left(1 + w\left(\theta, t\right)\right) \tag{27}$$

so that (16) becomes

$$\tau_\bullet^* \frac{\partial}{\partial t}\left[\eta\right] + \frac{\partial}{\partial \theta}\left[k_0 + k_0 w + \eta + \eta w\right] = 0. \tag{28}$$

Taking the first-order approximation yields

$$\tau_\bullet^* \frac{\partial}{\partial t}\left[\eta\right] + k_0 \frac{\partial}{\partial \theta}\left[w\right] + \frac{\partial}{\partial \theta}\left[\eta\right] = 0. \tag{29}$$

Rearranging (27) for w and substituting (17a) and (17b) for $v_\bullet$ give

$$\begin{aligned} w_{\mathrm{ON}} &= \frac{1}{\alpha}\left(\phi_{\mathrm{ON}}^* \theta - \frac{\beta_+}{T_+^* - T_{\mathrm{ON}}}\right)\dot{f}\left(t\right) - \frac{\delta\tau_{\mathrm{ON}}\left(t\right)}{\tau_{\mathrm{ON}}^*} \\ w_{\mathrm{OFF}} &= \frac{1}{\alpha}\left(\phi_{\mathrm{OFF}}^* \theta + \frac{\beta_+}{T_{\mathrm{OFF}} - T_+^*}\right)\dot{f}\left(t\right) - \frac{\delta\tau_{\mathrm{OFF}}\left(t\right)}{\tau_{\mathrm{OFF}}^*}, \end{aligned} \tag{30a}$$

$$\delta\tau_{\mathrm{ON}}\left(t\right) = -\frac{\phi_{\mathrm{ON}}^* \widetilde{f}\left(t\right)}{\alpha};\ \delta\tau_{\mathrm{OFF}}\left(t\right) = -\frac{\phi_{\mathrm{OFF}}^* \widetilde{f}\left(t\right)}{\alpha}.$$

Hence

$$\begin{aligned} \frac{\partial}{\partial \theta}\left[w_\bullet\left(t\right)\right] &= \frac{1}{\alpha}\left[\phi_\bullet^* \dot{f} + \left(w\left(t\right)|_{\theta=0^+} - w\left(t\right)|_{\theta=0^-}\right)\delta\left(\theta\right)\right. \\ &\quad \left. + \left(w\left(t\right)|_{\theta=-1} - w\left(t\right)|_{\theta=1}\right)\delta\left(\theta - 1\right)\right] \\ \frac{\partial}{\partial \theta}\left[w_\bullet\left(t\right)\right] &= \frac{1}{\alpha}\left[\phi_\bullet^* \dot{f} - \nu_0\delta\left(\theta\right) + \nu_1\delta\left(\theta - 1\right)\right]\dot{f}\left(t\right) \\ &\quad + \frac{\mu}{\alpha}\left[\delta\left(\theta - 1\right) - \delta\left(\theta\right)\right]\widetilde{f}, \end{aligned} \tag{31}$$

where we have defined

$$\nu_0 \coloneqq \frac{\beta_+}{T_+^* - T_{\mathrm{ON}}} + \frac{\beta_+}{T_{\mathrm{OFF}} - T_+^*} > 0 \tag{32a}$$

$$\nu_1 \coloneqq \frac{\beta_-}{T_-^* - T_{\mathrm{ON}}} + \frac{\beta_-}{T_{\mathrm{OFF}} - T_-^*} > 0 \tag{32b}$$

$$\begin{aligned} \mu &\coloneqq \frac{\phi_{\mathrm{OFF}}^*}{\tau_{\mathrm{OFF}}^*} - \frac{\phi_{\mathrm{ON}}^*}{\tau_{\mathrm{ON}}^*} \\ &> 0 \quad \text{if } \frac{\beta_+}{\beta_-} \text{ satisfies (7) with } T_\pm^*. \end{aligned} \tag{32c}$$

We have a time-invariant linear system (29), and so it is natural to look for solutions for which the time dependence of our variables $\widetilde{f}$ and η is $e^{\lambda t}$; $\lambda \in \mathbb{C}$ is called an eigenvalue of the system. Defining $k \coloneqq k_0/\alpha$ and renaming $\widetilde{f}$ to f, (29) becomes

$$\begin{aligned} &\tau_\bullet^* \lambda\eta + \frac{\partial \eta}{\partial \theta} + k\left[\phi_\bullet - \nu_0\delta\left(\theta\right) + \nu_1\delta\left(\theta - 1\right)\right]\lambda f \\ &\quad + k\mu\left[\delta\left(\theta - 1\right) - \delta\left(\theta\right)\right] f = 0. \end{aligned} \tag{33}$$

We introduce an integrating factor so that on the open intervals $(-1, 0) \cup (0, 1)$ we can find an expression for $\eta(\theta)$:

$$\begin{aligned} &\frac{\partial}{\partial \theta}\left(e^{\lambda\tau_\bullet^*\theta}\eta\right) + k\phi_\bullet \lambda f e^{\lambda\tau_\bullet^*\theta} = 0 \\ &\therefore \eta\left(\theta\right) = \left(\eta_\bullet\left(0\right) + kf\frac{\phi_\bullet^*}{\tau_\bullet^*}\right)e^{-\lambda\tau_\bullet^*\theta} - kf\frac{\phi_\bullet^*}{\tau_\bullet^*}. \end{aligned} \tag{34}$$

At the discontinuities $\theta = 0$ and $\theta = \pm 1$,

$$\eta_{\mathrm{ON}}\left(0\right) - \eta_{\mathrm{OFF}}\left(0\right) = kf\left(\lambda\nu_0 + \mu\right) \tag{35a}$$

$$\eta_{\mathrm{OFF}}\left(-1\right) - \eta_{\mathrm{ON}}\left(1\right) = -kf\left(\lambda\nu_1 + \mu\right). \tag{35b}$$

We can use (34) to find expressions for $\eta(-1)$ and $\eta(1)$ and substitute these into (35b). After substitution for $\eta_{\mathrm{OFF}}(0)$ (or $\eta_{\mathrm{ON}}(0)$) using (35a) and rearrangement we arrive at

$$\begin{aligned} &\eta_{\mathrm{ON}}\left(0\right) g\left(\lambda\right) \\ &\quad = -kf\left(\frac{\phi_{\mathrm{ON}}^*}{\tau_{\mathrm{ON}}^*} g\left(\lambda\right) + \lambda\left(\nu_1 - \nu_0 e^{\lambda\tau_{\mathrm{OFF}}^*}\right)\right) \end{aligned} \tag{36a}$$

$$\begin{aligned} &\eta_{\mathrm{OFF}}\left(0\right) g\left(\lambda\right) \\ &\quad = -kf\left(\frac{\phi_{\mathrm{OFF}}}{\tau_{\mathrm{OFF}}^*} g\left(\lambda\right) + \lambda\left(\nu_1 - \nu_0 e^{-\lambda\tau_{\mathrm{ON}}^*}\right)\right), \end{aligned} \tag{36b}$$

where

$$g\left(\lambda\right) = e^{\lambda\tau_{\mathrm{OFF}}^*} - e^{-\lambda\tau_{\mathrm{ON}}^*}. \tag{36c}$$

Rewriting our equation for the rate of change of grid frequency near equilibrium (9) as

$$\dot{f}\left(t\right) = -\gamma f\left(t\right) - cP_c\tau_{\mathrm{ON}}^* \int_0^1 \eta\left(\theta, t\right) \mathrm{d}\theta \tag{37}$$

and setting $\dot{f} = \lambda f$ give

$$\int_0^1 \eta\left(\theta, t\right) \mathrm{d}\theta = -\frac{\left(\lambda + \gamma\right) f}{cP_c\tau_{\mathrm{ON}}^*}. \tag{38}$$

Integrating (34) over $[0, 1)$ in θ (the switched on TCLs), setting the resulting expression equal to the right hand side of (38), and substituting our expression in (36a) for $\eta_{\mathrm{ON}}(0)$ establish the following implicit equation for λ:

$$\begin{aligned} &\left(\lambda + \gamma - Z\phi_{\mathrm{ON}}^*\right) g\left(\lambda\right) \\ &\quad = Z\left(\nu_1 - \nu_0 e^{\lambda\tau_{\mathrm{OFF}}^*}\right)\left(1 - e^{-\lambda\tau_{\mathrm{ON}}^*}\right), \end{aligned} \tag{39}$$

where we have defined $Z \coloneqq kcP_c$, which reflects the strength of the effect of the TCLs on grid frequency.

When $Z = 0$ (no effect of the TCLs on the grid frequency) the eigenvalue equation (39) reduces to $(\lambda+\gamma)g(\lambda) = 0$, so the eigenvalues are $\lambda = -\gamma$ and $\lambda = 2n\pi i/(\tau_{\mathrm{ON}}^* + \tau_{\mathrm{OFF}}^*)$ for $n \in \mathbb{Z}$ (the roots of $g(\lambda) = 0$). It can also be seen from (39) that for all Z there is an eigenvalue $\lambda = 0$. It corresponds to conservation of the number of TCLs. This eigenvalue 0 is removed by the

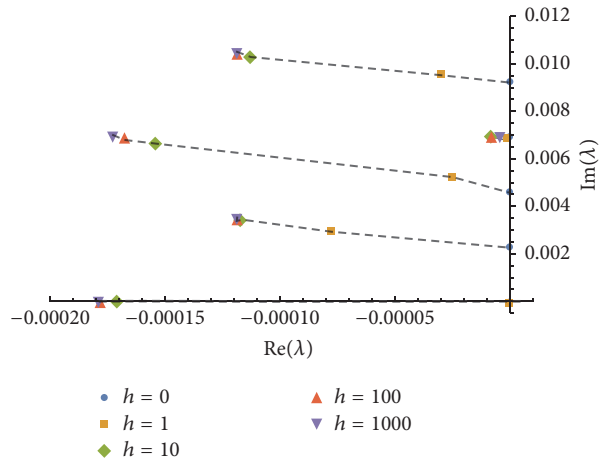

Figure 1: Numerical solutions for the first five eigenvalues above the real axis (there is an infinite sequence going further along the imaginary axis, and they are reflected in the real axis). We use multiplier h to increase Z, and the real part of each eigenvalue we have followed decreases from 0 as Z increases from 0.

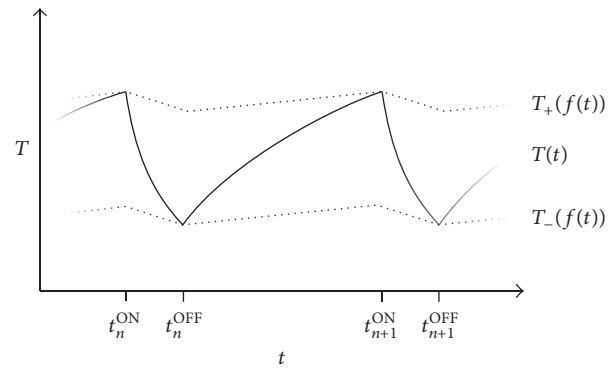

Figure 2: Illustration of the nth and $(n+1)$th switching events of the fully synchronised population and the frequency-sensitive temperature set points $T_-(f(t))$ and $T_+(f(t))$.

normalisation condition (25). The real and imaginary parts of λ that solve (39) can be solved for numerically, using, for example, [54]. Figure 1 shows numerical solutions for the first five eigenvalues above (or on) the real axis for the parameter values given in Table 2 in Section 2.3 and allowing Z to vary from its value Z_0 derived from the table, by $Z = hZ_0$. There is an infinite sequence of eigenvalues going upwards and their reflections in the real axis. Increasing Z from zero by powers of 10 is seen to decrease the real part of the eigenvalues from zero and therefore the system is stable to small perturbations.

This is a surprising result because intuitively identical TCLs are vulnerable to synchronisation which would cause instabilities on the system, which is the general view in the literature as discussed previously. The result is not due to the damping constant γ, because we chose $\gamma = 0$ so as not to mask the effect of the TCLs. What the analysis does not tell us is how small any perturbations would have to be for a population of TCLs to have a stabilising effect on grid frequency. It might be that a larger perturbation than valid for linearisation leads to instability. In Section 4 we study the effects of different sized perturbations using simulations and indeed find growth of synchronisation. In the next section we consider the behaviour of a population of TCLs under the opposite type of perturbation; namely, all TCLs synchronised into one or two groups.

3.2. Synchronised Groups of TCLs. In the previous section we studied the stability of a uniformly distributed (continuum) population of TCLs at the 50 Hz equilibrium and found it to be stable almost everywhere in parameter space. In this section we consider the opposite extreme of possible TCL distributions, the Dirac delta distribution. That is to say, we explore the behaviour of a fully synchronised population of TCLs, all switching on and off at the same time, all with the same temperature, and (again) identical parameters. This is equivalent to a single TCL with the power consumption of the whole population.

3.2.1. Mapping the Switch Times. We begin by constructing a map from one (whole population) switch on event to the next. We show that under certain conditions such a mapping is a contraction. Let the subscript n denote the nth switch on and nth switch off event. Without loss of generality, suppose that after our initial start time t_0 the next switch event is the population switching on. This implies that, for all $n \in \mathbb{N}$, $t_n^{\mathrm{OFF}} > t_n^{\mathrm{ON}}$. Figure 2 illustrates the notation. Hence the amount of time the population spends switched on following the nth switch on event is given by

$$t_n^{\mathrm{OFF}} - t_n^{\mathrm{ON}} = \frac{1}{\alpha} \log\left(\frac{T_+^0 - \beta_+ f_n^{\mathrm{ON}} - T_{\mathrm{ON}}}{T_-^0 - \beta_- f_n^{\mathrm{OFF}} - T_{\mathrm{ON}}}\right), \tag{40a}$$

where f_n^{ON}, f_n^{OFF} are the frequencies at the nth switch on and off times. The amount of time spent switched off following the nth switch off is given by

$$t_{n+1}^{\mathrm{ON}} - t_n^{\mathrm{OFF}} = \frac{1}{\alpha} \log\left(\frac{T_{\mathrm{OFF}} - T_-^0 + \beta_- f_n^{\mathrm{OFF}}}{T_{\mathrm{OFF}} - T_+^0 + \beta_+ f_{n+1}^{\mathrm{ON}}}\right). \tag{40b}$$

Assuming, as for the numerical analysis in Section 3.1, that the system has no damping, we set $\gamma = 0$ in (12) for $\dot{f}(t)$. In a synchronised population, at time t all TCLs are either on ($\rho(t) = 1$) or off ($\rho(t) = 0$). Then we can define constants $c_{\mathrm{ON}}, c_{\mathrm{OFF}} > 0$ such that

$$\dot{f} = \begin{cases} -c_{\mathrm{ON}} & := cP_c(\rho^* - 1) \text{ when the population is on} \\ +c_{\mathrm{OFF}} & := cP_c\rho^* \text{ when the population is off.} \end{cases} \tag{41}$$

Hence the values of f at the switch off and on times are given by the piecewise-linear functions

$$f_n^{\mathrm{OFF}} = f_n^{\mathrm{ON}} - c_{\mathrm{ON}}\left(t_n^{\mathrm{OFF}} - t_n^{\mathrm{ON}}\right) \tag{42a}$$

$$f_{n+1}^{\mathrm{ON}} = f_n^{\mathrm{OFF}} + c_{\mathrm{OFF}}\left(t_{n+1}^{\mathrm{ON}} - t_n^{\mathrm{OFF}}\right). \tag{42b}$$

After substituting for the switching times using (40a) and (40b) and rearranging, these become

$$f_n^{\mathrm{OFF}} - \frac{c_{\mathrm{ON}}}{\alpha}\log\left(T_-^0 - \beta_- f_n^{\mathrm{OFF}} - T_{\mathrm{ON}}\right) = f_n^{\mathrm{ON}} - \frac{c_{\mathrm{ON}}}{\alpha}\log\left(T_+^0 - \beta_+ f_n^{\mathrm{ON}} - T_{\mathrm{ON}}\right) \tag{43a}$$

$$f_{n+1}^{\mathrm{ON}} + \frac{c_{\mathrm{OFF}}}{\alpha}\log\left(T_{\mathrm{OFF}} - T_+^0 + \beta_+ f_{n+1}^{\mathrm{ON}}\right) = f_n^{\mathrm{OFF}} + \frac{c_{\mathrm{OFF}}}{\alpha}\log\left(T_{\mathrm{OFF}} - T_-^0 + \beta_- f_n^{\mathrm{OFF}}\right). \tag{43b}$$

Now since each side of (43a) and (43b) are functions of only one of the $f_n^\bullet$ variables, we can explicitly name them as such

$$\phi_{\mathrm{ON}}^-\left(f_n^{\mathrm{OFF}}\right) \coloneqq f_n^{\mathrm{OFF}} - \frac{c_{\mathrm{ON}}}{\alpha}\log\left(T_-^0 - \beta_- f_n^{\mathrm{OFF}} - T_{\mathrm{ON}}\right) \tag{44a}$$

$$\phi_{\mathrm{ON}}^+\left(f_n^{\mathrm{ON}}\right) \coloneqq f_n^{\mathrm{ON}} - \frac{c_{\mathrm{ON}}}{\alpha}\log\left(T_+^0 - \beta_+ f_n^{\mathrm{ON}} - T_{\mathrm{ON}}\right) \tag{44b}$$

$$\phi_{\mathrm{OFF}}^-\left(f_n^{\mathrm{OFF}}\right) \coloneqq f_n^{\mathrm{OFF}} + \frac{c_{\mathrm{OFF}}}{\alpha}\log\left(T_{\mathrm{OFF}} - T_-^0 + \beta_- f_n^{\mathrm{OFF}}\right) \tag{44c}$$

$$\phi_{\mathrm{OFF}}^+\left(f_{n+1}^{\mathrm{ON}}\right) \coloneqq f_{n+1}^{\mathrm{ON}} + \frac{c_{\mathrm{OFF}}}{\alpha}\log\left(T_{\mathrm{OFF}} - T_+^0 + \beta_+ f_{n+1}^{\mathrm{ON}}\right). \tag{44d}$$

Each of the four ϕ functions is increasing and therefore invertible, and so we can write

$$f_n^{\mathrm{OFF}} = \phi_{\mathrm{ON}}^{-^{-1}}\phi_{\mathrm{ON}}^+\left(f_n^{\mathrm{ON}}\right) \tag{45a}$$

$$f_{n+1}^{\mathrm{ON}} = \phi_{\mathrm{OFF}}^{+^{-1}}\phi_{\mathrm{OFF}}^-\left(f_n^{\mathrm{OFF}}\right) \tag{45b}$$

and therefore

$$f_{n+1}^{\mathrm{ON}} = \phi_{\mathrm{OFF}}^{+^{-1}}\phi_{\mathrm{OFF}}^-\phi_{\mathrm{ON}}^{-^{-1}}\phi_{\mathrm{ON}}^+\left(f_n^{\mathrm{ON}}\right), \tag{45c}$$

which is a mapping from the frequency at one switch on event to the frequency at the next. The mapping is a contraction iff

$$\left|\left(\phi_{\mathrm{OFF}}^{+^{-1}}\phi_{\mathrm{OFF}}^-\phi_{\mathrm{ON}}^{-^{-1}}\phi_{\mathrm{ON}}^+\right)'\right| < 1 \tag{46}$$

$$\text{iff } \left|\frac{\left(\phi_{\mathrm{OFF}}^-\right)'}{\left(\phi_{\mathrm{OFF}}^+\right)'}\frac{\left(\phi_{\mathrm{ON}}^+\right)'}{\left(\phi_{\mathrm{ON}}^-\right)'}\right| < 1 \tag{47}$$

$$\left(\text{evaluated at the appropriate places}\right).$$

Note that

$$\frac{\left(\phi_{\mathrm{OFF}}^-\right)'}{\left(\phi_{\mathrm{OFF}}^+\right)'} = \frac{1+\beta_- c_{\mathrm{OFF}}/\left[\alpha\left(T_{\mathrm{OFF}} - T_n^+\right)\right]}{1+\beta_+ c_{\mathrm{OFF}}/\left[\alpha\left(T_{\mathrm{OFF}} - T_{n+1}^+\right)\right]} < 1 \quad \text{iff } \frac{\beta_+}{\beta_-} > \frac{T_{\mathrm{OFF}} - T_{n+1}^+}{T_{\mathrm{OFF}} - T_n^-}. \tag{48}$$

Similarly

$$\frac{\left(\phi_{\mathrm{ON}}^+\right)'}{\left(\phi_{\mathrm{ON}}^-\right)'} = \frac{1+\beta_+ c_{\mathrm{ON}}/\left[\alpha\left(T_n^+ - T_{\mathrm{ON}}\right)\right]}{1+\beta_- c_{\mathrm{ON}}/\left[\alpha\left(T_n^- - T_{\mathrm{ON}}\right)\right]} < 1 \quad \text{iff } \frac{\beta_+}{\beta_-} < \frac{T_n^+ - T_{\mathrm{ON}}}{T_n^- - T_{\mathrm{ON}}}. \tag{49}$$

Therefore a sufficient condition for the mapping to be a contraction is that

$$\frac{\beta_+}{\beta_-} \in \left(\frac{T_{\mathrm{OFF}} - T_{n+1}^+}{T_{\mathrm{OFF}} - T_n^-}, \frac{T_n^+ - T_{\mathrm{ON}}}{T_n^- - T_{\mathrm{ON}}}\right) \tag{50}$$

which is a nonempty interval (containing $\{1\}$), so long as $T_{\mathrm{ON}} < T_n^- < T_n^+ < T_{\mathrm{OFF}}$ and $T_n^- < T_{n+1}^+$ for all n. It is worth recalling our earlier condition on the values of $\beta_\pm$ (7) which also imposed that β_+/β_- belong to an open interval containing $\{1\}$.

3.2.2. Solving for the Periodic Solution. The contraction property of the mapping $f_n^{\mathrm{ON}} \mapsto f_{n+1}^{\mathrm{ON}}$ (45c) under the above conditions implies that there is an attracting fixed point so long as $T_{\mathrm{ON}} < T_n^- < T_n^+ < T_{\mathrm{OFF}}$, and hence a periodic solution for the synchronised population. We now seek to solve for this periodic solution. Denote by l_{ON} and l_{OFF} the amount of time spent on and off during one (periodic) cycle, respectively. Since power consumption for the population is constant during each on/off phase, the frequency moves linearly between upper and lower values which we denote by f_+ and f_-. Therefore the temperature of the population will cycle between upper and lower set points, given by $T_+^0 - \beta_+ f_+$ and $T_-^0 - \beta_- f_-$, respectively. Equations (42a) and (42b) show us that

$$f_- = f_+ - c_{\mathrm{ON}} l_{\mathrm{ON}} \tag{51a}$$

$$f_+ = f_- + c_{\mathrm{OFF}} l_{\mathrm{OFF}}. \tag{51b}$$

The temperature evolution equations (3a) and (3b) allow us to express the switch on and switch off temperatures as follows:

$$T_+^0 - \beta_+ f_+ = \left(T_-^0 - \beta_- f_- - T_{\mathrm{OFF}}\right)e^{-\alpha l_{\mathrm{OFF}}} + T_{\mathrm{OFF}} \tag{52a}$$

$$T_-^0 - \beta_- f_- = \left(T_+^0 - \beta_+ f_+ - T_{\mathrm{ON}}\right)e^{-\alpha l_{\mathrm{ON}}} + T_{\mathrm{ON}} \tag{52b}$$

which after substituting for f_- using (51a) and rearranging become

$$f_+\left(\beta_- e^{-\alpha l_{\mathrm{OFF}}} - \beta_+\right) = \left(T_-^0 - T_{\mathrm{OFF}} + \beta_- c_{\mathrm{ON}} l_{\mathrm{ON}}\right)e^{-\alpha l_{\mathrm{OFF}}} + T_{\mathrm{OFF}} - T_+^0, \tag{53a}$$

$$f_+\left(\beta_+ e^{-\alpha l_{\mathrm{ON}}} - \beta_-\right) = \left(T_+^0 - T_{\mathrm{ON}}\right)e^{-\alpha l_{\mathrm{ON}}} + T_{\mathrm{ON}} - T_-^0 - \beta_- c_{\mathrm{ON}} l_{\mathrm{ON}}. \tag{53b}$$

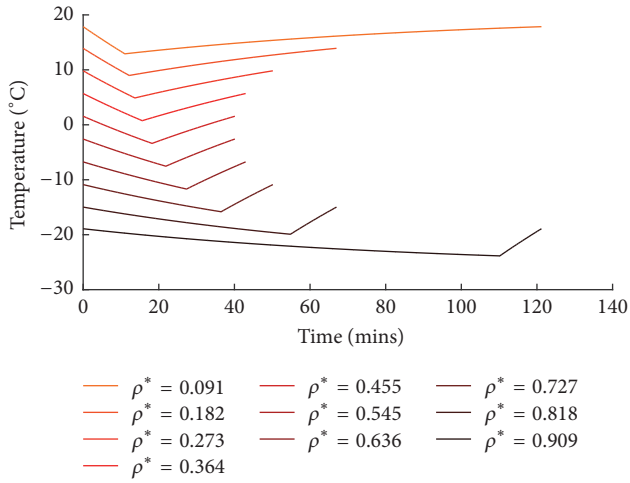

FIGURE 3: One cycle of the single group solution for different values of ρ^* when $\rho_0 \approx 0.3355$. They include values that lead to unrealistic results for real fridges but are there to illustrate the effect.

Now we have two equations in terms of f_+, l_{ON} and l_{OFF}, which we can combine into one equation and eliminate f_+,

$$\begin{aligned}&\left(\beta_+ e^{-\alpha l_{ON}} - \beta_-\right)\\&\cdot\left[\left(T_-^0 - T_{OFF} + \beta_- c_{ON} l_{ON}\right) e^{-\alpha l_{OFF}} + T_{OFF} - T_+^0\right]\\&= \left(\beta_- e^{-\alpha l_{OFF}} - \beta_+\right)\\&\cdot\left[\left(T_+^0 - T_{ON}\right) e^{-\alpha l_{ON}} + T_{ON} - T_-^0 - \beta_- c_{ON} l_{ON}\right].\end{aligned} \tag{54}$$

We can also express l_{OFF} in terms of l_{ON} by summing (51a) and (51b) to give

$$\begin{aligned}c_{ON} l_{ON} &= c_{OFF} l_{OFF} \text{ or, equivalently,}\\(1-\rho^*)\, l_{ON} - \rho^* l_{OFF} &= 0\end{aligned} \tag{55}$$

and so (53b) and (55) form a pair of coupled equations for l_{ON} and l_{OFF}, which can be solved numerically. Figure 3 shows one temperature cycle for the single group under different choices for ρ^*. Denote by ρ_0 the value of ρ when $f = 0$. As ρ^* gets further away from ρ_0 the solutions drift further from the uncoupled temperature range (2–7°C). The cycle lengths are symmetric about $\rho^* = 1/2$ but the TCLs consume more power per cycle as ρ^* increases.

To begin some analysis of the stability of this fully synchronised solution we address the question: given a population split into two synchronised groups, will the groups merge into one fully synchronised population, or will they remain distinct forever?

3.2.3. Two-Group Dynamics. Suppose we have a population of frequency-sensitive TCLs that are split into two synchronised groups. We would like to understand the dynamics of the switch times, and we ask whether, given sufficient time, the groups will merge, or whether they will remain distinct, possibly settling down to separated periodic solutions. In

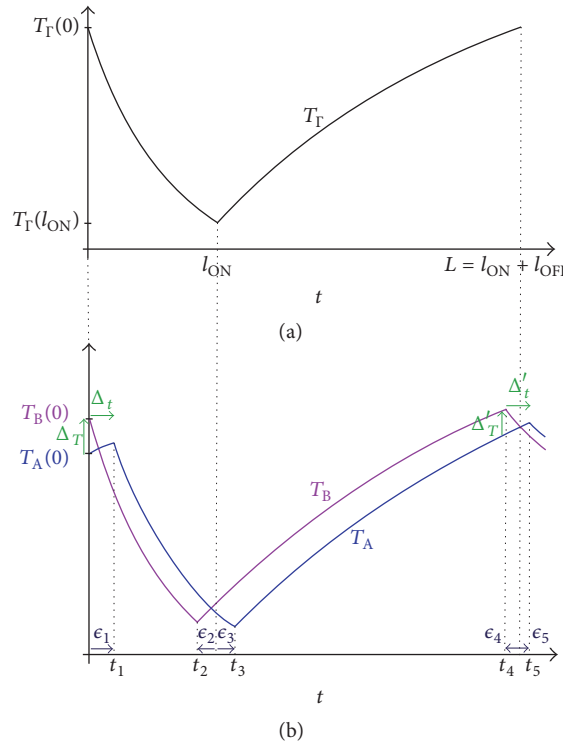

FIGURE 4: Linearisation about the single group solution. (a) Single group solution $T_\Gamma(t)$. (b) Temperature cycling of groups A and B close to the single group solution.

particular, we consider the initial difference between the switch on times Δ_t to be very small and the switch on temperatures very close to the single group periodic solution from the previous subsection.

Let Γ denote the single group periodic solution, which cycles periodically through temperature space with temperature $T_\Gamma(t)$. As before, we denote the switched on duration in this solution by l_{ON} and the switched off duration by l_{OFF}. Suppose that the population is split into two groups A and B, such that proportion σ belongs to group A, and proportion $1 - \sigma$ belongs to group B. Suppose also that group B switches on at time $t = 0$, followed soon after by group A switching on, at time $t_1 > 0$. Then after a time period of length similar to l_{ON} group B switches off, which is again followed shortly after by group A switching off. After a time period similar to l_{OFF} each of the groups then switches back on. We shall assume that the switching order does not change, since if they do swap, we need only repeat this process with σ replaced by $1 - \sigma$. Simulations show that the switching order will not continue to change indefinitely.

We would like to compare the temperature cycles of these two groups with the single group periodic solution Γ. Without loss of generality suppose that group B initially switches on at the same time as a fully synchronised population solution. We compare the cycling of the groups A and B using the following measures, along with all those shown in Figure 4. Let $\Delta_T := T_B(0) - T_A(0)$ and $\Delta'_T := T_B(t_4) - T_A(t_4)$, the temperature difference when B switches on the first and second times, respectively. In addition, let $\Delta_t := t_1 - 0 = t_1 = \epsilon_1$ and

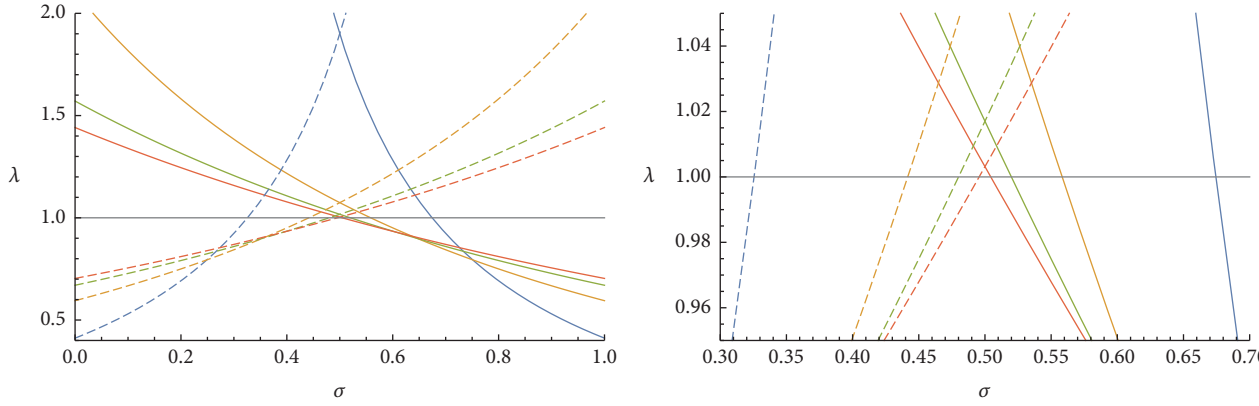

(a) Full interval (b) Enlargement

FIGURE 5: Solutions for λ (see (61)) (solid lines) for different values of ρ^*. Dashed lines show reflection in $\sigma = 1/2$ to show the effect of reversing the switching order of the groups. Blue: $\rho^* = 0.1$, yellow: $\rho^* = 0.2$, green: $\rho^* = 0.3$, and red: $\rho^* = 0.4$. Black line shows the boundary of stability (stable below, unstable above). The results are identical when ρ^* is replaced by $1 - \rho^*$. (b) shows an enlargement centred at $\sigma = 1/2$, showing that either switching order of the groups leads to $\lambda_2 > 1$ on a small interval of σ. In this case the groups never merge and in all other cases they will.

$\Delta'_t := t_5 - t_4$, the time difference between the two groups switching on the first and second times, respectively. Further notation is shown in Figure 4.

In order to calculate Δ'_T and Δ'_t we need to calculate the switch times and temperatures of the two groups at each switch event leading up to t_5. Solving for the switch times and temperatures when there are two groups is a little more complicated than for the fully synchronised case. It requires solving the temperature set point equations using the system conditions at the previous switch and the equation for $\dot{f}$ which now takes one of four values depending on which combination of groups is switched on (both, neither, A only, or B only). We begin by making the simplifying assumption $\beta_- = \beta_+ := \beta$. Now since group A is switching on at time t_1 and group B switched off at time 0,

$$\begin{aligned} T_A(t_1) &= T_+^0 - \beta f(t_1) \\ f(t_1) &= f(0) - cP_c(1 - \sigma - \rho^*)t_1 \\ f(0) &= \frac{1}{\beta}\left(t_+^0 - T_B(0)\right) \\ \therefore T_A(t_1) &= T_B(0) + \beta cP_c(1 - \sigma - \rho^*)t_1. \end{aligned} \tag{56a}$$

In addition, by the temperature evolution equations,

$$T_A(t_1) = (T_A(0) - T_{OFF})e^{-\alpha t_1} + T_{OFF}. \tag{56b}$$

Equating (56a) and (56b) and introducing our new notation give

$$\begin{aligned} &\beta cP_c(1 - \sigma - \rho^*)\Delta_t + \Delta_T \\ &\quad = (T_A(0) - T_{OFF})\left(e^{-\alpha\Delta_t} - 1\right). \end{aligned} \tag{57}$$

If we write $T_A(0) = T_\Gamma(0) + \delta T_A(0)$ and take $\delta T_A(0)$ and Δ_t small, then

$$\begin{aligned} \Delta_T &= (T_\Gamma(0) + \delta T_A(0) - T_{OFF})\left(e^{-\alpha\Delta_t} - 1\right) \\ &\quad - \beta cP_c(1 - \sigma - \rho^*)\Delta_t \end{aligned} \tag{58}$$

and linearising in Δ_t gives

$$\Delta_T \approx \xi\Delta_t, \tag{59}$$

where

$$\xi := \alpha(T_{OFF} - T_\Gamma(0)) - \beta cP_c(1 - \sigma - \rho^*). \tag{60}$$

More generally, at each switch event we have the temperature evolution equations that describe the temperature of each group as a function of their temperature at the previous switch (such as (56b)) and an additional equation for the temperature of the switching group, using the temperature set point equations (such as (56a)). Writing $\Delta'_T = T_B(t_4) - T_A(t_4)$ and linearising about the single group solution, we find in Appendix B that $\Delta'_T = \lambda\Delta_T$ where

$$\begin{aligned} \lambda := &\left(1 - \frac{\alpha(T_{OFF} - T_{ON})}{\alpha(T_{OFF} - T_\Gamma(0)) - \beta cP_c(1 - \sigma - \rho^*)}\right) \\ &\cdot \left(1 - \frac{\alpha(T_{OFF} - T_{ON})}{\alpha(T_\Gamma(l_{ON}) - T_{ON}) + \beta cP_c(\sigma - \rho^*)}\right) \\ &\cdot e^{-\alpha L}. \end{aligned} \tag{61}$$

So $[-1, +1]$ is a left eigenvector of the linearised map in the space of $\begin{pmatrix} \delta T_A \\ \delta T_B \end{pmatrix}$ with eigenvalue λ. We can plot λ against σ for various ρ^* to see whether $|\lambda| < 1$ (in which case the two groups merge into one) or whether $|\lambda| > 1$ (they move apart). The results are shown in Figure 5. We find that the second eigenvalue is within the interval $(-1, +1)$ for any σ and ρ^* for

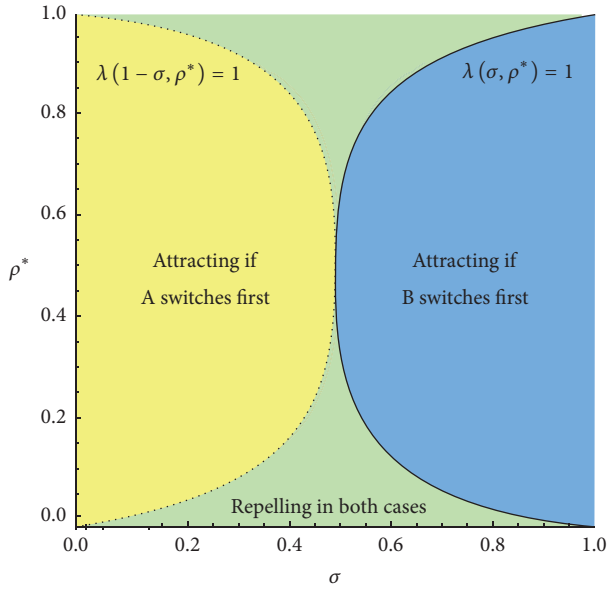

FIGURE 6: Bifurcation diagram for the stability of the single group solution to splitting in two. Stable if the parameters lie in the yellow or blue regions (the groups will ultimately merge); unstable in the green parameter region (the groups will never merge). Boundary lines are solutions to (61) as a function of σ (or $1-\sigma$ to capture switching order reversal) and ρ^*.

our parameter values (taken from Table 2 with the exception of $\beta = 0.1$ which has been reduced to limit the rate of change of the frequency and ensure model validity), see Appendix C for details, and therefore the stability is governed by λ.

By solving for the dividing case $\lambda = 1$ we can create a bifurcation diagram in terms of the parameters σ and ρ^* to show where the single group solution is attracting and repelling. Figure 6 sketches the solution, along with the solution for the case when the switching order of the groups is reversed, found by replacing σ with $1-\sigma$. If in either case (group A switching first or group B switching first) the solution is attracting, then the two groups will merge together into the one group solution. However, if both cases have unstable dynamics then the solutions will never merge. Simulations show that in this parameter region the two groups will settle down to a fixed phase distance apart. If the solution is attracting for one switching order and repelling for the other, we find that the typical behaviour is for a small separation in the unstable direction to grow until the phase difference becomes almost a whole cycle, when they merge. Figure 7 illustrates how the cycles of the two groups can change over time relative to one another, depending on which of the three regions in the bifurcation diagram their parameters belong to.

What these results show is that when a population is split into two groups, if they are sufficiently similar in size then they will remain apart, effectively trying to counteract one another and balance the frequency fluctuations. Conversely, if one of the groups is significantly larger ("significantly" here depends on the size of ρ^*, and may be very small if $\rho^* \approx 0.5$) than the other then it will have too strong an effect on the frequency and "pull" on the smaller group's cycle. The closer the proportion switched on in equilibrium is to the proportion switched off (i.e., the closer it is to 0.5), the more similar the groups have to be in size to remain distinct.

With more than two groups of TCLs the modelling becomes far more complicated, since there are now far more possibilities to be considered for the switching order of the groups. Simulations have shown that for three groups it is possible for all three cycles to settle down to a fixed, separated pattern. This occurs if the groups are very similar in size, just as in the two-group case. Once one group is too large (or too small), the groups collapse into two, before synchronising completely. Taking the number of groups to infinity is equivalent to modelling a continuum of TCLs as in Section 3.1. Taking all groups of equal size and uniformly distributed in phase θ is equivalent to the continuum population equilibrium studied earlier. From above we found analytically that small perturbations to the population distribution should relax back to the uniform distribution, that is, that the equilibrium was stable. Now we find that if the population is discretised into 2 (and hypothetically N) groups then so long as they are of close to equal sizes, they will attempt to settle the frequency back to its nominal value by "spreading out" their cycles.

In reality we will never have a continuum of TCLs, and they may exhibit nonlinear dynamics not captured by our analysis. This motivates our use of simulations to gain further insights into how a large population of TCLs would behave according to our switching rules and how the grid frequency would be affected.

4. Simulations

4.1. Perturbations of a Uniform Distribution of TCLs. In Section 3.1 we analysed the stability of a large population of TCLs uniformly distributed in each part of the on/off cycle. In this section we simulate a large population of fridges with initial conditions close to the equilibrium distribution (the uniform distribution) and compare the results with our analytical work.

The model is the same as presented in Section 2, and unless stated otherwise, the parameter values are as in Table 2. In Section 3.1 we modelled our population as a continuum. For our simulations we split the fridge population into 10^4 "agents" (groups of fridges) that are each represented by a temperature and state, and who operate according to the switching rules and temperature progression equations in Section 2.1. These 10^4 agents are representative of the million fridges we assume are participating in our DSR scheme (i.e., operating in frequency-sensitive mode), since one million (or more) individuals would require very large amounts of computing time and memory. The power consumption of each agent is taken to be the total possible population consumption P_c divided by the number of agents, 10^4. Each time step is taken to be 1 s, and at each time step each agent updates its temperature and based on the frequency at the previous time step may switch on or off. The exact switch time is approximated using linear interpolation between the current and previous time step, and the new temperature is adjusted accordingly.

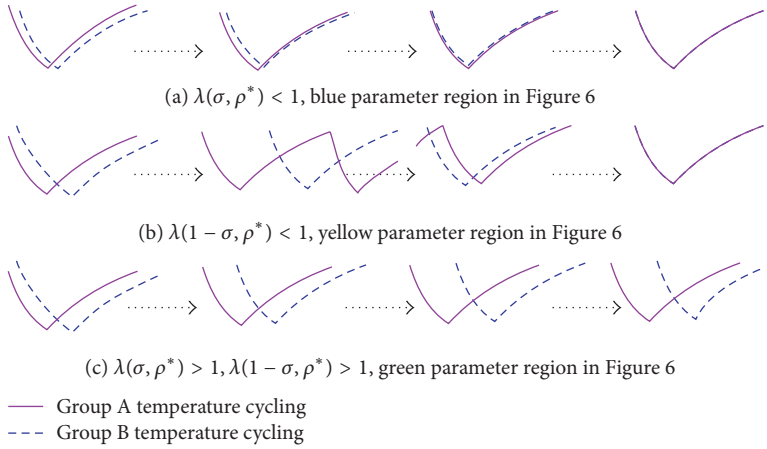

Figure 7: Illustration of the three types of cycling behaviour of two groups relative to one another, based on simulations. Arrows indicate the occurrence of many cycles and the central illustrations are snapshots of the cycling behaviour between the start and the final behaviour. Synchronisation occurs in cases (a) and (b), while in case (c) each group tends towards a fixed phase difference apart.

Table 3: Parameter values for plots in Figures 8, 9, and 10.

Plot number	$\rho_{on}(0)$	Δu
a(i)	ρ^*	0
a(ii)	ρ^*	0.1
a(iii)	ρ^*	0.25
a(iv)	ρ^*	0.5
b(i)	$1.5\rho^*$	0
b(ii)	$1.5\rho^*$	0.1
b(iii)	$1.5\rho^*$	0.25
b(iv)	$1.5\rho^*$	0.5

To perturb the TCL distribution $u(\theta)$ we can alter the number of TCLs switched on or off from the equilibrium proportions ρ^* and $(1-\rho^*)$, respectively, and we can perturb the uniform distributions within each on/off half of the θ interval. We choose to perturb the distributions by the addition of a sine wave to u^*, and we refer to the normalised wave peak amplitude Δu (normalised by dividing by u^*). This normalisation means that when we plot $u(\theta, 0)/u^*$, the zero perturbation case is 1 for all θ both on and off and the results are more clear. Table 3 shows eight combinations of choices for these perturbation parameters. All other parameters are as stated in Table 2.

Figure 8 shows the effects of these perturbations on the initial conditions in each case, plotting $u(\theta, 0)/u^*$ against θ. Figure 9 shows the final fridge distributions after ten days. The unperturbed case a(i) has remained uniform, while the peaks of the perturbation cases have all grown by varying amounts. In cases a(ii)–a(iv) (no perturbation to the proportion switched on) the final distributions exhibit increasing levels of synchronisation, but the clustering is far less than in cases b(i)–b(iv) which see the population synchronised into seven or fewer groups. The effects of this synchronisation on the electricity grid frequency can be seen in Figure 10.

Interestingly, in each case with perturbations, the frequency oscillations initially die down to close to 50 Hz. This means that to begin with the fridges are controlling the frequency oscillations caused by their initial condition perturbations. This aligns with our analysis from Section 3.1, in which we found that the uniform distribution of a continuum population is stable to small perturbations. What that analysis was unable to capture was the long-term effects of frequency sensitivity. In each case the frequency oscillations grow after less than a day, becoming very large in several cases. Before the large spikes in b(iii) we see that the frequency oscillations shrink down. This shows the inherently volatile nature of the system and potentially explains why the oscillations in b(iv) are ultimately less severe. It could be that these lower oscillations will shortly become much larger. In either case, the size of most of the final oscillations would be too large for the system to cope without frequency response from other providers.

These simulations reveal that while a homogeneous population of TCLs will act to dampen system perturbations, their behaviour to support the electricity grid will, given sufficient time, lead to further oscillations. The larger the perturbations are, the sooner these detrimental effects will occur.

4.2. Simulating TCLs on the GB Electricity Grid. Our model and simulations have thus far reduced the complexity of the problem by assuming that, apart from the TCL population and the grid frequency, all other network conditions remain constant. This was necessary for our model to be tractable and to ensure that any results from the simulations were attributable to the frequency-sensitive TCL population. An important next step is to consider the TCL population in the context of a real system. In collaboration with the GB System Operator National Grid, we are able to model the GB system with real data from 36 separate 10-day periods during 2015-2016 and simulate what would have happened if a frequency-sensitive fridge population had been active. We consider how the distribution of TCLs changes over this

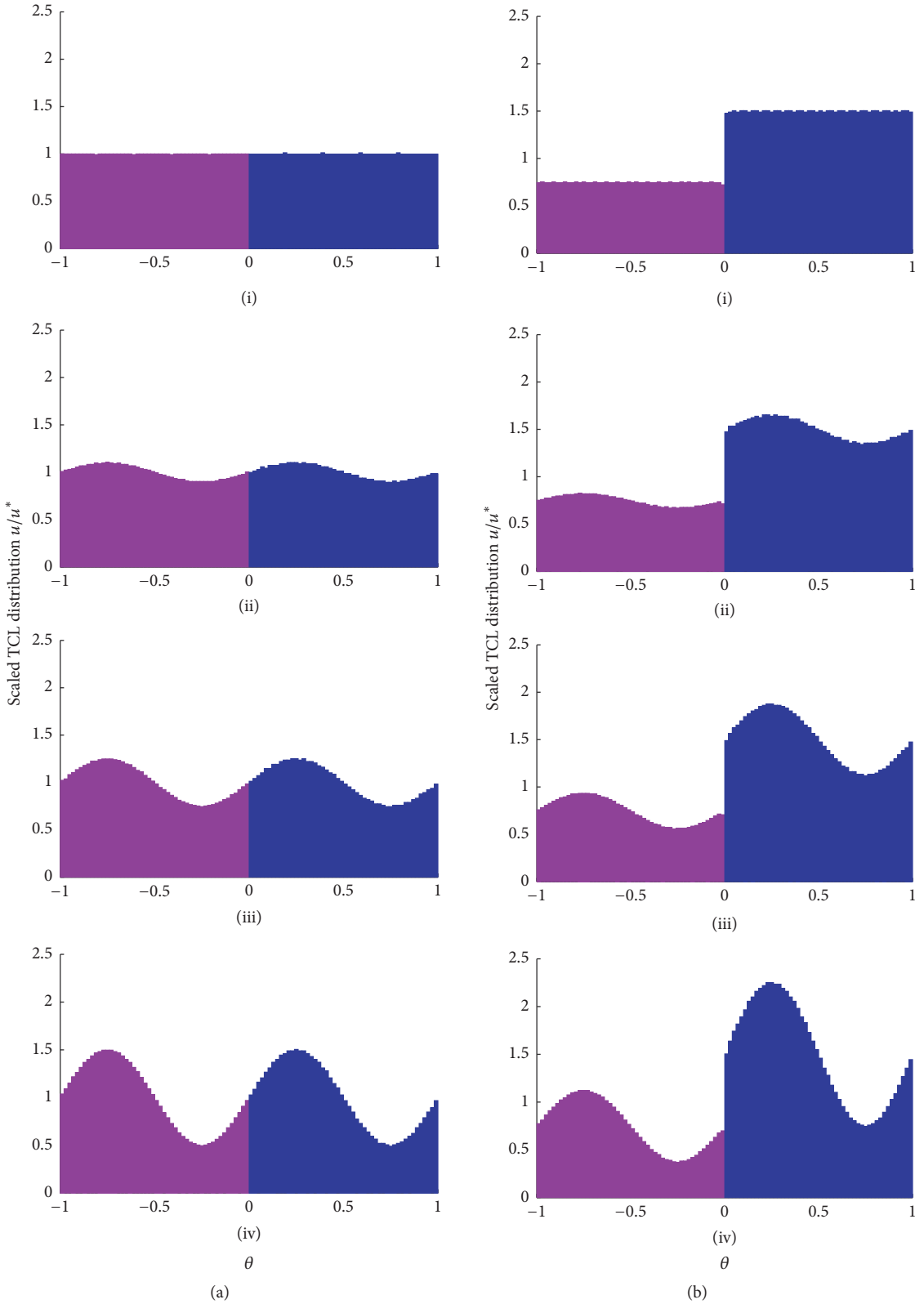

FIGURE 8: Initial fridge distributions in θ-space, with labels matching those in Table 3. Pink indicates switched off fridges, and blue indicates switched on. Distributions scaled by $1/u^*$ and histograms formed of 100 bins. (a) has no perturbation to the proportion of fridges switched on, and (b) has increasing perturbation (going downwards) to the number of fridges switched on. All involve sinusoidal distribution perturbations.

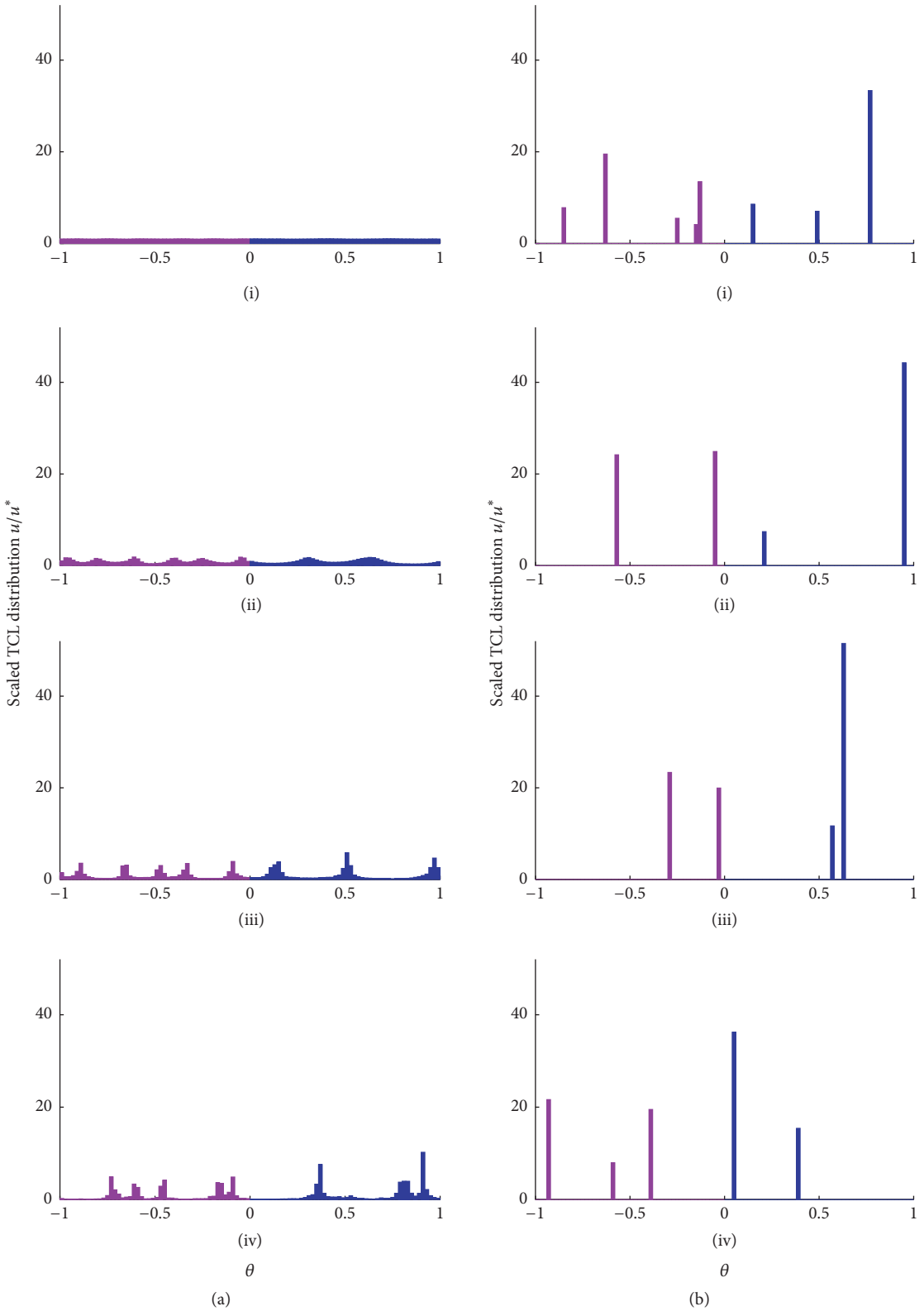

FIGURE 9: Final fridge distributions after 10 days in θ-space, with properties as given in Table 3 and initial distributions as shown in Figure 8. Perturbations have grown (except for the zero perturbation case a(i)).

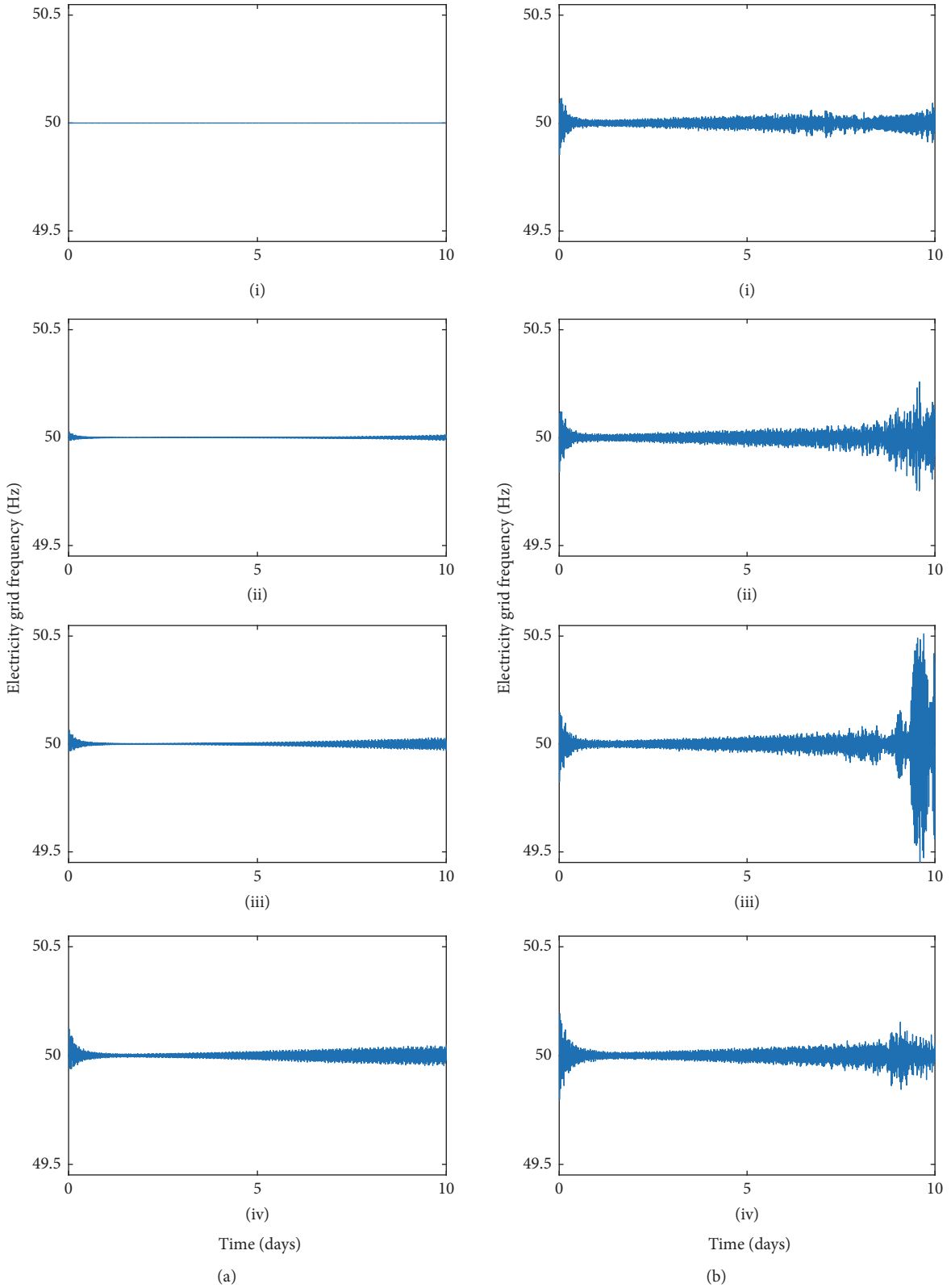

Figure 10: Electricity grid frequency over 10 days (values plotted once per 5 minutes), with fridge distributions as described in Table 3 and Figures 8 and 9. The perturbed systems (all but a(i)) see an initial reduction in oscillation amplitude followed by oscillation growth.

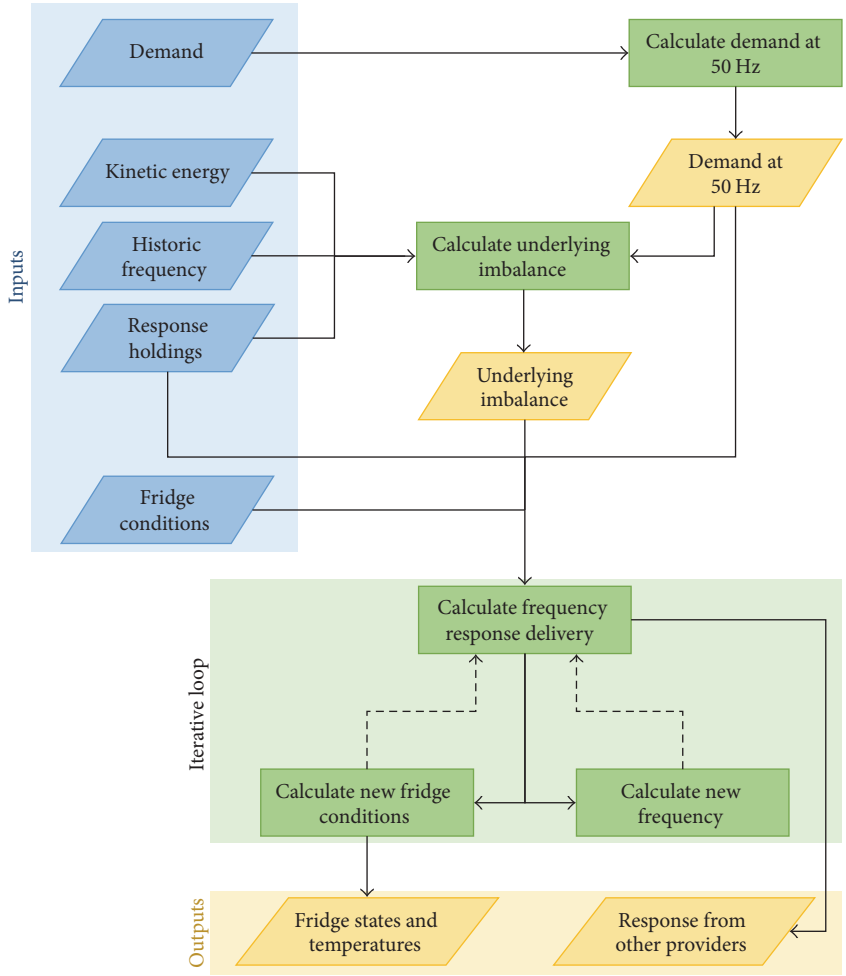

Figure 11: Simulation methodology diagram. Rhombi indicate input or calculated data/simulated data, and rectangles indicate methods/calculations. Events occur from top to bottom with the exception of the dashed arrows which form the iterative loop.

period, and the reduction in the amount of response that other providers needed to supply because of the contribution from the fridges.

4.2.1. Methods. We simulate a population of TCLs (specifically fridges) that respond to the grid frequency according to the rules in Section 2.1. We use various historic data from National Grid to model real system conditions and simulate the effects of a frequency-sensitive fridge population acting on the GB system. By considering the population in the context of real data including response provision from other sources such as power generators, we are able to get a better understanding of the potential impact of the fridges compared to, say, modelling them in isolation responding to a one-off frequency event.

Figure 11 gives an overview of the simulation process. Rhombi indicate inputs and outputs; rectangles indicate methods used in the simulation. Methods are applied working downwards, except for the dashed arrows which create an iterative loop.

4.2.2. Inputs. As shown in Figure 11, there are four types of data input, in addition to the fridge population initial conditions. We use 36 consecutive ten-day data samples from the period July 2015–June 2016.

Kinetic energy data is an estimate for the total kinetic energy in MVAs (megavolt-ampere seconds) [55]. Values are calculated by summing the kinetic energy of all running synchronised generators (a generator-specific constant provided to the System Operator by each power generator) with an estimate of kinetic energy from demand. The kinetic energy data provided (confidentially from National Grid) is per settlement period (settlement periods split the day into 48 half hour units starting on the hour and half hour) and repeats each value for the full 30 minutes (rather than interpolating). Typical kinetic energy values are in the range 20000–40000 MVAs.

Demand data consists of per-second metered demand from National Grid. This is a sum of the power leaving the electricity transmission system, including any power exports through the interconnectors. Half-hourly demand data is accessible via National Grid's "Data Explorer" [56].

Historic frequency data consists of per-second system frequency data in hertz. Frequency measurements are taken in multiple locations to ensure reliable data availability in the event of any metering faults. The frequency data provided by

Table 4: Illustrative historic response holding data behind Figure 12.

	Primary			Secondary		High	
Frequency trigger (Hz)	49.2	49.5	49.8	49.5	49.8	50.2	50.5
Response (MW)	850	800	430	950	500	−350	−680

National Grid has undergone a cleaning process that takes advantage of the multiple readings. It is available via National Grid's "Enhanced Frequency Response" [57].

Response holdings are the amount of frequency response delivery in MW (as a function of grid frequency) that National Grid expects each second. Response holdings are positive (or negative) for "low (high) frequency response delivery" when the frequency is below (above) 50 Hz, respectively. For each time step (1 second), 9 different values for response holding are listed. These take the form of primary, secondary, and high response.

Primary response values are given for trigger points at 49.9 Hz, 49.5 Hz, and 49.2 Hz. This means that at these frequencies the power response provided through various types of primary response service are the historic response holding values given, subject to a 1 second reaction delay. We assume that the response increases linearly from 0 between 49.985 Hz and 49.8 Hz and likewise linearly between all other frequency trigger values. Below 49.2 Hz the response is assumed to be the constant 49.2 Hz response value. The starting frequency trigger value of 49.985 Hz is used to take into account the Grid Code deadband of (50 ± 0.015) Hz, within which response is not required. Secondary response values are given for frequency trigger points 49.8 Hz and 49.5 Hz, and response is modelled in the same was as for primary response, only with an 11 s response delay. High response values have trigger points 50.2 Hz and 50.5 Hz. Just as for primary response, the time lag is 1 s and again, response is modelled as linear interpolation through these points, starting at the edge of the deadband at 50.015 Hz and remaining constant beyond 50.5 Hz. Figure 12 illustrates an example of how response holding data (Table 4) are interpreted in the model. Values given are indicative only of possible values.

Fridge conditions are the initial on/off state and initial temperature of each fridge in the population. For the simulations presented here we take the zero perturbation case a(i) in Table 3 from the previous section.

4.2.3. Calculating the Demand at 50 Hz. Deviations in grid frequency away from 50 Hz affect the total system demand. We make the assumption that demand increases linearly by approximately 2.5% of its value at 50 Hz for every 1 Hz increase in frequency above 50 Hz (and decreases by the same amount as frequency decreases below 50 Hz). In order to know the demand at the nominal frequency, "demand at 50 Hz," $\mathrm{Dem}_{\omega 0}(t)$, we need to calculate it from the (measured) demand data input, $D(t)$.

$$D(t) = \mathrm{Dem}_{\omega 0}(t)\left[1 + 0.025\left(f(t) - 50\right)\right] \quad (62)$$

$$\mathrm{Dem}_{\omega 0}(t) = \frac{D(t)}{1 + 0.025\left(f(t) - 50\right)}. \quad (63)$$

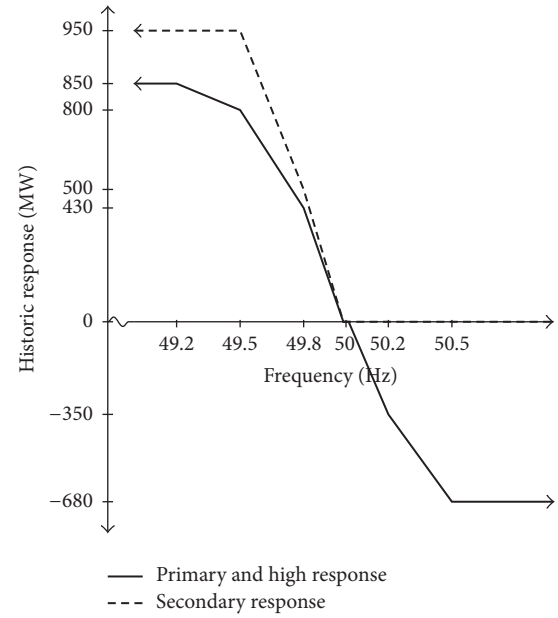

Figure 12: Representative historic response data with interpolation method for primary response (solid line below 50 Hz), secondary response (dashed line), and high response (solid line above 50 Hz). Zero response in the deadband (50 ± 0.015) Hz.

4.2.4. Calculating the Underlying Imbalance. In order to calculate the effects of the fridge population on the system frequency, we first need to calculate the underlying supply-demand imbalance (in MW) that caused the original system frequency deviations away from 50 Hz. At this point it is necessary to distinguish between two important, similar-sounding terms: *underlying imbalance* and *total imbalance*. By underlying imbalance, $\mathrm{Imb}_{\mathrm{under}}(t)$, we mean the generation-demand imbalance that occurs independently of the system frequency. This may be due to, for example, fluctuations in wind or solar power generation or discrepancies between the total predicted system demand and the actual real-time demand. In contrast, total imbalance, $\mathrm{Imb}_{\mathrm{tot}}(f, t)$, includes both the underlying imbalance and, additionally, what we shall refer to as *dynamic imbalance*.

There are two sources of dynamic imbalance: *generator response* (frequency response provided by power generators as the frequency changes) and *demand response* (the automatic change in demand as frequency changes). Note that in this context "demand response" is completely different to demand-side response services, which, given their current low penetration of the response market, we exclude from our simulations. Generator response, $\mathrm{Gen}_{\mathrm{resp}}$, consists of the actual response delivered by generators, calculated as described above from the response holdings and the historic

system frequency. Generator response is assumed to have a small time lag δt, which we take to be 1 second. In contrast, demand response, $\mathrm{Dem}_{\mathrm{resp}}$, is assumed to occur instantaneously and is defined as the measured system demand $D(t)$ minus the demand at 50 Hz, $D_{\omega 0}(t)$ (see "calculating demand at 50 Hz"). Therefore by (62)

$$\mathrm{Dem}_{\mathrm{resp}}\left(f\left(t\right),t\right)=0.025D_{\omega 0}\left(t\right)\left(f\left(t\right)-50\right). \tag{64}$$

Both sources of dynamic imbalance will change when we introduce the population of responsive fridges (because of their impact on the frequency) and will therefore need to be recalculated.

We use a linear approximation for the rate of change of frequency [51], which in our notation is given by

$$\frac{\mathrm{d}f}{\mathrm{d}t}=\frac{50\,\mathrm{Imb}_{\mathrm{tot}}\left(t\right)}{2E_k\left(t\right)}, \tag{65}$$

where 50 is the nominal frequency 50 Hz and $E_k = F_0 M/2$ is total stored kinetic energy in MVAs. Since

$$\begin{aligned}\mathrm{Imb}_{\mathrm{tot}}\left(t\right)=\mathrm{Imb}_{\mathrm{under}}\left(t\right)+\mathrm{Gen}_{\mathrm{resp}}\left(f\left(t-\delta t\right),t\right)\\-\mathrm{Dem}_{\mathrm{resp}}\left(f\left(t\right),t\right)\end{aligned} \tag{66}$$

we are able to find

$$\begin{aligned}\mathrm{Imb}_{\mathrm{under}}\left(t\right)=\frac{E_k\left(t\right)}{25}\frac{\mathrm{d}f}{\mathrm{d}t}-\mathrm{Gen}_{\mathrm{resp}}\left(f\left(t-\delta t\right),t\right)\\+\mathrm{Dem}_{\mathrm{resp}}\left(f\left(t\right),t\right)\end{aligned} \tag{67}$$

which for simulation time step size Δt gives

$$\begin{aligned}\mathrm{Imb}_{\mathrm{under}}\left(t\right)=\frac{E_k\left(t\right)\left[f\left(t\right)-f\left(t-\Delta t\right)\right]}{25\Delta t}\\-\mathrm{Gen}_{\mathrm{resp}}\left(f\left(t-\delta t\right),t\right)\\+\mathrm{Dem}_{\mathrm{resp}}\left(f\left(t\right),t\right).\end{aligned} \tag{68}$$

We take $\Delta t = 1$ s, so $\Delta t = \delta t$, the generator response time lag. Generator response is calculated using historic response holdings and the frequency $t-\delta t$ seconds ago along with some constraints on the generator ramp rates.

4.2.5. Iterative Loop. Once the underlying imbalance has been calculated for all time steps it can be used along with the response holdings and fridge conditions to begin a loop formed of three calculation steps that iterates over all time steps (see the "iterative loop" in Figure 11). The steps are as follows:

(1) *Calculate the frequency response delivery* from the fridge population and from the dynamic response providers based on the previous frequency value (the first iteration takes the first historic frequency value, after which the "new frequency" values are used). For the fridge population this requires summing the switched on fridges multiplied by their individual power consumption and subtracting the power consumption of the population if the fridges were not frequency-sensitive. Response from the dynamic response providers is described above.

(2) *Calculate the new frequency* $f^*(t)$ using the equations from "calculating the underlying imbalance" and beginning with the approximation

$$\begin{aligned}f^*\left(t\right)&=f^*\left(t-\Delta t\right)+\Delta t\frac{\mathrm{d}f^*}{\mathrm{d}t}\left(t\right)\\&=f^*\left(t-\Delta t\right)+\Delta t\frac{25\,\mathrm{Imb}^*_{\mathrm{tot}}\left(t\right)}{E_k\left(t\right)}\end{aligned} \tag{69}$$

and since

$$\begin{aligned}\mathrm{Imb}^*_{\mathrm{tot}}\left(t\right)=\mathrm{Imb}_{\mathrm{under}}\left(t\right)+\mathrm{Gen}_{\mathrm{resp}}\left(f^*\left(t-\delta t\right),t\right)\\-0.025\mathrm{Dem}_{\omega 0}\left(f^*\left(t\right)-50\right)\end{aligned} \tag{70}$$

we get

$$f^*\left(t\right)=\frac{f^*\left(t-\Delta t\right)+\left(25\Delta t/E_k\left(t\right)\right)\left(\mathrm{Imb}_{\mathrm{under}}\left(t\right)+\mathrm{Gen}_{\mathrm{resp}}\left(f^*\left(t-\delta t\right),t\right)+1.25\mathrm{Dem}_{\omega 0}\right)}{1+0.625\left(\delta t/E_k\left(t\right)\right)\mathrm{Dem}_{\omega 0}}. \tag{71}$$

Note that we let $f^*(0) = f(0)$, the original frequency value at time 0.

(3) *Calculate the new fridge conditions* by updating their temperature set points with the new frequency f^* calculated in step 2, according to (2a) and (2b). Each fridge temperature is evolved one time step according to (3a) or (3b). If a switch on or off should have occurred during the time step then the exact time of switch is estimated and the temperature is recalculated from the switch time to the end of the time step using linear interpolation.

4.2.6. Outputs. There are two key outputs for our analysis: firstly, the temperatures and states of each fridge over time and secondly, the frequency response supplied by all other providers on the grid. Since response can be positive or negative depending on the frequency, but both incur payment, we take the absolute value of the response at each time step. We take the cumulative sum of the difference between this response in the presence of TCLs and the original system response and call it "cumulative response savings," which we measure in MWh. This allows us to find out how much benefit (or detriment) the fridges provided the system and

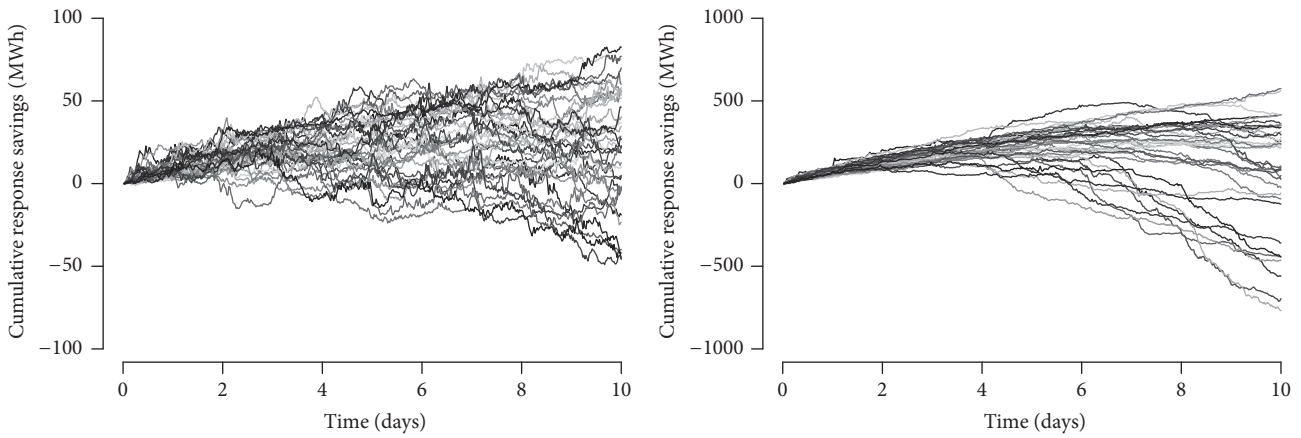

(a) $P_c = 70\,\text{MW}$ (b) $P_c = 700\,\text{MW}$

FIGURE 13: Cumulative response savings (MWh), the difference between other providers' response with and without the frequency-sensitive fridge population (cumulatively) for the 36 data samples over one year for two different participation levels. We sum high frequency response and the absolute value of low frequency response, in MWh. Negative results indicate that the other providers had to compensate for detrimental fridge behaviour. In both cases the population is homogeneous.

how that changes over time as they respond to frequency perturbations.

4.2.7. Results. We begin by comparing the results of two populations of fridges, one with total power consumption (if every fridge were switched on), $P_c = 70\,\text{MW}$, as in previous simulations, and the other with $P_c = 700\,\text{MW}$. The second case is the extreme with 10 million frequency-sensitive fridges, similar to Trovato et al. who modelled 11 million fridges in [33]. Rather than modelling all 1 million or 10 million fridges, we split the population into 10^4 groups, where the fridges within one group have the same temperature and state. We begin both simulations with the groups uniformly distributed in phase (the unperturbed case) just as in figures a(i) of the previous simulation section. We repeat these simulations on 36 10-day data samples from July 2015–June 2016.

Figure 13 shows cumulative response savings over time (introduced above) for the 36 data sample simulations in each case. For both values of P_c, in at least a third of the simulations, the fridge population ended up doing more harm than good (negative savings) due to synchronisation. Increasing participation tenfold increased the best results by about a factor of 7 but worsened the worst results by a factor of 15. When there were fewer participants ($P_c = 70\,\text{MW}$), the results were more erratic over time, which we attribute to there being less response on the system, and so a less smooth frequency trace to respond to. In light of these findings, we present the results from another set of 36 simulations over the year for $P_c = 700\,\text{MW}$, with the addition of a very small amount of diversity (less than 0.25% in relative terms) to the parameters.

We find that very small amounts of parameter diversification can eradicate the detrimental fridge behaviour in our simulations. A full presentation of all of our simulations can be found in Webborn Ph.D. thesis, to appear. As an example we take $P_c = 700$ and the other parameters to have the same

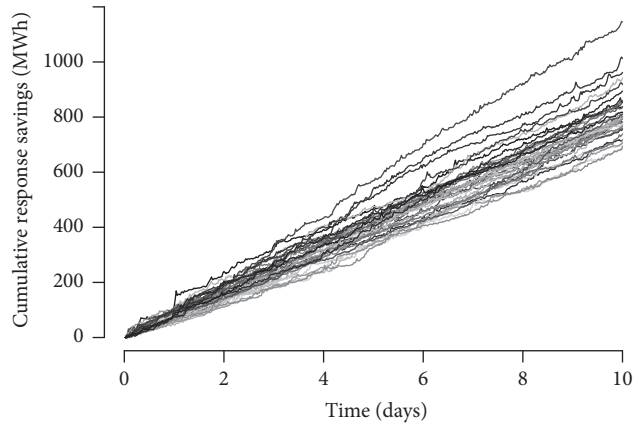

FIGURE 14: Cumulative response savings (MWh) (see Figure 13) for a heterogeneous fridge population with $P_c = 700\,\text{MW}$. The introduction of a very small amount of diversity has eradicated the detrimental behaviour in all cases and the fridge population provides a clear benefit to the system.

mean as in all of our previous simulations but draw them from normal distributions with nonzero standard deviation. We choose $T_{\text{ON}} \sim \mathcal{N}(-26, 0.020)$, $T_{\text{OFF}} \sim \mathcal{N}(20, 0.0133)$, $T_-^0 \sim \mathcal{N}(2, 0.005)$, $(T_+^0 - T_-^0) \sim \mathcal{N}(5, 0.003)$, and $\alpha \sim \mathcal{N}(18.08 \times 10^5, 0.030 \times 10^5)$. This results in $T_+^0 \sim \mathcal{N}(7, 0.005)$, the duty cycle approximately $\sim\mathcal{N}(33.55\%, 0.027\%)$, and the cycle period in minutes $\sim\mathcal{N}(41.144, 0.108)$. The results from these simulations are shown in Figure 14. We see that even with this very small amount of parameter diversity, all the simulations show a net and growing benefit to the system over the ten days. Since diversity naturally occurs in any real population, this offers reasonable evidence that TCLs could be a valuable resource for the grid, without the need for stochastic switching or regular communications from a central controller.

5. Discussion and Conclusions

The combination of our mathematical analysis and simulations has improved our understanding of how a population of frequency-sensitive TCLs might act on the electricity grid, in a number of ways. Our analysis in Section 3.1 was able to capture the short-term benefits of using identical TCLs for frequency response. However, the simulations of the model were important in showing that, in response to realistic forcing, in the long term, nonlinear dynamics occur that could not be captured with our linearisation. Studying the two-group case indicated that the fully synchronised periodic solution is unstable to splitting it into two synchronised groups of similar size. A continuum of TCLs, as analysed in Section 3.1, is the limit as N goes to infinity of N equally sized groups of TCLs. Therefore the stability found for the uniformly distributed continuum of TCLs can be compared to the case with two groups of similar size remaining separate. If the distribution of TCLs is perturbed too far from uniform, as in the simulations in Section 4, then this is similar to the two-group case in which the groups are not similarly sized.

Simulating a population of identical frequency-sensitive TCLs under typical system conditions revealed that for many of the data samples the short-term benefits were outweighed by switching behaviour that requires greater frequency response from the rest of the system than when the TCLs were not frequency-sensitive. In these cases regular communications would need to be sent to the TCLs to desynchronise. However, we find that the addition of a very small amount of parameter diversity, for example, 0.24% variation in the natural cycle period, which is likely to occur naturally in a population, can eradicate these issues. In our example the population was able to reduce the response required from other providers in all periods of the year studied.

A number of open questions remain. How would factors such as daily room temperature variations, opening the door, and changing the contents of TCLs like fridge-freezers affect the cycle distribution? How would a population cope during more severe frequency incidents than existed during 2015-16? What would be the effects of modelling the population on a network where frequency variations can be spatially dependent? How much diversity exists in real TCL populations and can the effects of diversity be understood theoretically?

In conclusion, this study indicates that a population of fridges might perform a valuable service to the grid without requiring centralised or stochastic control.

Appendix

A. Derivation of (7)

Sufficient condition (7) for a fridge to change its power consumption as required by the system frequency is derived as follows. We would like to know how the typical power consumption over one cycle changes as system frequency changes. Typical power consumption per TCL per cycle, $\overline{p}$, is given by

$$\overline{p} = \frac{p\tau_{\mathrm{ON}}}{(\tau_{\mathrm{ON}} + \tau_{\mathrm{OFF}})}, \tag{A.1}$$

where p is the instantaneous power consumption of a TCL when switched on (assumed to be independent of time in its on-phase). From (2a), (2b), (4a), and (4b),

$$\frac{\partial \tau_{\mathrm{ON}}}{\partial f} = \frac{\beta_- (T_+ - T_{\mathrm{ON}}) - \beta_+ (T_- - T_{\mathrm{ON}})}{\alpha (T_- - T_{\mathrm{ON}})^2} \tag{A.2a}$$

$$\frac{\partial \tau_{\mathrm{OFF}}}{\partial f} = \frac{\beta_- (T_{\mathrm{OFF}} - T_+) + \beta_+ (T_{\mathrm{OFF}} - T_-)}{\alpha (T_{\mathrm{OFF}} - T_+)^2}. \tag{A.2b}$$

Therefore

$$\frac{\partial \overline{p}}{\partial f} = \frac{p}{\alpha^2 (\tau_{\mathrm{ON}} + \tau_{\mathrm{OFF}})^2} \left[\frac{-\beta_+ (T_- - T_{\mathrm{ON}}) + \beta_- (T_+ - T_{\mathrm{ON}})}{(T_- - T_{\mathrm{ON}})^2} (\alpha\tau_{\mathrm{ON}} + \alpha\tau_{\mathrm{OFF}}) - \left(\frac{\beta_- (T_+ - T_{\mathrm{ON}}) - \beta_+ (T_- - T_{\mathrm{ON}})}{(T_- - T_{\mathrm{ON}})^2} + \frac{\beta_- (T_{\mathrm{OFF}} - T_+) + \beta_+ (T_{\mathrm{OFF}} - T_-)}{(T_{\mathrm{OFF}} - T_+)^2} \right) \alpha\tau_{\mathrm{ON}} \right]. \tag{A.3}$$

Since $p > 0$, $\partial\overline{p}/\partial f$ is strictly positive if and only if

$$\beta_+ \left(\frac{\tau_{\mathrm{ON}} (T_{\mathrm{OFF}} - T_-)(T_- - T_{\mathrm{ON}}) - \tau_{\mathrm{OFF}} (T_{\mathrm{OFF}} - T_+)^2}{(T_- - T_{\mathrm{ON}})(T_{\mathrm{OFF}} - T_+)^2} \right) + \beta_- \left(\frac{\tau_{\mathrm{OFF}} (T_{\mathrm{OFF}} - T_+)(T_+ - T_{\mathrm{ON}}) - \tau_{\mathrm{ON}} (T_- - T_{\mathrm{ON}})^2}{(T_{\mathrm{OFF}} - T_+)(T_- - T_{\mathrm{ON}})^2} \right) > 0 \tag{A.4}$$

which is the case if and only if

$$\tau_{\mathrm{ON}} (T_- - T_{\mathrm{ON}})^2 (\beta_+ (T_{\mathrm{OFF}} - T_-) - \beta_- (T_{\mathrm{OFF}} - T_+)) + \tau_{\mathrm{OFF}} (T_{\mathrm{OFF}} - T_+)^2 \cdot (\beta_- (T_+ - T_{\mathrm{ON}}) - \beta_+ (T_- - T_{\mathrm{ON}})) > 0. \tag{A.5}$$

Therefore a sufficient condition for the derivative of $\overline{p}$ with respect to Δf to be positive is that both terms in the preceding equation should be strictly positive. Since τ_{ON}, τ_{OFF}, and the

squared terms are always strictly positive this leaves us with two sufficient criteria:

$$\begin{aligned}\frac{\beta_+}{\beta_-} &< \frac{T_+ - T_{\mathrm{ON}}}{T_- - T_{\mathrm{ON}}},\\ \frac{\beta_+}{\beta_-} &> \frac{T_{\mathrm{OFF}} - T_+}{T_{\mathrm{OFF}} - T_-}.\end{aligned} \tag{A.6}$$

The upper bound is greater than 1 and the lower bound is less than 1 if $T_{\mathrm{ON}} < T_- < T_+ < T_{\mathrm{OFF}}$.

B. Derivation of (61): The First Eigenvalue in the Two-Group Case

The temperature evolution equations tell us that

$$T_{\mathrm{A}}(t_1) = (T_{\mathrm{A}}(0) - T_{\mathrm{OFF}})\, e^{-\alpha t_1} + T_{\mathrm{OFF}} \tag{B.1a}$$

$$T_{\mathrm{B}}(t_1) = (T_{\mathrm{B}}(0) - T_{\mathrm{ON}})\, e^{-\alpha t_1} + T_{\mathrm{ON}} \tag{B.1b}$$

$$T_{\mathrm{A}}(t_2) = (T_{\mathrm{A}}(t_1) - T_{\mathrm{ON}})\, e^{-\alpha(t_2 - t_1)} + T_{\mathrm{ON}} \tag{B.1c}$$

$$T_{\mathrm{B}}(t_2) = (T_{\mathrm{B}}(t_1) - T_{\mathrm{ON}})\, e^{-\alpha(t_2 - t_1)} + T_{\mathrm{ON}} \tag{B.1d}$$

$$T_{\mathrm{A}}(t_3) = (T_{\mathrm{A}}(t_2) - T_{\mathrm{ON}})\, e^{-\alpha(t_3 - t_2)} + T_{\mathrm{ON}} \tag{B.1e}$$

$$T_{\mathrm{B}}(t_3) = (T_{\mathrm{B}}(t_2) - T_{\mathrm{OFF}})\, e^{-\alpha(t_3 - t_2)} + T_{\mathrm{OFF}} \tag{B.1f}$$

$$T_{\mathrm{A}}(t_4) = (T_{\mathrm{A}}(t_3) - T_{\mathrm{OFF}})\, e^{-\alpha(t_4 - t_3)} + T_{\mathrm{OFF}} \tag{B.1g}$$

$$T_{\mathrm{B}}(t_4) = (T_{\mathrm{B}}(t_3) - T_{\mathrm{OFF}})\, e^{-\alpha(t_4 - t_3)} + T_{\mathrm{OFF}}. \tag{B.1h}$$

The temperature set point equations provide us with

$$T_{\mathrm{A}}(t_1) = T_{\mathrm{B}}(0) + \beta c P_c (1 - \sigma - \rho^*)\, t_1 \tag{B.2a}$$

$$\begin{aligned}T_{\mathrm{B}}(t_2) &= T_{\mathrm{A}}(t_1) + \beta c P_c (1 - \rho^*)(t_2 - t_1)\\ &\quad - \left(T_+^0 - T_-^0\right)\end{aligned} \tag{B.2b}$$

$$T_{\mathrm{A}}(t_3) = T_{\mathrm{B}}(t_2) + \beta c P_c (\sigma - \rho^*)(t_3 - t_2) \tag{B.2c}$$

$$T_{\mathrm{B}}(t_4) = T_{\mathrm{A}}(t_3) - \beta c P_c \rho^* (t_4 - t_3) + T_+^0 - T_-^0. \tag{B.2d}$$

Equations (B.1a) and (B.2a) determine t_1 in terms of $T_{\mathrm{A}}(0), T_{\mathrm{B}}(0)$, (B.1a) and (B.1b) determine $T_{\mathrm{A}}(t_1), T_{\mathrm{B}}(t_1)$ and so forth, and hence $T_{\mathrm{A}}(t_4), T_{\mathrm{B}}(t_4)$ are determined by $T_{\mathrm{A}}(0), T_{\mathrm{B}}(0)$. To analyse the linear stability of the fixed point of this map corresponding to the one group solution T_Γ (Section 3.2.2) we find that $\Delta'_T := T_{\mathrm{B}}(t_4) - T_{\mathrm{A}}(t_4)$ depends only on ΔT and some differences of switching times, by eliminating the temperatures at the intermediary switch times.

$$\begin{aligned}\Delta'_T &= (T_{\mathrm{B}}(0) - T_{\mathrm{A}}(0))\, e^{-\alpha(t_4 - t_1)} + (T_{\mathrm{OFF}} - T_{\mathrm{ON}})\\ &\quad \cdot \left(e^{-\alpha(t_4 - t_3)} - e^{-\alpha(t_4 - t_2)} - e^{-\alpha(t_4 - t_1)} + e^{-\alpha(t_4)}\right).\end{aligned} \tag{B.3}$$

Defining $L := l_{\mathrm{ON}} + l_{\mathrm{OFF}}$ and linearising about the single group solution using the ϵ_i notation from Figure 4 (signed displacement from the single group switch times) give

$$\begin{aligned}&\Delta'_T\\ &\quad \approx e^{-\alpha L}\Delta_T\\ &\qquad + \alpha (T_{\mathrm{OFF}} - T_{\mathrm{ON}}) \left[(\epsilon_3 - \epsilon_2)\, e^{-\alpha l_{\mathrm{OFF}}} - e^{-\alpha L}\Delta_t\right].\end{aligned} \tag{B.4}$$

Since (B.1a) and (B.2a) are two equations for $T_{\mathrm{A}}(t_1)$, (B.1d) and (B.2b) are two equations for $T_{\mathrm{B}}(t_2)$, (B.1e) and (B.2c) are two equations for $T_{\mathrm{A}}(t_3)$, and (B.1h) and (B.2d) are two equations for $T_{\mathrm{B}}(t_4)$, we have

$$\begin{aligned}&(T_{\mathrm{A}}(0) - T_{\mathrm{OFF}})\, e^{-\alpha t_1} + T_{\mathrm{OFF}}\\ &\quad = T_{\mathrm{B}}(0) + \beta c P_c (1 - \sigma - \rho^*)\, t_1\end{aligned} \tag{B.5a}$$

$$\begin{aligned}&(T_{\mathrm{B}}(t_1) - T_{\mathrm{ON}})\, e^{-\alpha(t_2 - t_1)} + T_{\mathrm{ON}}\\ &\quad = T_{\mathrm{A}}(t_1) + \beta c P_c (1 - \rho^*)(t_2 - t_1) - \left(T_+^0 - T_-^0\right)\end{aligned} \tag{B.5b}$$

$$\begin{aligned}&(T_{\mathrm{A}}(t_2) - T_{\mathrm{ON}})\, e^{-\alpha(t_3 - t_2)} + T_{\mathrm{ON}}\\ &\quad = T_{\mathrm{B}}(t_2) + \beta c P_c (\sigma - \rho^*)(t_3 - t_2)\end{aligned} \tag{B.5c}$$

$$\begin{aligned}&(T_{\mathrm{B}}(t_3) - T_{\mathrm{OFF}})\, e^{-\alpha(t_4 - t_3)} + T_{\mathrm{OFF}}\\ &\quad = T_{\mathrm{A}}(t_3) - \beta c P_c \rho^* (t_4 - t_3) + T_+^0 - T_-^0.\end{aligned} \tag{B.5d}$$

We used (B.5a) already to determine t_1 in terms of ΔT to first-order (59). Denote $\tau := \epsilon_3 - \epsilon_2$, then to find τ to first order we linearise (B.5c) to obtain

$$\begin{aligned}&\beta c p (\sigma - \rho^*)\tau + T_\Gamma(l_{\mathrm{ON}}) + (T_{\mathrm{B}}(t_2) - T_\Gamma(l_{\mathrm{ON}}))\\ &\quad = (T_\Gamma(l_{\mathrm{ON}}) + (T_{\mathrm{A}}(t_2) - T_\Gamma(l_{\mathrm{ON}})))\, e^{-\alpha\tau}\\ &\qquad + T_{\mathrm{ON}}(1 - e^{-\alpha\tau})\\ &\beta c p (\sigma - \rho^*)\tau + T_\Gamma(l_{\mathrm{ON}}) + (T_{\mathrm{B}}(t_2) - T_\Gamma(l_{\mathrm{ON}}))\\ &\quad = T_\Gamma(l_{\mathrm{ON}}) + T_{\mathrm{A}}(t_2) - T_\Gamma(l_{\mathrm{ON}})\\ &\qquad - \alpha\tau\left[T_\Gamma(l_{\mathrm{ON}}) + (T_{\mathrm{A}}(t_2) - T_\Gamma(l_{\mathrm{ON}}))\right]\\ &\qquad + T_{\mathrm{ON}}(1 - 1 + \alpha\tau)\\ &\therefore \left[\beta c p (\sigma - \rho^*) + \alpha (T_\Gamma(l_{\mathrm{ON}}) - T_{\mathrm{ON}})\right]\tau\\ &\quad = T_{\mathrm{A}}(t_2) - T_{\mathrm{B}}(t_2).\end{aligned} \tag{B.6}$$

Now we can find a substitution for $T_{\mathrm{A}}(t_2)$ and $T_{\mathrm{B}}(t_2)$

$$\begin{aligned}&T_{\mathrm{A}}(t_2) - T_{\mathrm{B}}(t_2)\\ &\quad = T_{\mathrm{A}}(0)\, e^{-\alpha t_2} + T_{\mathrm{OFF}}\left(e^{-\alpha(t_2 - t_1)} - e^{-\alpha t_2}\right)\\ &\qquad + T_{\mathrm{ON}}\left(1 - e^{-\alpha(t_2 - t_1)}\right) - (T_{\mathrm{B}}(0) - T_{\mathrm{ON}})\, e^{-\alpha t_2}\end{aligned}$$

$$
\begin{aligned}
&- T_{\mathrm{ON}} \\
&= -\left(T_{\mathrm{B}}(0) - T_{\mathrm{A}}(0)\right) e^{-\alpha(l_{\mathrm{ON}}+\epsilon_2)} \\
&\quad + T_{\mathrm{OFF}}\left(e^{-\alpha(l_{\mathrm{ON}}+\epsilon_2-\epsilon_1)} - e^{-\alpha(l_{\mathrm{ON}}+\epsilon_2)}\right) \\
&\quad + T_{\mathrm{ON}}\left(e^{-\alpha(l_{\mathrm{ON}}+\epsilon_2)} - e^{-\alpha(l_{\mathrm{ON}}+\epsilon_2-\epsilon_1)}\right) \\
&= -\Delta_T e^{-\alpha l_{\mathrm{ON}}} + T_{\mathrm{OFF}}\alpha\epsilon_1 e^{-\alpha l_{\mathrm{ON}}} - T_{\mathrm{ON}}\alpha\epsilon_1 e^{-\alpha l_{\mathrm{ON}}} \\
&= \left(\alpha\left(T_{\mathrm{OFF}} - T_{\mathrm{ON}}\right)\Delta_t - \Delta_T\right) e^{-\alpha l_{\mathrm{ON}}}
\end{aligned}
\tag{B.7}
$$

and we can use this substitution to arrive at

$$
\tau = \frac{\left(\alpha\left(T_{\mathrm{OFF}} - T_{\mathrm{ON}}\right)\Delta_t - \Delta_T\right) e^{-\alpha l_{\mathrm{ON}}}}{\beta c P_c\left(\sigma - \rho^*\right) + \alpha\left(T_\Gamma\left(l_{\mathrm{ON}}\right) - T_{\mathrm{ON}}\right)}. \tag{B.8}
$$

With our expression for τ and for Δ_t using (59), we arrive at $\Delta_T' = \lambda\Delta_T$ where

$$
\begin{aligned}
\lambda \coloneqq &\left(1 - \frac{\alpha\left(T_{\mathrm{OFF}} - T_{\mathrm{ON}}\right)}{\alpha\left(T_{\mathrm{OFF}} - T_\Gamma(0)\right) - \beta c P_c\left(1 - \sigma - \rho^*\right)}\right) \\
&\cdot \left(1 - \frac{\alpha\left(T_{\mathrm{OFF}} - T_{\mathrm{ON}}\right)}{\alpha\left(T_\Gamma\left(l_{\mathrm{ON}}\right) - T_{\mathrm{ON}}\right) + \beta c P_c\left(\sigma - \rho^*\right)}\right) \\
&\cdot e^{-\alpha L}.
\end{aligned}
\tag{B.9}
$$

C. Derivation of the Second Eigenvalue in the Two-Group Case

In Appendix B we found one of the eigenvalues λ (61) for the case of two groups of TCLs whose cycling was close to the single group solution and claimed that the other eigenvalue was insignificant for determining the stability of the system. Here we derive bounds on the second eigenvalue to prove this claim.

The temperature cycles of groups A and B are initially very close to the single group temperature cycle T_Γ and therefore, for $I \in \{\mathrm{A}, \mathrm{B}\}$, we write

$$
\begin{aligned}
T_I(0) &= T_\Gamma(0) + \delta T_I(0) \\
T_I(t_1) &= T_\Gamma(0) + \delta T_I(t_1) \\
T_I(t_2) &= T_\Gamma\left(l_{\mathrm{ON}}\right) + \delta T_I(t_2) \\
T_I(t_3) &= T_\Gamma\left(l_{\mathrm{ON}}\right) + \delta T_I(t_3) \\
T_I(t_4) &= T_\Gamma(0) + \delta T_I(t_4).
\end{aligned}
\tag{C.1}
$$

Our approach is to seek a map M such that

$$
\begin{pmatrix} \delta T_{\mathrm{A}}(t_4) \\ \delta T_{\mathrm{B}}(t_4) \end{pmatrix} = M \begin{pmatrix} \delta T_{\mathrm{A}}(0) \\ \delta T_{\mathrm{B}}(0) \end{pmatrix}. \tag{C.2}
$$

Taking linear approximations as in Section 3.2.3, (B.5a) approximates to

$$
\begin{aligned}
&T_\Gamma(0) + \delta T_{\mathrm{A}}(0) - \alpha t_1\left(T_\Gamma(0) - T_{\mathrm{OFF}}\right) \\
&\quad \approx T_\Gamma(0) + \delta T_{\mathrm{B}}(0) + \beta c P_c\left(1 - \sigma - \rho^*\right) t_1 \\
&t_1 \approx \frac{\delta T_{\mathrm{B}}(0) - \delta T_{\mathrm{A}}(0)}{\xi_1},
\end{aligned}
\tag{C.3}
$$

where

$$
\xi_1 \coloneqq \alpha\left(T_{\mathrm{OFF}} - T_\Gamma(0)\right) - \beta c P_c\left(1 - \sigma - \rho^*\right). \tag{C.4}
$$

We can use this expression for t_1 and take a first-order approximation of (B.1a) to find an expression for $\delta T_{\mathrm{A}}(t_1)$ in terms of $\delta T_{\mathrm{A}}(0)$:

$$
\begin{aligned}
&T_\Gamma(0) + \delta T_{\mathrm{A}}(t_1) \\
&\quad = \left(T_\Gamma(0) + \delta T_{\mathrm{A}}(0) - T_{\mathrm{OFF}}\right) e^{-\alpha t_1} + T_{\mathrm{OFF}} \\
&\delta T_{\mathrm{A}}(t_1) \approx \delta T_{\mathrm{A}}(0) - \alpha t_1\left(T_\Gamma(0) - T_{\mathrm{OFF}}\right) \\
&\delta T_{\mathrm{A}}(t_1) \\
&\quad \approx \delta T_{\mathrm{A}}(0) \\
&\qquad + \frac{\alpha}{\xi_1}\left(T_{\mathrm{OFF}} - T_\Gamma(0)\right)\left(\delta T_{\mathrm{B}}(0) - \delta T_{\mathrm{A}}(0)\right).
\end{aligned}
\tag{C.5}
$$

Similarly, using (B.1b) we find that

$$
\begin{aligned}
&\delta T_{\mathrm{B}}(t_1) \\
&\quad \approx \delta T_{\mathrm{B}}(0) \\
&\qquad - \frac{\alpha}{\xi_1}\left(T_\Gamma(0) - T_{\mathrm{ON}}\right)\left(\delta T_{\mathrm{B}}(0) - \delta T_{\mathrm{A}}(0)\right).
\end{aligned}
\tag{C.6}
$$

We repeat this process to find expressions for each time interval (recall that $t_1 = \epsilon_1 - 0$ is the first interval between switch times) $(\epsilon_i - \epsilon_{i-1})$ for $i \in \{2, 3, 4\}$ and each subsequent $\delta T_{\mathrm{A}}(t_i)$ and $\delta T_{\mathrm{B}}(t_i)$. We use (B.5b) to find

$$
\epsilon_2 - \epsilon_1 \approx \frac{\delta T_{\mathrm{B}}(t_1) e^{-\alpha l_{\mathrm{ON}}} - \delta T_{\mathrm{A}}(t_1)}{\xi_2}, \tag{C.7}
$$

where

$$
\xi_2 \coloneqq \alpha\left(T_\Gamma(0) - T_{\mathrm{ON}}\right) e^{-\alpha l_{\mathrm{ON}}} + \beta c P_c\left(1 - \rho^*\right). \tag{C.8}
$$

Equations (B.1c) and (B.1d) thus yield

$$
\begin{aligned}
\delta T_{\mathrm{A}}(t_2) \approx{}& \delta T_{\mathrm{A}}(t_1) e^{-\alpha l_{\mathrm{ON}}} - \frac{\alpha}{\xi_2}\left(T_\Gamma(0) - T_{\mathrm{ON}}\right) \\
&\cdot \left(\delta T_{\mathrm{B}}(t_1) e^{-\alpha l_{\mathrm{ON}}} - \delta T_{\mathrm{A}}(t_1)\right) e^{-\alpha l_{\mathrm{ON}}}
\end{aligned}
\tag{C.9}
$$

$$
\begin{aligned}
\delta T_{\mathrm{B}}(t_2) \approx{}& \delta T_{\mathrm{B}}(t_1) e^{-\alpha l_{\mathrm{ON}}} - \frac{\alpha}{\xi_2}\left(T_\Gamma(0) - T_{\mathrm{ON}}\right) \\
&\cdot \left(\delta T_{\mathrm{B}}(t_1) e^{-\alpha l_{\mathrm{ON}}} - \delta T_{\mathrm{A}}(t_1)\right) e^{-\alpha l_{\mathrm{ON}}}.
\end{aligned}
\tag{C.10}
$$

Using (B.5c) we find

$$\epsilon_3 - \epsilon_2 \approx \frac{\delta T_A(t_2) - \delta T_B(t_2)}{\xi_3}, \tag{C.11}$$

where

$$\xi_3 \coloneqq \alpha\left(T_\Gamma(l_{ON}) - T_{ON}\right) + \beta c P_c\left(\sigma - \rho^*\right). \tag{C.12}$$

Equations (B.1e) and (B.1f) yield

$$\begin{aligned}\delta T_A(t_3) &\approx \delta T_A(t_2) \\ &\quad - \frac{\alpha}{\xi_3}\left(T_\Gamma(l_{ON}) - T_{ON}\right)\left(\delta T_A(t_2) - \delta T_B(t_2)\right)\end{aligned} \tag{C.13}$$

$$\begin{aligned}\delta T_B(t_3) &\approx \delta T_B(t_2) \\ &\quad + \frac{\alpha}{\xi_3}\left(T_{OFF} - T_\Gamma(l_{ON})\right)\left(\delta T_A(t_2) - \delta T_B(t_2)\right).\end{aligned} \tag{C.14}$$

Finally (B.5d) gives

$$\epsilon_4 - \epsilon_3 \approx \frac{\delta T_A(t_3) - \delta T_B(t_3)\, e^{-\alpha l_{OFF}}}{\xi_4}, \tag{C.15}$$

where

$$\xi_4 \coloneqq \alpha\left(T_{OFF} - T_\Gamma(l_{ON})\right) e^{-\alpha l_{OFF}} + \beta c P_c \rho^* \tag{C.16}$$

and (B.1g) and (B.1h) give

$$\begin{aligned}\delta T_A(t_4) &\approx \delta T_A(t_3)\, e^{-\alpha l_{OFF}} + \frac{\alpha}{\xi_4}\left(T_{OFF} - T_\Gamma(l_{ON})\right) \\ &\quad \cdot \left(\delta T_A(t_3) - \delta T_B(t_3)\, e^{-\alpha l_{OFF}}\right) e^{-\alpha l_{OFF}}\end{aligned} \tag{C.17}$$

$$\begin{aligned}\delta T_B(t_4) &\approx \delta T_B(t_3)\, e^{-\alpha l_{OFF}} + \frac{\alpha}{\xi_4}\left(T_{OFF} - T_\Gamma(l_{ON})\right) \\ &\quad \cdot \left(\delta T_A(t_3) - \delta T_B(t_3)\, e^{-\alpha l_{OFF}}\right) e^{-\alpha l_{OFF}}.\end{aligned} \tag{C.18}$$

For each $i \in \{1, 2, 3, 4\}$ we can write

$$\begin{pmatrix}\delta T_A(t_i) \\ \delta T_B(t_i)\end{pmatrix} = M_i \begin{pmatrix}\delta T_A(t_{i-1}) \\ \delta T_B(t_{i-1})\end{pmatrix} \tag{C.19}$$

and so

$$\begin{pmatrix}\delta T_A(t_4) \\ \delta T_B(t_4)\end{pmatrix} = M \begin{pmatrix}\delta T_A(0) \\ \delta T_B(0)\end{pmatrix}, \tag{C.20}$$

where

$$M \coloneqq M_4 M_3 M_2 M_1. \tag{C.21}$$

We introduce the following simplifying notation before defining each matrix M_i. Let

$$\mathscr{A} = \alpha\left(T_{OFF} - T_\Gamma(0)\right) \tag{C.22a}$$

$$\mathscr{B} = \alpha\left(T_\Gamma(0) - T_{ON}\right) \tag{C.22b}$$

$$\mathscr{C} = \alpha\left(T_\Gamma(l_{ON}) - T_{ON}\right) \tag{C.22c}$$

$$\mathscr{D} = \alpha\left(T_{OFF} - T_\Gamma(l_{ON})\right). \tag{C.22d}$$

Then

$$M_1 = \frac{1}{\xi_1}\begin{pmatrix}\xi_1 - \mathscr{A} & \mathscr{A} \\ \mathscr{B} & \xi_1 - \mathscr{B}\end{pmatrix} \tag{C.23a}$$

$$M_2 = \frac{e^{-\alpha l_{ON}}}{\xi_2}\begin{pmatrix}\xi_2 + \mathscr{B} & -\mathscr{B} e^{-\alpha l_{ON}} \\ \mathscr{B} & \xi_2 - \mathscr{B} e^{-\alpha l_{ON}}\end{pmatrix} \tag{C.23b}$$

$$M_3 = \frac{1}{\xi_3}\begin{pmatrix}\xi_3 - \mathscr{C} & \mathscr{C} \\ \mathscr{D} & \xi_3 - \mathscr{D}\end{pmatrix} \tag{C.23c}$$

$$M_4 = \frac{e^{-\alpha l_{OFF}}}{\xi_4}\begin{pmatrix}\xi_4 + \mathscr{D} & -\mathscr{D} e^{-\alpha l_{OFF}} \\ \mathscr{D} & \xi_4 - \mathscr{D} e^{-\alpha l_{OFF}}\end{pmatrix}. \tag{C.23d}$$

We already know one of the eigenvalues of the system (λ), and the second eigenvalue is given by $\det(M)/\lambda$. Note that $\det(M) = \det(M_4)\det(M_3)\det(M_2)\det(M_1)$, and

$$\begin{aligned}\det(M_1) &= \xi_1 - (\mathscr{A} + \mathscr{B}) \\ &= -\mathscr{B} - \beta c P_c\left(1 - \sigma - \rho^*\right)\end{aligned} \tag{C.24a}$$

$$\begin{aligned}\det(M_2) &= \left(\xi_2 + \mathscr{B}\left(1 - e^{-\alpha l_{ON}}\right)\right) e^{-\alpha l_{ON}} \\ &= \left(\mathscr{B} + \beta c P_c\left(1 - \rho^*\right)\right) e^{-\alpha l_{ON}}\end{aligned} \tag{C.24b}$$

$$\det(M_3) = \xi_3 - (\mathscr{C} + \mathscr{D}) = -\mathscr{D} + \beta c P_c\left(\sigma - \rho^*\right) \tag{C.24c}$$

$$\begin{aligned}\det(M_4) &= \left(\xi_4 + \mathscr{D}\left(1 - e^{-\alpha l_{OFF}}\right)\right) e^{-\alpha l_{OFF}} \\ &= \left(\mathscr{D} + \beta c P_c \rho^*\right) e^{-\alpha l_{OFF}}.\end{aligned} \tag{C.24d}$$

We can rewrite λ (see (61)) in our new notation as

$$\begin{aligned}\lambda &= \frac{\left(\mathscr{B} + \beta c P_c\left(1 - \sigma - \rho^*\right)\right)\left(\mathscr{D} - \beta c P_c\left(\sigma - \rho^*\right)\right)}{\left(\mathscr{A} - \beta c P_c\left(1 - \sigma - \rho^*\right)\right)\left(\mathscr{C} + \beta c P_c\left(\sigma - \rho^*\right)\right)} \\ &\quad \cdot e^{-\alpha L}\end{aligned} \tag{C.25}$$

which allows us to write

$$\begin{aligned}\frac{\det(M)}{\lambda} &= \left[\mathscr{A} - \beta c P_c\left(1 - \sigma - \rho^*\right)\right] \\ &\quad \cdot \left[\mathscr{B} + \beta c P_c\left(1 - \rho^*\right)\right] \\ &\quad \cdot \left[\mathscr{C} + \beta c P_c\left(\sigma - \rho^*\right)\right]\left[\mathscr{D} + \beta c P_c \rho^*\right].\end{aligned} \tag{C.26}$$

Denote the second eigenvalue by λ_2, and use

$$\lambda_2 = \frac{\det(M)}{\lambda}. \tag{C.27}$$

Since $0 < \mathscr{A}, \mathscr{B}, \mathscr{C}, \mathscr{D} < \alpha(T_{\mathrm{OFF}} - T_{\mathrm{ON}})$, $\sigma \in (0, 1)$, and $\rho^* \in (0, 1)$,

$$|\lambda_2| < \left[\alpha\left(T_{\mathrm{OFF}} - T_{\mathrm{ON}}\right) + \beta c P_c\right]^4 \tag{C.28}$$

which for our choice of parameter values gives

$$|\lambda_2| < 7.70 \times 10^{-9}. \tag{C.29}$$

Therefore the absolute value of the second eigenvalue is (significantly) less than 1, and so the stability of the system is determined by the first eigenvalue λ.

Conflicts of Interest

Ellen Webborn was formerly an employee at National Grid. National Grid contributed code and data (but no financial support) to this project. The authors declare that there are no conflicts of interest regarding the publication of this paper.

Acknowledgments

This work was supported by the EPSRC through Grant no. EP/I01358X/1. The authors are very grateful to National Grid for data, code, and many engaging discussions, in particular to Roy Cheung, Matthew Roberts, and William Ramsay. They are also very grateful to Michael Waterson and Lisa Flatley for their valued input and to numerous colleagues at the Centre for Complexity Science at the University of Warwick for all of their support.

References

[1] C.-Y. Chong, "Statistical synthesis of physically based load models with applications to cold load pickup," *IEEE Transactions on Power Apparatus and Systems*, vol. 103, no. 7, pp. 1621–1628, 1984.

[2] R. Malhamé and C.-Y. Chong, "Electric Load Model Synthesis by Diffusion Approximation of a High-Order Hybrid-State Stochastic System," *IEEE Transactions on Automatic Control*, vol. 30, no. 9, pp. 854–860, 1985.

[3] R. Malhamé and C.-Y. Chong, "On the statistical properties of a cyclic diffusion process arising in the modeling of thermostat-controlled electric power system loads," *SIAM Journal on Applied Mathematics*, vol. 48, no. 2, pp. 465–480, 1988.

[4] R. E. Mortensen, K. P. Haggerty, and K. P. Haggerty, "A stochastic computer model for heating and cooling loads," *IEEE Transactions on Power Systems*, vol. 3, no. 3, pp. 1213–1219, 1988.

[5] P. J. Douglass, R. Garcia-Valle, P. Nyeng, J. Ostergaard, and M. Togeby, "Smart demand for frequency regulation: Experimental results," *IEEE Transactions on Smart Grid*, vol. 4, no. 3, pp. 1713–1720, 2013.

[6] P. Cappers, C. Goldman, and D. Kathan, "Demand response in US electricity markets: empirical evidence," *Energy*, vol. 35, no. 4, pp. 1526–1535, 2010.

[7] J. W. Zarnikau, "Demand participation in the restructured Electric Reliability Council of Texas market," *Energy*, vol. 35, no. 4, pp. 1536–1543, 2010.

[8] D. J. Hammerstrom, J. Brous, D. P. Chassin et al., "Pacific Northwest GridWise? Testbed Demonstration Projects; Part II. Grid Friendly? Appliance Project," Tech. Rep. PNNL-17079, 2007.

[9] B. J. Kirby, *Spinning reserve from responsive loads*, United States Department of Energy, 2003.

[10] D. S. Callaway and I. A. Hiskens, "Achieving controllability of electric loads," *Proceedings of the IEEE*, vol. 99, no. 1, pp. 184–199, 2011.

[11] Z. Xu, J. Østergaard, and M. Togeby, "Demand as frequency controlled reserve," *IEEE Transactions on Power Systems*, vol. 26, no. 3, pp. 1062–1071, 2011.

[12] D. S. Callaway, "Can smaller loads be profitably engaged in power system services?" in *Proceedings of the 2011 IEEE PES General Meeting: The Electrification of Transportation and the Grid of the Future*, pp. 1–3, July 2011.

[13] D. Angeli and P.-A. Kountouriotis, "A stochastic approach to "dynamic-demand refrigerator control"," *IEEE Transactions on Control Systems Technology*, vol. 20, no. 3, pp. 581–592, 2012.

[14] M. Aunedi, P. Aristidis Kountouriotis, J. E. Ortega Calderon, D. Angeli, and G. Strbac, "Economic and environmental benefits of dynamic demand in providing frequency regulation," *IEEE Transactions on Smart Grid*, vol. 4, no. 4, pp. 2036–2048, 2013.

[15] F. Bagagiolo and D. Bauso, "Mean-field games and dynamic demand management in power grids," *Dynamic Games and Applications*, vol. 4, no. 2, pp. 155–176, 2014.

[16] T. Borsche, U. Markovic, and G. Andersson, "A new algorithm for primary frequency control with cooling appliances," *Computer Science - Research and Development*, vol. 31, no. 1-2, pp. 89–95, 2016.

[17] K. Fikiin, B. Stankov, J. Evans et al., "Refrigerated warehouses as intelligent hubs to integrate renewable energy in industrial food refrigeration and to enhance power grid sustainability," *Trends in Food Science & Technology*, vol. 60, pp. 96–103, 2017.

[18] D. S. Callaway, "Tapping the energy storage potential in electric loads to deliver load following and regulation, with application to wind energy," *Energy Conversion and Management*, vol. 50, no. 5, pp. 1389–1400, 2009.

[19] K. Dehghanpour and S. Afsharnia, "Electrical demand side contribution to frequency control in power systems: A review on technical aspects," *Renewable & Sustainable Energy Reviews*, vol. 41, pp. 1267–1276, 2015.

[20] S. Koch, J. L. Mathieu, and D. S. Callaway, "Modeling and control of aggregated heterogeneous thermostatically controlled loads for ancillary services," in *Proceedings of the 17th Power Systems Computation Conference, PSCC 2011*, pp. 1–7, August 2011.

[21] E. Kremers, J. M. G. de Durana, O. Barambones, and A. Lachaud, *Synchronisation phenomena in electrical systems: emergent oscillation in a refrigerator population*, Springer, Berlin, Germany, 2013.

[22] E. Kremers, J. M. A. González de Durana, and O. Barambones, "Emergent synchronisation properties of a refrigerator demand side management system," *Applied Energy*, vol. 101, pp. 709–717, 2013.

[23] N. Lu and D. P. Chassin, "A state queueing model of thermostatically controlled appliances," in *Proceedings of the IEEE PES Power Systems Conference and Exposition*, vol. 190, pp. 1666–1673, New York, NY, USA, 2004.

[24] N. Lu, D. P. Chassin, and S. E. Widergren, "Modeling uncertainties in aggregated thermostatically controlled loads using a state queueing model," *IEEE Transactions on Power Systems*, vol. 20, no. 2, pp. 725–733, 2005.

[25] M. R. Vedady Moghadam, R. T. Ma, and R. Zhang, "Distributed Frequency Control in Smart Grids via Randomized Demand

Response," *IEEE Transactions on Smart Grid*, vol. 5, no. 6, pp. 2798–2809, 2014.

[26] A. Molina-García, F. Bouffard, and D. S. Kirschen, "Decentralized demand-side contribution to primary frequency control," *IEEE Transactions on Power Systems*, vol. 26, no. 1, pp. 411–419, 2011.

[27] F. Oldewurtel, T. Borsche, M. Bucher et al., "A framework for and assessment of demand response and energy storage in power systems," in *Proceedings of the 2013 IREP Symposium on Bulk Power System Dynamics and Control - IX Optimization, Security and Control of the Emerging Power Grid, IREP 2013*, pp. 1–24, August 2013.

[28] S. K. Pandey, S. R. Mohanty, and N. Kishor, "A literature survey on load-frequency control for conventional and distribution generation power systems," *Renewable & Sustainable Energy Reviews*, vol. 25, pp. 318–334, 2013.

[29] C. Perfumo, E. Kofman, J. H. Braslavsky, and J. K. Ward, "Load management: Model-based control of aggregate power for populations of thermostatically controlled loads," *Energy Conversion and Management*, vol. 55, pp. 36–48, 2012.

[30] J. A. Short, D. G. Infield, and L. L. Freris, "Stabilization of grid frequency through dynamic demand control," *IEEE Transactions on Power Systems*, vol. 22, no. 3, pp. 1284–1293, 2007.

[31] N. A. Sinitsyn, S. Kundu, and S. Backhaus, "Safe protocols for generating power pulses with heterogeneous populations of thermostatically controlled loads," *Energy Conversion and Management*, vol. 67, pp. 297–308, 2013.

[32] M. Stadler, W. Krause, M. Sonnenschein, and U. Vogel, "Modelling and evaluation of control schemes for enhancing load shift of electricity demand for cooling devices," *Environmental Modeling and Software*, vol. 24, no. 2, pp. 285–295, 2009.

[33] V. Trovato, S. H. Tindemans, and G. Strbac, "Controlling the synchronization and payback associated with the provision of frequency services by dynamic demand," in *Proceedings of the 22nd International Conference and Exhibition on Electricity Distribution, CIRED 2013*, pp. 1–4, June 2013.

[34] S. H. Tindemans, V. Trovato, and G. Strbac, "Decentralized Control of Thermostatic Loads for Flexible Demand Response," *IEEE Transactions on Control Systems Technology*, pp. 1–16, 2015.

[35] C. H. Wai, M. Beaudin, H. Zareipour, A. Schellenberg, and N. Lu, "Cooling devices in demand response: A comparison of control methods," *IEEE Transactions on Smart Grid*, vol. 6, no. 1, pp. 249–260, 2015.

[36] W. Zhang, J. Lian, C.-Y. Chang, and K. Kalsi, "Aggregated modeling and control of air conditioning loads for demand response," *IEEE Transactions on Power Systems*, vol. 28, no. 4, pp. 4655–4664, 2013.

[37] Y. Lin, P. Barooah, and S. P. Meyn, "Low-frequency power-grid ancillary services from commercial building HVAC systems," in *Proceedings of the 2013 IEEE International Conference on Smart Grid Communications, SmartGridComm 2013*, pp. 169–174, October 2013.

[38] S. Lu, N. Samaan, R. Diao et al., "Centralized and decentralized control for demand response," in *Proceedings of the 2011 IEEE PES Innovative Smart Grid Technologies, ISGT 2011*, pp. 1–8, January 2011.

[39] S. Esmaeil Zadeh Soudjani and A. Abate, "Aggregation and Control of Populations of Thermostatically Controlled Loads by Formal Abstractions," *IEEE Transactions on Control Systems Technology*, vol. 23, no. 3, pp. 975–990, 2015.

[40] S. Esmaeil Zadeh Soudjani, S. Gerwinn, C. Ellen, M. Fränzle, and A. Abate, "Formal synthesis and validation of inhomogeneous thermostatically controlled loads," *Lecture Notes in Computer Science (including subseries Lecture Notes in Artificial Intelligence and Lecture Notes in Bioinformatics): Preface*, vol. 8657, pp. 57–73, 2014.

[41] S. Borenstein, J. Michael, and A. Rosenfeld, *Dynamic pricing, advanced metering, and demand response in electricity markets*, Center for the Study of Energy Markets, 2002.

[42] D. S. Kirschen, "Demand-side view of electricity markets," *IEEE Transactions on Power Systems*, vol. 18, no. 2, pp. 520–527, 2003.

[43] F. C. Schweppe, M. C. Caramanis, R. D. Tabors, and R. E. Bohn, *Spot pricing of electricity*, Springer Science & Business Media, 2013.

[44] B. Schäfer, M. Matthiae, M. Timme, and D. Witthaut, "Erratum: Decentral smart grid control," *New Journal of Physics*, vol. 17, no. 5, Article ID 059502, 2015.

[45] S. H. Strogatz, *SYNC: The Emerging Science of Spontaneous Order*, Hyperion Press, New York, NY, USA, 2003.

[46] Y. Kuramoto, *Chemical Oscillations, Waves and Turbulence*, Springer, Berlin, Germany, 1984.

[47] S. H. Strogatz, "From Kuramoto to Crawford: exploring the onset of synchronization in populations of coupled oscillators," *Physica D: Nonlinear Phenomena*, vol. 143, no. 1-4, pp. 1–20, 2000.

[48] M. Klein, G. J. Rogers, and P. Kundur, "A fundamental study of inter-area oscillations in power systems," *IEEE Transactions on Power Systems*, vol. 6, no. 3, pp. 914–921, 1991.

[49] Energy & Industrial Strategy Department for Business, *Energy consumption in the UK*, 2016.

[50] Office for National Statistics, *Overview of the UK population*, 2015.

[51] National Grid, System operability framework, 2016, http://www2.nationalgrid.com/UK/Industry-information/Future-of-Energy/System-Operability-Framework/.

[52] S. H. Strogatz and R. E. Mirollo, "Stability of incoherence in a population of coupled oscillators," *Journal of Statistical Physics*, vol. 63, no. 3-4, pp. 613–635, 1991.

[53] G. Batchelor, *An introduction to fluid mechanics*, Cambridge Press, Cambridge, UK, 1967.

[54] Inc. Wolfram Research. Mathematica version 11.0, 2017.

[55] J. R. Cogdell, *Foundations of Electrical Engineering*, Prentice-Hall, Inc., 1995.

[56] http://www2.nationalgrid.com/UK/Industry-information/Electricity-transmission-operational-data/Data-Explorer/.

[57] http://www2.nationalgrid.com/Enhanced-Frequency-Response.aspx.

Hindawi
Complexity
Volume 2017, Article ID 3597010, 14 pages
https://doi.org/10.1155/2017/3597010

Research Article

Sociotechnical Network Analysis for Power Grid Resilience in South Korea

Daniel A. Eisenberg,[1] Jeryang Park,[2] and Thomas P. Seager[1]

[1]*School of Sustainable Engineering and the Built Environment, Arizona State University, Tempe, AZ, USA*
[2]*School of Urban and Civil Engineering, Hongik University, Seoul, Republic of Korea*

Correspondence should be addressed to Daniel A. Eisenberg; daeisenb@asu.edu

Received 31 May 2017; Accepted 5 September 2017; Published 23 October 2017

Academic Editor: Paul Hines

International efforts to improve power grid resilience mostly focus on technological solutions to reduce the probability of losses by designing hardened, automated, redundant, and smart systems. However, how well a system recovers from failures depends on policies and protocols for human and organizational coordination that must be considered alongside technological analyses. In this work, we develop a sociotechnical network analysis that considers technological and human systems together to support improved blackout response. We construct corresponding infrastructure and social network models for the Korean power grid and analyze them with betweenness to identify critical infrastructures and emergency management organizations. Power grid network analysis reveals important power companies and emergency management headquarters for responding to infrastructure losses, where social network analysis reveals how information-sharing and decision-making authority shifts among these organizations. We find that separate analyses provide relevant yet incomplete recommendations for improving blackout management protocols. In contrast, combined results recommend explicit ways to improve response by connecting key owner, operator, and emergency management organizations with the Ministry of Trade, Industry, and Energy. Findings demonstrate that both technological and social analyses provide important information for power grid resilience, and their combination is necessary to avoid unintended consequences for future blackout events.

1. Introduction

The increasing frequency and costs of catastrophic events have prompted concerted international efforts to study and design more resilient power systems. In the United States, national policy is encouraging technical efforts to improve the resilience of infrastructure systems, including energy, water, cyber security, communications, transportation, emergency management, healthcare, financial, and government systems [1, 2]. Global organizations like the United Nations [3] and Rockefeller Foundation [4] promote similar goals across partner nations to establish resilient cities to future catastrophes. In all cases, the resilience of electric power systems receives particular interest, as electricity is essential to the provision of nearly all other infrastructure services. Power grid resilience research now produces a constant stream of novel analytical techniques to predict and reduce systemic losses associated with infrastructure failures, natural disasters, and terrorist attacks [5–7]. Despite these efforts, even the most modern power grids continue to experience large-scale blackouts. Countries like the US [8], India [9], Ukraine [10], and Australia [11] suffered major brownouts and blackouts between 2011 and 2016 from a broad range of events from extreme weather to cyberattack.

We argue that the lack of resilience in critical infrastructure is, in part, due to overemphasizing technological solutions that underestimate crisis decision-making and social context [12–15]. Currently, power system protection focuses on hardening existing system components and designing automated, redundant, smart, or otherwise technological solutions to reduce the probability of losses [13, 14]. However, reducing the *probability* of losses via technological solutions alone does not reduce their *consequences* (i.e., outcome of emergencies), which is dictated by human actions. For

example, the 2003 US Northeast blackout included a combination of infrastructure, control system, and decision-making failures that exacerbated unstable conditions and led to cascading damages [16]. Since 2003, postmortem analysis of several major blackout events continue to recommend improved communication within and across organizations to enhance crisis response [12, 17, 18]. Thus, research should expand awareness beyond technological limitations to include the diverse institutions that influence human decision-making and failure consequences, such as operations and management practices, economic constraints, organizational and industry cultures, and affected parties. We refer to the joint consideration of technological systems with these and other social institutions hereafter as "sociotechnical" analysis [19].

Network science enables one to model the components and interactions of human and infrastructure systems [21], suggesting the potential to develop a sociotechnical network analysis (STNA) for infrastructure resilience. Both electric power grids and human interactions are now studied as networks, yet isolated research does not treat engineering and social science perspectives as equals for sociotechnical guidance. The term "sociotechnical" is primarily used in network science to describe the study of human processes organized or mediated by technology, such as the formation of online social networks like Facebook and Twitter [22], traffic flows on transportation systems [23], or human interactions on communication networks [24–26]. Instead, we use the term STNA to describe the application of sociotechnical systems theory [19] to technological and human networks coupled by a single context. The tenets of sociotechnical systems theory can be translated into infrastructure network models by analyzing both social and technological networks together to avoid unpredictable and harmful recommendations from narrow perspectives on a single system [27] and by considering the tasks taken by social units and the expected function of technological systems alongside network structure [28]. A STNA of blackout management, thus, requires both infrastructure networks of substations, generators, transmission lines, and transformers as nodes and links [29] alongside social networks of human constructs like actors and their relational ties (e.g., who knows whom) [30], not one or the other. A STNA also requires knowledge of how power systems provide electric power services and the tasks people and organizations take to ensure services remain available. We argue that this form of STNA better supports the design of resilient power grids than those extant in the literature by integrating knowledge from engineering and social science without marginalizing either. To the best of the authors' knowledge, this form of STNA is also novel as no network studies in the literature give built and human systems equal consideration.

In this work, we develop the first STNA of a power grid to improve blackout response. We construct corresponding infrastructure and social networks and study them to identify critical components. We use results from power grid analysis in a new way by converting knowledge of critical infrastructure into demographic data of the organizations that manage their failures when lost. We further combine these results with a social network analysis of the formal institutions that dictate crisis coordination during large-scale blackouts [31–33]. The social network analysis reveals important organizations that fulfill coordination roles among them. Together, these analyses uncover which organizations are critical to power system protection from both engineering and administrative perspectives and can offer ways to improve blackout management policies that either analysis is incapable of offering its own.

Due to the significant amount of context-specific data required for STNA, this work centers on a single case study location: the South Korean power grid (KPG). In 2011, the worst brownout experienced in Korea caused roughly half of Seoul to lose power and was exacerbated by slowed decision-making processes across operator and regulatory agencies [34]. In 2013, corruption among regulatory officials led to nationwide power shortages after components in Korean nuclear power plants were found to have forged reliability documentation [35]. In 2014, the national tragedy of a ferry capsizing and killing 295 people (mostly children) [36] triggered the reorganization of the entire Korean emergency management industry to centralize crisis coordination efforts into a single agency [37]. In 2016, a city-wide blackout in Jeonggwan New City was exacerbated by a failure to deploy backup infrastructure stored on the other side of the country. Taken together, a case study of the KPG will have broad impacts on Korean society as the South Korean grid in need of social and technological guidance for blackout response.

2. Background on Korean Electric Power and Emergency Management Industries

The KPG is an islanded power system which has two primary parts, a large mainland grid serving the majority of Korea and a smaller, self-contained grid on the island state of Jeju-Do. In this work, we focus on the mainland KPG. The mainland grid has voltage classes from 765 kV to as low as 3.3 kV, yet ~55.1% of substation and 96% of power line infrastructure are 345 and 154 kV (Figure 1) [38]. The 345 and 154 kV transmission infrastructures are geographically clustered in population-dense regions such as the Seoul Metropolitan Area in the northwest. Korean power generation is dominated by coal, natural gas, and nuclear power technologies, and this power production is geographically centralized, where roughly 95% of installed capacity is located in 55 separate sites throughout the county [39].

KPG infrastructure is owned and operated by a few, key organizations (Table 1). Korean power transmission and distribution are managed by a single company, the Korea Power Exchange (KPX), and infrastructure ownership and maintenance are dominated by a separate company, the Korean Electric Power Corporation (KEPCO). During crises, KPX and KEPCO act as focal points for grid status, health, and management across the nation: KPX managing power flow and operations decisions and KEPCO managing power line and infrastructure recovery. KEPCO has 6 generation subsidiaries that independently operate and manage ~97% of Korean grid [40]. Liquid fuel, natural gas, and coal-fired power plants are owned and operated by 5 of the 6

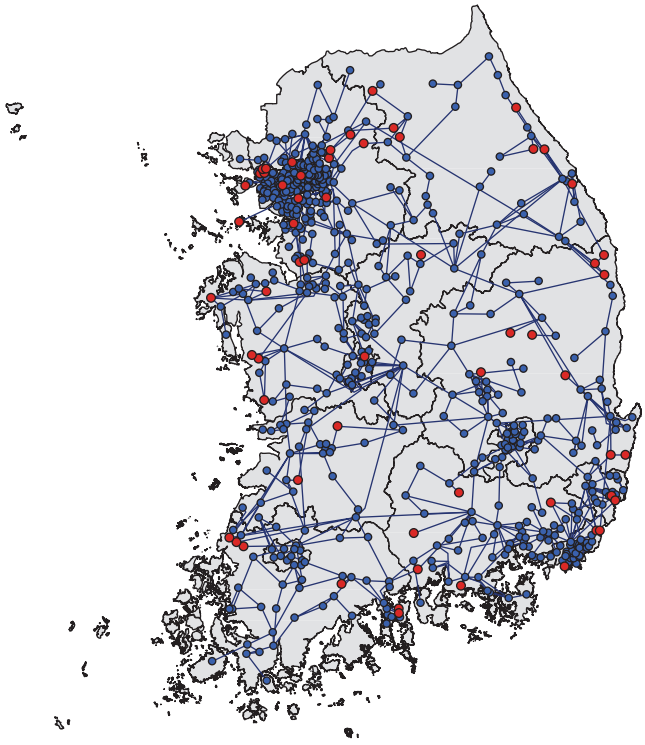

Figure 1: Map of the 2013 South Korean power grid. This map shows the connectivity of major power grid infrastructure in mainland Korea, that is, power plants (red circles), high-voltage transmission substations (dark blue circles), and power lines (dark blue lines). Transformers connect buses that are too close together to be shown in this image. For security purposes, data is simplified to only publicly available data from the Korean Power Exchange [20]. Jeju Island off the southern coast of Korea is also excluded from the image because it is not considered in the current analysis.

generation subsidiaries, each with roughly the same total generation capacity, 10–15 GW. The single largest generation subsidiary (~20 GW) is Korea's sole owner and operator of all nuclear power plants, Korea Hydro Nuclear Power (KHNP). Besides nuclear and fossil fuel generation, ~7% of electricity is generated from hydroelectric and renewable sources. KHNP and other KEPCO subsidiaries operate single purpose dams (power generation), whereas the Korean Water Administration (Kwater) manages all Korean multipurpose dams (power, water supply, and flood control).

Korean blackout response requires the coordination of electric power regulators (Table 1) and emergency managers for decision-making and crisis support (Table 2). KPX is the established hub for minor blackout incidents. Ministries and support organizations provide additional oversight in larger events depending upon the type of generation technologies involved (Table 1). For major fires, typhoons, earthquakes, and terrorist attacks, the power industry coordinates with first-responder and emergency management organizations (fire fighters, police, and crisis mangers) to mitigate and recover failed infrastructure. Federal regulatory and crisis coordination agencies also become involved in decision-making in worst case scenarios where national power availability is deemed vulnerable. The Ministry of Trade, Industry, and Energy (MOTIE) is the acting headquarters for man-made disasters including infrastructure failure due to human error or intentional attack and works with KPX and KEPCO to respond to national blackouts. MOTIE's disaster management division works with the National Emergency Management Agency (NEMA) and the Ministry of Security and Public Administration (MOSPA) to monitor and manage natural disasters. When MOTIE, NEMA, or MOSPA are involved in disaster management, MOTIE is the final decision-maker for built infrastructure and NEMA coordinates crisis support across a hierarchy of state and special city crisis headquarters to city, county, and district fire, police, and emergency management agencies.

Our description of the KPG and related crisis management organizations is based on 2013-2014 data collected from and verified by experts in formal interviews. We focus on this timeframe to ensure that power system analyses match with blackout management analyses. Since then, MOSPA and NEMA have become part of the same organization, the Ministry of Public Security and Safety (MPSS). Nonetheless, analysis of this blackout management system is a critical case relevant for many current policies and practices that remain intact, and all conclusions made in this work are applicable to the most recent organizational relationships.

3. Materials and Methods

3.1. Data for Network Analysis

3.1.1. Power Grid Networks. The KPG data was directly provided as a PSS/E (power system simulation for engineering) printout by KEPCO and was converted into a complex network using methods similar to those described in Kim et al. [38]. We assessed the extracted KPG model with MATLAB packages for optimal power flow [41] and complex network analysis [42, 43]. We use the Direct Current (DC) power flow approximation for all analyses [41]. Power flow analysis was calculated with the summer-time generation and demand dispatch for peak system load used by KEPCO for power system planning.

3.1.2. Korean Power Grid Emergency Response Networks. Primary data for the interorganizational blackout management social network was collected through semistructured interviews with Korean electric power industry experts. 14 expert interviews ranging from 30 minutes to 2 hours in length were held in South Korea over two 3-month periods in 2014 and 2015. A total of 12.7 hours of interviews were held. Experts interviewed include industry and academic experts from the following organizations: KEPCO, KPX, KHNP, NEMA, KMA, Kwater, Seoul National University, and Ulsan National Institute of Science and Technology. In these interviews, experts provided researchers with 208 pages of primary documents outlining various power system emergency protocols that were verified among interviewees. These primary documents were coded to determine the specific roles of different power system organizations identified in Tables 1 and 2. Additional interviews were then held to clarify

Table 1: Electric power industry organizations.

Operation & management		Regulation & decision-making
Power transmission:		*Industry-wide*:
Korea Electric Power Corp		Ministry of Trade, Industry, and Energy
Korean Power Exchange		Korea Electricity Commission
Thermoelectric power:	% *Gen capacity*	*Sector specific, nuclear*:
Korea Midland Power*	12.0%	Nuclear Safety and Security Commission
Korea Western Power*	10.6%	Korea Institute of Nuclear Safety
Korea East-West Power*	10.6%	*Sector specific, hydroelectric*:
Korea Southern Power*	9.6%	Ministry of Land, Infrastructure, and Transport
Korea Southeast Power*	9.6%	Kum River Flood Control Office
POSCO Power	3.1%	Youngsan River Flood Control Office
SK Energy	2.1%	Nakdong River Flood Control Office
K-Power Ltd.	1.2%	Han River Flood Control Office
Korea District Heating Corp	1.2%	
Meiya Power Company	1.2%	
GS EPS	1.1%	
Hyundai Corporation	1.1%	
Nuclear power:		
Korea Hydro Nuclear Power*	29.0%	
Hydroelectric power:		
Korea Water Administration	2.9%	
Korea Hydro Nuclear Power*	—	

*Subsidiary of Korean Electric Power Corporation. *Note*. Only companies with >1% of total generation capacity for Korea are listed.

Table 2: Disaster management industry organizations.

Local operations & management	Federal operations & management
Crisis operations, state:	*Crisis coordination*:
Gyeonggi Firefighting & Disaster HQ	Ministry of Trade, Industry, and Energy
Gangwon Fire HQ	Ministry of Security and Public Administration
Chungcheongbuk HQ of Fire Mgmt.	National Emergency Management Agency
Chungcheongnam Fire Safety Office	*Oversight*:
Jeollabuk Fire Dept. HQ	Prime Minister's Office
Jeollanam Fire Safety HQ	National Security Office
Gyeongsangbuk Fire Protection HQ	*Additional federal support*:
Gyeongsangnam Fire Service HQ	Ministry of Land, Infrastructure, and Transport
Jeju Fire & Disaster Mgmt. HQ*	Ministry of Strategy and Finance
Crisis operations, city:	Ministry of Employment and Labor
Seoul Fire & Disaster HQ	Ministry of Health and Wellness
Busan Fire Department	Ministry of Defense
Incheon Fire & Safety Mgmt. Dept.	National Police Agency
Daejeon Fire Fighting Head Office	Ministry of Culture, Sports, and Tourism
Gwangju Fire Safety HQ	Korean Communications Commission
Daegu Fire Fighting HQ	Korean Meteorological Agency
Ulsan Fire & Disaster HQ	

*Jeju Island is not included in the current analysis. *Note*. Table based on 2013 data.

roles and explicit information sharing and decision-making relationships among power grid and emergency management organizations.

Together, the interviews and coded documents resulted in social network models of the formal institutions for blackout management in South Korea, where nodes represent organizations in Tables 1 and 2 and links represent bidirectional information sharing and decision-making relationships. These networks are detailed representations of real policies and protocols to the best of the authors' knowledge

and incorporate additional expert input for their accuracy of relationships.

The shifting context of power grid operations and decision-making changes with power system health, defined by system reserve margin, and requires the creation and analysis of six blackout management social networks. Six reserve margin thresholds are defined in Korean policies, one for Normal Operations, one for minor events that do not reduce reserve margin past set thresholds, and four for increasing blackout risks as backup power becomes less available and the system becomes more unstable. We label these thresholds by associated titles denoted within the protocols themselves, with increasing risk of blackout from Prevention activities to Alarm Red.

(i) Normal Operations. State/city emergency management agencies coordinate infrastructure failure response directly with power infrastructure owners and operators. This network applies when infrastructure losses do not affect power grid reserve margin.

(ii) No Alarm: Prevention. KPX provides blackout coordination to protect the power grid and some coordination still exists between state/city emergency managers and infrastructure owner/operators.

(iii) Alarm Blue: Concern. KPX serves primary blackout coordination role between electric power and emergency management industries. Industry-specific regulators like the MOTIE provide industry oversight.

(iv) Alarm Yellow: Caution. Additional oversight ministries were involved in coordination efforts and first responder decision-making shifts from emergency management agencies to city/state governor offices.

(v) Alarm Orange: Alert. Crisis coordination and decision-making switch from electric power industry organizations to the MOSPA and the NEMA.

(vi) Alarm Red: Serious. All communication and decision-making between industries are mediated by Korean Federal Ministries with increasing ministerial participation (e.g., inclusion of military support).

3.2. Network Analysis Methods

3.2.1. Betweenness of Infrastructure and Social Networks. The resilience of a power grid must be understood with respect to the service it provides [27], the delivery of electricity from generation to distribution substations that then serve point of use. This generation-demand relationship corresponds to social network theory via "package" based flow processes [44]. Unlike other social processes such as gossip that transfers information among actors in an unregulated, probabilistic way, packages are assumed to have explicit destinations. Information sharing and decision-making among blackout crisis managers follow a similar package delivery relationship due to the regulated nature of the industry.

The "package delivery" structure and function of the KPG indicate that *betweenness*, which measures the flow contribution of network elements, can be used to identify critical components in both infrastructure and social networks. Betweenness in abstract graphs is based on the "geodesic path (or shortest path)" from nodes i to j. The set of all geodesic paths between any two nodes i and j is referred to as the "minimum cut set" of i and j. Following this definition, the "betweenness" of a node or link (B_v) is the total number of geodesic paths the network element v resides on (σ_{ij}^v) normalized by the total number of geodesic paths (σ_{ij}) in a network [21], following

$$B_v = \sum_{i \neq v \neq j \in N} \frac{\sigma_{ij}^v}{\sigma_{ij}}. \quad (1)$$

When used in power grid networks, betweenness identifies critical infrastructure whose loss may initiate cascading failures [45]. The same measure in crisis management networks identifies authoritative actors that broker emergency information and decision-making rights among disconnected groups [31, 33, 46]. Thus, betweenness analysis should identify infrastructures that have the greatest influence on power delivery and partnerships that dictate crisis coordination activities.

3.2.2. Additional Power Grid Betweenness Measures. B_v in (1) assumes that all links and nodes are equivalent (unweighted and homogeneous), which is not true for real power grids. Within the KPG, different characteristic infrastructures extract electricity from the network, constraining the total number of origin-destination flow paths within the resulting graph. Moreover, power system infrastructure (e.g., power lines) has electrical properties that impede and limit electricity from travelling along paths, further constraining potential flow. Thus, (1) may produce an unrealistic ranking of critical network elements by ignoring relevant power system characteristics.

In response to the perceived impracticality of (1) for power grids, researchers have developed betweenness measures that include relevant power system data for assessing flow contribution. At least two novel electrical betweenness metrics (EB_v^1 and EB_v^2) are proposed in the literature to build upon the formation and purpose of (1). The method developed by Nasiruzzaman et al. [47] combines network science and power system engineering by using geodesic paths weighted based on the amount of power flowing through them

$$EB_v^1 = \sum_{i \neq v \neq j \in N} \frac{P_{ij}^v}{P_{ij}}, \quad (2)$$

where P_{ij} is the maximum power flowing in the shortest path between nodes i and j and P_{ij}^v is the maximum of inflow and outflow of power at bus v on this shortest path. The feasibility of (2) for ranking nodes has been studied on numerous IEEE test power systems using both AC [48, 49] and DC [47, 50, 51] power flow models.

Another method developed by Arianos et al. [52–54] does not calculate shortest paths and instead uses simplified power grid vulnerability methods [55] and combines their output to recreate a measure comparable to betweenness. This method measures the sensitivity of nodes and links to the changes in generation and load throughout the system to assess their potential contribution to power flow. First, links are considered to be power lines and transformers ($|\mathbf{L}| = M_{\text{lines}}$) and nodes are power system buses organized into three sets: generation ($|\mathbf{G}| = N_{\text{Gen}}$), transmission ($|\mathbf{T}| = N_{\text{Trans}}$), and distribution ($|\mathbf{D}| = N_{\text{Dist}}$). Then, power transfer distribution factors [56], f_i^{gd}, are calculated for each power line, $l \in \mathbf{L}$, for a unit injection of electricity at a given generation bus, $g \in \mathbf{G}$, and a comparable increase in load at distribution bus, $d \in \mathbf{D}$. This value is used to determine how the structure of the KPG influences power transmission capacity across all g to d relationships. In addition, it is used to calculate a total transfer capability factor, C_g^d, to ensure all power lines remain within maximum power flow limits for each generation-demand relationship:

$$C_g^d = \min_{l \in \mathbf{L}} \left(\frac{P_1^{\max}}{f_1^{gd}} \cdots \frac{P_l^{\max}}{f_l^{gd}} \cdots \frac{P_M^{\max}}{f_M^{gd}} \right). \tag{3}$$

The bus betweenness of bus v combines these two elements, the sensitivity of power lines connected to it and total transfer capability of the grid, and is defined as

$$\text{EB}_v^2 = \frac{1}{2} \sum_{g \in \mathbf{G}} \sum_{d \in \mathbf{D}} C_g^d \sum_{l \in \mathbf{L}^v} \left| f_l^{gd} \right|, \quad g \neq v \neq d, \tag{4}$$

where $\mathbf{L}^v$ is the set of power lines connected to bus v and the factor of $1/2$ deals with double counting flow into and out of nodes. As $(1/2) C_g^d \sum_{l \in \mathbf{L}^v} |f_l^{gd}|$ can be interpreted as the security constrained contribution to power flow of node v for a single generation-load pair, (4) calculates the total power flowing through v relative to all generation, distribution pairs within the system. Thus, (4) directly measures the contribution of node v to flow without determining geodesic paths or minimum cut sets, which is computationally difficult for large networks. The feasibility of (4) for ranking nodes has been studied on numerous IEEE test power systems and the Italian high voltage transmission grid [52–54, 57, 58].

3.2.3. Converting Infrastructure Network Results into Demographic Results. We use all three betweenness measures to find critical power grid infrastructure in the KPG because there is no established "best" option among power grid betweenness measures. Then we aggregate results into demographic data useful to blackout management organizations. We treat each betweenness score as the relative importance of each power grid bus within the KPG characterizing its criticality. Then, we sum normalized scores based on demographic information of where each node is located in South Korea (longitude/latitude location) and ownership information. These two pieces of information aggregate individual node betweenness values into the infrastructure companies that own and operate them (Table 1) and the state or special city emergency management agency (Table 2).

3.2.4. Additional Social Network Measures. We use general social network analysis measures outlined below to characterize the six blackout management networks and (1) to identify the critical organizations that broker information for blackout coordination. Social network visualization and analysis were completed using ORA-LITE social network analysis software [59] developed by the Carnegie Mellon Center for Computational Analysis of Social and Organizational Systems.

To compare and contrast blackout management contexts, additional measures are used to characterize network-level properties of all six social networks, including the following [60]:

(i) Network Size. It is the number of organizations (nodes) in each network and the number of interactions (links) among organizations.

(ii) Network Density. Density is calculated as ratio of network interactions to the total number of possible interactions. Density is a normalized measure ranging from 0 to 1, where 0 indicates an unconnected network and 1 indicates a completely connected network.

(iii) Network Centralization (Degree and Betweenness). Network centralization measures the relative importance of highest ranking node for a single network measure to rest of the network. This is expressed as a ratio of the sum of the differences between the highest ranking node and the rest of the nodes in the network to the maximum possible sum of the differences. Freeman [61] defines standard ways to calculate degree and betweenness centralization with the following equations:

$$\begin{aligned} &\text{Network Centralization, Degree} \\ &= \frac{\sum_{i=1}^{n} \text{Deg}_{\max} - \text{Deg}_i}{(n-1)(n-2)}, \\ &\text{Network Centralization, Betweenness} \\ &= \frac{\sum_{i=1}^{n} \text{Bet}_{\max} - \text{Bet}_i}{(n-1)(n-2)(n-3)}, \end{aligned} \tag{5}$$

where Deg_i is the number of links connected to node i (referred to as the degree of i) and $\text{Deg}_{\max}$ is the degree of the node with the most links. Likewise, Bet_i is the betweenness of node i, and $\text{Bet}_{\max}$ is the highest betweenness in the network. All centralization values are between 0 and 1, where 0 indicates no centralization (all nodes equal) and 1 indicates complete centralization (one node dominates the measure).

4. Results

4.1. Aggregated Power Grid Criticality Results. Linking the Korean blackout management industry organizations and infrastructure criticality analysis results implicates the involvement of different power system and emergency management organizations in protecting infrastructure for future blackout events. Figure 2 presents the aggregated and

Power industry organizations	Generation and transmission				Generation only		
	B_v	EB_v^1	EB_v^2	% of installed gen capacity	B_v	EB_v^1	EB_v^2
KEPCO	100.0%	99.9%	49.9%	—	—	—	—
KHNP	0.0%	0.0%	12.7%	29.0%	0.0%	5.6%	25.3%
KOSEPO	0.0%	0.0%	5.4%	9.6%	0.0%	0.0%	10.8%
KOSPO	0.0%	0.0%	5.1%	9.6%	0.0%	16.9%	10.1%
EWP	0.0%	0.0%	7.0%	10.7%	0.0%	8.5%	13.9%
KOWEPO	0.0%	0.0%	4.5%	10.3%	0.0%	22.6%	8.9%
KOMIPO	0.0%	0.1%	6.3%	12.0%	100.0%	46.4%	12.5%
Kwater	0.0%	0.0%	0.4%	2.9%	0.0%	0.0%	0.7%
Posco Power	0.0%	0.0%	1.7%	3.1%	0.0%	0.0%	3.3%
GS Power Co	0.0%	0.0%	0.3%	0.9%	0.0%	0.0%	0.7%
K-Power Ltd.	0.0%	0.0%	0.5%	1.2%	0.0%	0.0%	0.9%
Korea District Heating	0.0%	0.0%	0.2%	1.2%	0.0%	0.0%	0.5%
Posco E&C LTD	0.0%	0.0%	1.0%	0.8%	0.0%	0.0%	2.0%
GS EPS	0.0%	0.0%	0.6%	1.1%	0.0%	0.0%	1.2%
Meiya Power Co	0.0%	0.0%	0.5%	1.2%	0.0%	0.0%	1.0%
STX Energy	0.0%	0.0%	0.0%	0.1%	0.0%	0.0%	0.0%
Korea Energy Mgmt. Corp	0.0%	0.0%	0.0%	0.0%	0.0%	0.0%	0.0%
Daelim Mitsubishi	0.0%	0.0%	1.5%	1.2%	0.0%	0.0%	3.0%
S-Power	0.0%	0.0%	0.1%	0.7%	0.0%	0.0%	0.2%
SK Energy	0.0%	0.0%	2.4%	2.2%	0.0%	0.0%	4.7%
Hyundai Corp	0.0%	0.0%	0.0%	1.1%	0.0%	0.0%	0.0%

Figure 2: Criticality of KPG buses aggregated by power industry organizations.

normalized criticality scores for the infrastructures owned by power system organizations. All measures implicate KEPCO as owning and operating the majority of critical KPG infrastructure. In particular, B_v and EB_v^1 only identify power generation companies owning and operating fractions of a percent of the critical infrastructure. In contrast, EB_v^2 identifies a much larger participation of power companies in owning and operating critical infrastructure, suggesting that KEPCO and KPX only operate ~50% of the critical infrastructure within the KPG.

The differences between power organizations become more apparent when excluding transmission infrastructure and only comparing the critical generation buses. Even though few power plants are identified as critical, it is important to pinpoint these infrastructures to identify the importance of generation assets to the KPG. We present the relative importance of just these infrastructures to determine which organizations may operate these few central plants. Here, B_v identifies only a single generation company, Korea Midland Power, as owning and operating critical infrastructure. EB_v^1 and EB_v^2 each identify multiple generation companies, but with varying importance of generation technologies. EB_v^1 implicates thermoelectric power companies as more important than nuclear, and, in contrast, EB_v^2 implicates the exact opposite. Moreover, EB_v^2 produces results quantitatively similar to the percent total installed generation capacity and is the only measure to suggest power producers not affiliated with KEPCO to own and operate critical buses.

We combine infrastructure scores for geographic regions to predict which emergency management headquarters may be involved in crisis response. Figure 3 presents the aggregated infrastructure results including a frequency plot of power generation and transmission infrastructure in South Korea compared and normalized criticality scores for infrastructure in each state and city region. Although more power system infrastructure is located in the northwest region surrounding the Seoul Metropolitan Area and the Southern coast (Figure 3(a)), the measures indicate that critical infrastructure may be located elsewhere. Method B_v suggests that the vast majority of critical infrastructure is located in the state Gyeonggi-do (GGD) surrounding Seoul and to a lesser extent the three states making up the center of the country: Chungcheongnam-do (CCND), Chungcheongbuk-do (CCBD), and Gyeongsangbuk-do (GSBD), from east to west, respectively (Figure 3(b)). Method EB_v^1 produces results similar to the physical location of infrastructure with greater emphasis on the central and northwest regions of the country instead of Seoul and Incheon cities (Figure 3(c)). Method EB_v^2

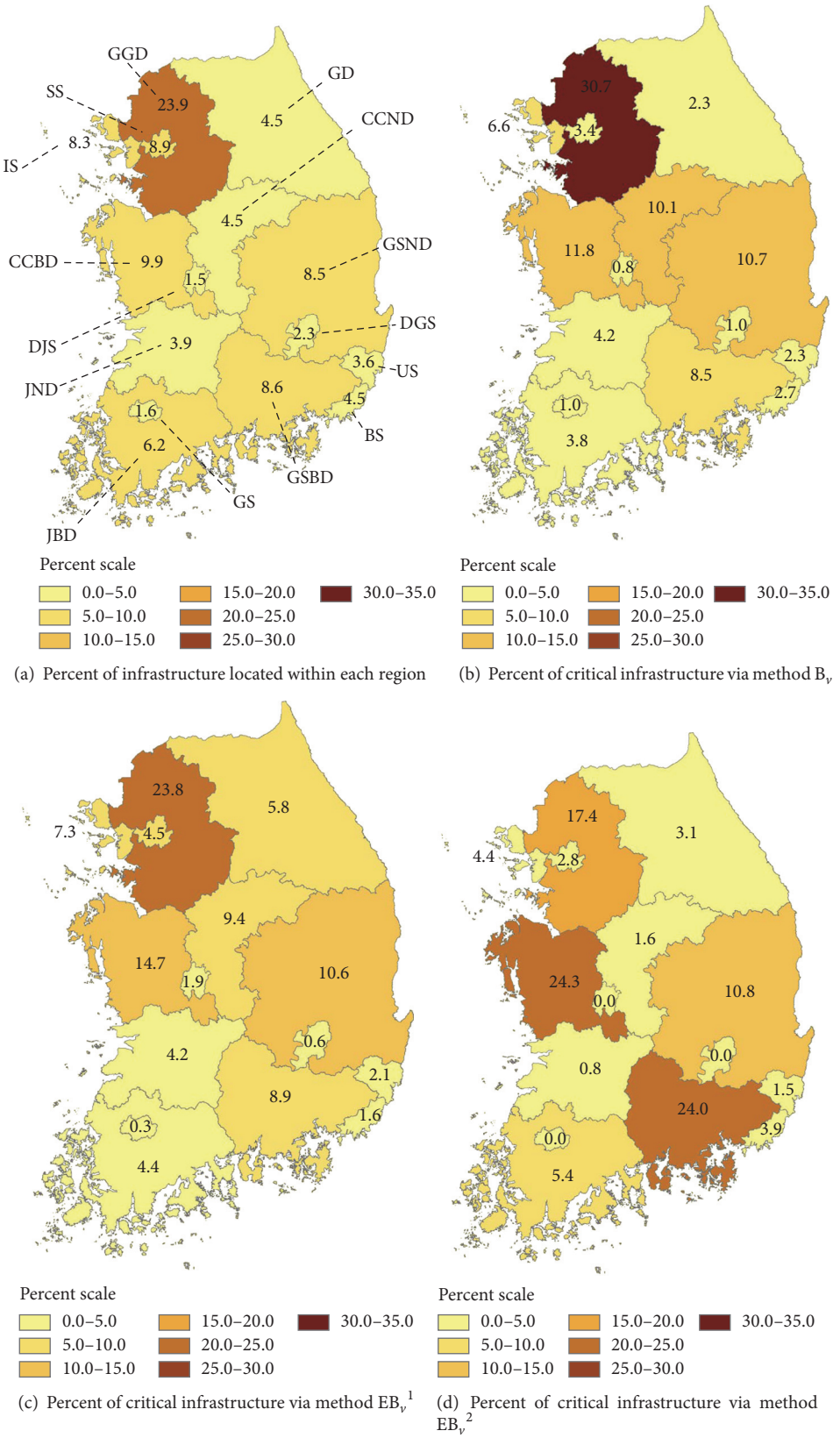

FIGURE 3: Aggregate criticality scores for Korean power grid infrastructure by emergency management region. The top left image of Korea presents the amount of generation and substation buses located in each region (a), where all other images show the normalized total criticality score for each region (b, c, and d). Thus, percent scale refers to quantity of infrastructure (a) and aggregated criticality score (b, c, and d). Regions are labelled in (a) with abbreviations: Gyeonggi-do (GGD), Gangwon-do (GD), Chungcheongnam-do (CCND), Chungcheongbuk-do (CCBD), Gyeongsangnam-do (GSND), Gyeongsangbuk-do (GSBD), Jeollanam-do (JND), Jeollabuk-do (JBD), Seoul-si (SS), Incheon-si (IS), Daejeon-si (DJS), Gwangju-si (GS), Daegu-si (DGS), Ulsan-si (US), and Busan-si (BS).

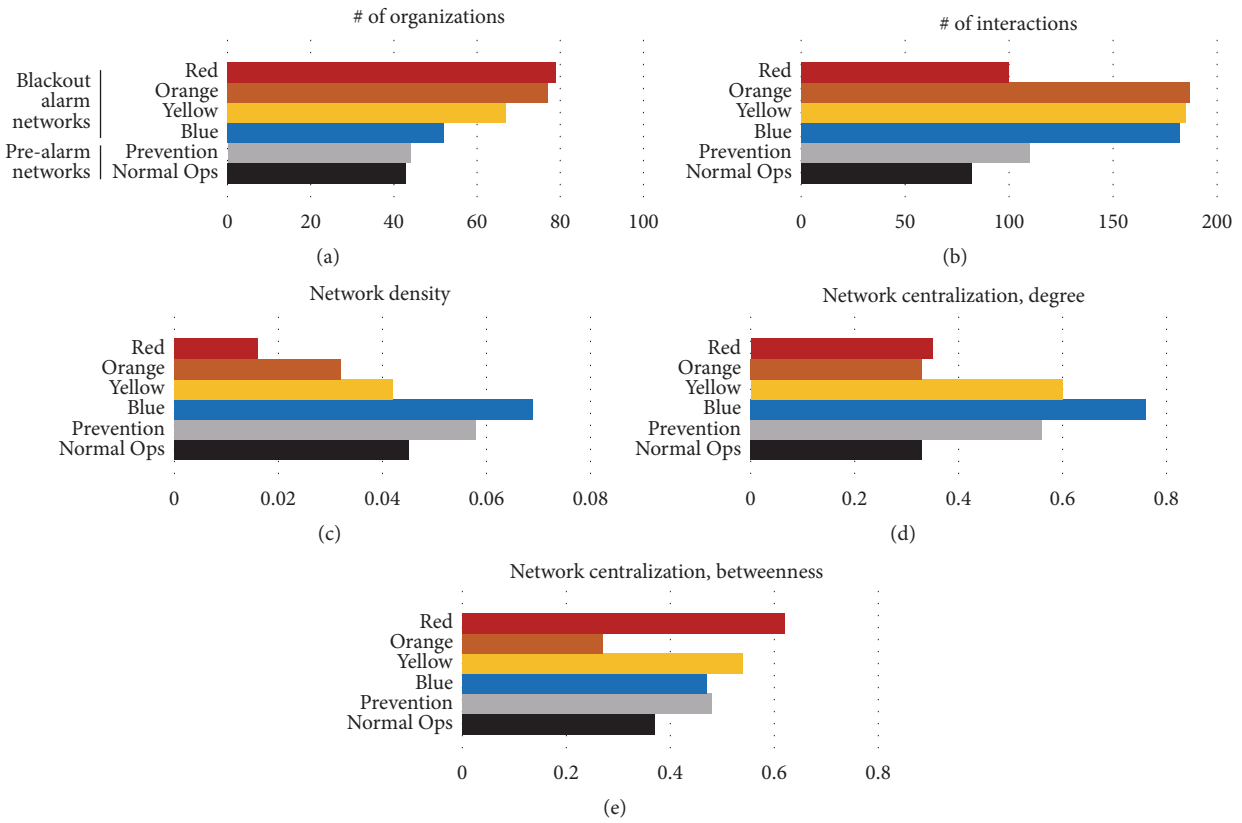

Figure 4: Network-level results for Korean blackout management social networks. We characterize the 6 blackout management social networks (y-axes) with five characteristic network-level measures (x-axes). (a-b) Social network size is measured by the total number of organizations and interactions (i.e., links). (c) Network density, (d) centralization of degree, and (e) centralization of betweenness are normalized values ranging from 0 to 1 (see Methods).

suggests that Gyeonggi-do (GGD) is not the most important region, but rather Chungcheongnam-do (CCND) and Gyeongsangnam-do (GSND), together, contain nearly 50% of all critical infrastructure (Figure 3(d)). Across all methods, the top ranked infrastructures are more often located in three states of Chungcheongnam-do (CCND), Gyeongsangnam-do (GSND), and Jeollabuk-do (JBD).

4.2. Blackout Management Social Network Results. Figure 4 presents general results of network analysis for the six blackout management social networks. Results show that formal policies produce social networks that have increasing organizational inclusion with blackout risk. Formal institutions assume that less risky scenarios require less regulated interactions among electric power and emergency management sectors, and vulnerable situations with lower reserve margins and greater grid instability require more oversight and federal involvement. This is represented in the network size (Figure 4(a)) as the number of organizations connected to the network almost doubles from 43 organizations in Normal Operations to 79 in Alarm Red. The majority of these new nodes represent either emergency managers or federal ministries not involved in minor blackouts, such as governor-level crisis management HQs and the Ministry of Defense.

The decision-making authority of the electric power industry peaks when the first blackout alarm is activated (Alarm Blue) and then shifts to the emergency management industry, as represented by the number of links (Figure 4(b)), network density (Figure 4(c)), and centralization of node degree (Figure 4(d)). All three measures show peaking trends as blackout alarms increase in severity. Even though the number of nodes among networks steadily increase with crisis risk level, the number of links peaks around ~180 links and then decreases to 100 at Alarm Red. This sudden drop in links corresponds with the transition of decision-making and information-sharing authority from the electric power to the emergency management industry. Moreover, the network density and centralization of degree peak at Alarm Blue and decrease across all four alarms, corresponding with the initial centralization of authority among the electric power industry and its diffusion into emergency management organizations as they join to the network.

Figure 4(e) also demonstrates variability in the centralization of blackout coordination activities among sectors with the centralization of betweenness. The centralization of betweenness increases across the first four networks, drops to its minimum at Alarm Orange, and is at its maximum in Alarm Red. The low centralization of betweenness of Alarm

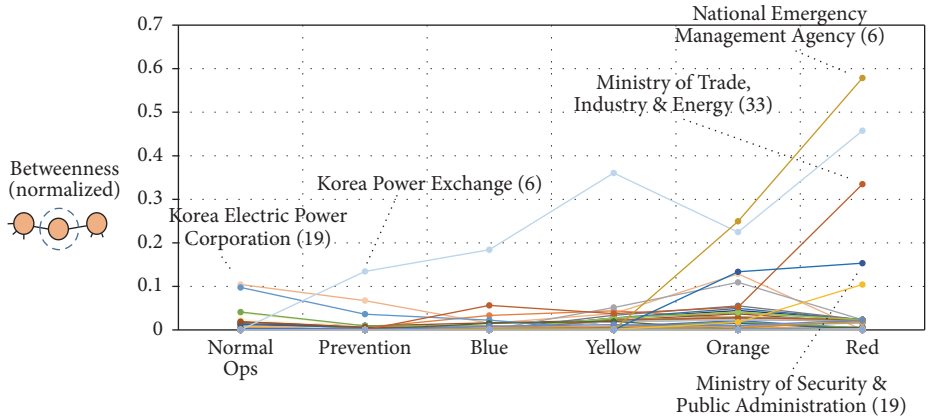

Figure 5: Betweenness and number of roles for Korean blackout management organizations. Each line represents a different organization. As the majority of organizations are periphery actors, they have low betweenness compared to few central, coordinating organizations. These central and important organizations are labelled: name (number of crisis management roles). Results demonstrate that few organizations from both electric power and emergency management sectors are the key crisis coordinator for different blackout risks, specifically KEPCO, KPX, and NEMA. In contrast, MOTIE and MOSPA are key decision-making organizations, yet they remain periphery to information brokerage.

Orange when compared to Alarm Yellow or Red corresponds to the electric power and emergency management industries sharing information brokerage activities almost equally for that interorganizational configuration. All other instances with high centralization of betweenness will have a single organization as the most central crisis coordinator.

Nodal betweenness identifies that organizations with fewer decision-making roles than others tend to broker information during blackouts. Betweenness results presented in Figure 5 identify the specific organizations that act as information hubs for blackout response. KEPCO and Gyeonggi-do Fire Mgmt. HQ share central crisis coordination roles for Normal Operations, KPX is the most central organization for Prevention, Alarm Blue, and Alarm Yellow, NEMA and KPX share coordination for Alarm Orange, and NEMA is the central coordinator for Alarm Red. These results correspond to general perspectives held by blackout management experts that either KPX or NEMA is the crisis management HQ for blackouts. Still, KPX and NEMA have fewer decision-making roles as outlined in formal protocols and may not be best suited for being the central information broker. The number of roles assigned to each organization (labelled next to its name) reveals that MOTIE (33), KEPCO (19), and MOSPA (19) have far more blackout management roles to fulfil than KPX (6) and NEMA (6). This result indicates that decisions made by authoritative organizations must travel through intermediary organizations before reaching their final destination.

5. Discussion

5.1. Implications for Blackout Management Protocols from the Infrastructure Perspective. Results suggest that certain generation companies may be more involved in future blackout scenarios. Current blackout management policies make limited differentiation between organizational roles between generation companies, which may be inappropriate when each company owns and operates different amounts of critical infrastructure. For example, both B_v and EB_v^1 would recommend that increased protection and recovery capacity be located at generation facilities owned and operated by Korea Midland Power, where EB_v^2 results emphasize nuclear power plants managed by KHNP and relatively equivalent treatment of other KEPCO subsidiaries. Moreover, EB_v^2 highlights differences among private power producers that manage an appreciable amount of critical infrastructure like SK Energy, Posco Power, and Daelim Mitsubishi that are not reflected in crisis management protocols. Based on these results, we recommend that crisis management policies make more explicit roles for the KEPCO subsidiaries and private power companies that operate these critical infrastructures to emphasize their potential involvement in blackout response.

Specific state and city headquarters have a greater chance of being the crisis management authority in large-scale blackout support activities than others. Combining results across measures, Chungcheongnam-do (CCND), Gyeongsangnam-do (GSND), and Jeollabuk-do (JBD) house more critical power grid infrastructure than other regions. Moreover, aggregate scores for regions consistently score states higher than cities, with Gyeonggi-do (GGD), Chungcheongnam-do (CCND), Gyeongsangbuk-do (GSBD), and Gyeongsangnam-do (GSND) receiving top ranks across multiple methods. Whereas existing national blackout management policies treat emergency management HQs equivalently, more focused policies may highlight power system protection and response in these regions. For example, the most recent blackout in Korea which occurred in the Southeastern region of Gyeongsangnam-do (GSND) was exacerbated as backup infrastructure was only housed in Seoul. Reorienting crisis response resources to match these results would have led to a shorter blackout duration by maintaining backup transformers near more critical substations.

5.2. Implications of Blackout Management Protocols from the Social Network Perspective. This analysis is the first to

take a system-wide perspective on blackout management and identify when decision-making and information-sharing authority shifts between industries. Policies and protocols outline explicit decision-making and information-sharing roles, and experts are aware of the interactions among multiple sectors. However, explicit transitions in authority are not outlined in formal institutions making it difficult for actors to predict which electric power or emergency management organization will be the central coordinating body when alarms are activated. Network-level analysis demonstrates a transition in authority between the electric power and emergency management industries associated with a drop in number of links, network density, average degree, and centralization of degree and an increase in centralization of betweenness. Decision-making is most centralized in the power industry for Alarm Blue and makes a transition to the emergency management industry between Alarms Orange and Red. Experts can use this information to determine if current reserve margin and power system stability measures are effective for creating the wanted decision-making context to handle blackout risk.

Betweenness results indicate that there may be a mismatch between blackout decision-making authority and information brokerage in South Korea, suggesting a need to restructure current policies. Although KPX and NEMA are identified as central hubs for power grid and emergency management information, they are not the central decision-makers. Having central actors involved in information-sharing is vital for successful blackout response, as effective coordination avoids the duplication of work, hindrance of first responders, delays due to misunderstanding, and inappropriate allocation of resources [62]. Crises including the 2011 Seoul Brownout, 2013 Corruption Scandal, 2014 Ferry Tragedy, and 2016 Blackout were exacerbated by hindrances like the infeasibility to centrally manage, role ambiguity, and unbalanced workload distribution. Restructuring blackout response policies to centralize actors with greater decision-making authority may alleviate this issue. MOTIE, in particular, is identified through interviews as an important organization for decision-making and oversight, yet a periphery node remains within all networks for information brokerage. Making MOTIE a central node is a possible way to improve coordination activities. We recommend doing this for intermediary networks that transition authority between sectors like Alarm Yellow and Orange as MOTIE has equal authority to other federal organizations where KPX does not. Thus, we recommend restructuring future policies to centralize MOTIE for Alarms Yellow and Orange to support decision-making and shifting authority among industries.

5.3. Combined Guidance. Completing infrastructure and interorganizational network analyses side-by-side offers combined recommendations to improve blackout management in South Korea. The results from both network analyses are complementary as infrastructure analysis identifies which periphery organizations own, operate, and respond to critical infrastructure failures and social network analysis identifies which organizations coordinate decision-making and information-sharing among them. Betweenness results for the social network further indicate that there is a mismatch between organizational authority and information brokerage that may require updating protocols to restructure the network. While the above recommendations for improving formal policies may be helpful, they remain superficial by not specifying how improvements are to be made. For example, social network analysis can offer the recommendation to restructure the social network to centralize MOTIE for Alarms Yellow and Orange but cannot specify which paths or organizations should be involved in restructuring. Instead, the results from infrastructure network analysis identify critical organizations that should be involved in these heightened blackout risk scenarios. Our combined recommendation is then to restructure formal institutions to increase information flow among the power companies, Korea Midland Power, SK Energy, Posco Power, and Daelim Mitsubishi, the emergency management agencies in Chungcheongnam-do, Gyeongsangnam-do, and Jeollabuk-do, and MOTIE.

6. Conclusion

Blackouts continue to occur across the globe due to failed blackout coordination activities, and power grid resilience depends upon effective formal policies and protocols to handle emergency response. We identify critical cases in which blackout coordination does not match infrastructure failure needs in South Korea by conducting STNA with matching data from 2013 for KPG infrastructure and blackout management policies. In the KPG, separate analysis of infrastructure and interorganizational networks provides insight into the cause of recent, exacerbated events. Power grid criticality analysis shows that some infrastructures and organizations may be disproportionately involved in large-scale events, yet formal policies do not distinguish between them. Social network analysis characterizes the transition of authority among sectors and organizations to help guide more precise use of policies to manage future events. Still, each analysis on its own can only provide broad recommendations for improving institutions rather than specific changes to policy. Combined results instead pinpoint the specific social networks and organizations that needed to be changed when updating future policies.

This work demonstrates that the growing number of studies comparing criticality measures for other real-world power systems [57, 63–65] or developing social networks around infrastructure systems [23] would benefit from linking technological analyses to social context. Since the majority of academic literature does not bridge infrastructure and social contexts, power grid protection and resilience may be undermined by overlooking the social consequences of technical recommendations. The inclusion of ownership and jurisdictional boundaries in this work revealed Korean organizations whose actions may have greater influence on power grid protection than others. In interconnected grids, a similar analysis may highlight local decision-makers that have disproportionate authority over power system security that crosses utility, state, and country borders. The same is true for social network analysis of actors that manage infrastructure systems. Taking a public administration

perspective while ignoring the interconnected and complex infrastructure system it surrounds may overlook salient interactions that connect social entities but exist in the technology. Crisis management protocols made without reference to the physical limitations of existing infrastructure creates latent weaknesses embedded in policy which may exacerbate damages in future emergencies. The sociotechnical network analysis presented herein offers one way to overcome these issues.

Disclosure

Any opinions, findings, conclusions, or recommendations expressed in this material are those of the authors and do not necessarily reflect the views of the NSF or NRF.

Conflicts of Interest

The authors declare that they have no conflicts of interest.

Acknowledgments

The authors would like to acknowledge Donghwan Kim for assistance with analysis, Younghan Chun for helping acquire South Korean power system data, and Taehun Lee for assisting with translation of technical documents. This material is based upon work supported by the National Science Foundation (NSF) (Grants nos. 1311230, 1441352, and 1415060). Jeryang Park was supported by Basic Science Research Program through the National Research Foundation of Korea (NRF) funded by the Ministry of Science, ICT & Future Planning (NRF-2016R1C1B1011770).

References

[1] R. L. Wilby and R. Keenan, "Adapting to flood risk under climate change," *Progress in Physical Geography*, vol. 36, no. 3, pp. 348–378, 2012.

[2] Department of Homeland Security (DHS), *National Infrastructure Protection Plan (NIPP): Partnering for critical infrastructure security and resilience*, 2013.

[3] United Nations International Strategy for Disaster Reduction, *Hyogo Framework For Action 2005-2015: Building the resilience of nations and communities to disasters*, 2007.

[4] The Rockefeller Foundation and ARUP, *City Resilience Index*, 2015, The Rockefeller Foundation and ARUP, "City Resilience Index," p. 16, 2015.

[5] *Committee on Determinants of Market Adoption of Advanced Energy Efficiency and Clean Energy Technologies, The Power of Change: Innovation for Development and Deployment of Increasingly Clean Electric Power Technologies*, The National Academies Press, 2016.

[6] *Committee on Analytical Research Foundations for the Next-Generation Electric Grid, Analytic Research Foundations for the Next-Generation Electric Grid*, The National Academies Press, 2016.

[7] *Quadrennial Energy Review Task Force, The Department of Energy (DOE), Quadrennial Review: Transforming the Nation's Electricity System: The Second Installment of the Quadrennial Energy Review*, 2017.

[8] North American Electric Reliability Corporation, *September 2011 Southwest Blackout Event*, 2011.

[9] O. P. Veloza and F. Santamaria, "Analysis of major blackouts from 2003 to 2015: Classification of incidents and review of main causes," *The Electricity Journal*, vol. 29, no. 7, pp. 42–49, 2016.

[10] C.-C. Sun, C.-C. Liu, and J. Xie, "Cyber-physical system security of a power grid: State-of-the-art," *Electronics (Switzerland)*, vol. 5, no. 3, article no. 40, 2016.

[11] Australian Energy Market Operator (AEMO), *Preliminary Report 3rd Oct – Black System Event in South Australia on 28 September 2016*, Report no. September, 2016.

[12] M. M. Adibi and L. H. Fink, "Restoration from cascading failures," *IEEE Power & Energy Magazine*, vol. 4, no. 5, pp. 68–77, 2006.

[13] M. Panteli and P. Mancarella, "The grid: Stronger, bigger, smarter?: Presenting a conceptual framework of power system resilience," *IEEE Power & Energy Magazine*, vol. 13, no. 3, pp. 58–66, 2015.

[14] M. Panteli and P. Mancarella, "Influence of extreme weather and climate change on the resilience of power systems: Impacts and possible mitigation strategies," *Electric Power Systems Research*, vol. 127, pp. 259–270, 2015.

[15] M. Panteli and P. Mancarella, "Modeling and evaluating the resilience of critical electrical power infrastructure to extreme weather events," *IEEE Systems Journal*, vol. PP, no. 99, 2015.

[16] P. Pourbeik, P. S. Kundur, and C. W. Taylor, "The anatomy of a power grid blackout," *IEEE Power & Energy Magazine*, vol. 4, no. 5, pp. 22–29, 2006.

[17] G. Andersson, P. Donalek, R. Farmer et al., "Causes of the 2003 major grid blackouts in North America and Europe, and recommended means to improve system dynamic performance," *IEEE Transactions on Power Systems*, vol. 20, no. 4, pp. 1922–1928, 2005.

[18] D. Kirschen and F. Bouffard, "Keep the Lights On and the Information Flowing," *IEEE Power & Energy Magazine*, vol. 7, no. 1, pp. 50–60, 2009.

[19] G. Walker, "Come back sociotechnical systems theory, all is forgiven . . .," *Civil Engineering and Environmental Systems*, vol. 32, pp. 170–179, 2015.

[20] Korea Power Exchange (KPX), *Korea Power Exchange Transmission Map*, 2016, https://www.kpx.or.kr/eng/contents.do?key=333.

[21] M. E. J. Newman, *Networks: An Introduction*, Oxford University Press, Oxford, UK, 2010.

[22] F. Hu, A. Mostashari, and J. Xie, Eds., Socio-Technical Networks: Science and Engineering Design, CRC Press, 2011.

[23] A. Vespignani, "Modelling dynamical process in complex sociotechnical systems," *Nature Physics*, vol. 8, no. 1, pp. 32–39, 2012.

[24] P. M. Salmon, N. A. Stanton, G. H. Walker, D. Jenkins, C. Baber, and R. McMaster, "Representing situation awareness in collaborative systems: A case study in the energy distribution domain," *Ergonomics*, vol. 51, no. 3, pp. 367–384, 2008.

[25] N. A. Stanton, "Representing distributed cognition in complex systems: How a submarine returns to periscope depth," *Ergonomics*, vol. 57, no. 3, pp. 403–418, 2014.

[26] N. A. Stanton and C. Harvey, "Beyond human error taxonomies in assessment of risk in sociotechnical systems: a new paradigm with the EAST 'broken-links' approach," *Ergonomics*, vol. 60, no. 2, pp. 221–233, 2017.

[27] D. A. Eisenberg, J. Park, D. Kim, and T. P. Seager, "Resilience analysis of critical infrastructure systems requires integration of multiple analytical techniques," *Urban Sustainability and Resilience*, 2014.

[28] S. Amir and V. Kant, "Sociotechnical Resilience: A Preliminary Concept," *Risk Analysis*, 2017.

[29] P. H. J. Nardelli, N. Rubido, C. Wang et al., "Models for the modern power grid," *The European Physical Journal Special Topics*, vol. 223, no. 12, pp. 2423–2437, 2014.

[30] K. M. Carley, "Computational organizational science and organizational engineering," *Simulation Modelling Practice and Theory*, vol. 10, no. 5-7, pp. 253–269, 2002.

[31] K. Jung and M. Song, "Linking emergency management networks to disaster resilience: Bonding and bridging strategy in hierarchical or horizontal collaboration networks," *Quality & Quantity*, vol. 49, no. 4, pp. 1465–1483, 2015.

[32] N. Kapucu and V. Garayev, "Designing, Managing, and Sustaining Functionally Collaborative Emergency Management Networks," *The American Review of Public Administration*, vol. 43, no. 3, pp. 312–330, 2013.

[33] N. Kapucu and V. Garayev, "Structure and Network Performance: Horizontal and Vertical Networks in Emergency Management," *Administration and Society*, vol. 48, no. 8, pp. 931–961, 2016.

[34] T. Kim, *Blackouts Hit Korea Nationwide*, The Korea Times, 2011.

[35] C. Sang-Hu, *Scandal in South Korea over nuclear revelations*, New York Times, 2013.

[36] T.-E. Kim, S. Nazir, and K. I. Øvergård, "A STAMP-based causal analysis of the Korean Sewol ferry accident," *Safety Science*, vol. 83, pp. 93–101, 2016.

[37] Y. Kim and H. Kim, "Improving Korea's societal security by preparing for unforeseen disasters: Focused on the horizontal collaboration approach," *International Journal of Security and Its Applications*, vol. 10, no. 3, pp. 11–20, 2016.

[38] D. H. Kim, D. A. Eisenberg, Y. H. Chun, and J. Park, "Network topology and resilience analysis of South Korean power grid," *Physica A: Statistical Mechanics and its Applications*, vol. 465, pp. 13–24, 2017.

[39] Korea Power Exchange (KPX), *Electric Power Statistics Information System*, 2016, http://epsis.kpx.or.kr/epsis/ekesStaticMain.do;jsessionid=Y0JXXWdKvpwzznLpXTn5fy0Z4sLvbZzlQytHgtwF2kN2phJJQjsR!241999982?cmd=001001&flag=&locale=EN.

[40] D. Ngar-yin Mah, J. M. van der Vleuten, J. Chi-man Ip, and P. Ronald Hills, "Governing the transition of socio-technical systems: A case study of the development of smart grids in Korea," *Energy Policy*, vol. 45, pp. 133–141, 2012.

[41] R. D. Zimmerman, C. E. Murillo-Sánchez, and R. J. Thomas, "MATPOWER: steady-state operations, planning, and analysis tools for power systems research and education," *IEEE Transactions on Power Systems*, vol. 26, no. 1, pp. 12–19, 2011.

[42] *Matlab Tools for Network Analysis (2006-2011)*, 2011, http://strategic.mit.edu/downloads.php?page=matlab_networks.

[43] D. Gleich, *MatlabBGL*, 2008, https://www.mathworks.com/matlabcentral/fileexchange/10922-matlabbgl?requestedDomain=www.mathworks.com.

[44] S. P. Borgatti, "Centrality and network flow," *Social Networks*, vol. 27, no. 1, pp. 55–71, 2005.

[45] M. Rosas-Casals, S. Bologna, E. F. Bompard et al., "Knowing power grids and understanding complexity science," *International Journal of Critical Infrastructures*, vol. 11, no. 1, pp. 4–14, 2015.

[46] N. Kapucu, "Interorganizational Coordination in Dynamic Context: Networks in Emergency Response Management," *Connections*, vol. 26, no. 2, pp. 33–48, 2005.

[47] A. B. M. Nasiruzzaman, H. R. Pota, and M. A. Mahmud, "Application of centrality measures of complex network framework in power grid," in *Proceedings of the 37th Annual Conference of the IEEE Industrial Electronics Society, IECON 2011*, pp. 4660–4665, aus, November 2011.

[48] A. B. M. Nasiruzzaman, H. R. Pota, and A. Anwar, "Comparative study of power grid centrality measures using complex network framework," in *Proceedings of the 2012 IEEE International Power Engineering and Optimization Conference, PEOCO 2012*, pp. 176–181, mys, June 2012.

[49] A. B. M. Nasiruzzaman, H. R. Pota, A. Anwar, and F. R. Islam, "Modified centrality measure based on bidirectional power flow for smart and bulk power transmission grid," in *Proceedings of the 2012 IEEE International Power Engineering and Optimization Conference, PEOCO 2012*, pp. 159–164, mys, June 2012.

[50] A. B. M. Nasiruzzaman and H. R. Pota, "Transient stability assessment of smart power system using complex networks framework," in *Proceedings of the 2011 IEEE PES General Meeting: The Electrification of Transportation and the Grid of the Future*, usa, July 2011.

[51] A. B. Nasiruzzaman and H. R. Pota, "Complex network framework based comparative study of power grid centrality measures," *International Journal of Electrical and Computer Engineering*, vol. 3, no. 4, 2013.

[52] S. Arianos, E. Bompard, A. Carbone, and F. Xue, "Power grid vulnerability: A complex network approach," *Chaos: An Interdisciplinary Journal of Nonlinear Science*, vol. 19, no. 1, Article ID 013119, 2009.

[53] E. Bompard, R. Napoli, and F. Xue, "Extended topological approach for the assessment of structural vulnerability in transmission networks," *IET Generation, Transmission & Distribution*, vol. 4, no. 6, pp. 716–724, 2010.

[54] E. Bompard, D. Wu, and F. Xue, "Structural vulnerability of power systems: A topological approach," *Electric Power Systems Research*, vol. 81, no. 7, pp. 1334–1340, 2011.

[55] G. C. Ejebe, J. Tong, J. G. Waight, J. G. Frame, X. Wang, and W. F. Tinney, "Available transfer capability calculations," *IEEE Transactions on Power Systems*, vol. 13, no. 4, pp. 1521–1527, 1998.

[56] A. J. Wood, B. F. Wollenberg, and G. B. Sheble, *Power Generation, Operation, and Control*, John Wiley & Sons, 2014.

[57] E. Bompard, L. Luo, and E. Pons, "A perspective overview of topological approaches for vulnerability analysis of power transmission grids," *International Journal of Critical Infrastructures*, vol. 11, no. 1, pp. 15–26, 2015.

[58] E. Bompard, E. Pons, and D. Wu, "Extended topological metrics for the analysis of power grid vulnerability," *IEEE Systems Journal*, vol. 6, no. 3, pp. 481–487, 2012.

[59] K. M. Carley, J. Pfeffer, J. Reminga, J. Storrick, and D. Columbus, "ORA User's Guide 2013," Defense Technical Information Center, 2013.

[60] A. Abbasi and N. Kapucu, "A longitudinal study of evolving networks in response to natural disaster," *Computational and Mathematical Organization Theory*, vol. 22, no. 1, pp. 47–70, 2016.

[61] L. C. Freeman, "Centrality in social networks conceptual clarification," *Social Networks*, vol. 1, no. 3, pp. 215–239, 1978-1979.

[62] B. Petrenj, E. Lettieri, and P. Trucco, "Towards enhanced collaboration and information sharing for critical infrastructure

resilience: Current barriers and emerging capabilities," *International Journal of Critical Infrastructures*, vol. 8, no. 2-3, pp. 107–120, 2012.

[63] E. P. R. Coelho, J. C. Thomazelli, M. H. M. Paiva, and M. E. V. Segatto, "A complex network analysis of the Brazilian Power Test System," in *Proceedings of the IEEE PES Innovative Smart Grid Technologies Latin America, ISGT LATAM 2015*, pp. 113–118, ury, October 2015.

[64] Z. Wang, A. Scaglione, and R. J. Thomas, "Electrical centrality measures for electric power grid vulnerability analysis," in *Proceedings of the 2010 49th IEEE Conference on Decision and Control, CDC 2010*, pp. 5792–5797, usa, December 2010.

[65] H. Bai and S. Miao, "Hybrid flow betweenness approach for identification of vulnerable line in power system," *IET Generation, Transmission & Distribution*, vol. 9, no. 12, pp. 1324–1331, 2015.

Hindawi
Complexity
Volume 2017, Article ID 7539089, 10 pages
https://doi.org/10.1155/2017/7539089

Research Article

Structural Evaluation for Distribution Networks with Distributed Generation Based on Complex Network

Fei Xue,[1] Yingyu Xu,[1] Huaiying Zhu,[2] Shaofeng Lu,[1] Tao Huang,[3] and Jinling Zhang[1]

[1] *Department of Electrical and Electronic Engineering, Xi'an Jiaotong-Liverpool University, No. 111 Ren'ai Road, Suzhou Industrial Park, Suzhou, China*
[2] *SDIC Baiyin Wind Power Co., Ltd., Lanzhou, China*
[3] *Politecnico di Torino, Torino, Italy*

Correspondence should be addressed to Fei Xue; fei.xue@xjtlu.edu.cn

Received 16 May 2017; Revised 1 September 2017; Accepted 12 September 2017; Published 17 October 2017

Academic Editor: Zofia Lukszo

Structural analysis based on complex network theory has been considered promising for security issues of power grids. At the same time, modern power distribution networks with more Distributed Generations (DGs) and Energy Storage Systems (ESS) have taken on more challenges in operation and security issues. This paper proposed a dedicated metric named as Power-Supply-Ability for power distribution networks based on net-ability. Special features of DGs, such as relations of capacities, identification of effective supply area, and limitation in continuous power supply, have been considered in definition. Furthermore, a novel opinion is proposed that the extent of improvement for operation and security by adding DGs also depends on the original structure of the distribution networks. This is an inherent ability of the original networks and could be quantitatively analyzed. Through case studies, this method has been proved to be effective in identifying potential structural vulnerabilities of distribution networks; particularly the impact of DGs on security has been studied. Furthermore, it can help in site selection for DGs by providing different priorities of locations compared with results of other works. This can help to complement other methods to construct a more comprehensive methodology by considering aspects of security, economy, and quality.

1. Introduction

The networks of power system, also named as power grids, are a critical infrastructure in modern social livings [1]. Serious outages of electrical power systems can impact the whole society [2, 3]. For instance, recent blackouts have occurred in the USA and Europe directly causing losses up to billions of dollars [4]. These serious consequences have drawn much attention to electrical security problems such as accidental or intentional attacks [4, 5].

However, with the increasing size and complexity in power grids [6], as well as increased consumption of power and other social developments, it is becoming more difficult and complex to analyze a large scale of whole power system and the complicated interconnectivity precludes us from understanding and evaluating an overall power system [6]. Complex network theory is a popular method to analyze networked systems in terms of a set of lines with connected nodes and fortunately recent studies have found that several properties of complex network (CN), such as small-world [7] and the characterization of scale-free [8], were related to power networks. It then allows structural analysis of power grids through pure topological metrics and brings a new analyzing method to overcome the above problems [9, 10]. In the theory of CN, Global Efficiency is a metric to measure the efficiency of the network for information transmission between vertices [10] and later is popularly referred to in assessing the vulnerability of power grids [5, 11–15]. Furthermore, with consideration of specific features in electrical engineering, it was updated as net-ability to evaluate power transmission networks [2, 4]. Based on complex network concept, net-ability analyzes the performance of transmission networks through considering extra physical features such as

power flow limits, electrical distance, and contributions of all involved transmission paths.

Although net-ability is effective in analyzing power transmission networks, due to different structural features among transmission and modern distribution networks, it could not be directly utilized for modern distribution networks. In conventional distribution networks, the main differences from transmission networks are their radial topology and impedance to resistance ratio. But it is not a problem for complex network theory to analyze any network structure including radial topology, and it is not a problem to adapt net-ability with appropriate impedance model. However, in modern power distribution networks, Distributed Generation (DG) and energy storage devices may increase its complexity. DGs, simply defined as small-scale electricity generation within distribution networks or on the customer side of the networks, are currently undergoing an increasing amount to relieve environmental problems, such as greenhouse gases from traditional electricity generation [16–23]. There are various categories of DGs, such as photovoltaic cells installed at homes or wind turbines on a farm land. Although these DGs could improve power supply to local loads, compared to conventional generation, they are highly dependent on climates or weather and could not provide continuous electricity [16, 17]. So battery Energy Storage Systems (BESS) can also be widely applied to improve power stability and demand/supply balance [17].

Up to now, to our best knowledge, few papers have considered direct applying of complex network approaches for analyzing modern distribution networks, especially to include impacts from DG and BESS. By comparing with conventional power distribution stations, [24, 25] consider DG with relevant small capacity and being placed to load node. Reference [24] pointed out that the power supply performance of DG should decrease rapidly with the increases of distance. Based on complex network concept, they raise some metrics to reflect that DG performance would decrease rapidly with increase of distance. The metrics used exponential form to show that DG contributed more power to relatively local load demand and less to remote loads, but exponential form cannot be fully justified and specific electrical features, such as impedance, power capacities of different devices, and contribution of different paths, were not fully considered. In this paper, the main impacts from DG on structural analysis of distribution networks are considered according to the channel capacity, supplying distance as well as intermittency and fluctuation of primary energy. These will be discussed in detail in Sections 2 and 3.

The rest of paper is organized as follows: global efficiency and net-ability will be discussed with their limitations for applying in distribution networks in Section 2. In Section 3, a new concept of Power-Supply-Ability (PSA) and its application in evaluating power distribution networks will be proposed. In Section 4, a novel opinion will be discussed to evaluate the inherent ability of original network structure to be improved by adding DGs. Simulation and results of application of PSA are shown in Section 5 with some examples and Section 6 contains some conclusions.

2. From Global Efficiency to Net-Ability

Global efficiency from the CN theory was initially defined by Latora [2, 4, 10] and was later widely used to evaluate performance of network, such as vulnerability assessment or location of critical components [4, 26]. It was also utilized in analyzing cascading failures for assessing power systems [27–29]. The definition for global efficiency can be written as

$$E(\mathbf{Y}) = \frac{1}{N(N-1)} \sum_{i \neq j} \frac{1}{d_{ij}}. \tag{1}$$

d_{ij} is the distance (length of the shortest path) between the pair of node i and node j, and N is the number of all nodes in the network. This formula is aimed at measuring network efficiency of information transmission by considering that the efficiency for sending information between a pair of nodes i and j is proportional to the reciprocal of their geodesic distance. For obtaining the general efficiency of the whole network, performance between each pair of nodes should be assessed to calculate an average value.

However, when applying this metric to evaluate power grids, the original concept of distance in (1) is not meaningful in electrical engineering [2, 4, 30]. Distance in power grids should be adjusted as the ability to overcome difficulties of transferring power between the pair of generator node g and load node d. Through considering the economic and technical aspects, power transmission difficulties should depend both on power flow capacity and on impedance. According to the electrical circuit theory, the equivalent impedance between bus g and bus d can be expressed as

$$Z_g^d = \frac{U_g^d}{I_g} = z_{gg} - 2z_{gd} + z_{dd}. \tag{2}$$

z_{gg}, z_{gd}, and z_{dd} are corresponding elements of the impedance matrix of the network.

Furthermore, the maximum power flow limit from g to d should also be considered, which can be calculated as

$$C_g^d = \min_{l \in L} \left(\frac{C_l^{\max}}{\left| f_l^{gd} \right|} \right). \tag{3}$$

C_g^d is power transmission capacity between the generator-load (g-d) pair. L is the set of all lines connecting g and d; $C_l^{\max}$ is the maximum power flow capacity for line l; f_l^{gd} is the power transfer and distribution factor (PTDF) when transferring power from bus g to d. PTDF here has overcome the assumption of transferring physical quantity only through the shortest path in global efficiency. Therefore, with the new definition of distance in power grids and taking into account power flow capacity characterized by PTDF, net-ability for power transmission network was defined as [3, 4, 9]

$$A(\mathbf{Y}) = \frac{1}{N_G N_D} \sum_{g \in G} \sum_{d \in D} \frac{C_g^d}{Z_g^d}. \tag{4}$$

G and D are, respectively, the sets of generator buses and load buses. N_G is the number of generator buses and N_D is the number of loads buses.

With fast development of smart grid technologies, distribution networks with DGs and BESS have become a hot topic in research and engineering. However, up to now, pure structural analysis has seldom been applied to this field. In fact, the evaluation of power supply security with penetration of DGs and BESS is meaningful and necessary; and site allocation for DGs and BESS from structural perspective can also contribute to real system planning and operation.

Although net-ability has been applied to evaluate structure vulnerabilities of power transmission network as an effective approach, it is not reasonable to directly apply it for modern distribution networks.

Firstly, only the capacity of transmission channel between any pair of generator bus and load bus was considered, because net-ability only targeted features of network and did not consider generators or loads as a part of networks. However, the power capacities of power sources and loads may impact on the final power supply performance if they are much different from the capacity of channel, especially for distribution networks where the capacities of power sources are not comparable with transmission networks. Therefore, the connotation of structural analysis should not be limited to pure topological features but should also include some static physical features of devices, such as capacities of power sources and BESS.

Secondly, in definition of net-ability, all generator buses are supposed to have large capacity to support long distance transmission, so any generator can be a power source for any load bus in the same network. However, in distribution networks, most DGs have much smaller power capacity and may only be effective power sources for a range of local loads. Therefore, DGs cannot be considered as equal power sources in set G with other traditional sources and cannot be an effective power source for any load bus in the network.

Thirdly, most DGs are renewable power generation, such as wind power or solar power. The output power of such power sources greatly depends on the availability of primary energy. Therefore, with intermittency and fluctuation, these power sources cannot supply continuous full rated output power for any required time period. Similar problem exists for BESS, which have to operate in charging and discharging modes in turn and cannot supply continuous full rated power for any required time period. As these features can seriously impact on the power supply performance of the distribution networks, they should not be neglected in structural analysis.

3. Power-Supply-Ability for Distribution Networks

To address the problems mentioned above, a new metric named as Power-Supply-Ability (PSA) dedicated to distribution networks is proposed based on net-ability.

To address the first problem mentioned in Section 2, the capacity of power source will be compared with the capacity of transmission channel defined in (3), and the minimum one will be applied in evaluating Power-Supply-Ability:

$$\frac{\min\left(C_g^d, C_g\right)}{Z_g^d}. \tag{5}$$

If the capacity of power source is smaller than the channel capacity, that means the channel capacity cannot be fully utilized by the power source, so it cannot be directly used in evaluating Power-Supply-Ability.

As for the second problem in Section 2, with development of renewable technology, focus of environmental-friendly energy, and demand/supply balance, new generation technologies of DG such as wind generation and energy storage are gradually considered in distribution networks [17, 31, 32]. However, according to their common small capacities [32, 33] and power generating efficiency, they should not be directly evaluated as above conventional power sources. So in definition of PSA, DGs will only be considered as backup or auxiliary power sources to improve power supply reliability and quality, which cannot be considered in a source-load pair in average calculation, but just as an additional compensation for a conventional source-load pair. Therefore, the net-ability can be extended as

$$\mathrm{PSA}\,(\mathbf{Y}) = \frac{1}{N_G N_D}\left\{\sum_{g\in G}\left[\sum_{d\in D}\left(\frac{\min\left(C_g^d, C_g\right)}{Z_g^d} + \sum_{g_B\in G_B^d}\frac{\min\left(C_{g_B}^d, C_{g_B}\right)}{Z_{g_B}^d}\right)\right]\right\}, \tag{6}$$

where G_B^d is the set of DG buses which are effective power sources for load bus d. And C_{g_B} is capacity of DG at bus g_B; $C_{g_B}^d$ is power transmission capacity from bus g_B to load d, which can also be calculated by (3). $Z_{g_B}^d$ is the equivalent impedance between g_B and the supplied load bus d. *The metric of net-ability calculates average network performance for all possible (generation + load) pairs. PSA considers a power supply layout in terms of main power source + load + auxiliary sources and calculates average power supply performance for all possible power supply layouts.* This means that when considering the power supply of one pair (g-d), additional power supply from local power supplies (DGs) to that load d will also be considered to improve the supply performance.

Since DGs in (6) are considered to have small capacities in this paper, it implies that DGs could not serve any load in the network like conventional power sources. It then needs a method to identify effective DG power sources G_B^d for a load bus d. From another point of view, we can say that we need a method to identify effective supply area of a DG bus g_B.

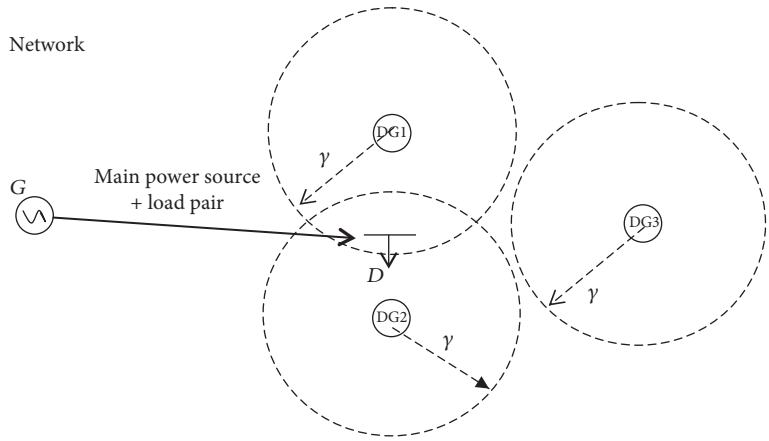

Figure 1: Sketch for effective supply area of DGs.

Then G_B^d is the set of DG buses whose supply areas all include load d. When considering effective supply area of DGs, the general idea is that, with the same impedance, higher power supply capacity increases the efficient supplying area; with the same power supply capacity, higher impendence reduces the efficient supplying area. Then, a criterion to identify effective supply area for a DG bus is proposed as

$$\frac{Z_{g_B}^d}{\min\left(C_{g_B}^d, C_{g_B}\right)} \leq \gamma, \quad g_B \neq d. \tag{7}$$

All DGs from G_B^d satisfy criterion $Z_{g_B}^d / \min(C_{g_B}^d, C_{g_B}) \leq \gamma$ and $g_B \neq d$. To be specific, when the criterion is satisfied, it means that the DG has the ability to supply power to load d with acceptable power quality. $g_B \neq d$ means that when analyzing power supplied to load d, any DG directly installed at load bus d will not be evaluated. The reason is that PSA in this paper is to evaluate the distribution network; once the DGs are placed at the load bus d, to some degree, they could not be considered as a part of network because their interactions are not through the network frame, and the power supply from these DGs to load d should be considered as an internal supply, which is isolated from the whole system performance. Additionally, γ is a parameter to define the DG supply area and it should be a value based on statistical analysis and simulation.

Figure 1 is a sketch to explain the meaning of effective supply area and power supply layout. A main power source G and a load bus D can be considered as a generation + load pair. There are three different DGs in the figure. Each DG could be considered as the center of a circle whose radius is γ. The circles could be considered as the effective area of each DG. The load bus D is inside the circles of DG1 and DG2 but outside of the circle of DG3. That means DG1 and DG2 are all effective auxiliary sources for D and should be included in G_B^d. And DG3 is not an effective auxiliary source for D; it should not be included in G_B^d. So the corresponding power supply layout could be (G + D + DG1 + DG2).

To address the third problem mentioned in Section 2, as some renewable DGs and BESS cannot supply continuous full rated power, a power supply factor is introduced:

$$\eta = \frac{T_S}{T_P} = \frac{\text{Equivalent Supply Time at Rated Power}}{\text{Total Time of One period}}. \tag{8}$$

For a DG or BESS with rated power P, suppose, in one calculating period T_P, the accumulated output energy is E_P; then the equivalent supply time at rated power during this period can be calculated as

$$T_S = \frac{E_P}{P}. \tag{9}$$

This is a method to unify all main power sources, DGs and BESS systems. For example, for a main power source g, such as a distribution substation which has ability to supply rated power during any required time period, the corresponding power supply factor η_g is equal to 1. This will not influence the calculation of net-ability. But for some DGs and BESS, this power supply factor needs to be calculated according to statistical data. For a wind power generator or PV panel, this needs to select a long term period with corresponding weather information and actual output energy statistical data. For BESS, the system needs specific time for charging and then to make discharging for some time. The power supply factor should be calculated based on an average charging and discharging period.

Furthermore, the power supply factor is an indicator to reflect the ability of a power source to make continuous rated power supply but not description for real operating state. For example, a main power source (distribution substation) may have power supply factor of 1 meaning ability to supply rated power for any required time period, but it does not mean it always operates at rated power for any time.

With this power supply factor, PSA can be finally defined as

$$\mathrm{PSA}(\mathbf{Y}) = \frac{1}{N_G N_D}\left\{\sum_{g\in G}\left[\sum_{d\in D}\left(\eta_g \frac{\min\left(C_g^d, C_g\right)}{Z_g^d} + \sum_{g_B\in G_B^d}\eta_{g_B}\frac{\min\left(C_{g_B}^d, C_{g_B}\right)}{Z_{g_B}^d}\right)\right]\right\} \quad \left(g \neq d,\ g_B \neq d\right). \tag{10}$$

Similar to calculation for net-ability, the relative change of PSA after removal of components can help to indicate the most important components in the targeted distribution network:

$$\Delta\mathrm{PSA} = \frac{\mathrm{PSA}(Y) - \mathrm{PSA}(Y-1)}{\mathrm{PSA}(Y)}, \tag{11}$$

where PSA($Y-1$) represents the Power-Supply-Ability of distribution network after one component is removed and ΔPSA is the relative drop of PSA normalized by PSA(Y) to identify critical components of a network. Higher value of ΔPSA implies that this component is more critical and removal of it could result in severer negative effects. Thus, this component needs more protection.

4. Overall Ability of Networks for DG Integration

In the field of complex networks, it has been widely acknowledged that the performance and vulnerabilities of networked infrastructures are tightly related to the original topology and structure. Furthermore, in analyzing performance and security issues for power grids, topology and extended structural factors, such as positions of generation and load buses, capacities of transmission lines, and contributions of all paths in power transmission have been taken into account. However, up to now, few research works have considered DGs in terms of their positions and capacities as structural factors and evaluated their possible contributions in improving network performance and security. This is the original motivation to propose PSA.

However, it is important to point out that such improvements are from bidirectional interactions between the original networks and the integrated DGs. Therefore, the final effects may depend not only on the features of DGs, but also on some inherent features of the original networks. In these inherent features, topology and structural factors of the original networks are very important. Therefore, there should be two different perspectives to consider the issues about integration of DGs with distribution networks. The first perspective is at a local level and from individual viewpoint of DGs to discuss possible optimal deployment and operation of DGs with structural factors as given conditions. The second perspective should be at a global level and from overall viewpoint of original networks to discuss the inherent potential abilities of networks about how their performance and security can be improved by penetration of DGs. That is to say, with the same extents of DG penetration, the extents of improvement for different distribution networks may be different due to their inherent characteristics, such as topology and structure. Up to now, most existent works related to DGs were from the first perspective; few works were from the second perspective or even aware of its existence. In this paper, we will propose methodologies based on PSA to evaluate and compare this inherent potential of networks from the second perspective.

The inherent potential abilities of networks for improvement by DG penetration are related to two aspects, that is, network performance and security. The first issue is to discuss how the network static performance can be improved by same extent of DG penetration. The second issue is to discuss how the vulnerabilities of the networks can be reduced by penetration of DGs.

For the first issue, to make overall evaluation, two networks can be considered, the original network Y and a modified network $Y+T$. In $Y+T$, we suppose all buses of Y are connected to DGs with same power supply factor and capacity; then the variance of PSA before and after adding these DGs could be used to evaluate the original system structure for its inherent ability to be improved by DGs.

Alternatively, we may suppose a unique DG with given power supply factor and capacity is connected to each bus of Y in turn; the increase of PSA corresponding to each bus could be used to evaluate which one may be the best location to install a DG. But, furthermore, we may also calculate the average value of increase in PSA for all buses to make overall evaluation for inherent ability of the network.

Both methods can be applied jointly to indicate the inherent ability of the network. The former one is mainly from an overall and accumulated point of view; the second one is mainly from an average point of view.

For the second issue, the vulnerability of the original network can be characterized by the relative drop of PSA calculated by (11); then the vulnerability of network Y can be defined as

$$\mathrm{VUL}(Y) = \max_{l\in L}\left\{\frac{\mathrm{PSA}(Y) - \mathrm{PSA}(Y-l)}{\mathrm{PSA}(Y)}\right\}. \tag{12}$$

The most critical line l_m can be identified as corresponding to the maximum PSA drop in (12). Similar to the former ideas, DGs with same power supply factor and capacity can be added to all buses of network Y, which can be indicated as $Y+T$. In $Y+T$, we can also calculate its maximum drop of PSA by (12). So this variance of PSA drop can reflect the original overall ability of the network to be improved for its security by adding DGs.

To give more detailed information, the adding of DGs can be performed according to the importance sequence of

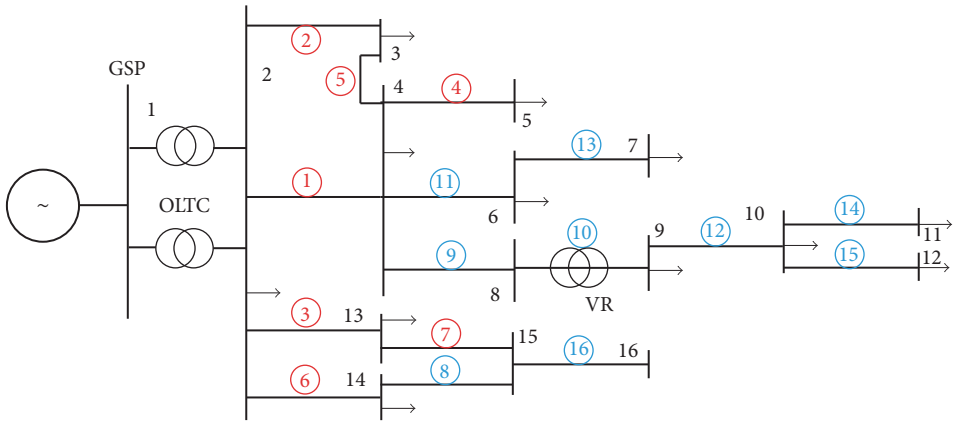

Figure 2: Ranking of branch in UKGDS_86.

buses step by step. The importance sequence is the sequence from larger to smaller PSA for different $(Y + DG_i)$. This may give direct expression of impacts from DGs on security for different locations.

For given networks, these methods can jointly evaluate and discover their difference in potential abilities to be improved by DG penetration. This can help analysis and decisions in overall planning and investment related to DG penetration. Possible application of these methods is that when limited resources of DG are given, if one distribution network needs to be selected from two or several candidate networks to install these DG resources, these methods can help to determine which one is the best choice according to their original structure features. And, furthermore, this also can help to identify structural bottlenecks of distribution networks in DG development.

5. Case Study

In this section, the PSA is applied to the IEEE-33-bus system and a real distribution network UKGDS_86. UKGDS_86 initially is tested without DGs and it will be assessed to compare and analyze corresponding power supply performance through PSA. The initial PSA for UKGDS_86 without DGs is calculated as

$$\text{PSA (UKGDS\_86)} = 57.1253. \quad (13)$$

When removing one branch from UKGDS_86, performance of power supply could be evaluated through PSA$(Y - 1)$ metric and relative drop ΔPSA could be used to rank the critical lines.

As in Table 1, once a branch is removed, it could result in decreases in PSA. For better visual effect, rankings are shown in Figure 2.

The red numbers in red circles represent five branches which would result in significant PSA drops once removed and need more protection. As is shown, these branches mainly occur close to power station. It seems that branches near power station play significant roles in power supply; removal of them would influence performance of the whole system more severely and need more protection for grid security. Branches in blue, which are relevantly away from power station and near loads, will cause less negative consequences when they are removed.

Table 1: Critical branches rankings in UKGDS_86.

$$\text{PSA}_{\text{initial}}(Y) = 57.1253$$
$$\Delta\text{PSA}(Y) = \frac{\text{PSA}(Y) - \text{PSA}(Y-1)}{\text{PSA}(Y)}$$

Rank	Branch	PSA	ΔPSA
1	2-4	14.426	0.747467
2	2-3	17.125	0.70022
3	2-13	17.144	0.699888
4	4-5	17.385	0.695669
5	3-4	17.572	0.692395
6	2-14	17.977	0.685306
7	13-15	18.193	0.681525
8	15-14	18.193	0.681525
9	4-8	18.589	0.674593
10	8-9	18.589	0.674593
11	4-6	18.72	0.672299
12	9-10	19.103	0.665595
13	6-7	19.32	0.661796
14	10-11	19.531	0.658102
15	10-12	19.57	0.65742
16	15-16	19.724	0.654724

When adding same DGs to each bus, which means there are now totally 16 DGs in network, PSA value of this new grid increases to 62.721. Similar to above analysis, branches of this grid are ranked and labeled as in Figure 3.

As is shown in Figure 3 comparing with former conventional network without DGs, removal of branches results in similar rankings. Only branch 2-3 and branch 4-5 have exchanged ranks, which are labeled in Figure 3, but they still keep top five as former. So installation of DGs can improve power supply performance of the network but does not change the protection properties of branches too much.

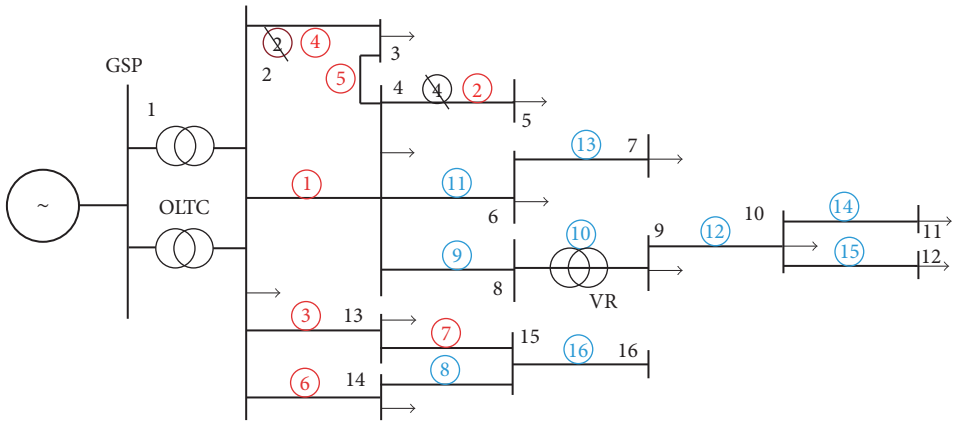

Figure 3: Ranking of branch in UKGDS_86 with DGs.

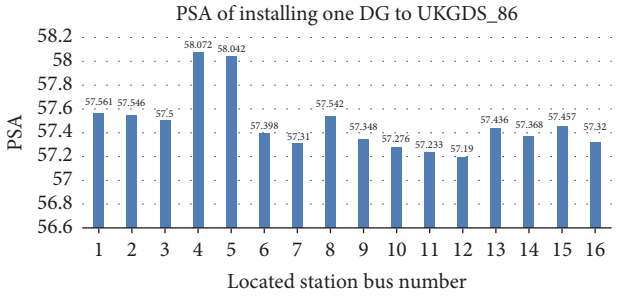

Figure 4: PSAs for adding one DG at different buses.

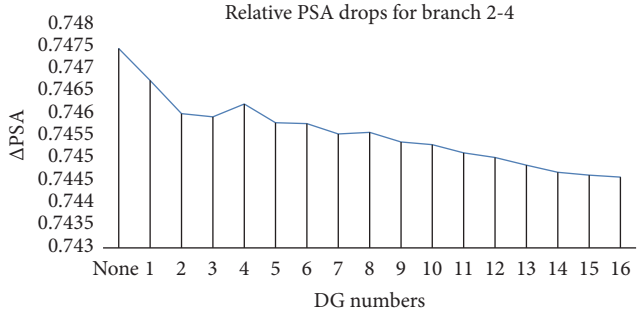

Figure 5: ΔPSA of branch 2-4 with different DGs.

Branches near power distribution station still need more attention for security.

To quantitatively identify which buses are best sites for installation of DG, one DG can be installed on each bus in turn and the corresponding increase of PSA is shown in Figure 4.

It shows that bus 4 is the best location for locating DG and bus 12 is the relevantly worst. Based on this, the first DG should be suggested to be located on bus 4 and then the second one will be added at bus 5. Through considering overall performance, bus 12 with worst PSA = 57.19 will be lastly planned to add a DG.

Based on the order in Figure 4, DGs are added one by one for further observation of DG influence. As is shown, initially there is no DG; based on orders in Figure 3, the first DG will be added to bus 4 and then add the second DG at bus 5. Add DGs one by one under above suggestion order and record relative PSA drops (ΔPSA) of (12) during DG addition procedure.

From Figures 2 and 3, branch 2-4 is the most critical line and needs the most protection. Thus, this branch is selected in Figure 5 to observe ΔPSAs under different number of DGs.

Figure 5 shows that, with increases of DGs, they generally decrease ΔPSA; in other words, addition of local power supplies could improve power grids performance and decrease the vulnerability of critical lines. At the beginning, the curve is steeper and indicates that the adding of DGs at beginning could obviously reduce system vulnerabilities. However, at the end of the curve, it becomes flat and indicates that the effect of adding DGs becomes weak step by step.

Furthermore, an ideal small-scale generation with power supply factor of 1 is utilized to test IEEE-33-bus system and compare with analytical methods reported earlier [34] through considering improvement of voltage profile and reduction of losses.

In Figure 6, the y-axis of ranking represents the performance of DG installation, the minimum number means best performance, and the largest number means the worst performance. For instance, in purple line, when DG location is 5, its priority ranking is 1 and it means that installing DG to bus location 5 will improve performance most.

There are three lines in Figure 6, the blue line is the ranking results from PSA metric in this paper, which is based on structural analysis. While voltage stability index and Exhaustive Load Flow Method (ELF) [34–36] are based on detailed power flow calculations, involving detailed load voltages, generator voltages, and load currents. These methods consider that addition of DGs may increase real power flow back to system and then cause voltage rise or may increase reactive power follow into feeder and then cause voltage to fall [34–36]. Thus, reduction of losses, which is aimed at minimizing total power losses and improvement of voltage stability, is the main purpose for these methods to consider DG optimum location. To some extent, methods

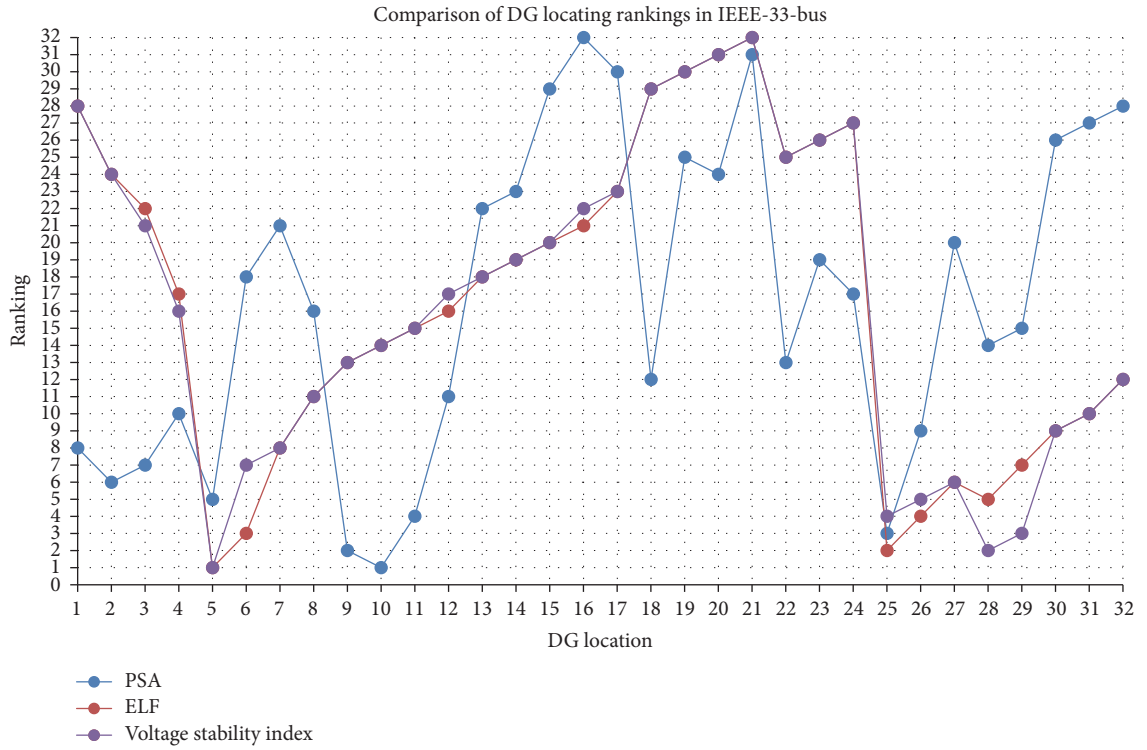

Figure 6: PSAs for installing DGs at different buses.

based on states pay more attention to economy and quality while PSA method based on structural analysis focuses on overall performance and security.

In other words, analyses based on operating states could not consider all possible system operative states through calculating and they mostly focus on economy through limited situations. However, security analysis should pay attention to emergencies such as intentional attacks, which are not the common conditions. Thus, safety analysis and above economic analysis have contradictions.

Since analyzing aspects of three methods are different, there are variances of rankings in Figure 6. However, there are still some installation locations with relevantly smaller priority variances. For these locations, they contain both aspects of security and aspects of economy and quality, which are more meaningful.

In Figure 7, bus locations 25, 5, and 26 have high rankings from perspectives of economy, quality, and security, which should be firstly suggested to install DGs while bus locations 13, 14, and 21 have low performance from three perspectives and may not be recommended to add DGs. There are also inconsistent locations such as bus locations 6, 9, 10, and 28. That means evaluation by limited operational states cannot identify possible problems in security analysis which is the contribution of the measure from this paper.

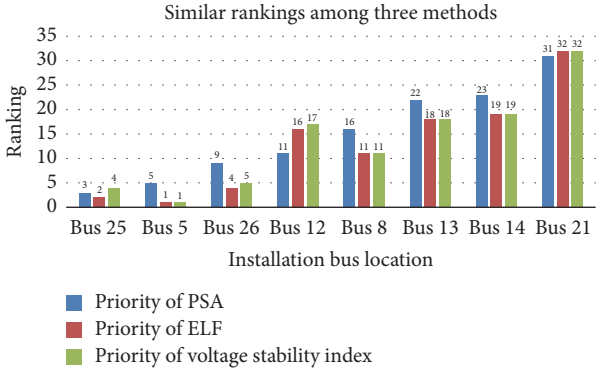

Figure 7: Similar rankings among three methods.

6. Conclusions

Structural analysis based on complex network theory has been considered promising for analyzing security issues of power grids. However, the meaning of "structure" has normally been limited to topological connections or some related physical features of networks. In fact, in broad sense, some static physical features of related components may also have tight relation with network performance, such as capacities, effective supply area, or intermittency of generators. Many effective metrics of complex networks are based on statistic evaluation. And these static physical features can also provide great valuable information from statistic perspective. Therefore, it is inevitable that these more static features would be integrated with network structures when the targeted issues are more specific and professional.

At the same time, with fast development of smart grid technology, modern power distribution networks with more

DGs and BESS have taken on more challenges in operation and security issues. By consideration of some specific defects of former metrics for distribution networks and DGs, it is necessary to update related methodologies by some further important and special features to extend the meaning of structural analysis. This paper proposed a dedicated metric named as Power-Supply-Ability for power distribution networks based on net-ability which was formerly applied to power transmission networks. Three defects of net-ability applying to distribution networks with DGs are identified. Based on solutions to these defects, the net-ability is updated and refined as Power-Supply-Ability for distribution networks. Furthermore, it is pointed out that it is an inherent ability depending on the original network structure to improve its performance and security by same extent of DG penetration. Through case studies, this method has been proved to be effective in identifying potential structural vulnerabilities of distribution networks. Furthermore, it can help in site allocation for DGs and complementing other methods which are only based on limited analysis of states. The analysis and judgment for DG plan and operation should consider perspectives of economy, quality, and security. This metric can help to construct a more comprehensive methodology. In the future, this method will try to be applied to real world systems in decision of DG allocation for further development and analysis.

Conflicts of Interest

The authors declare that there are no conflicts of interest regarding the publication of this paper.

Acknowledgments

This work has been supported by the SDIC Baiyin Wind Power Co., Ltd., through the joint research project "Study on Key Technologies for Energy-Internet-Oriented Microgrids."

References

[1] C. Liu, Q. Xu, Z. Chen, and C. L. Bak, "Vulnerability evaluation of power system integrated with large-scale distributed generation based on complex network theory," in *Proceedings of the 47th International Universities Power Engineering Conference (UPEC '12)*, 2012.

[2] E. Bompard, D. Wu, and F. Xue, "Structural vulnerability of power systems: A topological approach," *Electric Power Systems Research*, vol. 81, no. 7, pp. 1334–1340, 2011.

[3] E. Bompard, R. Napoli, and F. Xue, "Analysis of structural vulnerabilities in power transmission grids," *International Journal of Critical Infrastructure Protection*, vol. 2, no. 1-2, pp. 5–12, 2009.

[4] S. Arianos, E. Bompard, A. Carbone, and F. Xue, "Power grid vulnerability: a complex network approach," *Chaos: An Interdisciplinary Journal of Nonlinear Science*, vol. 19, no. 1, Article ID 013119, 2009.

[5] V. Latora and M. Marchiori, "Vulnerability and protection of infrastructure networks," *Physical Review E: Statistical, Nonlinear, and Soft Matter Physics*, vol. 71, no. 1, Article ID 015103, 2005.

[6] R. Albert, I. Albert, and G. L. Nakarado, "Structural vulnerability of the North American power grid," *Physical Review E: Statistical, Nonlinear, and Soft Matter Physics*, vol. 69, no. 2, Article ID 025103, 2004.

[7] D. J. Watts and S. H. Strogatz, "Collective dynamics of 'small-world' networks," *Nature*, vol. 393, no. 6684, pp. 440–442, 1998.

[8] A. L. Barabasi and R. Albert, "Emergence of scaling in random networks," *American Association for the Advancement of Science: Science*, vol. 286, pp. 509–512, 1999.

[9] E. Bompard, R. Napoli, and F. Xue, "Extended topological approach for the assessment of structural vulnerability in transmission networks," *IET Generation, Transmission & Distribution*, vol. 4, no. 6, pp. 716–724, 2010.

[10] L. D. F. Costa, F. A. Rodrigues, G. Travieso, and P. R. V. Boas, "Characterization of complex networks: a survey of measurements," *Advances in Physics*, vol. 56, no. 1, pp. 167–242, 2007.

[11] P. Hines, E. Cotilla-Sanchez, and S. Blumsack, "Do topological models provide good information about electricity infrastructure vulnerability?" *Chaos: An Interdisciplinary Journal of Nonlinear Science*, vol. 20, no. 3, Article ID 033122, 2010.

[12] U. Brandes and D. Fleischer, *Centrality Measures Based on Current Flow*, Springer, 2005.

[13] G. Chen, Z. Y. Dong, D. J. Hill, and G. H. Zhang, "An improved model for structural vulnerability analysis of power networks," *Physica A: Statistical Mechanics and its Applications*, vol. 388, no. 19, pp. 4259–4266, 2009.

[14] E. Bompard, D. Wu, and F. Xue, "The concept of betweenness in the analysis of power grid vulnerability," in *Proceedings of the Complexity in Engineering (COMPENG '10)*, pp. 52–54.

[15] S. Arianos, E. Bompard, A. Carbone, and F. Xue, "Power grid vulnerability: A complex network approach," *Chaos: An Interdisciplinary Journal of Nonlinear Science*, vol. 19, no. 1, Article ID 013119, 2009.

[16] A. Oudalov, D. Chartouni, and C. Ohler, "Optimizing a battery energy storage system for primary frequency control," *IEEE Transactions on Power Systems*, vol. 22, no. 3, pp. 1259–1266, 2007.

[17] Y. Hida, Y. Ito, R. Yokoyama, and K. Iba, "A study of optimal capacity of PV and battery energy storage system distributed in demand side," in *Universities Power Engineering Conference (UPEC)*, pp. 1–5, 2010.

[18] W. Y. Yang, X. Y. Yang, and J. J. Yang, "Research on distributed generation and application in power system," *Advances of Power System & Hydroelectric Engineering*, vol. 24, pp. 39–43, 2008.

[19] K. J. Qian and Y. Yuan, "Distributed generation technology and its impact on power systems," *Relay*, vol. 35, pp. 25–29, 2007.

[20] U. Doe, The potential benefits of distributed generation and rate-related issues that may impede their expansion, 2007.

[21] A. Yadav and L. Srivastava, "Optimal placement of distributed generation: an overview and key issues," in *Proceedings of the International Conference on Power Signals Control and Computations (EPSCICON '14)*, 2014.

[22] A. Borbely and J. F. Kreider, *Distributed generation: the power paradigm for the new millennium*, CRC press, 2001.

[23] M. K. Maribu, *Distributed Generation in Liberalised Electricity Markets [Ph.D. thesis]*, 2002.

[24] Y. Y. Wang, S. W. Mei, Y. B. Mao, and F. Liu, "Vulnerability assessment of power grid with distributed generation based on complex network theory," *Journal of Systems Science and Mathematical Sciences*, vol. 30, no. 6, pp. 859–868, 2010.

[25] F. Gullí, "Small distributed generation versus centralised supply: a social cost-benefit analysis in the residential and service sectors," *Energy Policy*, vol. 34, no. 7, pp. 804–832, 2006.

[26] P. Crucitti, V. Latora, and M. Marchiori, "Locating critical lines in high-voltage electrical power grids," *Fluctuation and Noise Letters*, vol. 5, no. 2, pp. L201–L208, 2005.

[27] R. Kinney, P. Crucitti, R. Albert, and V. Latora, "Modeling cascading failures in the North American power grid," *The European Physical Journal B*, vol. 46, no. 1, pp. 101–107, 2005.

[28] B. C. Lesieutre, S. Roy, V. Donde, and A. Pinar, *Power system extreme event screening using graph partitioning*, Lawrence Berkeley National Laboratory, 2006.

[29] J. Li, "Identification of Cascaded Generator Over-Excitation Tripping Events," ProQuest, 2007.

[30] E. Bompard, E. Pons, and D. Wu, "Extended topological metrics for the analysis of power grid vulnerability," *IEEE Systems Journal*, vol. 6, no. 3, pp. 481–487, 2012.

[31] L. Kang, H. Guo, J. Wu, and S. Chen, "Characteristics of distributed generation system and related research issues caused by connecting it to power system," *Power System Technology*, 2010.

[32] R. Viral and D. K. Khatod, "Optimal planning of distributed generation systems in distribution system: a review," *Renewable & Sustainable Energy Reviews*, vol. 16, no. 7, pp. 5146–5165, 2012.

[33] L. Li, "A study on distributed generation and its effects in power system," *Journal of Modern Power Systems and Clean Energy*, pp. 55–59, 2010.

[34] S. Kalambe, G. Agnihotri, and A. K. Bohre, "An Analytical Approach for Multiple DG Allocation," in *Proceedings of the in Distribution System*, vol. 2, 2013.

[35] D. Q. Hung and N. Mithulananthan, "Multiple distributed generator placement in primary distribution networks for loss reduction," *IEEE Transactions on Industrial Electronics*, vol. 60, no. 4, pp. 1700–1708, 2013.

[36] N. Acharya, P. Mahat, and N. Mithulananthan, "An analytical approach for DG allocation in primary distribution network," *International Journal of Electrical Power & Energy Systems*, vol. 28, no. 10, pp. 669–678, 2006.